New insights on classical-quantum gravitational backreaction

By

Emanuele Panella

A thesis submitted to

University College London

for the degree of

Doctor of Philosophy

Department of Physics and Astronomy

University College London

June 2025

I, Emanuele Panella, confirm that the work presented in this thesis is my own. Where information has been derived from other sources, I confirm that this has been indicated in the thesis.

Signed ..... Date .....

New insights on classical-quantum gravitational backreaction

Emanuele Panella

Doctor of Philosophy of Physics

University College London

Prof. Jonathan Oppenheim, Supervisor

Prof. Andrew Pontzen, Supervisor

Abstract

This thesis treats the backreaction of quantum degrees of freedom on classical systems, with a focus on gravitational physics. We consider both fundamental and effective classical subsystems.

Assuming fundamental classicality of a subsystem leads to classical-quantum (CQ) dynamics, a framework that requires both decoherence and classical diffusion for consistency. We first apply the CQ formalism to study the evolution of two coupled oscillators – one classical, one quantum – with classical friction. Using path integrals, we show that the system relaxes to a unique non-equilibrium steady state, which becomes thermal in the high-diffusion limit. We derive the phase-space representation of hybrid dynamics and show that for harmonic potentials it maps exactly to a Fokker-Planck equation.

We then examine the proposal that gravity could remain fundamentally classical. Consistency of the theory at all scales implies that the combined matter and gravitational evolution has be of CQ form. We first analyse a stochastic Klein-Gordon field (the classical sector of a CQ Yukawa model) as a toy model for linearised CQ gravity. We address the issue of unbounded diffusion and discuss the implication of the infinite energy production in the model. Next, we study a CQ model of cosmology. In a stochastic FLRW Universe, we show that diffusion during inflation, if strong enough, could mimic dark matter (CDM) effects.

The second part discusses "braneworld holography" as a method to compute semiclassical backreaction of conformal quantum fields on an effectively classical metric. We apply this framework and find an exact quantum Kerr–de Sitter solution to the (2+1)-dimensional semiclassical Einstein's equations with higher-curvature corrections, and derive its thermodynamic

properties. We compare the exact solution with the non-holographic, but limited, perturbative approach to the backreaction problem. We conclude with prospects for future work.

Impact Statement

This thesis presents and analyses models that can be useful to study the problem of gravitational backreaction, and quantum-classical backreaction more generally.

The hybrid damped classical-quantum oscillator we discuss provides the first non-thermal steady-state in a consistent hybrid system. It provides the stepping stone towards the study of non-equilibrium thermodynamics when both classical and quantum degrees of freedom are present. It also shows that classical friction can be enough for the hybrid system to flow to a steady-state. The phase-space representation of hybrid dynamics we present provides a novel approach to efficiently simulate CQ evolution.

The techniques we introduce to solve for the classical stochastic Klein-Gordon – such as the regularisation of the divergences and the pole-prescription in Fourier space – can be easily generalised to any classical stochastic out-of-equilibrium field. This is key for the study of linearised hybrid gravity, a natural next step towards the development of a theory of fundamental classical gravity interacting with quantum matter.

The stochastic model of cosmology we present gives a novel mechanism to generate cold dark matter phenomenology without the need of a hidden dust fluid. Further, it can be used, together with our result on relativistic stochastic scalars, to explore how CQ cosmology diverges from LambdaCDM, in order to come up with cosmological and table-top tests on the quantum nature of the gravitational field. Indeed, falsifying CQ gravity would indirectly prove the quantumness of the spacetime geometry.

The quantum black hole solution we discuss is the first rotating black hole in (2+1)-dimensional de Sitter space. It – and braneworld holography in general – provides a fertile ground of investigation to study the role of quantum corrections to classical GR results.

List of Publications and Preprints

The work presented in this thesis contains material from the following publications and preprints:

1. Classical-quantum oscillators as diffusive processes in phase space; Emanuele Panella. In preparation [1];

2. Diffusion in the stochastic Klein-Gordon equation; J. Oppenheim, Emanuele Panella. In preparation [2];

3. J. Oppenheim, Emanuele Panella, A. Pontzen. Emergence of phantom cold dark matter from spacetime diffusion. arXiv:2407.13820 [3];

4. Three-dimensional quantum black holes: a primer, Emanuele Panella, J. Pedraza, A. Svesko. Universe **2024**, 10(9) 358 [4];

5. Quantum Kerr-de Sitter black holes in three dimensions, Emanuele Panella, A. Svesko. J. High Energ. Phys. 2023, **127** (2023) [5];

Other publications and preprints published during the doctorate period by the author are:

6. Nucleation of charged quantum dS_3 black holes, A. Climent, R. Hennigar, Emanuele Panella, A. Svesko. J. High Energ. Phys. 2025, **86** (2025) [6];

7. Stochastic Dark Matter: Covariant Brownian Motion from Planckian Discreteness, E. Albertini, A. Nasiri, Emanuele Panella. Phys. Rev. D **111**, 023514 [7];

Acknowledgments

This thesis would have not been possible without the support of my advisors Jonathan and Andrew. I never felt "just a student" in these four years – I had all the freedom, support and challenges needed to develop as an independent researcher. To Jonathan I owe the open-minded critical approach I now welcome new ideas with. The stimulating, yet relaxed, environment he set up in our group is a uniquely delicate system – something I hope to recreate in the future. I need to thank Andrew for the constant advice, an eternal reservoir of quietude, and for being a model of pure intellectual honesty and impressive breadth of knowledge. Further, I want to thank Johannes Noller and Gautam Satishchandran for the insightful comments on my work – not only they improved this thesis, they are useful pointers for future investigations.

Then, I cannot understate the immense gratitude I feel towards my parents. To my mom Cristina and my dad Alessandro, thank you for the emotional sacrifices you made, for being challengingly supportive of my choices and for the daily doses of affection, from which I could not escape even when I tried! It is because of you that I had the courage and the means to follow my aspirations – the greatest present I will ever receive. To my brother Dado, I'm grateful for the love and respect you constantly invest me with — it warms me and gifts me sense of responsibility. I have deep admiration for your unique kindness, intelligence and integrity. I could not hope for a better sibling.

Who I am is the result of a united and caring family. I want to thank grandma Bianca for having taught me rigor and respect, grandpa Andrea for the hard-working role model he has been (and for the occasional tire punctures on the street!), grandma Marina for her purity of heart and for keeping me up to date through delicious gossip lunches. A special thought to grandpa Sandro, who was the first to feed my young scientific curiosity — I would have loved to

share this moment with you. I'm grateful to Massimiliano, Paola and Fabio for having always been my extra parents in times of need, and to my "little sisters" Marta and Francesca for keeping me in touch with the young, cool, world.

To the superbly talented C-Office gang, I was so lucky to share with you parts of my doctorate. I want to thank Zach for "having picked all the low-hanging fruit", Andrea for the unselfish paternal role, Maite for understanding my emotive language in times of need and Isaac for being my mischievous brother — we did some good nailing. To Rhys and Muhammad, thanks for having indulged my chaos in the last year – you have bright futures. I'd then like to thank Lorenzo for having shown me the truest Italian deli in London — excellent fuel to complete this thesis. To Andy, however, goes a particularly heartfelt acknowledgment. You've been way more than a great friend and mentor in these four years — I owe to you a good chunk of my current serenity. I didn't need a "bigger boat" after all.

Finally, I'd like to thank my non-scientific friends. First, my household, for having been my second — Legendary — family, in rigorous numerical order. To Tan: our cigar sessions are amongst the most treasured moments of my English life – pure emotional honesty and a pinch of pretentious philosophy. Ignoring all the banana-stealing, I am grateful to Henry for constantly allowing my inner child to take control. I then need to thank Lollo for having constantly put us back on the course of decency and Pit for the inebriated bus rides of chats and hopes. I then need to thank the rest of my London friends for being ever so unique, interesting, thought-provoking and crazy. You made these eight years truly special. In particular, I want to thank Cari and Andrea for having helped me to discover many new faces of the city I love. Then, to my friends in Rome: whenever I've come back, I've never felt as an expat. Instead, I've always found a special seat reserved – it means the world to me. My wife-de-facto Barto, Luca, Gialuca, Nene, Pisi and Bianca deserve an exceptional mention for being my unconditional supporters, ever since day one of high-school (and earlier still).

Much like for my Master's, I'd like to reserve my final words to my physics twins Emma, Tan and Capo. We started on this path together as clueless teenagers in Blackett, and now we're (almost) fully-fledged scientists. It was a privilege to share this absurd journey with you.

Contents

Chapter 1

Introduction

The split between the classical and quantum world is a blurred line of demarcation. Importantly, such a separation can sometimes lie in between interacting subsystems: the same object can have some degrees of freedom which behave classically and others whose description requires the quantum toolkit.

The situation in which it is only the evolution of the quantum subsystem to be influenced by the classical one is well-understood and under good analytical control. It encompasses a range of physical settings of interest, from a spin evolving in a magnetic field to quantum field theory in curved spacetime. There, it suffices to have the parameters controlling the quantum evolution operator being dependent on the value of some classical, independently-evolving, variable. In all other aspects, it is simply standard – often even unitary – quantum mechanics.

In this thesis we will focus on the much harder problem of handling quantum backreaction: we will take the evolution law of the classical degrees of freedom to depend on the state of the quantum subsystem. In particular, we will study the problem of quantum matter bakcreacting on a (fundamentally or effectively) classical geometry.

1.1 A brief history of consistent hybrid evolution

In most situations of interest the classicality of a subsystem of a hybrid system is only effective: it is always assumed – or known – that there exists a fundamental quantum evolution governing the full object, with the *semi-classical* description being only a useful effective theory. This

is the case, for example, in quantum chemistry [8, 9] and measurement-and-feedback [10, 11] (a framework used to describe quantum control, in which the measurement device is explicitly treated as an effectively classical object). These cases can be successfully described by *effective* theories of classical-quantum interaction, with some particular breakdown scale or time, after which the quantum effects in the approximately classical system become important. The most common techniques are the mean-field approximation, or the truncated Wigner approach.

It is, however, when the classicality of the C subsystem is assumed to be fundamental that one needs to be extremely careful. We call systems in which such an assumption is taken *classical-quantum* (CQ) models. Historically, a number of no-go theorems have been disrupting the way towards a unified consistent framework of hybrid classical-quantum dynamics. The motivation towards the search of these models was originally gravitational physics itself: the geometric description of gravity provided by Einstein's theory of general relativity had proven to be somewhat resistent to a straightforward description in terms of quantum fields. It was then a natural question to ask whether a fundamentally classical spacetime interacting with quantum field could have been seriously considered as an alternative to a fundamentally quantum theory of gravity.

1.1.1 The failure of the mean-field equations

To see why consistent classical-quantum backreaction is problematic, consider the semiclassical Einstein's equations

$$G_{\mu\nu} = 8\pi G_N \langle T_{\mu\nu} \rangle \tag{1.1}$$

to be the evolution equations for the classical sector of a hybrid theory of classical gravity interacting with quantum fields. This was postulated by some of the first champions for fundamentally classical gravity (e.g. [12, 13]). However, argues Bryce DeWitt in a famous article [14], even if the quantum matter obeyed a Schrödinger equation of the form

$$i\frac{\partial|\psi\rangle}{\partial x^\mu} = \mathcal{H}_\mu(g_{\mu\nu})|\psi\rangle \ , \tag{1.2}$$

linearity in the quantum system would be violated by the expectation value of the stress-energy tensor in Equation 1.1, prohibiting quantum superpositions – a cornerstone of quantum mechanics. Non-linearities in the quantum evolution also allow for superluminal signalling [15].

Within the context of the semiclassical Einstein's equations, local changes to stress-energy tensor can be used to send information using entangled particles at space-like separated points. This is not a result of the gravitational theory nor does it depend on a specific quantum matter content – it is solely a feature of quantum evolution laws that are unitary but depend non-linearly on the state. In particular, this issue is not related to small violations of causality in low-energy effective field theory, that can be dealt with [16]. Of course, there is no a priori reason why the classical metric would have to satisfy the semiclassical Einstein's equations in a hybrid theory of gravity, nor the evolution of the quantum state be unitary – indeed it turns out that in CQ evolution one needs to give *both* up. DeWitt himself admits that there might exist a way to have a classical gravitational theory, and that a way to couple a classical metric to quantum fields existed has appeals of its own, possibly allowing for a solution to the measurement problem [14]. However, that the simplest approach to semiclassical gravity suffered of such a great pathology was a significant blow for the supporters of a fundamentally classical theory of gravitation.

1.1.2 No-go theorems for classical-quantum dynamics

The Chapel Hill conference set the community on the definite path towards quantum gravity [17]. As reported by the proceedings of the conference, Richard Feynman came up with a convincing gedanken experiments against the fundamental classicality of the gravitational field. Feynman originally imagined a thought Stern-Gerlach experiment involving a massive spin-1/2 particle, but we quickly present a modern reformulation by Aharonov [18] instead. Consider the classic double-slit experiment: the state of the fired electron is driven to a quantum superposition of having gone through the right and left slit, producing an interference pattern at the end-screen. If, the gravitational field is quantum-mechanical, then it becomes entangled with the trajectory of the electron that sources it, and no inconsistency arises. A classical field, however, can never be in a quantum superposition.

Something needs to be postulated about how the classical gravitational field reacts to the state of the electron. We know we need to exclude the case of a mean-field backreaction, i.e. Equation 1.1, not to incur in pathologies due to the non-linear nature of the hybrid evolution. The other natural option, postulated by Feynman, is that of a deterministic coupling – the

gravitational field knows about the objective position of the electron, and reacts to it. Said in another way, the classical gravitational field encodes the information about which slit the particle went through. Therefore, measuring gravitational forces with infinite accuracy (which would be allowed in principle, as the metric would be a classical object) allows one to infer which slit the electron goes through. That would obviously collapse any superposition and, therefore, the intereference pattern – which we instead observe. Note that, crucially, the act of actually measuring the gravitational field would be irrelevant: the fact that the information is encoded in a classical degree of freedom is enough to make the superposition collapse.

At first sight, it seems hard to argue against this reasoning. In fact, progress can be made by realising that, in this thought experiment, the gravitational field acts in all effect as a measurement device. More precisely, it performs a projective measurement of the state of the electron on the position basis. Then, as we will see, the way out is simply to make the gravitational field a "worse" measurement device: this makes the collapse of the quantum particle in the position basis slower, at the cost of adding uncertainty in the gravitational equations.

Other gedanken experiments that supposedly prove the quantumness of gravity have piled up over the years, the most famous of which were provided by DeWitt himself [19], Eppley and Hannah [20] and Caro (their arguments are however contentious, see [21]) and Salcedo [22]. The first two revolve around the idea that classical-quantum interaction inevitably leads to violation of the Heisenberg uncertainty principle. The latter shows that the most popular approaches at the time for a hybrid classical-quantum dynamics all suffer from some serious pathologies, from breaking of positivity to failing to recover the correct evolution equations in the limit of small coupling. All these rely on strong assumptions on what the hybrid dynamics has to look like and can be easily circumvented. In fact, over the years, many examples of hybrid consistent dynamics have been explicitly found, as we now see.

1.1.3 The first consistent hybrid evolution

Semiclassical equations in which the classical system simply reacts to the expectation values of quantum operators [23, 24] suffer from the critical problem of non-linearities that we have highlighted before, and can therefore be used solely as effective theories applicable when the

quantum system is "sharply peaked". In that sense, they can be seen as the semiclassical limit of the Hartree approximation in quantum mechanics.

A crucial shift in perspective towards consistent CQ dynamics was introduced in [25], where a hybrid density matrix $\varrho(z)$, i.e. a subnormalised operator-valued function on phase space, was first adopted as the state of a classical-quantum model. Nonetheless, the CQ Liouville equation, namely the first proposals for the evolution equations of such a state, failed to satisfy trivial positivity conditions on ϱ [23]. That is, a well normalised and positive probability distribution over the classical degrees of freedom evolved generically into a non-positive function over the classical state-space. This was the inevitable faith of all the linear, yet reversible, classical-quantum dynamics proposed throughout the years [26, 25, 27, 28, 29, 30]. Eventually, this technical problem was overcome, first for jumping dynamics in the classical degrees of freedom [31, 32] and later to models with continuous classical phase-space [33, 34]. The continuous dynamics was obtained by treating the semiclassical backreaction problem as a measurement-and-feedback dynamics, i.e. treating the classical variable as the outcome of a weak measurement on the quantum system, conditioned on which a specific unitary is applied to evolve the quantum state.

This theoretical result sparked new interest in hybrid dynamics, and in particular for the potential applications of these techniques to a consistent theory of fundamentally classical gravity [35, 36, 37, 38]. Hybrid gravity models can be seen as a natural completion of stochastic collapse models, theories proposed to explain the macroscopic emergent of classicality. In stochastic collapse models [39, 40, 41, 42], the quantum state spontaneously collapses in a specific basis with a fixed rate, a free parameter in these theories. The conceptual weakness of collapse models, other than the fine-tuning required to minimise energy production due to the spontaneous collapse [43, 44, 45, 46], is that the decoherence is added ad-hoc. The first theories of consistent hybrid gravity, though restricted only to the Newtonian regime, successfully bridged spontaneous collapse theories to the historical proposal that gravitational interaction could be the source of wavefunction collapse [14, 47, 48, 49].

The key property that emerged from these first consistent models of hybrid dynamics is the irreversibility of the evolution. This was later established to be an inescapable property of CQ dynamics [50, 51, 52], with the quantum subsystem undergoing decoherence and the classical

one having a stochastic evolution. We describe in detail recent advances in the characterisation of CQ models in Part I.

1.1.4 CQ gravity for quantum gravity tests

Although few challenge the fundamental quantum nature of the gravitational field, there is still no agreed-upon model of quantum gravity. Since the first attempts by Rosenfeld [53] and Bronstein [54], a wealth of alternatives has been put forward, each with their own degree of success. Whilst the quantisation of low-energy perturbations of the metric is well-understood – although the theory is non-renormalisable and therefore unpredictive at high energies [55] – all ultraviolet (UV) complete quantum theories of gravity still fall short of both experimental verification and creating consensus in the community. Moreover, no experiment yet has confirmed the quantum nature of the gravitational degrees of freedom – let alone any prediction of specific theories.

The last few years have seen a surge in proposals for model-independent low-energy signatures of quantum gravity. Current proposals include measuring gravitationally-induced entanglement [56, 57], quantum-induced noise in the gravitational field [58, 59] (which is, however, only expected to be measurable for highly squeezed states [60]) and others [61, 62, 63]. However, these proposed tabletop experiments still require some significant technological developments to reach the precision needed to observe these subtle effects [64]. As such, the recent precise characterisation of theories that describe *fundamentally classical* degrees of freedom interacting with quantum systems [50, 51] opens new interesting avenues to test the fundamental quantumness of the gravitational field.

As mentioned, a condition for hybrid theories to be consistent is that they necessarily need to allow for both decoherence of quantum states and stochasticity in the classical degrees of freedom [50, 51, 52], two effects that can produce observable phenomenology [65]. Crucially, the decoherence and diffusion coefficients of a CQ theory are not independent, but need to satisfy a relation known as the decoherence-diffusion trade-off [33, 65], implying that both effects cannot be made arbitrarily small. Since *any* theory of fundamentally classical gravity interacting with quantum matter must satisfy the decoherence-diffusion trade-off, measuring its violation (by experimentally bounding both decoherence and diffusion coefficients) is a simple way to test

indirectly the quantum nature of the gravitational field.

1.2 Effective semiclassical theories

When the classicality of a quantum degree of freedom is effective, consistency of the hybrid model at all scales and all times is not a necessity. In fact, as long as one is aware of the limitations of a model, alternative approaches to the full hybrid framework can be used, often offering the appealing prospect of a simpler analysis.

The two most common approximations, especially in the gravitational community, are the mean-field and "truncated Wigner" approaches. The semiclassical Einstein's equation fall neatly in the former: the classical system responds to the expectation value of some quantum observable. They correspond to the semiclassical limit of the Hartree approximation – i.e. the approach of treating the dynamics of a single subsystem as moving in the mean-field of the rest of the system, which is well-motivated for a large number of particles (or fields). That is, whenever the system of interest interacts with another whose fluctuations around the mean are negligible [66, 67, 68]. The "truncated Wigner" approximation, instead, treats the evolution of the classical system as an ensemble average over independent realisations evolved from initial conditions drawn from the initial, classical-like, Wigner distribution [69]. Although the evolution map is non-positive [70], it is extremely popular in cosmology [71, 72] and condensed matter systems [73, 74]. Both of these methods successfully capture aspects of the quantum dynamics up to some quantum breakdown time, when quantum effects in the effectively classical system are no longer negligible [75, 76, 77].

The CQ formalism itself, involving both diffusion and decoherence, can be derived from the partial classical limit of a bipartite quantum system [78]. However, when used as an effective theory, the decoherence-diffusion trade-off needs not to be satisfied, and the dynamics might be non-positive in general. In these cases, the decoherence or diffusion effects can appear as subleading effects, providing only marginal improvements to other simpler approximations.

1.2.1 Semiclassical Einstein's equations

In quantum gravity research, the semiclassical Einstein's equations have long been used as the main tool to assess the backreaction effect of the quantumness in the matter degrees of freedom on an effectively classical geometry. The validity of the solution is restricted to regions of spacetime whose local radius of curvature is far above the Planck length L_P [79] and for quantum states of matter whose averaged stress-energy tensor has small fluctuations with respect to its mean [66]. As an effective theory, there have been proposals to go beyond the semiclassical equations themselves. The most relevant one, which shares certain features with the CQ formalism, is Bei Lok Hu's stochastic gravity (SG) [80]. There, the semiclassical Einstein's equations are supplemented with a stochastic driving force, which is intended to model the fluctuations around the mean of the expected stress-energy tensor. This is the first main difference with CQ gravity, where, for the evolution to be consistent, the noise kernel cannot depend on the quantum state of the matter. Secondly, the evolution of the quantum sector is still the standard unitary quantum field theory in curved spacetime – there is no decoherence in the quantum degrees of freedom. As such, SG suffers from the same issue of non-linearity as the standard semiclassical gravitational equations. Another key difference between SG and CQ gravity is the origin of the noise process. In SG, the stochasticity is effective, coming from the integration of some "fast" microscopic degrees of freedom – as standard [81]. Generally, such a procedure does not produce a Markovian dynamics, with memory kernels appearing in the reduced equations of motion. Still, at weak coupling with the bath, such stochastic equations are well approximated by the memoryless, time-local, form if there is a clear-cut separation of scale [82]. Further, as we explain in the next section, the effective nature of the noise term implies, naturally, a distinct definition of the stochastic differential equations modelling the dynamics with respect to the one representing the fundamental noise in CQ.

Nonwithstanding their popularity, the interpretation of the semiclassical Einstein's equation is contentious. Taken at face value, they caused the worst prediction in physics – popularly known as the cosmological constant problem [83]. Indeed, were the full divergent vacuum stress tensor to backreact on a semiclassical geometry, it would correspond to a vastly larger cosmological constant than observed (irrespective of whether one uses as cutoff for the quantum fluctuations the Planck scale or the QCD scale, and of supersymmetric cancellations between

bosonic and fermionic loops [84]). Today, we understand that it is the *renormalised* stress tensor that backreacts on the geometry [85, 86, 87, 88], with the vacuum fluctuations being subtracted off. Other loop effects such as vacuum polarisation can still potentially backreact and contribute to an effective cosmological constant [84].

One of the main sources of interests on the semiclassical Einstein's equation has been the observation that, in general, the expectation value of the quantum stress tensor does not satisfy the usual positive energy conditions [89] which sits at the base of a wealth of classic GR results. Violation of positive-energy conditions allow for the construction of exotic gravitational solutions, like traversable wormholes and closed timelike curves. A weaker version of the null-energy condition, the *averaged* null energy condition, is itself violated [90] in curved space. Nevertheless, other generalisations hold, such as the achronal averaged null-energy condition [91], forbidding these exotic solutions. Moreover, taking quantum backreaction into the picture suggests that any violation of the averaged null-energy condition by the quantum stress-tensor are at most Planckian in size [79].

Solving the semiclassical Einstein's equations themselves is a great challenge. Explicit, exact self-consistent solutions have been found for highly symmetric cases (e.g. when the fields possess conformal invariance and the matter stress tensor is fully determined by the conformal anomaly [92, 93, 94]). For more general settings, the perturbative approach is required [95, 96, 97], in which one iteratively solves for corrections to both the classical geometry and the quantum correlations sourcing it. Fortunately, a novel, powerful techniques has been recently uncovered to extract *exact* solutions to the semiclassical Einstein's equations – braneworld holography.

1.2.2 Braneworld holography and quantum backreaction

Braneworld models were historically introduced as a possible solution to the hierarchy problem [98, 99]. They treat the four-dimensional world we experience as a (mem)brane sitting in a spacetime with large extra-dimensions. Although over the years their phenomenological appeal faded due to experimental constraints on the size of these "large" extra dimensions [100], the discovery of the AdS/CFT correspondence [101] has opened the doors to new applications of these models.

Born out of studies in string theory, AdS/CFT is a non-perturbative candidate model of quantum gravity, where gravitational physics in a bulk $d+1$-dimensional asymptotically AdS spacetime has a dual description in terms of a CFT living on the d-dimensional conformal boundary of AdS. This duality is therefore a concrete realization of gravitational holography [102, 103]. More specifically, in a large-N expansion, the planar diagram limit of the CFT, the bulk is well-approximated by classical gravity. A powerful feature of the AdS/CFT correspondence is strong-weak coupling duality: coupling constants between the bulk and boundary theories are inversely related, $G_N \sim N^{-1}$. Thus, computations of strongly coupled field theories may instead be performed via a classical gravity calculation. While the boundary geometry on which the CFT lives may be curved (and even contain black holes [104]), it is fixed. Consequently, standard AdS/CFT holography alone is insufficient for addressing the problem of semi-classical backreaction.

It is when combined with braneworlds that holography functions as a useful toolkit to address difficult problems in semi-classical gravity. In this framework, AdS/CFT duality is adapted to incorporate situations where a portion of the bulk, including its boundary, is removed by a d-dimensional Randall-Sundrum [105, 99] or Karch-Randall [106, 107] braneworld. Crucially, the geometry of the end-of-the-world (ETW) brane is dynamical, having an induced theory of gravity. More precisely, the brane serves as an infrared cutoff in the bulk, translating to a ultraviolet cutoff for the holographic CFT. As in holographic renormalization [108, 109, 110, 111, 112], a tower of higher-derivative corrections to the d-dimensional Einstein-Hilbert action are induced by the holographic cutoff CFT_d. From the brane perspective, the induced theory may thus be interpreted as a semi-classical theory of gravity [113], where the higher-derivative corrections incorporate backreaction effects due to the CFT living on the brane. By the AdS/CFT correspondence, the induced metric on the brane is guaranteed to solve the higher-curvature semiclassical Einstein's equations:

$$G_{ij} + \Lambda_d g_{ij} + (\text{higher-curvature}) = 8\pi G_d \langle T_{ij}^{\text{CFT}} \rangle_{\text{planar}} \ , \tag{1.3}$$

Here Λ_d and G_d are induced cosmological and Newton constants on the brane, and the right-hand side indicates the holographic CFT is in its planar limit. This is the focus of Part II of the thesis, where we describe a specific holographic construction in 3+1-dimensions that computes a novel solution to the semiclassical gravitational equations – a quantum-corrected rotating de

Sitter black hole in 2+1-dimensions.

1.3 Structure of the thesis

The thesis treats two different approaches to the quantum backreaction problem on (semi)-classical systems, with an interest towards gravitational physics. As such, it is divided in two main parts, plus some final remarks in Part III bridging the two main topics of discussion.

1.3.1 Classical-quantum gravity

Part I concerns quantum backreaction on *fundamentally* classical systems, and contains Chapters 2 to 5.

In Chapter 2 we review the most general form of self-consistent classical-quantum dynamics. We begin with a quick summary of the main ideas in the theory of stochastic processes and open quantum systems, in all of their three equivalent descriptions: master equation, unravelling in terms of trajectories and path integrals. They will be important to understand the main features of hybrid CQ dynamics. We then proceed to introduce the most general form of Markovian, self-consistent, hybrid dynamics – again in all of its three equivalent representations.

Chapter 3 is the first result section of the thesis. Here, we solve a simple toy model of hybrid classical-quantum dynamics: two interacting harmonic oscillators, one quantum and the other classical, with the latter experiencing friction. By mapping the problem exactly to a classical Ornstein–Uhlenbeck process, we show that the hybrid system reaches a steady state for any value of the couplings. We then compute its properties, such as correlations, response to external perturbations and occupation in the quantum system. Crucially, we show that the combined state becomes thermal when the diffusion in the classical sector is large. We also perform the Wigner-Moyal transform of the hybrid dynamics, deriving the phase-space representation of CQ evolution. This chapter is based on yet unpublished work [1].

The next two chapters focus on the phenomenology of the classical sector of a potential CQ theory of gravity. In Chapter 4, we consider the evolution of a classical field in a hybrid Yukawa model. We begin by reviewing the classical thermal Klein-Gordon (KG) field, the steady-state of a damped stochastic KG evolution. Then, we move on to the non-equilibrium random

system, We describe how to compute the non-equilibrium two point function of the scalar field, showing explicitly the role of the initial state in regulating divergences. In particular, we use a "mod-squared-retarded" pole-prescription to find that the covariance in the field is non-zero only outside the lightcone, scales inversely with the spatial distance of the spacetime points and grows linearly in time. We show how these results map to the thermal state correlations. We conclude by discussing the implications for hybrid theories of gravity, in particular regarding energy production and the induced brownian motion on test particles due to the fluctuations generated in the classical field. This chapter is based on currently unplublished work with Jonathan Oppenheim [2]

Chapter 5 presents a stochastic model of cosmology motivated by CQ gravity. In particular, on comsological scales, the quantum matter can be taken to be decohered on classical-like states. However, the decoherence-diffusion trade-off is independent on the state of the quantum, meaning that the classical degree of freedom – in this case the cosmological scale factor – would still experience stochastic fluctuations. We investigate what that would imply in a homogeneous and isotropic model of cosmology – the Friedmann-Leimatre-Robertson-Walker Universe. We find that the stochastic evolution results in the spatial metric diffusing away from its deterministic value, generating phantom cold dark matter (CDM). This is produced primarily at the end of the inflationary phase of the Universe's evolution, with a statistical distribution that depends on the specifics of the early-times cosmological model. We find the energy density of this phantom cold dark matter is positive on average, a necessary condition to reproduce the cosmological phenomenology of CDM, although further work is required to calculate its mean density and spatial distribution. If the density is cosmologically significant, phantom dark matter acts on the geometry in a way that is indistinguishable from conventional CDM. As such, it has the potential to reproduce phenomenology such as structure formation, lensing, and galactic rotation curves. We conclude by discussing the possibility of testing hybrid theories of gravity by combining measurements of the Cosmic Microwave Background with tabletop experiments. This section is based on work done in collaboration with Jonathan Oppenheim and Andrew Pontzen [3].

1.3.2 Quantum-corrected black holes

Part II of the thesis contains Chapters 6 and 7 where we discuss how to use braneworld holography to exactly solve the backreaction problem on an *effectively* classical geometry.

We begin in Chapter 6, where we introduce and motivate the braneworld holography approach to semiclassical gravity. After having summarised briefly the main ideas needed from the standard AdS/CFT correspondence, we derive the equations of motion for the induced metric on a dynamical brane in AdS, showing that – under the holographic principle – they solve a higher-order theory of semiclassical gravity. We follow by discussing a perturbative calculation to compute the semiclassical backreaction of a conformally coupled quantum scalar onto the rotating (2+1)-dimensional Kerr-de Sitter spacetime, a GR solution of lower-dimensional gravity that presents a naked conical singularity. We present the limitations of the standard perturbative calculation, but highlight the suggestive result that quantum backreaction sets up a Planckian-sized event horizon hiding the naked singularity – saving cosmic censorship. This section is based on a review on the topic of braneworld holography written in collaboration with Juan Pedraza and Andrew Svesko [4] with the perturbative calculations based on work with Andrew Svesko [5].

In Chapter 7 we construct an explicit, novel, solution to the semiclassical Einstein's equation in 2+1 dimensions by means of braneworld holography – the quantum-corrected Kerr-de Sitter black hole. The quantum Kerr black hole shares many qualitative features with the classical four-dimensional Kerr-de Sitter solution. Of note, backreaction induces inner and outer black hole horizons which hide a ring singularity. Moreover, the quantum-corrected geometry has extremal, Nariai, and ultracold limits, which appear as fibered products of a circle and two-dimensional anti-de Sitter, de Sitter, and Minkowski space, respectively. The thermodynamics of the classical bulk black hole, described by the rotating four-dimensional anti-de Sitter C-metric, has an interpretation on the brane as thermodynamics of the quantum black hole, obeying a semi-classical first law where the Bekenstein-Hawking area entropy is replaced by the generalized entropy. We conclude by comparing the exact solution of the higher-curvature theory with the perturbative results derived from the semiclassical Einstein's equations. This chapter is based on work done in collaboration with Andrew Svesko [5].

Conventions

Unless explicitly stated, we use the mostly positive convention for the Minkowski metric $(-,+,+,+)$. We also take $\hbar = c = k_B = 1$.

Part I

Classical-Quantum dynamics

Chapter 2

Consistent classical-quantum dynamics

We now present the general classical-quantum (CQ) framework to describe consistent coupling of classical and quantum degrees of freedom. First, we summarise the main concepts in classical stochastic dynamics and open quantum system. Then, we merge these two frameworks and discuss the most general form of CQ dynamics. In all cases, we describe three equivalent representations of the dynamics: master equation, unravelling and path integral.

2.1 Stochastic classical dynamics

We denote a (deterministic or stochastic) classical degree of freedom by $z \in \mathcal{M}$, where $\mathcal{M}$ is the m-dimensional space of physical states. In most occasions, we take $\mathcal{M}$ to be the canonical phase-space, with the coordinates chosen to represent $m/2$ positions and their conjugate momenta. We refer to a realised trajectory through $\mathcal{M}$ via $z = Z_t$.

Contrary to deterministic physics, in which one can compute the unique trajectory of the classical degree of freedom in state space given the initial condition and the physical law, in stochastic dynamics the best we can do is to predict the evolution of the probability density $p(z,t)$ over state space, or, equivalently, the probability of a given trajectory Z_t being realised.

Probability density and its evolution

The probability density is a positive, normalised, scalar density, i.e.:

$$p(z,t) \geq 0 \ , \qquad \int_{\mathcal{M}} \mathrm{d}z \ p(z,t) = 1 \ . \tag{2.1}$$

It encodes the probability of finding the classical degree of freedom within the infinitesimal volume $\mathrm{d}^m z$ in state space at time t. It can also be used to compute the expectation value with respect to the ensemble of any function $\mathcal{O}(z)$ of the stochastic degrees of freedom by integration over state space:

$$\mathbb{E}[\mathcal{O}_t] = \int_{\mathcal{M}} \mathrm{d}z \ \mathcal{O}(z) p(z,t) \ . \tag{2.2}$$

The evolution map for probability distribution needs to satisfy some basic properties, irrespective of the physical model it is supposed to describe. Indeed, consider an operator that takes a probability distribution at time $t = 0$ and computes its future state at time t:

$$p(z,t) = \mathcal{L}_t[p(z,0)] \ . \tag{2.3}$$

Requiring that the final state $p(z,t)$ is a valid probability distribution imposes clear restrictions on the form of the map. Indeed, it needs to be linear, positive and norm-preserving. The latter two conditions are obvious from the definition of a probability distribution. The first one comes from the observation that the set of valid probability distributions is convex, meaning that for any $0 \leq \theta \leq 1$ we can decompose $p(z,t)$ as:

$$p(z,t) = \theta p_1(z,t) + (1-\theta) p_2(z,t) \ , \tag{2.4}$$

with $p_{1,2}$ being two other probability distributions. Requiring that the map preserves this decomposition imposes that $\mathcal{L}$ must be a linear operator.

These three requirements are themselves not restrictive enough to fully characterise the most general form of valid evolution operators acting on probability distributions. Yet, a simple assumption simplifies the matter greatly – Markovianity. A stochastic dynamics is Markovian if it is time-local, or memoryless. That is, information about the system in the past is irrelevant if one knows already the current probability distribution. Markovianity is a strong assumption: most effective stochastic systems do have memory [82]. Yet, as long as one coarse grains on time-scales large enough with respect to the memory timescales, the Markovian approximation

is effective and simplifies greatly the description of the system. Moreover, it might be a natural expectation for any fundamental stochastic theory – CQ gravity falls necessarily in this category, as we will shortly see – to be Markovian. This is the nature of the laws of physics that have been so successful in describing fundamental interactions so far – both in QFT and GR it suffices to know the current state to predict future ones. In fact, any Hamiltonian theory is by construction time-local. It does not seem a stretch to require such a property to be retained, even when we relieve the dynamics from fundamental determinism. For these reasons, and for the sake of simplicity, we solely restrict to memoryless dynamics in this thesis.

Requiring $\mathcal{L}$ to be Markovian, linear, positive, norm-preserving and time-local yields to the following partial differential equation as the unique evolution equation for a probability density:

$$\frac{\partial p(z,t)}{\partial t} = \sum_{n=1}^{n=\infty} \frac{(-1)^n}{n!} \frac{\partial^n}{\partial z_{i_1} ... \partial z_{i_n}} [D_{n,i_1,...,i_n} p(z,t)] \ . \tag{2.5}$$

Here, D_n are the Kramers-Moyal coefficients defined in terms of the central moments of the infinitesimal transition probability function. That is, expanding the infinitesimal Markovian conditional distribution as:

$$p(z,t|z',t-\delta t) = \delta(z,z') + W(z|z')\delta t + \mathcal{O}(\delta t^2) \ , \tag{2.6}$$

the Kramers-Moyal coefficients are defined as

$$D(z')_{n,i_1...i_n} = \int_{\mathcal{M}} \mathrm{d}z \ W(z|z')(z-z')_{i_1} ... (z-z')_{i_n} \ . \tag{2.7}$$

Note that different conventions exist with respect to the factor of $n!$. The moments of the Kramers-Moyal expansion fully characterise the evolution of a Markovian process via Equation 2.5, known as the Kolgomorov forward equation.

Positivity enforces an important requirement on the Kramers-Moyal coefficients. Indeed, the Pawula theorem [114] states that the derivative expansion of the Kolgomorov forward equation can truncate only at 1st or 2nd order. If any of the D_n with $n > 2$ is non-zero, then the whole tower of moments is non-vanishing and the higher derivative terms have to be kept into account. The latter is the case for jumping processes. Drift-only processes, i.e. deterministic processes which might have uncertainty in the initial state, but not in the evolution, truncate at 1st order. Those that truncate at 2nd order are diffusive processes, i.e. stochastic systems with continuous

trajectories in phase space. For the latter family of systems, the forward Kolgomorov equation is commonly known as the *Fokker-Planck equation*:

$$\frac{\partial p(z,t)}{\partial t} = -\frac{\partial}{\partial z_i}[D_{1,i}\ p(z,t)] + \frac{1}{2}\frac{\partial^2}{\partial z_i \partial z_j}[D_{2,ij}\ p(z,t)]\ , \tag{2.8}$$

where Einstein's summation convention is understood and D_1 is called the drift vector, controlling the average force on each of the degrees of freedom of the system, whilst the positive semi-definite $D_{2,ij}$ is known as the diffusion matrix and encodes the correlation in the stochastic random kicks. Note that the adjective "vector" to D_1 is a misnomen – it is a pseudovector under coordinate transformation on state space. Yet, it is possible to repackage the Fokker-Planck equation in a covariant manner [115].

When the deterministic part of the dynamics is taken to derive from some classical Hamiltonian H_C, the Fokker-Planck equation can be written as:

$$\frac{\partial p(z,t)}{\partial t} = \{H_C, p(z,t)\} + \frac{1}{2}\frac{\partial^2}{\partial z_i \partial z_j}[D_{2,ij}\ p(z,t)]\ , \tag{2.9}$$

where for $D_2 = 0$ we recover the standard Liouville equation evolving the initial uncertainty over the state of a deterministic Hamiltonian system. Here, $\{\cdot,\cdot\}$ are the standard Poisson brackets.

Trajectories

Sometimes, we desire to understand the property of specific realisations, or trajectories, of the classical stochastic system in state space. These two pictures are obviously equivalent: given all the allowed trajectories Z_t of the stochastic dynamics with their associated probabilities, the probability distribution $p(z,t)$ is just the expectation value over all realisations of the trajectory passing through the point z at time t:

$$p(z,t) = \mathbb{E}[\delta(z - Z_t)]\ . \tag{2.10}$$

The evolution of any continuous stochastic variable can be therefore equivalently described in terms of stochastic differential equations (SDEs). For a continuous Markovian process Z_t, the evolution equation is given by

$$\mathrm{d}Z_t^i = \mu^i(Z_t,t)\mathrm{d}t + \sigma_k^i(Z_t,t)\mathrm{d}W_t^k\ , \tag{2.11}$$

where μ and σ determine the deterministic and stochastic forces respectively, whilst $\mathrm{d}W_t^i$ is a vector of independent Wiener increments. A Wiener process is an almost surely continuous stochastic process with Gaussian increments distributed as:

$$\Delta W = W_t - W_t' \sim \mathcal{N}(0, t - t') \ , \tag{2.12}$$

i.e. with vanishing mean and variance Δt, with $\mathrm{d}W_t$ being defined as the infinitesimal limit of the increment. W_t is also often called "Brownian motion" in the mathematics literature, but we will reserve that characterisation for the dynamics of a particle experiencing a random white noise force – i.e. a Wiener process specifically in momentum. It is useful to think of $\mathrm{d}W_t$ as order $\sqrt{\mathrm{d}t}$, with Itô's lemma making this precise [116]. For the results in this thesis, it is sufficient to know that the Wiener increments satisfy Itô's rules:

$$\mathrm{d}W_t^i \mathrm{d}W_t^j = \mathrm{d}t \ \delta^{ij} \ , \qquad \mathrm{d}W_t^i \mathrm{d}t = 0 \ . \tag{2.13}$$

and that their expectation value is zero. Often, in the physics literature Equation 2.11 is represented as:

$$\dot{Z} = \mu + \sigma \xi(t) \ , \tag{2.14}$$

where $\xi \sim \mathrm{d}W/\mathrm{d}t$ is a δ-correlated white noise process. Equation 2.14 is commonly referred to as a *Langevin equation*. When it comes to Langevin equations, however, their interpretation is not unique. This comes from the fact that, unlike Riemann integrals, stochastic integrals give different results for different discretisations. That is, the definition of Riemann integrals

$$\int_0^t f \mathrm{d}t = \lim_{n \to \infty} \sum_{[t_{i+1}, t_i] \in \pi_n} f(\alpha Z_{t_i} + (1 - \alpha) Z_{t_{i+1}})(t_{i+1} - t_i) \ , \tag{2.15}$$

where π_n is a sequence of partition of $[0, t]$ with mesh going to zero, gives the same interpretation of the integral for every $\alpha \in [0, 1]$ as $\delta t \to 0$. In contrast, a stochastic integral defined similarly as:

$$\int_0^t f \mathrm{d}W_t = \lim_{n \to \infty} \sum_{[t_{i+1}, t_i] \in \pi_n} f(\alpha Z_{t_i} + (1 - \alpha) Z_{t_{i+1}})(W_{i+1} - W_i) \ , \tag{2.16}$$

gives different results for different choices of α. Choosing $\alpha = 0$, the update of the state Z_t from t to $t + \Delta t$ is given by:

$$Z_{t+\Delta t} = Z_t + \mu(Z_t)\Delta t + \sigma(Z_t)\Delta W_t \ . \tag{2.17}$$

This is known as Itô integration. It is non-anticipative (i.e. the increment is evaluated with information of the functions μ and σ at the current time-step only) and it is easier to handle numerically, but it does not obey the standard chain rule. Instead, the total derivative of a function of a stochastic variable Z_t obeys Itô's lemma instead:

$$\mathrm{d}f(Z_t,t) = \left(\frac{\partial f}{\partial t} + \frac{\partial f}{\partial z}\mu\right)\mathrm{d}t + \frac{\partial f}{\partial z}\sigma \mathrm{d}W_t + \frac{1}{2}\frac{\partial^2 f}{\partial z^2}\sigma^2 \mathrm{d}t \ . \tag{2.18}$$

The usual interpretation of the extra $\mathrm{d}t$ term appearing in the formula for the total derivative relies on the intuition, mentioned earlier, that the Wiener process is of fractional order in time. In particular, $\mathrm{d}W_t^2 \sim \mathrm{d}t$. All the stochastic equations in this thesis will be assumed to be in Itô sense, unless otherwise stated. Itô's lemma will be at the basis of key results in Chapters 4 and 5. The non-anticipative nature of the integration makes Itô's SDEs the natural choice to define a fundamentally stochastic theory – to compute the next timestep it suffices to know the current state and the stochastic increment.

On the other hand, $\alpha = 1/2$ leads to:

$$\Delta Z_t = f\left(\frac{Z_t + Z_{t+\Delta t}}{2}\right)\Delta t + \sigma\left(\frac{Z_t + Z_{t+\Delta t}}{2}\right)\Delta W_t \ . \tag{2.19}$$

This choice is known as Stratonovich interpretation and does respect the usual chain rule, but the background noise is anticipative, meaning that $\mathbb{E}[f(Z)\mathrm{d}W_t] \neq 0$ in general. The Stratonovich definition appears naturally when deriving stochastic differential equations through coarse-graining. Indeed, when the stochastic force comes from the elimination of some fast degrees of freedom, it is natural to expect the force acting in a time-step Δt to be the result of the time-average of the forces acting on the system of interest over the coarse-graining timescale. This is precisely the physical interpretation of the $\alpha = 1/2$ choice – reason why it is commonly used in effective random systems where the noise models the interaction with some microscopic environment [117].

Whilst the same SDE yields different probability distributions for the final state whether it is intended in the Stratonovich or Itô sense, it is always possible to transform any Itô SDE into a Stratonovich one, and vice-versa [117]. Specifically, the process described by the following SDE

$$\mathrm{d}Z^i = \mu(Z)^i \mathrm{d}t + \sigma(z)^i_j \mathrm{d}W_t^j \ , \tag{2.20}$$

(where "∘" indicates that the stochastic increment is of Stratonovich type) can be equivalently be described by the following Itô process

$$\mathrm{d}Z^i = \left(\mu(Z)^i + \delta\mu(Z)^i\right)\mathrm{d}t + \sigma(z)^i_j \mathrm{d}W^j_t \ , \tag{2.21}$$

where the Itô correction amounts to

$$\delta\mu(Z)^i \equiv \frac{\sigma^j_k}{2}\frac{\partial\sigma^i_j}{\partial Z^k} \ . \tag{2.22}$$

Generally, when one is to simulate a Stratonovich process, it is convenient to map it to an Itô SDE like so, and then deploy a simple forward Euler-Maruyama scheme [118].

Given an SDE, there exists a unique Fokker-Planck equation describing the evolution of the probability distribution of the process. When expressed in Itô sense, we can read off the Fokker-Planck drift and diffusion coefficient as:

$$D^i_1 = \mu^i \ , \qquad D^{ij}_2 = \frac{1}{2}(\sigma\sigma^T)^{ij} \ . \tag{2.23}$$

OM and MSR path integrals

There exists a third, equivalent, representation of stochastic processes in terms of functional integration. In particular, given an initial probability distribution $p_0(z)$, the final state can be computed in terms of the following functional integral:

$$p(z', T) = \int^{z(T)=z'} \mathcal{D}z \int \mathcal{D}\tilde{z}\ \mathcal{N} e^{-S_{MSR}[z,\tilde{z}]} p_0(z), \tag{2.24}$$

where z is the vector state of the system as before, whilst $\tilde{z}$ is a vector of equal dimensions encoding the purely imaginary *response variables* and $\mathcal{N}$ ensures the appropriate normalisation. This formalism is known as the Martin-Siggia-Rose (MSR) [119] formalism with the action representing the Itô process in Equation 2.11 given by:

$$S_{MSR}[z,\tilde{z}] = \int_{t_0}^{T} dt \left[\tilde{z}^T\left(\partial_t z - D_1\right) - \frac{1}{2} z^T D_2 \tilde{z}\right] \ . \tag{2.25}$$

As usual, the expectation value of any observable $\mathcal{O}_i$ at time $t_0 \leq t_i \leq T$ can be computed by insertion in the path integral:

$$\mathbb{E}[\prod_i \mathcal{O}_i(t_i)] = \int \mathcal{D}z \int \mathcal{D}\tilde{z}\ \mathcal{N} e^{-S_{MSR}[z,\tilde{z}]} \prod_i \mathcal{O}_i(t_i) p_0(z) \ . \tag{2.26}$$

From here, it is explicit why the variables $\tilde{z}$ are known as response variables. Indeed, imagine that the system is pertubed with a delta-impulse I at t_0. This amounts to a perturbed action:

$$S_{MSR} \to S_{MSR} + \tilde{z}^T I \delta(t - t_0) z \ . \tag{2.27}$$

If the impulse I is "small", the action can be Taylor expanded. To first order, this corresponds to the original path integral with an extra $\tilde{z}(t_0)$ overall – meaning that $\mathbb{E}[\tilde{z}(t_0)\mathcal{O}]$ computes the change in the observable $\mathcal{O}$ *given* a small perturbation at t_0 to the system.

The MSR path integral is useful in many settings – it is particularly apt to perturbation theory and shares a similar structure to the quantum path integral approach for open quantum systems that we describe in the next section. It is therefore the formalism we adopt throughout, in particular in Chapters 3 and 4. Still, it is in principle possible to integrate out the quadratic response variables. The resulting path integral, known as Onsager-Machlup [120], is commonly used in the theory of large deviations [121].

2.2 Open quantum systems

The next section is dedicated to a quick review of the theory of open quantum systems – quantum mechanics beyond unitary evolution.

The quantum state as a density matrix

The most general quantum state, which supports both classical and quantum correlations, is not a ray in some Hilbert space $\mathcal{H}$, but rather a density matrix $\hat{\rho}$. A density matrix is a positive, Hermitian and normalised (with respect to the trace) operator on $\mathcal{H}$ representing the state of the system. Given an operator $\hat{O}$ on $\mathcal{H}$, we can use the density matrix to evaluate its expectation value (we drop hats from now on):

$$\langle O \rangle = \mathrm{Tr}[O\rho] = \sum_i \langle i|O\rho|i\rangle \ , \tag{2.28}$$

where the sum is over all the basis states chosen for $\mathcal{H}$.

The advantage of dealing with density operators is that they allow us to consider not only pure states, for which $\rho = |\psi\rangle\langle\psi|$, but also mixed states. Mixed states are quantum states with

classical uncertainty. That is, if we have probability p_i of finding ourselves on the pure state $|\psi_i\rangle$, the state is described by the following mixed density matrix:

$$\rho = \sum_i p_i |\psi_i\rangle\langle\psi_i| \ . \tag{2.29}$$

Whilst both pure and quantum states are unit trace, as classical probabilities must sum to one, the trace of ρ^2 tells the two families of states apart. In particular:

- $\mathrm{Tr}[\rho^2] = 1$ for pure states,
- $\mathrm{Tr}[\rho^2] < 1$ for mixed states.

In unitary quantum theory, mixed states arise naturally when one considers bipartite quantum systems, i.e. quantum systems whose Hilbert space can be split into two factors, $\mathcal{H}_A$ and $\mathcal{H}_E$ for the system A and E respectively. When tracing out the environment E, a general quantum state on the combined systems produces a mixed state on the Hilbert space A. Specifically, any time there exists entanglement between the system and the environment, the tracing operation deletes the quantum correlations between E and A, yielding a mixed state. It is straightforward to see this by considering the simple example of a Bell state between E and A

$$|\Psi\rangle = \frac{1}{\sqrt{2}}(|0\rangle_A|0\rangle_E + |1\rangle_A|1\rangle_E) \ , \tag{2.30}$$

which, after the partial trace over the environment, produces the maximally mixed state

$$\rho_A = \mathrm{Tr}_E(|\Psi\rangle\langle\Psi|) = \mathbf{1}_A \ . \tag{2.31}$$

The GKSL equation

In unitary quantum mechanics, the density matrix obeys the quantum Liouville equation:

$$\partial_t \rho = -i[H, \rho] \ . \tag{2.32}$$

Yet, this is not the most general form of dynamics that preserves the quantum state. The evolution map preserving the density matrix can be in principle non-unitaty, as long as it satisfies some key requirements. In general, when viewed as a map acting on density operators, the evolution has to be a CPTP (completely positive and trace preserving) map – a *quantum channel*. Quantum channels $\Phi(\cdot)$ are:

1. linear: $\Phi(\lambda\rho_1 + (1-\lambda)\rho_2) = \lambda\Phi(\rho_1) + (1-\lambda)\Phi(\rho_2)$,

2. hermiticity preserving, meaning that $\rho = \rho^\dagger \implies \Phi(\rho) = \Phi(\rho)^\dagger$,

3. trace preserving: $\mathrm{Tr}[\rho] = \mathrm{Tr}[\Phi(\rho)]$,

4. completely positive: for any auxiliary Hilbert space $\mathcal{H}_A$, $\rho \geq 0 \implies \Phi \otimes \mathbf{1}_{\mathcal{H}_A}(\rho) \geq 0$.

Linearity and trace preservation (TP) are necessary in order to retain the statistical interpretation of the density matrix, whilst complete positivity (CP) is required in order for the evolution to give positive probabilities even when it acts only on part of a larger system. Kraus theorem states that any quantum channel can be rewritten as:

$$\Phi(\rho) = \sum_{\alpha\beta} \Lambda^{\alpha\beta} K_\alpha \rho K_\beta^\dagger \ , \tag{2.33}$$

where $\Lambda^{\alpha\beta}$ is a positive Hermitian matrix, whilst K_α are called the *Kraus operators* and can always be taken to describe an orthogonal set of operators on the Hilbert space. Trace preservation implies:

$$\sum_{\alpha\beta} \Lambda^{\alpha\beta} K_\beta^\dagger K_\alpha = \mathbf{1} \ . \tag{2.34}$$

With stochastic dynamics, much can be said on the form of the generator if one introduces the assumption of time-locality. In the same spirit, we focus on Markovian open quantum systems, i.e. systems for which the CTPT maps only takes the current state at t to evaluate the state at $t + \delta t$. A map is then time-local if:

$$\dot{\rho}_t = \mathcal{L}(\rho_t) \ . \tag{2.35}$$

It is an important result that any quantum channel with these properties can, via the appropriate choice of Kraus operators, be written in the following form:

$$\frac{\partial \rho}{\partial t} = -i[H, \rho] + \lambda^{\alpha\beta} \left(L_\alpha \rho L_\beta^\dagger - \frac{1}{2}\{L_\beta^\dagger L_\alpha, \rho\}_+ \right) \ , \tag{2.36}$$

where $\{\cdot,\cdot\}_+$ represents the anticommutator (to avoid confusion with the Poisson bracket $\{\cdot,\cdot\}$) and $\lambda^{\alpha\beta}$ is a positive semi-definite matrix, with no additional requirement imposed on the *Lindblad operators* L_α. Here, the Lindblad operators are the leading order correction away

from the identity to the Kraus operators up to order δt, i.e. they can be expressed, without loss of generality, as

$$K_0 = \mathbf{1} - L_0 \delta t \ , \qquad K_{\alpha \neq 0} = \sqrt{\delta t} L_\alpha \ . \tag{2.37}$$

Note that, to satisfy the normalisation condition of the Kraus operators to linear order in δt, the following must be true:

$$L_0 = iH + \frac{1}{2} \sum_{\alpha \neq 0} L_\alpha^\dagger L_\alpha \tag{2.38}$$

where H is some Hermitian operator which is to be matched to the generator of the unitary evolution of the system – hence the Liouville-like term in Equation 2.36.

Equation 2.36 is commonly known as the Gorini–Kossakowski–Sudarshan–Lindblad (GKSL) equation, or simply as the Lindblad equation. When $\lambda^{\alpha\beta} = 0$ we recover the von Neumann equations, the quantum version of the Liouville equation, corresponding to unitary dynamics. Whilst the GKSL equation can be assumed as the fundamental law for a non-unitary quantum system, it can be also be shown, under certain assumptions, to be the evolution of a system in contact with a bath when the combined evolution is unitary and the environment is traced out. From this, the name "open quantum systems" is often used to describe the family of systems undergoing Lindbladian evolution. More generally, any Lindblad evolution can be embedded in a larger, unitary system [122]. This is known as dilation, or *purification*.

In Lindbladian evolution, pure states tend to evolve into mixed state, a process known as *decoherence*. That is, quantum states evolve into statistical mixture of pure states. From the point of view of the total system (or purifying system), the system of interest gets entangled with the bath degrees of freedom via the unitary dynamics, but the tracing out of E destroys the quantum correlation, leaving us with a mixed state. From the point of view of the GKSL equation, this is done by the Lindblad operators, which act to suppress the off-diagonal terms in the density matrix. To see that this is the case, consider the Lindblad equation with a single Hermitian operator L. Then, we can diagonalise the operator as $L = \sum_i L_i |i\rangle\langle i|$. Expanding the density operator in the basis that diagonalises the Lindblad operator we see explicitly that the Lindblad term acts to dampen exponentially the off-diagonal components of the density matrix with rate $\lambda(L_i - L_J)^2$:

$$\partial_t \rho_{ij} \approx -\frac{\lambda}{2}(L_i - L_j)^2 \tag{2.39}$$

Quantum trajectories

The evolution given by the GKSL equation can be unravelled in terms of trajectories. Unlike the classical version, however, these trajectories are not objective (as one cannot observe which trajectory the quantum state actually follows) and, more importantly, are not unique (as one can decompose a mixed state density matrix in terms of pure states in multiple equivalent ways). A common choice for the unravelling of Equation 2.36 is given by:

$$\begin{aligned} \mathrm{d}|\psi\rangle_t = &-iH|\psi\rangle_t \mathrm{d}t \\ &- \frac{1}{2}\lambda^{\alpha\beta}(L_\beta^\dagger - \langle L_\beta^\dagger\rangle)(L_\alpha - \langle L_\alpha\rangle)|\psi\rangle_t \mathrm{d}t + \frac{1}{2}\lambda^{\alpha\beta}(\langle L_\beta^\dagger\rangle L_\alpha - \langle L_\alpha\rangle L_\beta^\dagger|\psi\rangle_t \mathrm{d}t \\ &+ (\lambda^{1/2})^{\alpha\beta}(L_\alpha - \langle L_\alpha\rangle)\mathrm{d}\xi_{\beta,t} \ , \end{aligned} \tag{2.40}$$

where $\lambda = \lambda^{1/2}\lambda^{1/2\dagger}$ and $\mathrm{d}\xi_{\alpha,t}$ is a complex-valued Wiener process obeying:

$$\mathrm{d}\xi_{\alpha,t}\mathrm{d}\xi_{\beta,t} = 0 \ , \qquad \mathrm{d}\xi_{\alpha,t}\mathrm{d}\xi^*_{\beta,t} = \delta_{\alpha\beta}\mathrm{d}t \ . \tag{2.41}$$

The unravelling has the advantage of fleshing out the decoherence effect. This is given by the first term in the second line and the third line in Equation 2.36. Indeed, we see that the pure state is pushed in Hilbert space towards eigenstates of the Lindblad operators, where such terms stop contributing. The non-uniqueness of the quantum trajectories has a phenomenological interpretation. Indeed, in specific settings, one can explicitly derive the different representations of the unravelling by starting from the unitary evolution and supplementing it with a specific measurement protocol [123, 124]. For example, the jumping Poisson representation for the dynamics is related to photon counting in quantum optics, whilst the continuous Wiener unravelling maps to a homodyne detection scheme. By including the evolution of the measurement record itself, one obtains a CQ-type dynamics that lifts the redundancy in the description. In fact, if one does have access to the specific measurement outcomes, there exist observables that can distinguish the particular unravelling that describes the physical evolution of the quantum state. If one, however, ignores the measurement record, they are forced to average over the noise – leading to the same result for every choice of trajectories.

From the unravelling, it is sufficient to use Itô's lemma and the definition of the density matrix $\rho(t) = \mathbb{E}[|\psi(t)\rangle\langle\psi(t)|$, where the expectation value is take over all the noise realisations, to show that this is equivalent to the GKSL equation. Whilst all the unravellings give back

the same Lindblad equations, they can be assigned different operational meanings [123]. In particular, different trajectories can be associated with different "measurement protocols" on the quantum state. As such, they can be supplemented with the evolution of the measurement record itself, a classical variable – this is the first contact with consistent classical-quantum evolution.

Schwinger-Keldysh path integral

The evolution of the density matrix can be expressed in terms of path integrals also for non-unitary dynamics. The starting point is to expand the density matrix in a complete basis:

$$\rho(t) = \int \mathrm{d}\psi^L \mathrm{d}\psi^R \rho(\psi^L, \psi^R, t) |\psi^L\rangle\langle\psi^R| \ . \tag{2.42}$$

The main idea behind non-unitary path integrals is to treat the evolution of the left L and right R branches as independent degrees of freedom (one evolving forward in time, the other backwards). For dynamics at most quadratic in the conjugate momenta, the Lindblad equation is equivalent to the following path integral:

$$\rho(\psi_T^L, \psi_T^R, T) = \mathcal{N} \int \mathcal{D}\psi^L \mathcal{D}\psi^R e^{iS_{OS}[\psi^L, \psi^R]} \rho(\psi^L, \psi^R, t_0) \ , \tag{2.43}$$

where $\mathcal{N}$ is a normalisation factor and the open system action is given by

$$iS_{OS}[\psi^L, \psi^R] = \int_{t_0}^{T} dt \left[iL[\psi^L] - iL[\psi^R] + iS_{FV}[\psi^L, \psi^R] \right] \tag{2.44}$$

with

$$iS_{FV}[\psi^L, \psi^R] = \int_{t_0}^{T} dt \left[\lambda^{\alpha\beta} L_\alpha(\psi^L) L_\beta(\psi^R) - \frac{1}{2} L_\beta^*(\psi^L) L_\alpha(\psi^L) - \frac{1}{2} L_\beta^*(\psi^R) L_\alpha(\psi^R) \right] \tag{2.45}$$

is known as the Feynman-Vernon (FV) functional. The FV contribution is the unitary-breaking term which pictorially corresponds to a coupling of the left and right branches.

Taking the trace at the final time and inserting sources for the left and right branches gives the Schwinger-Keldysh generating functional for moments of the operator $\mathcal{O}$:

$$Z[J^L, J^R] = \frac{1}{Z[0,0]} \int^{\psi^L(T)=\psi^R(T)} \mathcal{D}\psi^L \mathcal{D}\psi^R e^{iS_{OS}[\psi^L, \psi^R] + i(J^L \mathcal{O}^L - J^R \mathcal{O}^R)} \ , \tag{2.46}$$

obeying the normalisation condition $Z[0,0] = 1$. Note that the boundary condition at T on the two branches, coming from taking the trace, implies that the path integral is performed along a closed-time contour with precise ordering. First, evolve the ket along the forward branch; then, propagate the bra along the backward one – sources need to be time-ordered accordingly.

2.3 Hybrid classical-quantum dynamics

Now that we have described the basic ingredients of the theory, we can combine them to introduce a consistent framework that allows coupling between quantum and classical degrees of freedom [50, 51, 125, 126, 127, 67, 128]. As before, we start from a master equation approach, but we also discuss briefly how to interpret the dynamics in terms of trajectories and path integrals.

The space in which the CQ state evolves is a tensor product between a Hibert space $\mathcal{H}$ and phase space $\mathcal{M}$. CQ assigns to each point in phase space an un-normalised density matrix $\varrho(z,t)$ – the CQ state is an operator-valued probability measure. As such, the state has to satisfy the following two properties:

- tracing out over the quantum degrees of freedom yields a normalised probability distribution p in phase space : $\mathrm{Tr}[\varrho(z,t)] = p(z,t) \geq 0$,
- marginalising over all the classical degrees of freedom produces a normalised density matrix ρ on $\mathcal{H}$: $\int \mathrm{d}z \varrho(z,t) = \rho$.

These two requirements imply the following normalisation condition:

$$\int_{\mathcal{M}} \mathrm{d}z \mathrm{Tr}[\varrho(z,t)] = 1 \ . \tag{2.47}$$

Operators are defined as usual, but they are allowed to depend on the phase-space coordinates.

The CQ master equation

The dynamics has to map a CQ state to another valid CQ state. This, with the addition of the conditions of linearity and CP implies that the only allowed maps are the ones that can be rewritten as [50]:

$$\varrho(z,t_f) = \int \mathrm{d}z' \sum_{\alpha\beta} \Lambda^{\alpha\beta}(z,t_f|z',t_i) K_\alpha \varrho(z',t_i) K_\beta^\dagger \ , \tag{2.48}$$

where Λ is a positive Hermitian matrix kernel for each z, z' and K_α are arbitrary orthogonal set of Kraus operator in Hilbert space (note that we have absorbed all the phase space dependence of the map in the transition matrix Λ). This is just a generalisation of Kraus' theorem.

Normalisation forces:

$$\int \mathrm{d}z \sum_{\alpha\beta} \Lambda^{\alpha\beta}(z, t_f|z', t_i) K_\beta^\dagger K_\alpha = 1 \ . \tag{2.49}$$

As for the classical and quantum case, we are interested in dynamics with additional requirements. First of all, we desire Markovian dynamics. Again, an effective CQ dynamics needs not to be Markovian at all (and in general will not be), but, when it comes to adopting it as the fundamental description of a physical system, Markovianity is a natural thing to ask. Very much in the same spirit of the derivation of the Fokker-Planck equation, it is possible to do a short time expansion for Λ:

$$\Lambda^{\alpha\beta}(z, t + \delta t|z', t) = \delta_0^\alpha \delta_0^\nu + \delta t W^{\alpha\beta}(z|z', t) \ , \tag{2.50}$$

where we have chosen a basis in which $K_\alpha = \{\mathbf{1}, L_i\}$. Then it can be shown that the CQ master equation for a linear, CPTP and Markovian dynamics takes the form:

$$\begin{aligned} \frac{\partial \varrho(z,t)}{\partial t} = &\sum_{n=1}^{\infty} \frac{(-1)^n}{n!} \left(\frac{\partial^n}{\partial z_{i_1} \dots \partial z_{i_n}} \right) \left(D^{00}_{n,i_1 \dots i_n}(z, \delta t) \varrho(z,t) \right) \\ &- i[H(z), \varrho(z)] + D_0^{ij}(z) L_i \varrho(z) L_j^\dagger - D_0^{ij} \frac{1}{2} \{ L_j^\dagger L_i \varrho(z) \}_+ \\ &+ \sum_{\alpha\beta \neq 00} \sum_{n=1}^{\infty} \frac{(-1)^n}{n!} \left(\frac{\partial^n}{\partial z_{i_1} \dots \partial z_{i_n}} \right) \left(D^{\alpha\beta}_{n,i_1 \dots i_n}(\bar{z}) L_\alpha \varrho(z,t) L_\beta^\dagger \right) , \end{aligned} \tag{2.51}$$

where, for convenience, we have split the indices $\alpha = 0, i$ and $H(z) = \frac{i}{2}(D_0^{i0} L_i - D_0^{0i} L_i^\dagger)$ is a Hermitian operator which gives the leading unitary evolution, acting as an Hamiltonian that depends on the classical degrees of freedom.

It is useful at this point to compare the CQ master equation with Equation 2.5 and Equation 2.36. Indeed, the first line is nothing but the evolution of the probability distribution for a classical jumping process. That is, we identify D_n^{00} as the components of the CQ moments encoding the classical drift and diffusion. The second line strongly resembles the GKSL Equation, highlighting that D_0^{i0} controls the unitary part of the quantum evolution, with decoherence effects encoded in D_0^{ij}. In practice, D_0^{ij} map exactly to the Lindblad couplings $\lambda^{\alpha\beta}$ in the GKSL Equation2.36, with the added freedom of possibly depending on the classical variable Z. As the couplings can depend on the classical system, the second line also allows for the classical system to act on the quantum one. Finally, the last line represents non-trivial CQ backreaction, describing how the quantum system controls the classical degrees of freedom.

Positivity conditions on Λ trivially translate in conditions on $W^{\alpha\beta}$, since:

$$\Lambda^{\alpha\beta}(z,t+\delta t|z',t) = \begin{bmatrix} \delta(z,z') + \delta t W^{00}(z|z',t) & \delta t W^{0i}(z|z',t) \\ \delta t W^{j0}(z|z',t) & \delta t W^{ij}(z|z',t) \end{bmatrix} + O(\delta t^2) \ . \tag{2.52}$$

In particular, both $\delta(z,z') + \delta t W^{00}(z|z',t)$ and $W^{ij}(z|z',t)$ have to be positive matrices. Moreover, if either W^{ij} or W^{00} vanish, then also $W^{0,\alpha}$ must be zero except for its $\delta(z,z')$ component, which generates pure Hamiltonian evolution. Physically, this means that any non-trivial CQ coupling requires a non-zero W^{ij} and, therefore, decoherence.

The positivity conditions are clearer when studied in the context of continuous dynamics in phase space. As with for the FP equation, there is a CQ version of the Pawula theorem [51] saying that, in the case of continuous dynamics, the moments truncate at second order. Therefore, the most general CQ, autonomous, linear, CPTP and *continuous* dynamics is of the form:

$$\begin{aligned} \frac{\partial \varrho(z,t)}{\partial t} = &- \frac{\partial}{\partial z_l}(D^{00}_{1,l}\varrho(z,t)) + \frac{1}{2}\frac{\partial^2}{\partial z_l \partial z_k}(D^{00}_{2,lk}\varrho(z,t)) \\ &- \frac{\partial}{\partial z_l}(D^{0i}_{1,l}\varrho(z,t)L_i^\dagger) - \frac{\partial}{\partial z_l}(D^{i0}_{1,l}L_i\varrho(z,t)) \\ &- i[H(z),\rho(z,t)] + D_0^{ij}(z)L_i(z)L_j^\dagger - \frac{1}{2}D_0^{ij}\{L_j^\dagger, L_i, \rho(z)\}_+ \ , \end{aligned} \tag{2.53}$$

where the positivity conditions translate into:

$$2D_2 \geq D_1 D_0^{-1} D_1^\dagger \ , \qquad (1 - D_0 D_0^{-1}) D_1 = 0 \ , \tag{2.54}$$

with A^{-1} referring to the generalised inverse – recall that these are matrix multiplications for multidimensional systems. Note that, here, we have simplified the notation by dropping indices for the decoherence, diffusion and drift matrices

$$D_0 \equiv D_0^{ij} \ , \qquad D_1 = D^{0i}_{1,j} \ , \qquad D_2 \equiv D^{00}_{2,ij} \ , \tag{2.55}$$

These relations, dubbed the "decoherence-diffusion trade-off" showcase exactly the intuition developed before. The first one simply tells us that, unless $D_1 = 0$, the decoherence matrix D_0 (equivalent to λ in the GKSL equation) cannot vanish. Further, the second relation elucidates that the decoherence rates (the eigenvalues of D_0) bound from below the amount of diffusion in the classical degrees of freedom encoded in D_2, as long as there is backreaction ($D_1 \neq 0$). We restrict our attention to dynamics that saturate the bound given by Equation 2.54. The

reason for the following is that the exact saturation of the decoherence-diffusion is a special point in the parameter space of the theory – in that case there is no information destruction. Specifically, by keeping a record of the evolution of the classical system, it is always possible to reconstruct the pure state of the quantum system [67]. If the diffusion of the system is not minimal, instead, the quantum system in general evolves to a mixed state even if the classical system is monitored.

We will be in general interested in dynamics that can be seen as generated by some interaction Hamiltonian

$$H_{CQ} = H_C(x,p) + H_Q(\psi,\pi) + V_I(x,\psi) \tag{2.56}$$

coupling the classical and the quantum system, i.e. the minimal form of consistent CQ dynamics that, modulo the irreversible terms, corresponds to the standard mean-field semiclassical evolution. Specifically, H_C and H_Q are the Hamiltonians of the classical and quantum systems respectively, (x,p) and (ψ,π) their respective phase-space variables, and V_I an interaction potential coupling only to the generalised positions of the two systems. Then, by minimally coupling the classical system to the noise field (i.e. modelling it as a stochastic white noise force) and choosing as basis for the Lindblad operators $L_i = \frac{\partial V_I}{\partial x^i}$, the master equation greatly simplifies to

$$\begin{aligned}\frac{\partial \varrho(x,p)}{\partial t} &= \{H_C,\varrho\} + \frac{1}{2}\frac{\partial^2}{\partial p_i \partial p_j}\left(D_{2,ij}(x)\varrho\right) + \frac{1}{2}\left(\{V_I,\varrho\} - \{\varrho,V_I^\dagger\}\right) \\ &\quad - i[H_Q + V_I,\varrho] + D_0^{ij}\left(\frac{\partial V_I}{\partial x_i}\varrho\frac{\partial V_I^\dagger}{\partial x_j} - \frac{1}{2}\left\{\frac{\partial V_I^\dagger}{\partial x_j}\frac{\partial V_I}{\partial x_i},\varrho\right\}_+\right) \\ &= \{H_{CQ},\varrho\}_A + \mathbf{D}[\varrho]\ ,\end{aligned} \tag{2.57}$$

where we have grouped the reversible part of the dynamics in the Aleksandrov bracket

$$\{H_{CQ},\varrho\}_A \equiv \{H_C,\varrho\} - i[H_Q + V_I,\varrho] + \frac{1}{2}\left(\{V_I,\varrho\} - \{\varrho,V_I\}\right) \tag{2.58}$$

and the irreversible part in the decoherence-diffusion operator

$$\mathbf{D}[\varrho] \equiv \frac{1}{2}\frac{\partial^2}{\partial p_i \partial p_j}\left(D_{2,ij}(x)\varrho\right) + D_0^{ij}\left(\frac{\partial V_I}{\partial x_i}\varrho\frac{\partial V_I^\dagger}{\partial x_j} - \frac{1}{2}\left\{\frac{\partial V_I^\dagger}{\partial x_j}\frac{\partial V_I}{\partial x_i},\varrho\right\}_+\right)\ . \tag{2.59}$$

CQ trajectories are objective

Continuous hybrid dynamics can also be represented in terms of trajectories of the quantum state ρ and classical state z. We restrict to the dynamics that saturate the decoherence-diffusion trade-off. Under this assumption the quantum state remains pure once conditioned on the classical trajectory [67]. The following SDEs describes the evolution for the classical degrees of freedom:

$$dZ_{t,l} = \{Z_{t,l}, H_C(Z_t)\}dt + \langle\{Z_{t,l}, V_I(Z_t)\}\rangle dt + \sigma_{lk}(Z_t)dW_{t,k} \ , \tag{2.60}$$

whilst the pure quantum state follows:

$$\begin{aligned} d|\psi\rangle_t = &-i(H_0 + V_I(Z_t))|\psi\rangle_t dt + \frac{1}{2}\sigma^{-1}_{lk}\left(\{Z_k, V_I\} - \langle\{Z_k, V_I\}\rangle\right)|\psi\rangle_t dW_l \\ &- \frac{1}{8}\sigma^{-1}_{lk}\sigma^{-1}_{lm}\left(\{Z_k, V_I\} - \langle\{Z_k, V_I\}\rangle\right)\left(\{Z_m, V_I\} - \langle\{Z_m, V_I\}\rangle\right)|\psi\rangle_t dt \ . \end{aligned} \tag{2.61}$$

Whilst the unravelling equations look non-linear, upon averaging they reduce to the linear master equation, much like for the case of the GKSL unravelling. We can recover the combined CQ state by averaging over all realisations of the noise:

$$\varrho(z,t) = \mathbb{E}[\rho_t \delta(z - Z_t)] \ . \tag{2.62}$$

Indeed, by taking Equation 2.62 and applying Itô's lemma, it is easily verified that ϱ satisfies Equation 2.53 if Z_t and ρ_t evolve as per the unravelling equations. Contrary to the pure Lindbladian case, the trajectories of CQ dynamics are unique, due to the objectivity of the classical evolution. If the decoherence-diffusion trade-off is not saturated, an unravelling in terms of trajectories still exists, but Equation 2.61 is modified to handle mixed states instead.

CQ path integral

The time-local dynamics can be trotterized and, therefore, expressed in terms of integration over paths. The deterministic part of the dynamics of hybrid system can be derived from the CQ *proto-action*:

$$W_{CQ} = \int \mathrm{d}t \left(L_Q[\psi] + L_C[z] - V_I[z,\psi]\right) = \int \mathrm{d}t \ L_{CQ} \ . \tag{2.63}$$

The prefix "proto" here indicates that, whilst the functional encodes all the information about the deterministic part of the dynamics, it is not the action of the path-integral itself. Instead,

continuous hybrid dynamics of the form of Equation 2.53 involving z and ψ (the classical and quantum degree of freedom respectively) can be equivalently represented via the following configuration-space path integral:

$$\varrho(z,\psi^L,\psi^R,T)=\int\mathcal{D}\psi^{L/R}\int\mathcal{D}z\int\mathcal{D}\tilde{z}\;e^{iI_{CQ}}\varrho(z,\psi_0^L,\psi_0^R,t_0)\;, \tag{2.64}$$

where

$$\begin{aligned} iI_{CQ}=\int\mathrm{d}t\Bigg[&i\Delta L_{CQ}[z,\psi^{L/R}]-\frac{1}{2}\frac{\delta\Delta W_{CQ}}{\delta z^i}D_0^{ij}\frac{\delta\Delta W_{CQ}}{\delta z^j}\\ &-\tilde{z}^i\frac{\delta}{\delta z^i}\bar{W}_{CQ}[z,\psi^{L/R}]+\frac{1}{2}\tilde{z}_i(D_2^{-1})^{ij}\tilde{z}_j\Bigg]\;. \end{aligned} \tag{2.65}$$

For simplicity of notation we have defined the averaged and subtracted proto-actions:

$$\Delta W_{CQ}=W_{CQ}[z,\psi^L]-W_{CQ}[z,\psi^R]\;,\qquad \bar{W}_{CQ}=\frac{1}{2}\left(W_{CQ}[z,\psi^L]+W_{CQ}[z,\psi^R]\right)\;. \tag{2.66}$$

The path integral neatly splits up in a SK-like and a MSR-like term, the first and second lines in Equation 2.65 respectively. The usual path integral techniques to compute expectation values of operators apply.

2.4 CQ gravity

As mentioned, the main scope of the first half of the thesis is to study the phenomenological plausibility of theories of hybrid gravity theories – models of fundamental classical gravity interacting with quantum matter.

Such a theory is currently active area of research. Consequently, there is a wealth of open problems and unanswered questions even at the level of the fundamental gravitational equations themselves, let alone on the key consistency conditions that the theory needs to satisfy – such as agreeing with Einstein's gravity where the latter is known to perform incredibly well. Nonetheless, we will here attempt to provide a brief summary of the main results, proposals and open questions on the topic – to prepare the discussion in the following chapters.

2.4.1 The fundamental dynamics

The master equation representation of the CQ framework is closer to the canonical formalism than a covariant approach. As such, the first attempt at describing such dynamics came

from adapting the canonical Arnowitt–Deser–Misner (ADM) [129] formalism of GR to the CQ framework.

In the ADM approach, we explicitly pick a foliation of spacetime, inducing the following 3+1 decomposition of the metric:

$$g_{00} = -N^2 + h^{ij}N_iN_j \ , \qquad g_{0i} = N_i \ , \qquad g_{ij} = h_{ij}. \tag{2.67}$$

Here, h_{ij} is the spatial metric on the chosen foliation, while N and N^i (called the lapse function and shift vector respectively) tell us how the 3-geometry is embedded in the 4-dimensional manifold. Further, we introduce the canonical momentum π_{ij} conjugate to the 3-metric. The deterministic (GR) dynamics is fully encoded by the gravity and matter Hamiltonians, $H_{\rm GR}[g, \pi, N, \underline{N}]$ and $H_{\rm m}[g, \psi, \pi_\psi, N, \underline{N}]$ respectively. Here, ψ is a quantum matter degree of freedom and π_ψ its conjugate momentum. In Chapter 5 we spell the gravitational Hamiltonian out explicitly for the FLRW model.

It is important to know that $H_{\rm GR}$ encodes the autonomous gravitational evolution only, whilst $H_{\rm m}$ the matter evolution *and* the backreaction. Then, the natural guess for the CQ equation of a hybrid gravitational theory would be schematically:

$$\frac{\partial \varrho}{\partial t} = \{H_{GR} + H_m, \varrho\}_A + \mathbf{D}\left[\varrho\right] \ , \tag{2.68}$$

where the diffusion-decoherence operator $\mathbf{D}$ is what needs modelling and is in principle unspecified – other than the requirement to satisfy the decoherence diffusion trade-off.

Imposing that the decoherence-diffusion trade-off is exactly saturated for simplicity (and because it seems natural for a fundamental theory of Nature), the decoherence-diffusion term $\mathbf{D}[\varrho] = \mathbf{D}_C[\varrho] + \mathbf{D}_Q[\varrho]$ can be compactly expressed as

$$\mathbf{D}_C[\varrho] = \frac{1}{2}\int \mathrm{d}^3x\mathrm{d}^3y\sqrt{h(x)h(y)}\frac{\delta^2(D^{ijkl}(x,y)\varrho)}{\delta\pi^{ij}(x)\delta\pi^{kl}(y)} \tag{2.69}$$

and

$$\mathbf{D}_Q[\varrho] = -\frac{1}{8}\int \mathrm{d}^3x\mathrm{d}^3y\sqrt{h(x)h(y)}\ D_{ijkl}(x,y)\left[\frac{\delta H_m}{\delta h_{ij}(x)}, \left[\frac{\delta H_m}{\delta h_{kl}(y)}, \varrho\right]\right] \ , \tag{2.70}$$

with D^{ijkl} and $D : ijkl$ the (possibly non-local) diffusion kernel and its inverse. The choice of D^{ijkl} already poses a difficulty. Again, it seems natural to impose the saturation of the decoherence-diffusion trade-off since it is equivalent to require that information about the

quantum state is not destroyed if one keeps a record of the classical evolution. Covariance is an incredibly restrictive requirement, forcing it to be related to the DeWitt metric

$$D^{ijkl} = \frac{N(x)D}{2\sqrt{h(x)}}\left(h^{ik}h^{jl} + h^{il}h^{jk} - 2\beta h^{ij}h^{kl}\right)\delta^{(4)}(x-y)\ , \tag{2.71}$$

with $\delta^{(4)}(x-y)$ being the 4-dimensional delta-*function* (rather than the equivalent object transforming as a density). Here is the D constant diffusion coefficient. Note, positive-semidefiniteness of the diffusion tensor requires that $\beta < 1/3$. Whilst the choice of the DeWitt metric is covariant, it has the unpleasant side-effect of adding energy to the system (on average) at infinite rate [130]. This can be seen by looking at the evolution of the Hamiltonian itself in the Heisenberg picture – the double derivative on π acting on $H_{GR} \sim \pi^2$ will generate a further δ-function which, upon integration, yields a contact $\delta(0)$ divergence. Yet, this is not a problem for local CQ gravity only, but of any theory with diffusion and/or decoherence if the respective kernel is local [43]. Indeed, the relativistic stochastic field theory we study in Chapter 4 features the same divergences. How these divergences can be renormalised – if at all – is an open question to be dealt with.

An alternative that has been discussed in the literature is relaxing the locality of the kernel, or essentially regularising the local one. Whilst this softens the energy production problem – energy conservation is still violated, but at a finite constant rate given by the small-distance cutoff – it spoils covariance and, locally, Lorentz invariance. In the Newtonian limit, the non-local kernel that minimises the decoherence in the matter degrees of freedom gives the famous Diosi-Penrose kernel [131, 132].

There are, however, further conceptual questions on Equation 2.68. Indeed, GR is a so-called "constrained system", due to diffeomorphism invariance [133]. The choice of lapse function and shift vectors is equivalent to a choice of gauge – under *any* such allowed choice the final state of the evolution must be physically equivalent. In Hamiltonian systems, invariance under transformations in field space results in one or more constraints [134] – algebraic relations between phase-space variables that need to be satisfied on-shell and that are preserved by the evolution equations. In GR, there are four of such constraints: one "Hamiltonian" and three "momentum" constraints. Curcially, and this is at the heart of the result in Chapter 5, the diffusive part of the evolution in Equation 2.68 necessarily breaks the deterministic constraint, even if

the decoherence-diffusion terms superficially respect the symmetries of the deterministic system. For the gravitational system, this can be seen as follows. A linear combination of the four GR constraint is equivalent to the Hamiltonian of the hybrid system itself. However, both the diffusion and decoherence terms do not preserve the energy of the system, that heats on average (much like a Brownian particle undergoing undamped diffusion will heat up indefinitely).

The expectation is that this should not be taken to signify loss of covariance [135]. This relies on the simple observation that the derivation of the constraints themselves uses the Hamiltonian structure of the dynamics, which CQ explicitly breaks. The role of the constraints even just in classical stochastic systems – let alone hybrid ones – is still an open question. Indeed, whilst the deterministic form of the constraint may be broken spontaneously by the stochastic terms, there might exist a generalisation that applies to stochastic gauge theories. Indeed, the constraints in the ADM formalism act to restrict the number of physical degrees of freedom, since they provide algebraic relations between the field variables. Unless we are ready to give up the idea that linearised perturbations of the metric can be described as a massless spin-2 field, there needs to be a mechanism in the stochastic gravitational dynamics to ensure that exactly only 2 gravitational degrees of freedom are independent. Of course, this consideration is valid only for models that do preserve local Lorentz invariance – where effectively in the linearised regime the theory behaves as GR with random sources. These considerations aside, there is however no convincing proof yet that the dynamics in Equation 2.68 is indeed covariant either – even if the decoherence-diffusion terms are taken to be local.

Path integral representation

To side-step the issue of the constraints that arises from the master equation approach, a path integral definition of CQ gravity has been proposed [126] with action:

$$iI_{CQ} = \int d^4x\sqrt{-g}\left[i\Delta\mathcal{L}_m - \frac{\sqrt{-g}}{8}\Delta T^{\mu\nu}D_{\mu\nu\rho\sigma}\Delta T^{\rho\sigma} \right. \\ \left. -\frac{\sqrt{-g}}{128\pi^2 G_N^2}\left(G^{\mu\nu} - 8\pi G_N\bar{T}^{\mu\nu}\right)D_{\mu\nu\rho\sigma}\left(G^{\rho\sigma} - 8\pi G_N\bar{T}^{\rho\sigma}\right)\right] , \tag{2.72}$$

where the natural Lorentzian extension to the local covariant kernel in Equation 2.71 was chosen, namely

$$D^{\mu\nu\rho\sigma} = \frac{D}{2\sqrt{-g}}(g_{\mu\rho}g_{\nu\sigma} + g_{\mu\rho}g_{\nu\sigma} - 2\beta g_{\mu\nu}g_{\rho\sigma}) . \tag{2.73}$$

The action is manifestly covariant, which is a necessary condition for the path integral itself to be invariant under diffeomorphisms. Moreover, expanding the action, it can be shown that it has a similar structure to the quantum quadratic gravity action, an observation that has been used to argue for renormalisability of the classical sector [136]. Of course, covariance of the action is not in itself a sufficient condition for diffeomorphism invariance – there are subtleties due to the normalisation and invariance of the measure which need to be investigated. Nonetheless, explicit covariance at the level of the action comes at a price: the path integral is not of standard CQ form. Crucially, the standard CQ path integral in configuration space for the theory in Equation 2.68, after integration of the response variables, would only involve the "square" of the spatial parts of the Einstein's equations, not the full set. Indeed the $G_{0\mu}$ components of Einstein's equation are intimately related to the constraint – it is unclear how such terms could appear in the action starting from the master equations approach, nor whether including them spoils any of the key properties that the master equation dynamics is known to possess – complete positivity, trace preservation or linearity. There are specific instances, however, where the master equation approach and the path integral definition of the dynamics are known to be equivalent (e.g. in the Newtonian limit [137]).

A related observation is that, contrary to the Riemannian DeWitt metric, the kernel in Equation 2.73 is dangerously not positive semidefinite on the space of 2-tensors. It has been shown that it is so on the sub-space of physical gauge-invariant degrees of freedom (e.g. on traceless tensor modes in the linearised regime) [136], but it is to be understood whether that in itself would be enough to guarantee consistency of the theory.

2.4.2 Recent results

The path integral representation of the dynamics has been the starting point for a number of recent advances in the understanding of CQ gravity.

First of all, it has been shown to be consistent in the case of Nordström CQ gravity [127]. Nordström gravity is a fully relativistic theory of gravitation that involves a single scalar degree of freedom. In such a theory, the dynamical spacetime metric is conformally flat, with the conformal factor being expressed in terms of a single scalar. Whilst Nordström gravity correctly reproduces Newton's law, it fails to account for light deflection and produces inconsistent esti-

mates for the effect of perihelion precession. However, it has the virtue of being conceptually much easier than GR – having a single degree of freedom implies the absence of Dirac constraints in the theory. Still, having a consistent theory of CQ gravity is a strong signal towards the fact the main obstacles towards an Einstein CQ gravity theory are not the classicality of the metric in itself, but rather the more subtle problem of covariance.

In both the path integral and master equation formulations of CQ gravity, the Newtonian limit has been derived [137]. Crucially, it matches previous models of self-consistent Newtonian CQ gravity [37], showing that they can be recovered from a fully relativistic theory. In the Newtonian limit, the gravitational field is stochastic, whilst particles decohere in the position basis as expected. The CQ Nordström model has the same relativistic limit as the Einstein CQ gravity [127].

Beyond the Newtonian regime, CQ gravity seems to favour metrics that can explain the rotational curves of galaxies without the need for dark matter. Indeed by studying vacuum spherically symmetric solution it was found that the leading order corrections to the Schwarzschild metric are of the form of the so-called MK metric [138] – a solution to conformal gravity that has the potential to explain galactic rotation curves without the need of dark matter [139, 138, 140]. Interestingly, by conditioning on the parameter that fits the rotational curves the best, the CQ gravity path integral yields a probability distribution for the cosmological constant parameter that is sharply peaked over the one favoured by observations. There are, however, assumption in the work that require further justification. The biggest challenge is to explain why all galaxies have correlated values for such a parameter term, which the path integral of the model suggests should be drawn independently at random for each realisations of the stochastic gravitational field – and therefore for each galaxy.

2.4.3 Cosmological evolution and dark matter

Since the main discussion in Chapter 5 will deal with cosmology and dark matter in particular, a brief review of the current state of arts on the topic is in order. This will be extremely quick, and it is no way intended to be a comprehensive summary of current research in cosmology, but will serve the purpose of contextualising the results in Chapter 5.

The briefest history of cosmology

The Standard Model of cosmology, also known as LambdaCDM, supplemented by the inflationary paradigm, is currently the most successful description we have of the cosmological history of our Universe. It explains a variety of observations, from local supernovae measurements, to anomalous galactic rotation curves all the way back to the main features of the cosmic microwave background (CMB) – the early relic radiation produced by our young Universe. We now attempt to give an extremely succint review of the evolution of our cosmos under such a model – for a more detailed one, see for example [141]. It all begins with a spacelike singularity, affectionately known as the Big Bang. Experimental data place the Big Bang approximately 14 billion years ago.

Shortly after the Big Bang, the Universe underwent a period of rapid expansion: inflation. The inflationary paradigm was originally introduced as a solution to the flatness and horizon problems [142]. The former is the apparent fine-tuning of the cosmological extrinsic curvature of our Universe, which is measured to be near-zero. A period of exponential expansion has the virtue of washing out any initial spatial curvature to zero, lifting the necessity of carefully-chosen initial conditions to reproduce observations. The latter, instead, is the early realisation that regions of the cosmic microwave background that could have never influenced each others within the "hot Big Bang" model, appeared correlated. The same accelerated expansion that had the potential to solve the flatness problem, could also solve the horizon problem – the exponential expansion successfully puts in causal contact region of the observable sky which would have never otherwise been able to develop correlated fluctuations in the observed temperature [142]. Several models have been put forward over the years, all realising the main features of the inflationary proposal [143, 144]. The most popular involve single [145] (or multiple [146]) scalar fields, "slow-rolling" down their potential and causing the exponential increase in the scale factor of the Universe. Other options include Starobinsky inflation [93] (where the so-called inflaton field emerges from higher-curvature corrections to GR) and Linde's chaotic inflation [147].

After about 10^{-32} s after the Big Bang, inflation halts and the inflaton field decays into the Standard Model particles we observe – this is the period known as "reheating". Shortly after, the first nuclei are produced (Big Bang nucleosynthesis). The Universe remains opaque for a long time, until 10^5 years ago, when it has cool down enough for neutral atoms to form

and light to travel with minimal scattering. It is now that the cosmic microwave background was released. Inflation left a definite, testable mark in the statistics of the CMB, beyond being a solution to the horizon problem. Moreover, the mechanism also explains other features of the power spectrum itself. Of these, famously, it explains its near scale-invariance and the suppression of tensor modes fluctuations. The CMB provides a powerful testing ground for inflationary models [144].

The next period of the expansion of the Universe is mainly of astrophysical significance, with the first stars igniting (and galaxy forming). Still, different components of the energy budget of the Universe dilute at unequal rate with the expansion. As such, whilst the main source of the cosmic evolution has been pressureless dust (non-relativistic matter), approximately 4 billion years ago the expansion of the Universe started accelerating again [148, 149]. Within the LambdaCDM model, the late-time expansion is attributed to a cosmological constant Λ, which is driving our Universe towards an asymptotically de Sitter state (since $\Lambda > 0$). Still, there exist many proposal in which the late-time acceleration is not due to a cosmological constant [150, 151] at all, but to other more exotic types of gravitational sources instead. In particular, recent data seems to point towards an evolving, rather than constant, dark energy fluid [152, 153].

Still, it is not all well for LambdaCDM. Recent years have uncovered tension between late-time and early time estimation of the model's parameters (famously, the Hubble parameter and matter clustering). Whilst both the Hubble tension and the so-called $S8$ tension can be hints of new physics, it is still up to debate whether they can be the result of systematics in the different measurement procedures. However, so far all the efforts in exploring the latter hypothesis have not managed to reduce the observed tensions [154, 155].

Dark matter

The CDM portion of the standard model of cosmology refers to the hypothesised presence of so-called "cold" dark matter. That is, non-relativistic pressureless dust that interacts only (or, in many models, mainly) gravitationally with baryonic (observable) matter.

Dark matter was originally introduced to explain anomalous flattening of the rotation curves of galaxies – incompatible with the observed luminous matter. Other theories that do not in-

clude an elusive matter species exist, the most famous of which is MOND (modified Newtonian dynamics). MOND proposes as a solution to the galactic rotation curves problem the existence of a fundamental acceleration scale below which new physics emerges. However, over the years, other evidence piled in favour of particle dark matter. In particular, the existence of specific peaks in the CMB power spectrum, known as baryonic acoustic oscillations, could be explained neatly just by assuming the esistence of CDM – matter species that do not feel radiation pressure since they are completely decoupled from electromagnetism. Moreover, particle CDM leaves its imprints also via gravitational light deflection, which allows for CDM to be mapped. Although there exists relativistic extensions to the MOND paradigm that can explain these phenomena as well [156], observational constraints strongly disfavour MOND models with respect to LambdaCDM [157].

The abundance of dark matter is constrained by various independent observations (though there are some model-dependent assumptions). In particular, both Pantheon+ [158] (low-redshift supernovae data) and Planck [149] (high-redshift measurements of the CMB) suggest the same value for the energy budget of the total pressureless dust ($\Omega \approx 0.3$). Of this, only a small fraction is baryonic matter, with the vast majority being assigned to CDM. Galactic measurements place strong bounds on models of hot or warm dark matter [159], in which the dark matter stress-tensor does have pressure terms (i.e. the matter particles are relativistic).

Whilst it is true that there are some mysteries regarding the CDM model, and that some other proposals can accomodate at least some of the phenomenology that CDM explains, the particle proposal is by far the most successful one – and the one that claims most support. There are many models to describe the nature of this invisible particle – from axions to primordial black holes [160, 151] – which are being extensively tested. As of now, however, all of the experiments have been unsuccessful at detecting dark matter particles, leaving the problem of the origin of CDM open [151]. In Chapter 5 we will present a novel mechanism, within CQ gravity, to generate CDM phenomenology without the need of a physical, elusive, particle. Instead, we will see that the stochasticity in the evolution equation can generate fluctuations of energy excess which remain frozen in the gravitational field. These do not interact other than gravitationally and behave exactly as a pressureless fluid, mimicking completely the phenomenology of dark matter. It is unclear, however, whether the amount of diffusion needed in the hybrid theory to

generate the entire energy budget of dark matter is already excluded by table-top gravitational experiments.

Chapter 3

Hybrid oscillators

In this chapter we study an exactly solvable CQ system – a classical-quantum oscillator. The first treatment of a classical oscillator interacting with a quantum one appeared in [161]. There, the quantum and classical oscillators did undergo decoherence and diffusion respectively, but there was no damping. As a consequence, the hybrid system heats up indefinitely. A more recent work studied the most general form of the dynamics for the coupled hybrid oscillator that preserves the CQ thermal state – finding that the evolution needs, other than friction in the classical sector, a specific (temperature dependent) type of Lindblad operators that are not generated by simply taking the Poisson brackets from the interaction Hamiltonian [162].

In this chapter, we consider the middle road in between the two approaches. We consider the Hamiltonian CQ evolution for the hybrid system of coupled oscillators. We show that it is sufficient to include friction in the classical system for the evolution to flow univocally towards a hybrid steady-state – which we compute. Such a state is not in equilibrium in general, except in the large diffusion regime, where the dynamics indeed matches the one discussed in [162]. We also present a phase-space representation of CQ dynamics by performing the Wigner-Moyal transform of the hybdrid generator.

Note, that here we use the definition of thermal state as being the canonical Gibbs' state with respect to the Hamiltonian of the system H_{CQ}. That is, the same Hamiltonian generates the equal-time and unequal-time correlations for the system. This is in contrast with looser definition of thermal state, which we do not adopt here, where the Hamiltonian in the Gibbs' state is allowed to be not the system's, but some other – e.g. the "mean-field hamiltonian"

–which usually has to depend on the temperature of the state itself [163].

3.1 The classical case

We begin by considering two coupled – stochastically driven – classical oscillators, of which only one is damped:

$$\begin{aligned} m_1\ddot{q}_1 + \kappa_1 q_1 + \alpha\dot{q}_1 + \lambda(q_1 - q_2) &= \sqrt{D_1}\xi_1 \\ m_2\ddot{q}_2 + \kappa_2 q_2 + \lambda(q_2 - q_1) &= \sqrt{D_2}\xi_2 \ , \end{aligned} \tag{3.1}$$

where $m_{1,2}$ and $\kappa_{1,2}$ are, respectively, the mass and the spring constant of each oscillator. λ, on the other hand, is the coupling constant between the two particles, and α is the friction coefficient. The stochastic forces $\xi_{1,2}$ are white noise processes obeying:

$$\mathbb{E}[\xi_i(t)] = 0 \ , \qquad \mathbb{E}[\xi_i(t)\xi_j(t')] = \delta_{ij}\delta(t - t') \ , \tag{3.2}$$

meaning they are two mean-zero independent processes of unit variance. Physically, we are driving the two masses with independent random kicks of typical size $\sqrt{D_i}$. Recall, we'll intend all the stochastic differential equations in the Itô sense - i.e. the noise process is non-anticipative.

Uncoupled oscillators

Before moving onto the coupled system, it is useful to review the behaviour of a single stochastically driven damped and undamped oscillator. Let's start with the latter:

$$m_2\ddot{q}_2 + \kappa_2 q_2 = \xi_2 \ , \tag{3.3}$$

i.e. an oscillator of natural frequency

$$\omega_2 = \sqrt{\frac{\kappa_2}{m_2}} \tag{3.4}$$

and no friction. It is useful to express this second-order stochastic equation in terms of a first order system introducing the momentum p_2 of the particle:

$$\begin{aligned} \dot{q}_2 - \frac{p_2}{m_2} &= 0 \\ \dot{p}_2 + \kappa_2 q_2 &= \sqrt{D_2}\xi_2 \ . \end{aligned} \tag{3.5}$$

Formally, this is an Ornstein-Uhlenbeck (OU) process – a multidimensional stochastic process of the form:

$$dz^i = -\Theta^i_j z^j \, dt + \Sigma^i_j \, dW^j_t \ , \tag{3.6}$$

where z^i are the components of the vector representing the degrees of freedom of the system whilst $\mathrm{d}W^i_t$ is a vector of independent Wiener increments – here we have assumed, without loss of generality, that the two have the same dimensions. The constant matrices Θ^i_j and Σ^i_j encode the mean dirft of z^i and covariance of the stochastic kicks respectively. For Equation 3.12 they are given by:

$$\mathbf{\Theta} = \begin{pmatrix} 0 & -\frac{1}{m_2} \\ \kappa_2 & 0 \end{pmatrix} \ , \qquad \mathbf{\Sigma} = \begin{pmatrix} 0 & 0 \\ 0 & \sqrt{D_2} \end{pmatrix} \ . \tag{3.7}$$

Intuitively, the system undergoes unbounded diffusion and heats up forever, which can be easily proven using Equation 2.18, Itô's lemma. Applying it to the energy of the particle:

$$H_2 = \frac{p_2^2}{2m_2} + \frac{1}{2}\kappa_2 q_2^2 \tag{3.8}$$

we obtain:

$$\dot{H}_2 = \frac{\sqrt{D_2}}{m_2}\xi_2 + \frac{D_2}{2m_2} \ . \tag{3.9}$$

Note for $D_2 = 0$ the energy of the system stays constant as expected, since the deterministic system is conservative. However, this means that the energy in the stochastic oscillator ($D_2 \neq 0$) is going to increase linearly in time on average:

$$\mathbb{E}[H_2] = H_0 + \frac{\sqrt{D_2}}{m_2} t \ . \tag{3.10}$$

This is a signature that the system does not reach a steady-state, as easily checked using standard results from stochastic systems (and in agreement with expectations). Indeed, for a multidimensional OU process, a steady-state exists if and only if the deterministic system is strongly stable – i.e. the eigenvalues θ_i of Θ^i_j have strictly positive real parts [164]. For Equation 3.12 this is clearly not the case, since they are purely imaginary:

$$\theta_{1,2} = \pm i\omega_2 \ . \tag{3.11}$$

Adding any amount of damping to the system is enough for the oscillator to eventually reach a steady-state. Indeed, consider the damped stochastic oscillator in isolation (in first

order representation):

$$\begin{aligned} \dot{q}_1 - \frac{p_1}{m_1} &= 0 \\ \dot{p}_1 + \frac{\alpha}{m_1} p_1 + \kappa_1 q_1 &= \sqrt{D_1}\xi_1 \ . \end{aligned} \tag{3.12}$$

Studying the evolution of the energy of the system suggests that indeed this system will have a steady-state:

$$\dot{H}_1 = -\frac{\alpha}{m_1^2} p_1^2 + \frac{\sqrt{D_1}}{m_1}\xi_1 + \frac{D_1}{2m_1} \ . \tag{3.13}$$

Note that, here, we are only looking at the single damped oscillator. Taking the expectation value of both sides, we can see that the average energy stops growing when:

$$\mathrm{Var}(p_1) = \frac{D_1}{2\gamma_1} \ . \tag{3.14}$$

In principle, we can use this result together with the equations of motion to extract all the moments of the stochastic degrees of freedom. To show that the system does indeed reach a steady-state, however, it is quicker to note that this is still an OU process in the form of Equation 3.6 with

$$\mathbf{\Theta} = \begin{pmatrix} 0 & -\frac{1}{m_1} \\ \kappa_1 & \frac{\alpha}{m_1} \end{pmatrix} \ , \qquad \mathbf{\Sigma} = \begin{pmatrix} 0 & 0 \\ 0 & \sqrt{D_1} \end{pmatrix} \ . \tag{3.15}$$

The eigenvalues of Θ are then:

$$\theta_{1,2} = \frac{\gamma_1}{2} \pm \frac{1}{2}\sqrt{\gamma_1^2 - 4\omega_1^2} \ . \tag{3.16}$$

They can be completely real or have an imaginary components (corresponding to the over-damped and underdamped regimes respectively), but they have positive real parts for any $\omega_1 \neq 0$ and $\gamma_1 > 0$, where

$$\omega_1 = \sqrt{\frac{\kappa_1}{m_1}} \ , \qquad \gamma_1 = \frac{\alpha}{m_1} \ , \tag{3.17}$$

proving the existence of steady-state formally.

For an OU process, if the steady-state exists then it is Gaussian [164]:

$$P_{st} = (2\pi)^{-N/2} \det(\mathbf{C}_\infty)^{-1/2} \exp\left(\frac{1}{2} z_i (C_\infty^{-1})^i_j z^j\right) \tag{3.18}$$

The equal-time covariance of the OU process $\mathbf{C}^i_{\infty\ j} = \mathrm{cov}(z^i, z^j)$ in such a state can be computed from the Lyapunov equation [164]:

$$\mathbf{\Theta}\mathbf{C}_\infty + \mathbf{C}_\infty \mathbf{\Theta}^T = \mathbf{\Sigma}\mathbf{\Sigma}^T \ . \tag{3.19}$$

For Equation 3.15, this can be readily solved giving:

$$\mathbf{C}_\infty = \frac{D_1}{2\gamma_1}\begin{pmatrix} \frac{1}{m_1\kappa_1} & 0 \\ 0 & 1 \end{pmatrix} , \tag{3.20}$$

which indeed matches the variance of the momentum we calculated earlier, and gives the spread in position for free as well. Equation 3.20 is, of course, just the covariance associated with the thermal state:

$$p(q_1, p_1) = \frac{1}{Z} e^{-\beta H_1} , \tag{3.21}$$

where $\beta = 2\gamma_1 m_1 / D_1$.

3.1.1 Coupling the two classical oscillators

We now re-introduce the spring with constant λ that couples the two systems and analyse the combined behaviour, showing that the two oscillators reach a steady-state nonetheless. Evidence that this is the case is obtained by looking at the average evolution of the energy under Equation 3.1:

$$\mathbb{E}[\dot{H}] = -\frac{\alpha}{m_1^2}\mathrm{Var}(p_1) + \frac{D_1}{2m_1} + \frac{D_2}{2m_2} , \tag{3.22}$$

meaning that the energy stops increasing once the variance in the momentum of the damped oscillator reaches:

$$\mathrm{Var}(p_1) = \frac{1}{2\gamma_1}\left(D_1 + \frac{m_1}{m_2}D_2\right) . \tag{3.23}$$

To make sure the steady-state exist, however, it is enough to know that the evolution of the state vector $\underline{z} = (q_1, p_1, q_2, p_2)$ for the combined system given by Equation 3.1 is in the form of Equation 3.6 where:

$$\mathbf{\Theta} = \begin{pmatrix} 0 & -\frac{1}{m_1} & 0 & 0 \\ \kappa_1 + \lambda & \frac{\alpha}{m_1} & -\lambda & 0 \\ 0 & 0 & 0 & -\frac{1}{m_2} \\ -\lambda & 0 & \kappa_2 + \lambda & 0 \end{pmatrix} , \qquad \mathbf{\Sigma} = \begin{pmatrix} 0 & 0 & 0 & 0 \\ 0 & \sqrt{D_1} & 0 & 0 \\ 0 & 0 & 0 & 0 \\ 0 & 0 & 0 & \sqrt{D_2} \end{pmatrix} . \tag{3.24}$$

We need to show that the eigenvalues of $\mathbf{\Theta}$ are all all strictly positive. To prove it, consider the eigenvalue equation:

$$\theta^4 - \gamma_1\theta^3 + \left(\omega_1^2 + \omega_2^2 + \frac{\lambda}{m_1} + \frac{\lambda}{m_2}\right)\theta^2 - \gamma_1\left(\omega_2^2 + \frac{\lambda}{m_2}\right)\theta + \omega_1^2\omega_2^2 + \omega_2^2\frac{\lambda}{m_1} + \omega_1^2\frac{\lambda}{m_2} = 0 . \tag{3.25}$$

The roots of the characteristic polynomial $P(\theta)$ are analytically solvable for being the solutions of a quartic equation. However, these solutions are extremely complicated expressions in general, so extracting them and requiring positivity of their real part is a very inefficient strategy. Instead, we make use of the Routh-Horowitz criteria [165, 166], i.e. a series of criteria that need to be satisfied for all the solutions of a polynomial of order n to have positive (or, equivalently, negative) real parts. These are more intuitive for the latter case, so we consider $\theta \to -\theta$ and prove that $P(-\theta)$ has solutions with only real negative parts. The first four conditions are equivalent to requiring that all the coefficients of the quartic are positive, which is always true if $\lambda, \gamma_1 > 0$ – a trivial condition. The remaining two criteria can be easily shown to reduce to:

- $\left(\omega_2^2 + \frac{\lambda}{m_2}\right)^2 + \frac{\lambda^2}{m_2^2} > 0$,
- $\frac{\lambda^2}{m_2^2} > 0$,

both trivially satisfied for real couplings. This shows that all the eigenvalues θ_i have positive real parts, meaning that the system will reach a steady-state.

The reason for the existence of the steady-state for any coupling λ is clearer when we explicitly solve (in perturbation theory) for the eigenvalues of the system – we will see that the undamped oscillator develops an effective damping coefficient of order λ^2 due to the interaction. Physically, however, one can see that this has to be the case by a simple thermodynamics argument. The rate at which the energy is added into the system (for both oscillators) is fixed, and depends solely on the diffusion coefficient. However, the energy is extracted by the damped oscillator at a rate that depends on its typical velocity (and, hence, amplitude of oscillation). Since there is energy exchange between the two oscillators, the damped one will heat up until it reaches the typical size of the swings for which it ejects energy at the rate equal to the one at which it is being added to the combined system.

The covariance at equal times can be obtained by solving explicitly the Lyapunov equation.

The variance of the positions and momenta of the two oscillators are given by:

$$\mathbb{E}[p_1^2] = \frac{1}{2\gamma_1}\left(D_1 + \frac{m_1}{m_2}D_2\right) \tag{3.26}$$

$$\mathbb{E}[p_2^2] = \frac{1}{2\gamma_1}\left[D_2\left(1 + \frac{m_1 m_2}{\lambda^2}\left(\left(\omega_1^2 - \omega_2^2 + \frac{\lambda}{m_1} - \frac{\lambda}{m_2}\right)^2 + \gamma_1^2\left(\omega_2^2 + \frac{\lambda}{m_2}\right)\right)\right) + \frac{m_2}{m_1}D_1\right] \tag{3.27}$$

$$\mathbb{E}[q_1^2] = \frac{1}{2\gamma_1}\frac{D_1\left(\frac{\lambda}{m_2} + \omega_2^2\right) + \frac{m_1}{m_2}D_2\left(\frac{\lambda}{m_1} + \omega_1^2\right)}{m_1^2\left(\omega_2^2\frac{\lambda}{m_1} + \omega_1^2\left(\omega_2^2 + \frac{\lambda}{m_2}\right)\right)} \tag{3.28}$$

$$\mathbb{E}[q_2^2] = \frac{1}{2\gamma_1}\frac{1}{m_2^2\left(\omega_2^2\frac{\lambda}{m_1} + \omega_1^2\left(\omega_2^2 + \frac{\lambda}{m_2}\right)\right)}\left[\frac{m_2}{m_1}D_1\left(\omega_1^2 + \frac{\lambda}{m_1}\right) + D_2\frac{m_1 m_2}{\lambda^2}\left(\left(\omega_1^2 + \frac{\lambda}{m_1}\right)^3 + \left(\omega_1^2\left(\omega_2^2 + \frac{\lambda}{m_2}\right) + \omega_2^2\frac{\lambda}{m_1}\right) \times \left(\omega_2^2 - 2\omega_1^2 + \frac{\lambda}{m_2} - 2\frac{\lambda}{m_1} + \gamma_1^2\right)\right)\right] , \tag{3.29}$$

Whilst the non-zero covariances are given by:

$$\mathbb{E}[p_1 p_2] = \frac{D_2}{2\gamma_1}\frac{m_1}{\lambda}\left(\omega_1^2 - \omega_2^2 + \frac{\lambda}{m_1} - \frac{\lambda}{m_2}\right) \tag{3.30}$$

$$\mathbb{E}[q_1 p_2] = -\frac{D_2}{2\lambda} \tag{3.31}$$

$$\mathbb{E}[q_2 p_1] = \frac{D_2}{2\lambda}\frac{m_1}{m_2} \tag{3.32}$$

$$\mathbb{E}[q_1 q_2] = \frac{1}{2\gamma_1}\frac{1}{m_2 m_1}\frac{D_1\frac{\lambda}{m_1} + D_2\frac{m_1}{\lambda}\left(\left(\omega_1^2 + \frac{\lambda}{m_1}\right)^2 - \omega_2^2\frac{\lambda}{m_1} - \omega_1^2\left(\omega_2^2 + \frac{\lambda}{m_2}\right)\right)}{\omega_2^2\frac{\lambda}{m_1} + \omega_1^2\left(\omega_2^2 + \frac{\lambda}{m_2}\right)} \tag{3.33}$$

The steady state variances have been checked numerically for a range of parameters – the stochastic differential equations describing the trajectories of the system in phase space can be straightforwardly simulated with an Euler-Maruyama forward scheme [118].

MSR path integral

We will now take another, more generalisable route, to extract the unequal time two-point functions, by studying the MSR path integral of the process. As we will see, this is exactly solvable in theory, but requiring the roots of a quartic with general coefficients the exact solution

is not illuminating. We will therefore work in the small λ regime for the rest of the chapter and look for a more informative – although approximate – result.

The MSR path intregral representation of the stochastic process in Equation 3.1(integrating out the momenta and working in configuration space) is given by:

$$P(\underline{q}_T) = \int \mathcal{D}\underline{q} \int \mathcal{D}\underline{\tilde{q}} e^{-S[\underline{q},\underline{\tilde{q}}]} P(\underline{x}_0), \tag{3.34}$$

where $\underline{q} = (q_1, q_2)^T$ is the vector state of the system with the position of the oscillators, whilst $\underline{\tilde{q}} = (\tilde{q}_1, \tilde{q}_2)^T$ are the so-called (purely imaginary) response variables. The MSR action for the process is given by:

$$\begin{aligned} S[\underline{q}, \underline{\tilde{q}}] = \int_{t_0}^{T} dt \Big[& \tilde{q}_1 \left(m_1 \partial_t^2 + \kappa_1 + \alpha \partial_t + \lambda \right) q_1 - \frac{D_1}{2} \tilde{q}_1^2 - \lambda \tilde{q}_1 q_2 + \\ & \tilde{q}_2 \left(m_2 \partial_t^2 + \kappa_2 \lambda \right) q_2 - \frac{D_2}{2} \tilde{q}_2^2 - \lambda \tilde{q}_2 q_1 \Big] \ . \end{aligned} \tag{3.35}$$

It is always possible to extend the upper limit of integration to $+\infty$ since observables in unconditional stochastic processes are independent of future evolution. At the same time, if we are interested only in the properties of the steady-state, we can send $t_0 \to -\infty$. The path integral prepares the steady-state in such a limit starting irrespective of the initial state, meaning that the latter can be dropped without loss of generality (we can imagine the system starts diffusing from a delta-function on $q_1 = q_2 = 0$ and zero momenta).

The steady-state of a OU process – if it exists – is Gaussian, and therefore is completely characterised by its mean and covariance. The mean of the process converges to zero in all its variables after sufficiently long times. To compute the unequal time 2-point function of the positions of the two oscillators, being the path integral itself Gaussian, it suffices to invert the kinetic matrix in the MSR action. Indeed:

$$S[z] = \frac{1}{2} \int dt z^i A_i^j z_j \ , \tag{3.36}$$

and, for a Gaussian process, one has:

$$\mathbb{E}[z^i(t) z^j(t')] = [A^{-1}(t,t')]_j^i \equiv (G(t,t'))_j^i \ . \tag{3.37}$$

It is easier to invert the operator in Fourier space and only then Fourier transform back into

t-space. In frequency domain, the operator is given by:

$$\mathbf{G}^{-1}(\omega) = \begin{pmatrix} 0 & m_1\omega^2 + i\alpha\omega - \kappa_1 - \lambda & 0 & \lambda \\ m_1\omega^2 - i\alpha\omega - \kappa_1 - \lambda & -D_1 & \lambda & 0 \\ 0 & \lambda & 0 & m_2\omega^2 - \kappa_2 - \lambda \\ \lambda & 0 & m_2\omega^2 - \kappa_2 - \lambda & -D_2 \end{pmatrix}, \tag{3.38}$$

which can be easily inverted using standard formulas for block 2x2 matrices [167]. The non-zero components are:

$$G_1^1(\omega) = \frac{D_1(m_2\omega^2 - \kappa_2 - \lambda)^2}{|D(\omega)|^2} + \frac{\lambda^2 D_2}{|D(\omega)|^2} \tag{3.39}$$

$$G_2^2(\omega) = \frac{D_2|-m_1\omega^2 + \kappa_1 + \lambda + i\omega\alpha|^2}{|D(\omega)|^2} + \frac{\lambda^2 D_1}{|D(\omega)|^2} \tag{3.40}$$

$$G_2^1(\omega) = \frac{\lambda D_1(-m_2\omega^2 + \kappa_2 + \lambda)}{|D(\omega)|^2} + \frac{\lambda D_2(-m_1\omega^2 + i\omega\alpha + \kappa_1 + \lambda)}{|D(\omega)|^2} = G_1^{2*} \tag{3.41}$$

$$G_{\tilde{1}}^1(\omega) = \frac{m_2\omega^2 - \kappa_2 - \lambda}{D(\omega)^*} = G_1^{\tilde{1}*} \tag{3.42}$$

$$G_{\tilde{2}}^2(\omega) = \frac{m_1\omega^2 - i\omega\alpha - \kappa_1 - \lambda}{D(\omega)^*} = G_2^{\tilde{2}*} \tag{3.43}$$

$$G_{\tilde{1}}^2(\omega) = G_{\tilde{2}}^1(\omega) = -\frac{\lambda}{D(\omega)^*} = G_2^{\tilde{1}*} = G_1^{\tilde{2}*}\ , \tag{3.44}$$

$$\tag{3.45}$$

where

$$D(\omega) = (m_1\omega^2 - i\alpha\omega - \kappa_1 - \lambda)(m_2\omega^2 - \kappa_2 - \lambda) - \lambda^2\ , \tag{3.46}$$

and

$$D(\omega)^* = (m_1\omega^2 + i\alpha\omega - \kappa_1 - \lambda)(m_2\omega^2 - \kappa_2 - \lambda) - \lambda^2\ , \tag{3.47}$$

that is, we conjugate the coefficient only, not the argument. Then $|D(\omega)|^2 \equiv D(\omega)D(\omega)^*$.

The inverse Fourier transform of these frequency-domain two-point function can be easily computed using contour integration, once the roots of the quartic equation with complex coefficients $D(\omega) = 0$ are known. These are in principle possible to find analytically, but they are extremely complicated expression in general. However, some general statements can be made without knowing the exact form of the solutions. First, for contour integration it is crucial to

know the sign of their imaginary part. To see this, consider:

$$D(\theta = i\omega) = \theta^4 - \gamma_1\theta^3 + \left(\omega_1^2 + \omega_2^2 + \frac{\lambda}{m_1} + \frac{\lambda}{m_2}\right)\theta^2 - \gamma_1\left(\omega_2^2 + \frac{\lambda}{m_2}\right)\theta + \omega_1^2\omega_2^2 + \omega_2^2\frac{\lambda}{m_1} + \omega_1^2\frac{\lambda}{m_2} = 0 \ , \quad (3.48)$$

which is the same quartic that appeared in Equation 3.25. We therefore already know that its roots θ_i have strictly positive real parts and that, consequently, the imaginary parts of ω are strictly negative. This means, on the other hand, that the imaginary parts of the solutions to $D(\omega)^*$ are strictly positive. As a consequence, no pole ever lies exactly on the real axis, making the use of Cauchy's residue theorem in the Fourier transform straightforward (no pole prescription is needed).

The structure of the poles for the propagators is such that they can all be generated by two independent complex roots. Let's call:

$$\Omega_1 = \tilde{\omega}_1 + i\tilde{\gamma}_1 \qquad \Omega_2 = \tilde{\omega}_2 + i\tilde{\gamma}_2 \quad (3.49)$$

the two independent roots of $D(\omega)^*$ living in the positive quadrant of the complex plane for some $\tilde{\omega}_1, \tilde{\omega}_2, \tilde{\gamma}_1, \tilde{\gamma}_2 > 0$. Then, we can generate all the other roots of both $D(\omega)$ and $D(\omega)^*$ and, consequently $|D(\omega)|^2$ by a combination of conjugation and reflection about the real axis:

- $\Omega_1, \Omega_2, -\Omega_1^*, -\Omega_2^*$ are solutions to $D(\omega)^*$
- $\Omega_1^*, \Omega_2^*, -\Omega_1, -\Omega_2$ are solutions to $D(\omega)$.

For convenience, we show the pictorial position in the complex plane of the poles in Figure 3.1.

It is useful to find the approximate roots for small coupling. In particular, we know the roots for $\lambda = 0$ – they are simply the eigenvalues of the two coupled systems:

$$\Omega_{1,0} \equiv \Omega_1^{(\lambda=0)} = \sqrt{\omega_1^2 - \frac{\gamma_1^2}{4}} + i\frac{\gamma_1}{2} \qquad \Omega_{2,0} \equiv \Omega_2^{(\lambda=0)} = \omega_2 \ . \quad (3.50)$$

Then, as we deform the system with $\lambda \neq 0$, the roots will receive some small corrections, both real and imaginary (necessarily positively imaginary in the case of Ω_2 as shown earlier). We can easily work out what that will be by expanding:

$$\Omega_i = \Omega_i^{(0)} + \lambda\Omega_i^{(1)} + \lambda^2\Omega_i^{(2)} + \mathcal{O}(\lambda^3) \equiv \Omega_i^{(0)} + \delta\Omega_i \quad (3.51)$$

and requiring $D(\Omega_i) = 0$, to hold up to quadratic order in λ we obtain:

$$\delta\tilde{\omega}_1 = \frac{\lambda}{2m_1\sqrt{\omega_1^2 - \frac{\gamma_1^2}{4}}}\left[1 + \frac{\lambda}{m_2\left((\omega_1^2-\omega_2^2)^2+\gamma_1^2\omega_2^2\right)}\left(\omega_1^2 - \omega_2^2 - \frac{\gamma^2}{2} - \frac{m_2}{4m_1}\frac{\gamma^2\omega_2^2 + (\omega_1^2-\omega_2^2)^2}{\omega_1^2 - \frac{\gamma^2}{4}}\right)\right] \tag{3.52}$$

$$\delta\tilde{\gamma}_1 = -\frac{\lambda^2}{2m_1m_2\left((\omega_1^2-\omega_2^2)^2+\gamma_1^2\omega_2^2\right)}\gamma_1 \tag{3.53}$$

$$\delta\tilde{\omega}_2 = \frac{\lambda}{2m_2\omega_2}\left[1 - \frac{\lambda}{m_1\left((\omega_1^2-\omega_2^2)^2+\gamma_1^2\omega_2^2\right)}\left(\frac{m_1}{4m_2}\frac{\left((\omega_1^2-\omega_2^2)^2+\gamma_1^2\omega_2^2\right)}{\omega_2^2} + \omega_1^2 - \omega_2^2\right)\right] \tag{3.54}$$

$$\delta\tilde{\gamma}_2 = \frac{\lambda^2}{2m_1m_2\left((\omega_1^2-\omega_2^2)^2+\gamma_1^2\omega_2^2\right)}\gamma_1 \ , \tag{3.55}$$

A good sanity check is that the imaginary component of Ω_2 is indeed positive. More importantly, corrections linear in λ only shift the poles along the real axis, whilst the corrections to the imaginary components come only at second order in λ. Naturally, by small λ we really mean that the frequencies associated with the interaction spring are much smaller than the natural frequencies of the two oscillators:

$$\frac{\lambda^2}{m_1m_2} \ll \omega_1\omega_2\gamma_1^2 \ . \tag{3.56}$$

For identical oscillators (i.e. $m_1 = m_2 = m_*$ and $\omega_1 = \omega_2 = \omega_*$) the corrections reduce to:

$$\delta\tilde{\omega}_1 = \frac{\lambda}{2m_*\sqrt{\omega_*^2 - \frac{\gamma_1^2}{4}}}\left(1 - \frac{\lambda}{2m_*\omega_*^2}\left(1 + \frac{1}{2}\frac{\omega_*^2}{\omega_*^2 - \frac{\gamma_1^2}{4}}\right)\right) \tag{3.57}$$

$$\delta\tilde{\gamma}_1 = -\frac{\lambda^2}{2m_*^2\gamma_1\omega_*^2} \tag{3.58}$$

$$\delta\tilde{\omega}_2 = \frac{\lambda}{2m_*\omega_*}\left(1 - \frac{\lambda}{4m_*\omega_*^2}\right) \tag{3.59}$$

$$\delta\tilde{\gamma}_2 = \frac{\lambda^2}{2m_*^2\gamma_1\omega_*^2} = -\delta\tilde{\gamma}_1 \ , \tag{3.60}$$

To illustrate the behaviour of the system, we will focus on the small (yet finite) λ limit. When performing the inverse Fourier transform of the two-point function, it is important to keep in mind that the residues of $|D(\omega)|^2$ for the Ω_2 poles are of order λ^{-2}, as this is the scaling of the difference between such pole and their complex conjugate. This is since they have no finite imaginary part in the $\lambda \to 0$ limit. It will result in the two-point functions having some leading order λ^{-n} terms – a signature of the fact that for vanishing coupling the system does not have a steady-state. Again, it is in principle possible to compute the general solutions explicitly

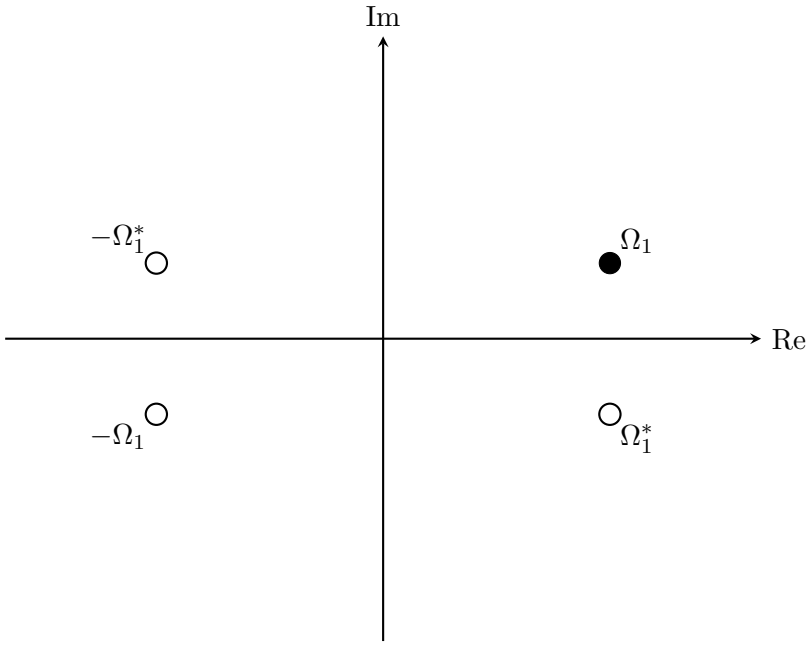

Figure 3.1: The Ω_1 pole and its reflections in the complex plane.

in terms of the roots of $D(\omega)$, but we refrain from reporting them as their are cumbersome and not particularly illuminating.

Performing the Fourier transform and keeping only terms leading order in λ that do not vanish in the $\lambda \to 0$ limit we obtain the following non-vanishing correlators:

$$G_1^1(t) = \frac{1}{2\gamma_1\omega_*^2 m_*^2}\left[D_1 e^{-\frac{\gamma_1}{2}|t|}\left(\cos\left(\sqrt{\omega_*^2 - \frac{\gamma_1^2}{4}}|t|\right) + \frac{\gamma_1}{2\sqrt{\omega_*^2 - \frac{\gamma_1^2}{4}}}\sin\left(\sqrt{\omega_*^2 - \frac{\gamma_1^2}{4}}|t|\right)\right) + D_2\cos(\omega_*|t|)\right] \tag{3.61}$$

$$G_2^2(t) = \frac{D_2}{2}\frac{\gamma_1}{\lambda^2}\cos(\omega_*|t|) \tag{3.62}$$

$$G_2^1(t) = \frac{D_2}{2}\frac{1}{\lambda\omega_* m_*}\sin(\omega_*|t|) = G_1^2(t) \tag{3.63}$$

$$G_{\tilde{1}}^1(t) = \frac{1}{m_*}\frac{e^{\frac{\gamma_1}{2}t}}{\sqrt{\omega_*^2 - \frac{\gamma_1^2}{4}}}\sin\left(\sqrt{\omega_*^2 - \frac{\gamma_1^2}{4}}t\right)\theta(-t) = G_1^{\tilde{1}}(-t) \tag{3.64}$$

$$G_{\tilde{2}}^2(t) = \frac{1}{m_*}\sin(\omega_* t)\theta(-t) = G_2^{\tilde{2}}(-t) \tag{3.65}$$

where we have defined

$$G_j^i(t) = \mathbb{E}[z^i(\tau)z^j(\tau+t)]\ . \tag{3.66}$$

An important check is that they match the equal-time covariances match Equations 3.26 to 3.33, which were obtained from solving the Lyapunov equation instead. Note that the covariance $q_1 q_2$ in Equation 3.33 goes to zero in the case of equal mass and coupling.

A few interesting properties emerge. First of all, the ratio between the typical size of the oscillations in the first spring with respect to the second one depends linearly on the coupling constant:

$$\frac{\sigma_1}{\sigma_2} = \sqrt{\frac{G_1^1(0)}{G_2^2(0)}} = \frac{\lambda}{\gamma_1 m_*}\sqrt{1 + \frac{D_1}{D_2}} \tag{3.67}$$

Secondly, and more curiously, the covariance between the displacement of the first oscillator at different times for time intervals greater than the typical decay time of its fluctuations $t \gtrapprox 1/\gamma_1$ is long-lived and completely dominated by effects due to the second oscillator even at leading order in λ:

$$G_1^1(t) \to \frac{D_2}{2}\frac{1}{\gamma_1 \omega_*^2 m_*^2}\cos(\omega_* |t|) \ . \tag{3.68}$$

This reflects a key behaviour of the steady-state: the two oscillators synchronise. This is due to the fact that the anti-symmetric normal mode in which the two oscillators will be out-of-phase with each others will have a larger damping coefficient than the in-phase relative motion, leading over time to synchronisation. Of course, in general, the stochastic perturbation will excite both modes, but the out-of-phase will always dies quicker. This means that the in-phase mode dominates the steady-state distribution if one coarse-grains on time-scales larger than the decay time of the damped oscillator. The fact that the two oscillators are synchronised is even more obvious when one looks at the mutual information between q_1 and q_2. Recalling that the probability distribution on the combined state is Gaussian, this is trivially given by:

$$I_{ij}(t) \equiv I(x_i(\tau), x_j(\tau + t)) = -\frac{1}{2}\log\left(1 - r_{ij}(t)^2\right) \ , \tag{3.69}$$

where r_{ij} is the correlation between the two sytems:

$$r_{ij}(t) = \frac{C_j^i(t)}{\sqrt{C_i^i(0) C_j^j(0)}} \ . \tag{3.70}$$

where the correlation functions are explicitly given by:

$$r_{11} = \frac{1}{1+\frac{D_1}{D_2}}\left[\cos(\omega_* t) + \frac{D_1}{D_2}e^{-\frac{\gamma_1}{2}|t|}\left(\cos\left(\sqrt{\omega_*^2 - \frac{\gamma_1^2}{4}}|t|\right)\right.\right. \tag{3.71}$$
$$\left.\left. + \frac{\gamma_1}{2\sqrt{\omega_*^2 - \frac{\gamma_1^2}{4}}}\sin\left(\sqrt{\omega_*^2 - \frac{\gamma_1^2}{4}}|t|\right)\right)\right]$$

$$r_{22} = \cos(\omega_* t) \tag{3.72}$$

$$r_{12} = \frac{1}{\sqrt{1+\frac{D_1}{D_2}}}\cos(\omega_* t)\ . \tag{3.73}$$

It is interesting to focus on the behaviour of the mutual information for the displacement of the damped oscillator at different times. Initially, it decays in magnitude until it asymptotes an oscillatory behaviour:

$$\lim_{t\to\infty} I_{11} = -\frac{1}{2}\log\left[1 - \frac{\cos^2(\omega_* t)}{\left(1+\frac{D_1}{D_2}\right)^2}\right]\ . \tag{3.74}$$

This shows that information is scrambled about the position of the first oscillator after the half-life $1/\gamma_1$. After that, however, the mutual information between two observations oscillate between 0 and some positive value set by the ratio of the two diffusion coefficients with period ω_*. A similar functional dependence appears in I_{12}. This elucidates the fact that whilst the damped oscillator synchronises and vibrates at the natural frequency of the frictionless one in the steady-state, its dynamics is less regular that its counterpart. That is, if the diffusion coefficient of the first oscillator is large enough. Indeed, in the $D_1/D_2 \to 0$ limit, both I_{11} and I_{12} asymptote to I_{22} – the relative states of the two oscillators in the steady-state become completely deterministic.

3.2 The classical-quantum case

Having analysed the system when both oscillators are classical, from the existence of the steady-state to its properties in the small coupling regime, we now study the classical-quantum case. In particular, we quantise the frictionless oscillator, in the attempt to answer the question of whether classical friction is enough for the combined CQ system to reach a steady-state. This is of interest especially in the case of effective CQ theories, where the quantum system is well

isolated except for the interaction with the classical one, whose classicality is effective and comes from the interaction with some bath. If thermal, implies the presence of classical friction via the fluctuation-dissipation relations.

We tackle the problem from the path-integral formulation of the dynamics. For a classical oscillator with displacement q coupled to a quantum one with displacement Q, we have that the proto-action encoding the CQ interaction is given by:

$$\mathcal{W}_{CQ} = -\frac{\lambda}{2}(q-Q)^2 \ . \tag{3.75}$$

Then, in the L/R basis for the quantum system, the action I_{CQ} for the hybrid path integral is given by:

$$\begin{aligned} I_{CQ} = \int_0^T dt \Bigg[i \left(\frac{1}{2} m_Q \left(\dot{Q}_L^2 - \dot{Q}_R^2 \right) - \frac{1}{2}\kappa_Q \left(Q_L^2 - Q_R^2 \right) - \left(\frac{\lambda}{2}(q-Q_L)^2 - \frac{\lambda}{2}(q-Q_R)^2 \right) \right) \\ - \frac{D_0}{2}\lambda^2 (Q_L - Q_R)^2 - \tilde{q}(m_C \partial_t^2 + \alpha \partial_t + \kappa_C + \lambda) q + \frac{D}{2}\tilde{q}^2 + \frac{\lambda}{2}\tilde{q}(Q_L + Q_R) \Bigg] \ , \end{aligned} \tag{3.76}$$

with $m_{Q,C}$ and $\kappa_{Q,C}$ being respectively the masses and coupling constants of the classical and quantum springs. As before, λ is the coupling constant between the two oscillators and α the friction coefficient of the classical system. Finally, D and D_0 are, respectively, the diffusion coefficient for the classical oscillator and the decoherence rate in the quantum one.

It is useful to expand the coupling term in the unitary part of the quantum action:

$$\begin{aligned} I_{CQ} = \int_0^T dt \Bigg[i \left(\frac{1}{2} m_Q \left(\dot{Q}_L^2 - \dot{Q}_R^2 \right) - \frac{1}{2}\kappa_Q \left(Q_L^2 - Q_R^2 \right) + \lambda q (Q_L - Q_R) \right) - \frac{D_0}{2}\lambda^2 (Q_L - Q_R)^2 \\ - \tilde{q}(m_C \partial_t^2 + \alpha \partial_t + \kappa_C + \lambda) q + \frac{D}{2}\tilde{q}^2 + \frac{\lambda}{2}\tilde{q}(Q_L + Q_R) \Bigg] \ . \end{aligned} \tag{3.77}$$

It is suggestive that only the average of the left and right branches of the path integral acts as a source to the classical system, whilst the difference appears to couple to the classical system in the quantum sector of the path integral. Indeed, moving to the average-difference basis (suggestively also known as the classical-quantum basis, but we'll avoid that nomenclature to minimise confusion):

$$Q_+ = \frac{Q_L + Q_R}{2} \ , \qquad Q_- = Q_L - Q_R \ , \tag{3.78}$$

one obtains the suggestive action:

$$I_{CQ} = \int_0^T dt \Big[-iQ_- \left(m_Q \partial_t^2 + \kappa_Q + \lambda \right) Q_+ - \frac{D_0}{2} \lambda^2 q_-^2 + i\lambda q Q_- \\ -\tilde{q}(m_C \partial_t^2 + \alpha \partial_t + \kappa_C + \lambda) q + \frac{D}{2} \tilde{q}^2 + \lambda \tilde{q} Q_+ \Big] \ . \quad (3.79)$$

where we have integrated by parts the kinetic term in the unitary sector of the action. This transformation elucidates a symmetry between the classical and quantum sectors of the hybrid system. Indeed, recall that the response variable $\tilde{q}$ in the MSR formalism is a purely imaginary auxiliary field. Making it explicit via the transformation $\tilde{q} \to i\tilde{q}$, we see that the average degree of freedom Q_+ is in exact correspondence with the classical displacement q, whilst Q_- plays the role of the response variable. Of course, this is just a mathematical equivalence in the propagator of the theory: the reduced states of the classical and quantum systems will be a probability distribution and a density matrix respectively.

This arises due to a well-known equivalence between Lindblad evolution and Fokker-Planck equations in the case of Gaussian-preserving dynamics. Indeed, for quadratic potentials and Lindblad operators at most linear in P and Q (where P is the conjugate momentum of a quantum particle with position Q) the evolution of the Wigner quasi-probability distribution representing the state of the system in phase-space follows exactly a Fokker-Planck-like equation. Introducing anharmonicities breaks this nice symmetry bewteen diffusive and Lindbladian dynamics [168, 169]. This is since, as se show explicitly in Section 3.3, the quantum sector of the dynamics can be mapped exactly to a classical stochastic processes (modulo constraints on the initial state) if and only if the potential is at most quadratic in the generalised position of the system. As soon as the potential has a power expansion that goes beyond the quadratic term, such a mapping becomes at best approximative – and only allowed in a region of phase space where the potential is effectively harmonic. Still, when the path integral is Gaussian, the Hubbard-Stratonovich transformation allows for an exact mapping between the classical stochastic evolution and the Lindbladian one. This is a powerful result, as it allows to use the properties of the equivalent diffusive generator to compute the steady-state of the quantum system [170]. We will return to this point more formally in Section 3.3

This simplifies greatly the problem: we can use all the results from our classical-classical

system, under the mapping

$$\tilde{q}_2 \to iQ_- \ , \qquad q_2 \to Q_+ \ , \qquad D_2 \to D_0\lambda^2 \ , \qquad D_1 \to D. \tag{3.80}$$

If the backreaction is non-zero ($\lambda \neq 0$), the decoherence diffusion trade-off requires $4DD_0 \geq 1$. We choose to saturate the trade-off setting $D_0 = 1/4D$ – the special case of hybrid dynamics in which the quantum state remains pure conditioned on the classical trajectory. Most importantly, we can conclude that the combined system reaches a steady-state, meaning that we can extend the limits of integration in the CQ action of Equation 3.79 to past and future infinity, preparing the asymptotic state. What changes is the interpretation of the correlators and how they map to physical observables.

Occupation number

Much like in the classical systems, the correlations between Q_- and Q_+ encode both correlations and the response of the system to external perturbations. In particular [171]:

$$\langle Q_+(t)Q_+(t')\rangle \equiv G^K(t,t') \ , \tag{3.81}$$

$$\langle Q_-(t)Q_+(t')\rangle \equiv iG^A(t,t') \ , \tag{3.82}$$

$$\langle Q_+(t)Q_-(t')\rangle \equiv iG^R(t,t') \ , \tag{3.83}$$

$$\langle Q_-(t)Q_-(t')\rangle = 0 \ . \tag{3.84}$$

The fact that the insertion of the difference field Q_- computes the perturbation to the system due to the external source can be understood in terms of the observation that a real external source is physical and therefore equal on the L and R branches. However, by performing the Keldysh rotation at the level of the source, it is straightforward to see that Q_+ couples to the difference of the sources J_- and vice-versa. Therefore, differentiating with respect to the physical source brings down a factor of Q_-.

Whilst the off-diagonal components of the quantum Green's function encode the response of the system to external perturbations, the Keldysh propagator G^K encodes the correlations in the system. In particular, introducing the usual bosonic raising $a^\dagger$ and lowering a operators, it is straighforward to see that the equal-time Keldysh Green's function computes the average

occupation of the oscillator:

$$G^K(t,t) = \frac{1}{m_Q \omega_Q}\left(N + \frac{1}{2}\right) \ , \tag{3.85}$$

with N being the expectation value of the number operator $aa^\dagger$.

The non-zero correlator $\langle\langle \tilde{q} Q_+ \rangle\rangle$ (where double-angled brackets indicate quantum *and* classical expectation value) econde instead the response in the quantum degrees after a perturbation to the classical system, and vice-versa for $\langle\langle q Q_- \rangle\rangle$. The decoherence-diffusion trade-off forced the decoherence coefficient to have quadratic dependence on λ, meaning that with respect to the classical results the relative weights of certain terms is shifted towards the ones involving the classical oscillator only. Indeed, keeping only leading terms up to order λ^0, the non-zero correlators are given by:

$$\begin{aligned}\langle\langle q(0)q(t)\rangle\rangle = \frac{1}{2\gamma_1 \omega_*^2 m_*^2}\Bigg[& D e^{-\frac{\gamma_1}{2}|t|}\left(\cos\left(\sqrt{\omega_*^2 - \frac{\gamma_1^2}{4}}|t|\right)\right. \\ & \left. + \frac{\gamma_1}{2\sqrt{\omega_*^2 - \frac{\gamma_1^2}{4}}}\sin\left(\sqrt{\omega_*^2 - \frac{\gamma_1^2}{4}}|t|\right)\right)\Bigg]\end{aligned} \tag{3.86}$$

$$\langle\langle Q_+(0)Q_+(t)\rangle\rangle = \left(\frac{\gamma_1}{8D} + \frac{D}{2\gamma_1 \omega_*^2 m_*^2}\right)\cos(\omega_*|t|) \tag{3.87}$$

$$\langle\langle q(0)\tilde{q}(t)\rangle\rangle = \frac{1}{m_*}\frac{e^{\frac{\gamma_1}{2}t}}{\sqrt{\omega_*^2 - \frac{\gamma_1^2}{4}}}\sin\left(\sqrt{\omega_*^2 - \frac{\gamma_1^2}{4}}t\right)\theta(-t) \tag{3.88}$$

$$\langle\langle Q_+(0)Q_-(t)\rangle\rangle = -\frac{i}{m_*}\sin(\omega_* t)\theta(-t) \tag{3.89}$$

Note that, contrary to the classical-classical case, there are no divergences when $\lambda \to 0$, since saturating the decoherence-diffusion trade-off implies that the decoherence (and hence the energy increase) in the quantum state vanishes when the two systems decouple.

The energy in the quantum system is independent (to leading order) of the coupling constant between the two oscillators – again a result of the decoherence-diffusion trade-off. Specifically, in analogy with the classical-classical case, the typical size of the oscillation in the quantum system would be $Q_+^2 \sim D_0/\lambda^2$ (since the induced friction is of quadratic order in the coupling constant), where D_0 is the decoherence strength – effectively the diffusion constant in the quantum oscillator. However, the decoherence diffusion trade-off forces $D_0 \sim \lambda^2$, meaning that the two dependences on λ cancel each other, giving an order 1 effect irrespective of the coupling

strength. We see that two terms contribute to its average energy (essentially Q_+^2, the Keldysh propagator at equal times). The first one is direct decoherence in the system, controlled by $1/D$; the second one is linear in D and is a result of the *secondary* decoherence coming from the diffusion in the classical oscillator. Defining the effective temperature of the classical system to be:

$$T_C = \frac{D}{2\alpha} = \frac{D}{2\gamma_1 m_*} \tag{3.90}$$

we see that we can re-express the average number of excitations in the quantum system as

$$N = \frac{1}{2}\left(\frac{\omega_*}{2T_C} + \frac{2T_C}{\omega_*} - 1\right) \ . \tag{3.91}$$

The first thing to note is that the quantum oscillator can never be empty of excitations. Tuning the temperature of the classical system to be the critical value $T_C^{crit} = \omega_*/2$ we can drive the quantum system to the lowest energy configuration allowed, namely the one that has $N_{min} = 1/2$. In the large diffusion regime (i.e. when the classical oscillator is much hotter than the zero-point energy of the quantum one), the direct decoherence is negligible and the energy in the classical and quantum oscillators exactly match to leading order in λ. In fact, we have that $N \approx T_C/\omega_*$, meaning that the quantum oscillator thermalises to T_C as well.

We have used the correlations computed from the MSR path integral to find the two-point functions of the hybrid system to leading order in λ (again, the system is in principle exactly solvable, but the roots of the quartic are extremely complicated and not at all illuminating). However, if we are only interested in equal-time *correlations* – that is we only care about symmetrised observables in the quantum system at equal times – we can use the exact covariance computed from Equation 3.19 (after appropriate rescalings of the coefficients). To see that the evolution of the average observables Q_+ is described by Equation 3.1, we need to find the equation of motion for the conjugate momentum P_+. It suffices to take the momentum part of the full Schwinger-Keldysh action (the purely quantum sector of the CQ action) and perform the rotation in the average-difference basis before integrating out P:

$$\begin{aligned} S_{SK}[Q_L, P_L, Q_R, P_R] &= i\left[P_L\dot{Q}_L - \frac{P_L^2}{2m_Q} - P_R\dot{Q}_R + \frac{P_R^2}{2m_Q}\right] + ... \\ &= i\left[P_-\left(\dot{Q}_+ - \frac{P_+}{m_Q}\right) + P_+\dot{Q}_-\right] + ... \ . \end{aligned} \tag{3.92}$$

Integration over P_- then sets $P_+ = m_Q\dot{Q}_+$, and complete equivalence follows.

The non-zero equal-time two-point functions of the hybrid state are given by:

$$\langle\langle p^2\rangle\rangle = \frac{1}{2\gamma_1}\left(D + \frac{m_C}{m_Q}\frac{\lambda^2}{4D}\right) \tag{3.93}$$

$$\langle\langle P^2\rangle\rangle = \frac{1}{2\gamma_1}\left[\frac{\lambda^2}{4D}\left(1 + \frac{m_C m_Q}{\lambda^2}\left(\left(\omega_C^2 - \omega_Q^2 + \frac{\lambda}{m_C} - \frac{\lambda}{m_Q}\right)^2 + \gamma_1^2\left(\omega_Q^2 + \frac{\lambda}{m_Q}\right)\right)\right) + \frac{m_Q}{m_C}D\right] \tag{3.94}$$

$$\langle\langle q^2\rangle\rangle = \frac{1}{2\gamma_1}\frac{D\left(\frac{\lambda}{m_Q} + \omega_Q^2\right) + \frac{m_C}{m_Q}\frac{\lambda^2}{4D}\left(\frac{\lambda}{m_C} + \omega_C^2\right)}{m_C^2\left(\omega_Q^2\frac{\lambda}{m_C} + \omega_C^2\left(\omega_Q^2 + \frac{\lambda}{m_Q}\right)\right)} \tag{3.95}$$

$$\langle\langle Q^2\rangle\rangle = \frac{1}{2\gamma_1}\frac{1}{m_Q^2\left(\omega_Q^2\frac{\lambda}{m_C} + \omega_C^2\left(\omega_Q^2 + \frac{\lambda}{m_Q}\right)\right)}\left[\frac{m_Q}{m_C}D\left(\omega_C^2 + \frac{\lambda}{m_C}\right) + \frac{m_C m_Q}{4D}\left(\left(\omega_C^2 + \frac{\lambda}{m_C}\right)^3 + \left(\omega_C^2\left(\omega_Q^2 + \frac{\lambda}{m_Q}\right) + \omega_Q^2\frac{\lambda}{m_C}\right) \times \left(\omega_Q^2 - 2\omega_C^2 + \frac{\lambda}{m_Q} - 2\frac{\lambda}{m_C} + \gamma_1^2\right)\right)\right] \tag{3.96}$$

$$\langle\langle qQ\rangle\rangle = \frac{1}{2\gamma_1}\frac{m_C}{m_Q}\frac{D\frac{\lambda}{m_C} + \frac{m_C\lambda}{4D}\left(\left(\omega_C^2 + \frac{\lambda}{m_C}\right)^2 - \omega_Q^2\frac{\lambda}{m_C} - \omega_C^2\left(\omega_Q^2 + \frac{\lambda}{m_Q}\right)\right)}{\omega_Q^2\frac{\lambda}{m_C} + \omega_C^2\left(\omega_Q^2 + \frac{\lambda}{m_Q}\right)} \tag{3.97}$$

$$\langle\langle Pq\rangle\rangle = -\frac{\lambda}{8D} \tag{3.98}$$

$$\langle\langle pQ\rangle\rangle = \frac{\lambda}{8D}\frac{m_C}{m_Q} \tag{3.99}$$

$$\langle\langle pP\rangle\rangle = \frac{\lambda}{8D\gamma_1}m_C\left(\omega_C^2 - \omega_Q^2 + \frac{\lambda}{m_C} - \frac{\lambda}{m_Q}\right) \ . \tag{3.100}$$

Thermal limit

In [162], the temperature-dependent hybrid dynamics that preserves the CQ thermal state at any β was derived – and a CQ oscillator was studied as a toy model. In that work, the authors find that, in order to preserve the thermal state, a temperature-dependent decoherence in P is required. Still, in the high-temperature limit the momentum decoherence term drops out, and their dynamics coincides with ours – meaning that the model we discuss must flow to the CQ thermal state in the high-temperature regime as well – as we now straightforwardly show.

A large effective temperature for the classical system at fixed γ_1 corresponds to the high

diffusion limit. At large D, the non-zero 2-point functions are

$$\langle\langle p^2\rangle\rangle = m_C T_C \tag{3.101}$$

$$\langle\langle P^2\rangle\rangle = m_Q T_C \tag{3.102}$$

$$\langle\langle q^2\rangle\rangle = \frac{T_C}{m_C}\left(\frac{\omega_Q^2\frac{\lambda}{m_C}}{\frac{\lambda}{m_Q}+\omega_Q^2}+\omega_C^2\right)^{-1} \tag{3.103}$$

$$\langle\langle Q^2\rangle\rangle = \frac{T_C}{m_Q}\left(\frac{\omega_C^2\frac{\lambda}{m_Q}}{\frac{\lambda}{m_C}+\omega_C^2}+\omega_Q^2\right)^{-1} \tag{3.104}$$

$$\langle\langle qQ\rangle\rangle = \frac{T_C}{m_Q}\left(\omega_Q^2+\frac{m_C\omega_C^2}{\lambda}\left(\omega_Q^2+\frac{\lambda}{m_Q}\right)\right)^{-1} \tag{3.105}$$

It is straightforward to see that in the high temperature regime the correlations converge exactly towards those of the thermal state:

$$\varrho_\beta(q,p) = \frac{1}{\mathcal{Z}}e^{-\beta H(q,p)}\ , \tag{3.106}$$

with $\beta = 1/T_C$ as $\beta \to 0$. In that limit the hybrid thermal state limits the classical one, and the correlations can be easily extracted from the Gaussian state without worrying about the discreteness of the energy levels in the quantum system. That is, the partition function of the quantum oscillator is well-approximated by the classical one.

3.3 CQ in phase space

The dynamical equivalence between the CQ and the CC stochastic oscillators is not a coincidence. As mentioned, it is just an extension of the statement that classical and quantum generators are equivalent for harmonic potentials. To see this more explicitly, let's introduce the phase-space description of CQ dynamics by peforming a Wigner-Moyal transform, in the spirit of [168]. For simplicity, we restrict to minimal CQ dynamics of the form of Equation 2.57. We further take the CQ Hamiltonian to be Hermitian and the quantum degree of freedom being described by a single point-particle. Extensions to higher-dimensional Hilbert space and more general CQ evolution are conceptually trivial.

The Wigner-Moyal transform assigns to every classical phase-space dependent operator $\hat{A}(z)$ (we introduce hats for operators and powers of $\hbar$ in this section to minimise confusion) a function

over the combined phase space $\mathcal{M}_C \times \mathcal{M}_Q$

$$\mathcal{W}\left[\hat{A}(z)\right] = A(z,Q,P) = \int dZ e^{ipZ/\hbar} \langle Q - Z/2|\hat{A}(z)|Q + Z/2\rangle \ , \tag{3.107}$$

where P and Q are the position and momentum respectively of the quantum particle, whilst $|Q\rangle$ is its position eigenstate with eigenvalue Q. The classical phase space dependence of the operators does not add any complication here. The Wigner-Moyal transform of the CQ state then corresponds to the hybrid Wigner quasi-probability distribution W

$$\mathcal{W}\left[\frac{1}{2\pi\hbar}\hat{\varrho}(z)\right] = W(z,P,Q) \ , \tag{3.108}$$

where the numerical factor is needed to appropriately normalise the state, since

$$\int dQ \int dP \ \mathcal{W}\left[\hat{A}(z)\right] = 2\pi\hbar \mathrm{Tr}[\hat{A}(z)] \ . \tag{3.109}$$

This is just the usual Wigner function. The twist is that it is subnormalised on the quantum phase-space, and it has classical-phase space dependence.

The time evolution of the hybrid phase-space state W is given by the Wigner-Moyal transform of Equation 2.57, the evolution map of the CQ state. In order to compute what that is in phase space, it is useful to keep in mind the following

$$\begin{aligned} \mathcal{W}\left[\hat{A}(z)\hat{B}(z)\right] &= A(z,Q,P) \exp\left(\frac{\hbar\Lambda}{2i}\right) B(z,Q,P) \\ &= B(z,Q,P) \exp\left(-\frac{\hbar\Lambda}{2i}\right) A(z,Q,P) \ , \end{aligned} \tag{3.110}$$

where the differential operator Λ is essentially the negative of the Poisson brackets

$$\Lambda = \partial_P^{\leftarrow}\partial_Q^{\rightarrow} - \partial_Q^{\leftarrow}\partial_P^{\rightarrow} \ , \tag{3.111}$$

with the arrow indicating what the derivative acts on. It then follows that the Wigner transform of the commutator is (from now on we drop the phase space dependence for notational economy)

$$\mathcal{W}\left[[\hat{A}(z),\hat{B}(z)]\right] = -2i \ A \sin\left(\frac{\hbar\Lambda}{2}\right) B \ , \tag{3.112}$$

whilst for the anticommutator we obtain

$$\mathcal{W}\left[\{\hat{A}(z),\hat{B}(z)\}_+\right] = 2 \ A \cos\left(\frac{\hbar\Lambda}{2}\right) B \ . \tag{3.113}$$

Using these relations, we can easily see that the reversible part of the CQ evolution equation, the Aleksandrov brackets, gets mapped to

$$\frac{1}{2\pi\hbar}\mathcal{W}\left[\{H_{CQ},\varrho\}_A\right] = \left\{H_C + V_I\cos\left(\frac{\hbar\Lambda}{2}\right), W\right\} - \frac{2}{\hbar}H_Q\sin\left(\frac{\hbar\Lambda}{2}\right)W \tag{3.114}$$

Here we have often used that the Wigner-Moyal transformation commutes with derivatives with respect to the classical degrees of freedom z. Note that, in the $\hbar \to 0$ limit, this is exactly the classical Liouville equation

$$\frac{1}{2\pi\hbar}\mathcal{W}\left[\{H_{CQ},\varrho\}_A\right] = \{H_C + V_I + H_Q, W\} + \mathcal{O}(\hbar)^2 \ , \tag{3.115}$$

as required for consistency. For the minimal models we consider, that is where the CQ interaction potential only involves generalised positions of the hybrid system ($V_I = V_I(q,Q)$) and similarly the quantum Hamiltonian is given by $H_Q = P^2/2m_Q + V_Q(Q)$, we can expand Equation 3.114 as

$$\begin{aligned}\frac{1}{2\pi\hbar}\mathcal{W}\left[\{H_{CQ},\varrho\}_A\right] = &\{H_C + V_I + H_Q, W\} \\ &+\sum_{n=1}^{\infty}(-1)^n\left(\frac{\hbar}{2}\right)^{2n}\left[\frac{1}{2n!}\frac{\partial^{2n}}{\partial Q^{2n}}\left(\frac{\partial V_I}{\partial q^i}\right)\frac{\partial^{2n}}{\partial P^{2n}}\left(\frac{\partial W}{\partial p_i}\right)\right. \\ &\left.+\frac{1}{(2n+1)!}\frac{\partial^{2n+1}U}{\partial Q^{2n+1}}\frac{\partial^{2n+1}W}{\partial P^{2n+1}}\right] \ .\end{aligned} \tag{3.116}$$

This explicitly shows that, if $H_Q + V_I$ is at most harmonic, the reversible part of the dynamics is equivalent to the classical evolution – generalising the standard quantum result to CQ systems. This is since the tower of derivatives vanishes identically for any value of $\hbar$.

What about the dissipative contribution instead? The Wigner-Moyal representation of the diffusive term is trivial, again because the map commutes with the derivatives with respect to z. On the other hand, the decoherence term is essentially equivalent to what has been computed in [168], under the appropriate rescalings, modulo the classical phase-space dependence. Indeed it is easy to show that

$$\frac{1}{2\pi\hbar}\mathcal{W}\left[\mathbf{D}[\varrho]\right] = \frac{1}{2}\frac{\partial^2}{\partial p_i \partial p_j}\left(D_{2,ij}\ W\right) + 2D_0^{ij}\frac{\partial V_I}{\partial q^i}\sin\left(\frac{\hbar\Lambda}{2}\right)\frac{\partial V_I}{\partial q^j}\sin\left(\frac{\hbar\Lambda}{2}\right)W \ . \tag{3.117}$$

Again, this can be expanded in powers of $\hbar$ in terms of an infinite tower of derivatives (using

the Cauchy product for the two infinite series coming from the sines)

$$\frac{1}{2\pi\hbar}\mathcal{W}\left[\mathbf{D}[\varrho]\right] = \frac{1}{2}\frac{\partial^2}{\partial p_i \partial p_j}\left(D_{2,ij}\ W\right) + \frac{\hbar^2 D_0^{ij}}{2}\frac{\partial^2 V_I}{\partial Q \partial q^i}\frac{\partial^2 V_I}{\partial Q \partial q^j}\frac{\partial^2 W}{\partial P^2} + 2D_0^{ij}\sum_{n=1}^{\infty}\sum_{m=0}^{n}\frac{(-1)^n}{c_{m,n}}\left(\frac{\hbar}{2}\right)^{2n+2}\frac{\partial^{2m+2}V_I}{\partial Q^{2m+1}\partial q^i}\frac{\partial^{2(n-m)+2}V_I}{\partial Q^{2(n-m)+1}\partial q^j}\frac{\partial^{2n+2}W}{\partial P^{2n+2}}\ , \tag{3.118}$$

where we defined $c_{m,n} \equiv (2m+1)!(2(n-m)+1)!$. We have explicitly isolated the $n = m = 0$ component of the sum, since it obviously maps to a diffusion term under the Wigner-Moyal transform. Moreover, under the assumption of harmonic Hamiltonian, as before, that's the only term surviving. In which case we see again that the CQ master equation for quadratic potentials can be mapped exactly to a diffusion problem in phase space. This is indeed the parallel of what we have observed at the level of the path integral.

A word of caution: the decoherence-induced diffusion in the quantum system is negligible with respect to the classical one, unless the decoherence constant itself is of the order of $1/\hbar^2$. In effective open system, the induced decoherence rate is exactly of that order, meaning that in the $\hbar \to 0$, both effects contribute equally [172]. For CQ systems, instead, this corresponds – via the deco-diff trade-off – to the small-diffusion regime. By inserting the explicit form of the potentials for the coupled CQ oscillators, and imposing the decoherence-diffusion trade-off, one can indeed see that the diffusion coefficient in the quantum variables is given by $\lambda^2\hbar^2/4D$, as in the discussion at the level of the path integral.

The phase-space description we have introduced here nicely mirrors the purely quantum-mechanical counterpart. Whilst it is an exact alternative representation of CQ dynamics, it can – in analogy to the quantum case – provide great computational advantage in evaluating the evolution of hybrid systems. For example, the Wigner formalism in quantum mechanics is useful when simulating molecular dynamics or highly transient phenomena [173].

3.4 Summary of the main results

In this chapter, we explored a solvable system of classical-quantum interaction: the hybrid oscillator. We began with two classical stochastic oscillator, one of which experiencing friction, showing that such a system univocally flows to a non-equilibrium steady-state. We then computed the out-of-time correlators for the steady-state in the small coupling regime. Next,

we quantised the undamped oscillators, and studied the system with the CQ framework. By mapping the generator of the dynamics to the classical stochastic system, we should that also the hybrid state flows to a non-equilibrium steady-state, which we computed. We demonstrated that in the high-diffusion regime of CQ, such a state becomes thermal. We concluded by formally deriving the phase-space description of CQ dynamics by performing the Wigner-Weyl transformation of the CQ generator. We showed explicitly that for quadratic potentials the hybrid evolution is equivalent to a Fokker-Planck equation with diffusion in both the classical and quantum phase space.

Chapter 4

Stochastic scalar

The aim of this chapter is to study the classical sector of a relativistic CQ theory as a toy model which may share some phenomenology with a fundamentally classical theory of gravity. In particular, we consider the free classical sector of a CQ field theory with a classical relativistic scalar – for example the quartic theory presented in [126] or the CQ Yukawa model [136] in which scattering has been recently discussed [174] – to compute its dynamically-generated correlations and the induced motion on test particles. It can also be seen as the classical sector of CQ Nordström gravity [127]– a scalar theory that correctly reproduces the Newtonian potential in the weak-field non-relativistic limit, but fails on accounting a series of other phenomena, such as light-bending and gravitational waves. While the propagating degree of freedom in CQ Einstein's gravity is the tensor mode, and the theory is non-linear, the study of a linear, scalar theory serves as an interesting toy model which is useful for building up an intuition for the gravitational case.

Here, we compute the two-point function of the non-dissipative Klein-Gordon field in Minkowski space, showing that the covariance in the field is free of divergences, zero for time-like separated spacetime points, grows linearly with the total time of diffusion, and drops as $1/r$ for spacelike separated events. We find that the size of the fluctuations, and their spatial variation, is large at short distances, meaning that linearised models of CQ gravity will likely break down at small scales, where non-linearities become important – possibly acting to smooth off the magnitude of the short-distance fluctuations. We further show that a particle reacting to the spatial gradient of the field will undergo diffusion, and compute the typical size of the white-noise stochastic

force that is induced by the classical stochastic fluctuations.

Conventions

Note that in this chapter of the thesis we work in the *mostly negative* convention for the Minkowski metric $(+---)$, the most common choice in the quantum field theory community. Unless stated otherwise, we set $G = 1$ in this chapter.

4.1 CQ scalar Yukawa

Our starting point is the one of a classical Klein-Gordon field interacting with its quantum counterpart, and in particular the Yukawa model of [136, 126]. Scattering in this model was recently discussed in [174] where it was shown that stochastic fluctuations can affect non-trivially scattering probabilities in CQ theories. The CQ scalar Yukawa theory corresponds to two dynamical Klein-Gordon scalars, the classical ϕ and quantum ψ. Specifically, the CQ proto-action can be obtain with the following choices:

$$\mathcal{L}_0^Q[\psi] = \frac{1}{2}\psi(\Box + m^2)\psi \ , \qquad \mathcal{L}_0^C[\phi] = \frac{1}{2}\phi(\Box + m^2)\phi \tag{4.1}$$

and

$$\mathcal{L}_{int}[\psi, \phi] = \lambda\phi\psi^2 \tag{4.2}$$

In fact, we will focus on the free part of the classical sector of the theory, whose understanding is crucial to construct perturbation theory and explore the renormalisation of the model. The equations of motion for the stochastic Klein-Gordon field (re-introducing momentarily factors of G, c and $\hbar$ and treating ϕ as having the unit of a gravitational potential):

$$\left(\frac{1}{c^2}\partial_t^2 - \nabla^2 + \frac{m^2c^2}{\hbar^2}\right)\phi(x) = \xi(x) \ , \tag{4.3}$$

with the Gaussian random field ξ (with units of inverse length squared) having the following statistics:

$$\mathbb{E}[\xi(x)] = 0 \ , \qquad \mathbb{E}[\xi(x)\xi(y)] = \frac{D_2}{c}\ \delta^{(4)}(x - y) \ . \tag{4.4}$$

Note that the diffusion coefficient is dimensionless, and the delta-function correlation is required for a local, Lorentz invariant noise. Surprisingly little is known regarding this stochastic field

theory. In the mathematics literature, this is mainly due to the fact that divergences occur in the stochastic wave equation in more than a single spatial dimensions – meaning that a regular solution does not exist – so deformations of the theory are usually studied instead [175, 176, 177]. In the physics literature, the non-dissipative system has not been studied to the best of our knowledge – although the thermal Klein-Gordon state has been explored in detail and is now textbook material [178, 179]. It is useful at this point to discuss the latter – it will serve to develop an intuition to interpret the non-dissipative results. Therefore, we now consider the modified dynamics that has as a fixed-point the thermal scalar field, breaking Lorentz invariance. As we will see in Section 4.3, the thermal field covariances are closely related to the ones of the non-dissipative system.

4.2 The Klein-Gordon thermal state, with friction

Consider now the following modification to the equations of motion:

$$(\Box + m^2)\phi(x) + 3\frac{\gamma_H}{c^2}\dot{\phi} = \xi(x) \ , \tag{4.5}$$

where γ_H is some constant friction coefficient – which breaks Lorentz invariance. The factor of 3 is there in analogy with the equations of motion of a Klein-Gordon field on an inflationary FLRW background with Hubble constant γ_H [180]. Of course, the analogy is imperfect since in the cosmological case the d'Alembertian is the one of the FLRW geometry, whilst we consider the flat-space operator instead. In the cosmological analogy, the loss of Lorentz invariance is natural: there is a preferred frame provided by the expansion of the Universe.

For completeness, let us write these equations of motion in first order formalism, re-introducing factors of c (again, we take the field to have the units of a gravitational potential):

$$\partial_t \phi = \pi_\phi \tag{4.6}$$

$$\partial_t \pi_\phi = c^2 \left(\nabla^2 - \frac{c^2 m^2}{\hbar^2} \right) \phi - 3\gamma_H \pi_\phi + c^2 \xi_t \ , \tag{4.7}$$

where ξ obeys Equation 4.4. The stochastic differential equations (SDE) of motion, here, are given in Langevin form for cosmetic reason. Recall that the white noise field corresponding to the formal time-derivative of a three-dimensional Brownian sheet [181].

Because of the friction term, the system achieves a steady state. Determining that steady state is achieved by considering the evolution of the probability density $P(\phi, \pi_\phi)$ in field space. This follows from the Fokker-Planck equation:

$$\frac{\partial P}{\partial t} = -\int d^3x \frac{\delta}{\delta\phi}\left(D_\phi P\right) - \int d^3x \frac{\delta}{\delta\pi_\phi}\left(D_\pi P\right) + \frac{1}{2}\int d^3x \int d^3y \frac{\delta^2}{\delta\pi_\phi(x)\delta\pi_\phi(y)}\left(D_{\pi\pi} P\right) \ , \quad (4.8)$$

where the drift coefficients are:

$$D_\phi = \pi_\phi \quad (4.9)$$

$$D_\pi = c^2\nabla^2\phi - \frac{c^2m^2}{\hbar^2}\phi - 3\gamma_H\pi_\phi \ , \quad (4.10)$$

whilst the diffusion coefficient is:

$$D_{\pi\pi} = D_2 c^3 \delta^{(3)}(\underline{x} - \underline{y}) \ . \quad (4.11)$$

A natuaral ansatz for the steady state ($\partial_t P = 0$) is the thermal state:

$$P_T = \frac{1}{\mathcal{Z}} e^{-\beta H} \ , \quad (4.12)$$

with:

$$H = \frac{1}{2G}\int d^3x \left(\frac{\pi_\phi^2}{c^2} + (\nabla\phi)^2 + \frac{c^2m^2}{\hbar^2}\phi^2\right) \ , \quad (4.13)$$

and β to be determined ($\mathcal{Z}$ ensures normalisation on field space, whilst the numerical pre-factor is needed from dimensional analysis). Plugging this into the Fokker-Planck equation and demanding that this is a steady state imposes:

$$\beta = \frac{6G\gamma_H}{D_2 c^5} \ . \quad (4.14)$$

The steady-state distribution is a field whose modes have an average energy of $1/\beta$. Without a cutoff, the energy of the field would be divergent, as there would be infinite modes, each contributing to $1/\beta$ to the total energy. If a natural UV cutoff Λ exists for the theory, however, the total energy depends cubically on such a scale, i.e. $H \propto \Lambda^3$ – the volume of the physical states in reciprocal space.

Seeing that this is the case is straightforward, and amounts to computing the two point functions of π_ϕ and ϕ in the thermal state. First, note that the probability distribution over

phase space factorises between π_ϕ and ϕ, meaning that we can compute the two separately. Let's introduce sources J and $\tilde{J}$ for ϕ and π_ϕ respectively, defining the generating function:

$$\begin{aligned} Z[J,\tilde{J}] &= \mathcal{N}\int \mathcal{D}\phi\mathcal{D}\pi_\phi e^{-\beta H+\int d^3x(J\phi+\tilde{J}\pi_\phi)} \\ &= \mathcal{N}\int \mathcal{D}\phi e^{-\frac{\beta}{2G}\int d^3x\left((\nabla\phi)^2+\frac{c^2m^2}{\hbar^2}\phi^2\right)}e^{\int d^3xJ\phi}\int \mathcal{D}\pi_\phi e^{-\frac{\beta}{2Gc^2}\int d^3x\pi_\phi^2}e^{\int d^3x\tilde{J}\pi_\phi} \\ &= Z_\phi[J]Z_\pi[\tilde{J}]\ . \end{aligned} \tag{4.15}$$

Performing the Gaussian integrals we obtain:

$$\begin{aligned} Z_\phi[J] &= \mathcal{N}\int \mathcal{D}\phi e^{-\frac{\beta}{2G}\int d^3x\left((\nabla\phi)^2+\frac{c^2m^2}{\hbar^2}\phi^2\right)}e^{\int d^3xJ\phi} \\ &= \mathcal{N}\int \mathcal{D}\phi e^{-\frac{\beta}{2G}\int\int d^3xd^3y\ \phi(x)\delta^{(3)}(x-y)\left(-\nabla^2+\frac{c^2m^2}{\hbar^2}\right)\phi(y)}e^{\int d^3xJ\phi} \\ &= \mathcal{Z}_\phi e^{\frac{1}{2}\int\int d^3xd^3y\ J(x)G(x-y)J(y)} \end{aligned} \tag{4.16}$$

where $\mathcal{Z}_\phi$ is the normalisation constant of the ϕ probability distribution and

$$\frac{\beta}{G}\left(-\nabla^2+\frac{c^2m^2}{\hbar^2}\right)G(\underline{x}-\underline{y}) = \delta^{(3)}(\underline{x}-\underline{y})\ . \tag{4.17}$$

As expected, $G(\underline{x}-\underline{y})$ is the Green's function of the Laplacian operator with a mass term. We can easily find this in Fourier space:

$$G(k) = \frac{G}{\beta}\frac{1}{k^2+(mc/\hbar)^2}\ . \tag{4.18}$$

The inverse Fourier transform is well known [179]

$$G(\underline{x}-\underline{y}) = \frac{G}{4\pi\beta}\frac{1}{r}e^{-mcr/\hbar} = \frac{D_2c^5}{24\pi\gamma_H}\frac{1}{r}e^{-mcr/\hbar} \tag{4.19}$$

and corresponds to the two-point function of the field ϕ

$$\mathbb{E}[\phi(\underline{x})\phi(\underline{y})] = \frac{D_2c^5}{24\pi\gamma_H}\frac{1}{r}e^{-mcr/\hbar}\ . \tag{4.20}$$

Differentiating in space the point-split two-point function gives the covariance for the gradient of the field at equal times

$$\mathbb{E}[\partial_i\phi(\underline{x})\partial_j\phi(\underline{y})] = \frac{D_2c^5}{24\pi\gamma_H}\left[\left(\delta_{ij}-\frac{r_ir_j}{r^2}\right)\left(\frac{1}{r^3}+\frac{mc}{\hbar r^2}\right)-\frac{r_ir_j}{r^2}\left(\frac{2}{r^3}+\frac{mc}{\hbar r^2}+\frac{m^2c^2}{\hbar^2r}\right)\right]e^{-mcr/\hbar}\ . \tag{4.21}$$

We sum over all directions (recall $x^i = -x_i$ in this signature of the metric). Carefully handling the coincident limit

$$\begin{aligned}\mathbb{E}[\nabla\phi(x)\nabla\phi(y)] &= -\nabla^2 G(\underline{x}-\underline{y}) = \frac{G}{\beta}\delta^{(3)}(\underline{x}-\underline{y}) - \frac{\beta c^4 m^2}{G\hbar^2}G(\underline{x}-\underline{y}) \\ &= \frac{D_2 c^5}{6\gamma_H}\delta^{(3)}(\underline{x}-\underline{y}) - \frac{6\gamma_H m^2}{D_2 c\hbar^2}G(\underline{x}-\underline{y}) \ .\end{aligned} \tag{4.22}$$

In the massless case, the appearance of the δ-function is even more obvious: the probability distribution in terms of $\nabla\phi$ has a δ-function kernel, whose inverse is a delta-function itself.

Repeating the same calculations with the momentum instead, we find that in the thermal state we have

$$\mathbb{E}[\pi(x)\pi(y)] = \frac{Gc^2}{\beta}\delta^{(3)}(\underline{x}-\underline{y}) = \frac{D_2 c^7}{6\gamma_H}\delta^{(3)}(\underline{x}-\underline{y}) \ . \tag{4.23}$$

This implies that the energy of the state has a contact divergence similarly to that found in the quantum field theory case. Indeed:

$$\begin{aligned}\mathbb{E}[H] &= \frac{1}{2G}\mathbb{E}\left[\int d^3x\ d^3y \left(\frac{\pi_\phi(x)\pi_\phi(y)}{c^2} + \nabla\phi(x).\nabla\phi(y) + \frac{c^2 m^2}{\hbar^2}\phi(x)\phi(y)\right)\delta^{(3)}(\underline{x}-\underline{y})\right] \\ &= \frac{V}{\beta}\delta(0) = \frac{D_2 c^5 V}{6G\gamma_H}\delta(0) \ .\end{aligned} \tag{4.24}$$

The δ-like divergence is due to the infinite number of modes contributing equally to the energy. Again, if a cutoff scale Λ exists, the divergence is regularised with a cubic scaling Λ^3. The total energy of the field does scale with the spatial volume V – here we regulate it with some IR cutoff which might be taken to be naturally the Hubble scale – but of course the energy density is insensitive to the IR and only feels the contribution from the UV modes. From these two-point functions, covariances at unequal times can be computed by studying the eigenvalue problem of the Fokker-Planck equation [182]. We instead stop here and now progress to the main results of the chapter – the covariance function of the non-dissipative system. We will continuously refer to the thermal results for comparison.

4.3 Correlations out of equilibrium

Let's consider again Equation 4.3. Contrary to the damped case, the probability distribution over field space does not converge to a steady state, with the variance growing unbounded instead. This means that we cannot ignore the initial state, nor the total time of evolution.

Assuming that we can initialise the system at the past timelike infinity, providing a Lorentz-invariant initial condition, leads to divergent results precisely for this reason. It is therefore necessary to specify an initial state on a spacelike hypersurface Σ_0, and foliate spacetime along the time-like vector specified by the initial condition.

The initial condition means that the solution for the two-point functions will not look Lorentz-invariant: correlators will fail to be invariant under boosts. However, this has nothing to do with the property of the evolution itself – the equations of motion are perfectly Lorentz invariant.

Without loss of generality – due to linearity of the Klein-Gordon equation – we are free to consider the initial state and its time derivative to be the identically vanishing, i.e. $\phi(t_0, \underline{x}) = \dot{\phi}(t_0, \underline{x}) = 0$. Indeed, we can always add any solution to the (deterministic) homogeneous problem that satisfies any other initial condition. Effectively, this means we are focusing only on the deviation from the deterministic dynamics due to the stochastic fluctuations: any non-zero initial condition can be simply propagated by the deterministic equation, contributing only to a non-vanishing mean.

The weak solution to Equation 4.3 can be rewritten as [175]:

$$\phi(x) = \int_{\Sigma_0}^{\Sigma_f} d^4y \; G_R(x,y)\xi(y) \; , \tag{4.25}$$

where G_R is the retarded Green's function of the Klein-Gordon equation. Recall that for a massive field this is given by [183]:

$$G_R(x-y) = \Theta(x^0 - y^0)\left(-\frac{1}{2\pi}\delta(\tau_{xy}^2) + \Theta(\tau_{xy}^2)\frac{mJ_1(m\tau_{xy})}{4\pi\tau_{xy}}\right) \; , \tag{4.26}$$

where τ_{xy} is the proper time elapsed on a geodesic between x and y, whilst J_1 is a Bessel function of the first kind. The propagator of the massless field trivially follows

$$G_R^0(x-y) = -\frac{\Theta(x^0 - y^0)}{2\pi}\delta(\tau_{xy}^2) \; . \tag{4.27}$$

It is entirely localised on the past lightcone of x.

As we intend the stochastic equation in the Itô sense, the expectation values over realisations of the noise acts only on the random field ξ. Therefore:

$$\mathbb{E}[\phi(x)] = \int_{\Sigma_0}^{\Sigma_f} d^4y \; G_R(x,y)\mathbb{E}[\xi(y)] = 0 \; , \tag{4.28}$$

as expected. The two-point function of the field, however, is non-zero:

$$\begin{aligned}\mathcal{C}(x,y|t_0) \equiv \mathbb{E}[\phi(x)\phi(y)|\phi_0 = \dot{\phi}_0 = 0] &= \int_{\Sigma_0}^{\Sigma_f} d^4z \int_{\Sigma_0}^{\Sigma_f} d^4z' \; G_R(x,z)G_R(y,z')\mathbb{E}[\xi(z)\xi(z')] \\ &= D_2 \int_{\Sigma_0}^{\Sigma_f} d^4z \; G_R(x,z)G_R(y,z) \; ,\end{aligned} \tag{4.29}$$

where we have used the fact that the random field is δ-correlated in spacetime. $\mathcal{C}$ is the covariance of the field at the spacetime points x and y *given the initial condition* of a vanishing field and conjugate momentum at the initial spacelike surface. That covariances can be expressed as convolutions of Green's functions applies to any stochastic field theory with linear equations of motion. However, performing the convolution in spacetime for a general theory is complicated – it is much easier to go to the Fourier domain where the convolution becomes a simple multiplication, and then perform the inverse Fourier transform.

For the massless KG field, solving Equation 4.29 directly is possible, as we show now. This serves as a check for the main results of this articles – how to handle the Fourier-space divergences of the two-points function in a stochastic field theory.

4.3.1 Explicit spacetime convolution for the massless field

We now perform the convolution:

$$\mathcal{C}(x,y|t_0) = D_2 \int_{t_0}^{\infty} dz^0 \int d^3z \; G_R(x-z)G_R(y-z) \; , \tag{4.30}$$

directly by calculating the integral in the spacetime representation. First, expand

$$\begin{aligned}G_R(x-z) &= -\frac{1}{2\pi}\Theta(x^0-z^0)\delta(s_{xz}^2) \\ &= -\frac{1}{4\pi}\frac{\delta(x^0-z^0-|\underline{x}-\underline{z}|)+\delta(x^0-z^0+|\underline{x}-\underline{z}|)}{|\underline{x}-\underline{z}|}\Theta(x^0-z^0) \; .\end{aligned} \tag{4.31}$$

Here we will assume $x^0 \geq y^0$. It is useful to perform the following change of variable:

$$\tilde{z} = y - z \; , \tag{4.32}$$

trasforming the integral into:

$$\begin{aligned}\mathcal{C}(x,y|t_0) \propto \int_{-\infty}^{y^0-t_0} d\tilde{z}^0 \int d^3\tilde{z} \; &\frac{\delta(\tilde{z}^0-|\underline{\tilde{z}}|)+\delta(\tilde{z}^0+|\underline{\tilde{z}}|)}{|\underline{\tilde{z}}|}\Theta(x^0-y^0+\tilde{z}^0)\Theta(\tilde{z}^0)\times \\ &\times \frac{\delta(x^0-y^0+\tilde{z}^0-|\underline{x}-\underline{y}+\underline{\tilde{z}}|)+\delta(x^0-y^0+\tilde{z}^0+|\underline{x}-\underline{y}+\underline{\tilde{z}}|)}{|\underline{x}-\underline{y}+\underline{\tilde{z}}|}\end{aligned} \tag{4.33}$$

Due to the theta-function imposing positivity on $\tilde{z}^0$, the $\delta(\tilde{z}^0 + |\underline{\tilde{z}}|)$ does not contribute. Integrating over $\tilde{z}^0$ we obtain:

$$\mathcal{C}(x,y|t_0) \propto \int d^3\tilde{z}\ \frac{\delta(x^0-y^0+|\underline{\tilde{z}}|-|\underline{x}-\underline{y}+\underline{\tilde{z}}|)+\delta(x^0-y^0+|\underline{\tilde{z}}|+|\underline{x}-\underline{y}+\underline{\tilde{z}}|)}{|\underline{x}-\underline{y}+\underline{\tilde{z}}||\underline{\tilde{z}}|}\times \\ \times\,\Theta(y^0-t_0-|\underline{\tilde{z}}|)\ . \tag{4.34}$$

Since $x^0 \geq y^0$, the second delta-function is irrelevant. The theta-function imposes the restriction on $|\underline{\tilde{z}}|$ due to the finite evolution in time. It is now convenient to perform the spatial integral in spherical polars $(\tilde{z},\theta,\phi)$, where the role of the unit $\hat{k}$ vector with respect to which the angles are defined is played by $(\underline{x}-\underline{y})/|\underline{x}-\underline{y}|$. Then, using:

$$|\underline{x}-\underline{y}+\underline{\tilde{z}}| = \sqrt{|\underline{x}-\underline{y}|^2+\tilde{z}^2+2|\underline{x}-\underline{y}|\tilde{z}\cos\theta}\ , \tag{4.35}$$

meaning that the delta-function condition is satisfied for θ_* s.t.:

$$\cos\theta_* = \frac{(x^0-y^0)^2-|\underline{x}-\underline{y}|^2}{2\tilde{z}|\underline{x}-\underline{y}|}+\frac{x^0-y^0}{|\underline{x}-\underline{y}|} \tag{4.36}$$

This clearly implies that x and y must be spacelike separated spacetime events – if timelike the RHS is larger than 1 (recall that $x^0-y^0 \geq 0$). In terms of $\cos\theta$, the delta-function can be expressed as:

$$\delta(x^0-y^0+|\underline{\tilde{z}}|-|\underline{x}-\underline{y}+\underline{\tilde{z}}|) = \frac{\sqrt{|\underline{x}-\underline{y}|^2+\tilde{z}^2+2|\underline{x}-\underline{y}|\tilde{z}\cos\theta_*}}{\tilde{z}|\underline{x}-\underline{y}|}\delta(\cos\theta-\cos\theta_*)\times \\ \times\,\Theta(-(x^0-y^0-|\underline{x}-\underline{y}|))\ . \tag{4.37}$$

Now, in spherical polars the integral becomes simply (ignoring the theta-function for brevity):

$$\mathcal{C}(x,y|t_0) \propto \int_0^{2\pi} d\phi \int_{-1}^{1} d(\cos\theta) \int_0^{y^0-t_0} d\tilde{z}\frac{\sqrt{|\underline{x}-\underline{y}|^2+\tilde{z}^2+2|\underline{x}-\underline{y}|\tilde{z}\cos\theta_*}}{\sqrt{|\underline{x}-\underline{y}|^2+\tilde{z}^2+2|\underline{x}-\underline{y}|\tilde{z}\cos\theta}}\times \\ \times\,\delta(\cos\theta-\cos\theta_*)\ . \tag{4.38}$$

Meaning that the final result is:

$$\mathcal{C}(x,y|t_0) = \frac{D_2}{16\pi}\left(\frac{y^0+x^0-2t_0}{|\underline{x}-\underline{y}|}-1\right)\Theta(-s^2_{xy})\Theta(x^0+y^0-2t_0-|\underline{x}-\underline{y}|)\ . \tag{4.39}$$

Before moving on and computing the two-point function in Fourier space instead, let's pause and analyse this result. The fluctuations in the field at time-like separated points are

uncorrelated. This is caused by the structure of the massless retarded propagator – which is completely localised on the lightcone. In order for the field in two different spacetime points to be correlated, they need to share signal from the same stochastic fluctuation. Since these travel strictly at the speed of light, x and y need to have intersecting light-cones – hence the first Θ-function. The second Θ-function follows from the initial condition $\phi = 0$ for $t < t_0$. Only if the Θ-condition is satisfied, then the two lightcones intersect before the stochastic white noise is turned on, i.e. before t_0. Indeed, the covariance between x and y drops as $1/r$ until it reaches zero at a critical distance r_*. Further than r_*, the two space-like separated points do not have an intersecting lightcone and are completely uncorrelated. Figure 4.1 visually clarifies this point. Note that the critical distance r_* grows linearly with the time coordinate elapsed from the initial spacelike hypersurface.

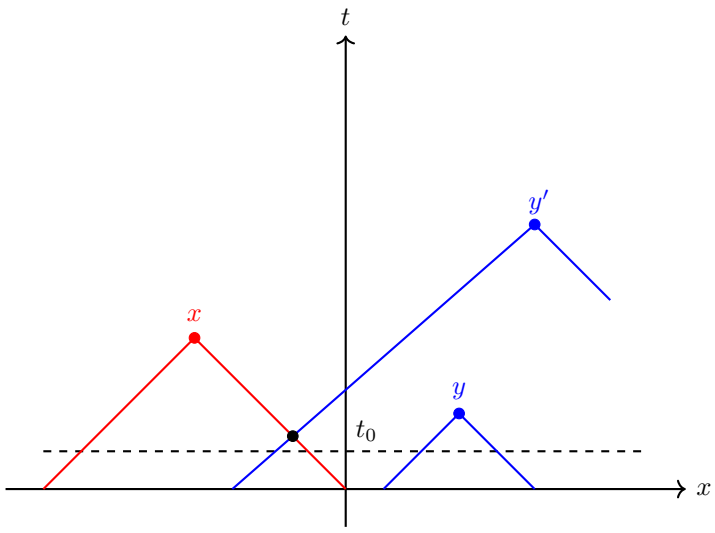

Figure 4.1: Spacetime diagram in $1 + 1$ dimensions. The points x and y, even if spacelike separated, are not correlated – their lightcones intersect *before* the initial condition (dashed line). On the other hand, the field at x and y' will have non-zero covariance, as their intersection (black dot) lies in the future of the initial spacelike hypersurface.

A useful analysis, for a further sanity check, is to compare Equation 4.39 for simultaneous events (with respect to the initial time hypersurface) to Equation 4.20, i.e. the thermal 2-point function. By taking the time elapsed to be $t_0 \sim 1/3\gamma_H$, i.e. the thermalisation scale, we see that in the massless limit both the $1/r$ scaling and size of the correlations match. Of course, for

the thermal state the Θ-function depending on the initial time is absent – in the equilibrium configuration enough time has elapsed such that all space-like separated points have intersecting lightcones.

4.3.2 Mod-squared retarded pole prescription

We now discuss solving Equation 4.29 in Fourier space. We derive the corresponding pole-prescription, which we call the *mod-squared retarded* prescription, and analyse the role of the divergent terms that appear in the computations.

Before considering the regularised evolution with an initial space-like surface, let's study the simpler situation in which we can extend the time integral to $\pm\infty$. The upper limit is always allowed: when computing expectation values of local observables $\mathcal{O}(x)$, we are free to extend the upper limit of the time integration to infinity – the future evolution of the probability distribution has no bearing on the expectation value of observables at some intermediate time. Initialising the state at $-\infty$ is more problematic if the evolution does not have a fixed point, since, as mentioned before, the variance of the probability distribution in field space grows unbounded. In the case in which there exists a steady-state (e.g. [162]), however, extending the time integration to infinitely far away in the past would prepare such a state, as we saw in Chapter 3.

For now, let's assume we are indeed allowed to push the lower limit of integration to time-like infinity both in the past and in the future: this uncovers the general pole-structure in Fourier space of classical correlators. Let's insert the Fourier representation of the retarded propagator in Equation 4.29:

$$\begin{aligned}\mathcal{C}(x,y|t_0) &= D_2\int_{-\infty}^{\infty} d^4z \int \frac{d^4p}{(2\pi)^4}\int \frac{d^4k}{(2\pi)^4}\frac{e^{-ip(x-z)}e^{-ik(y-z)}}{\left[(p_0+i\epsilon)^2-E(\underline{p})^2\right]\left[(k_0+i\epsilon)^2-E(\underline{k})^2\right]} \\ &= D_2\int \frac{d^4p}{(2\pi)^4}\frac{e^{-ip(x-y)}}{\left[(p_0+i\epsilon)^2-E(\underline{p})^2\right]\left[(p_0-i\epsilon)^2-E(\underline{p})^2\right]}\ ,\end{aligned} \tag{4.40}$$

where $E(\underline{p})^2 = m^2 + |\underline{p}|^2$ is the relativistic energy. This structure is perfectly general for stochastic processes – see Appendix A for the case of a point Brownian particle, where we show it explicitly recovers standard results – and we refer to it as the retarded-mod-squared prescription, in contrast with the Feynman-mod-squared prescription assumed in [136] to discuss stochastic propagators. Whilst the two point function is manifestly real and symmetric under exchange

of the field $\phi(x) \leftrightarrow \phi(y)$ as required for a classical two-point function for both prescriptions, the retarded one follows naturally from the weak solution to the stochastic equations. In fact, the MSR path integral itself calls for the retarded prescription, in analogy with the Keldysh propagator in quantum open-system path integrals [184].

Performing the inverse Fourier transform in Equation 4.40 would lead to divergent results in the limit $\epsilon \to 0$, with the leading divergence of order $1/\epsilon$. Indeed, in the $\epsilon \to 0$ limit the 4 first-order poles become 2 second-order poles on the p_0 real line. Then, when computing the residue for one of them – let's call it P – its conjugate P^* will contribute with a $1/\epsilon$ factor. These are very much physical divergences – it is not possible to map the result to distributions as it is commonly done for the spacetime representation of QFT propagators. To understand their physical origin instead, consider an undamped Brownian particle. It is a standard result that the variance in the velocity $\dot{X}(t)$ of the particle grows linearly with time, the diffusion coefficient being the constant of proportionality – namely $\dot{X}^2 \sim D_2 t$. As $t \to \infty$, the probability distribution over momenta limits to a uniform distribution – the variance diverges. The same happens for the scalar undamped field when driven by a white noise process.

We now explicitly see how these divergences drop out of the correlators once an initial state is defined at finite coordinate time, and what this implies for the heating rate of the classical non-dissipative field.

4.3.3 Pole prescription from MSR

To see how the MSR path integral selects naturally the mod-squared retarded prescription, consider the MSR path-integral representation of the stochastic process given by Equation 4.3:

$$P(\phi_f, t_t) = \int \mathcal{D}\phi \mathcal{D}\tilde{\phi} e^{I_{MSR}[\phi,\tilde{\phi}]} P(\phi_0, \dot{\phi}_0, t_0) \ , \tag{4.41}$$

where

$$I_{CQ}[\phi, \tilde{\phi}] = \int_{\Sigma_0}^{\Sigma_f} d^4x \left[-\tilde{\phi} \left(\Box + m^2 \right) \phi + \frac{D_2}{2} \tilde{\phi}^2 \right] \ . \tag{4.42}$$

The two-point function of the vector $\Phi = (\phi, \tilde{\phi})$ is, as usual, given by the inverse of the differential operator appearing in the action, subject to the boundary conditions. For simplicity, we choose as initial condition $P(\phi_0, \dot{\phi}_0, t_0) = \delta(\phi)\delta(\dot{\phi}_0)$ – any other initial condition can

be accounted for by adding the solution to the homogeneous equation satisfying the relevant boundary conditions.

As explained in the previous subsection, when computing expectation values of local observables $\mathcal{O}(x)$, we are free to extend the upper limit of the time integration to time-like infinity since the evolution is time-local and causal. The same cannot be done for the lower limit of integration. Evaluating the Green's function is then more easily computed in the Fourier domain, where the inversion of the operator is straightforward. We have:

$$\begin{aligned} I_{CQ}[\phi,\tilde{\phi}] &= \int_{t_0}^{\infty} dx^0 \int d^3x \int \frac{d^4p}{(2\pi)^4}\frac{d^4q}{(2\pi)^4}\left[-\tilde{\phi}(q)\left(p^2-m^2\right)\phi(p)+\frac{D_2}{2}\tilde{\phi}(q)\tilde{\phi}(q)\right]e^{-i(p+q)x} \\ &= -\frac{1}{2}\int \frac{d^4p}{(2\pi)^4}\frac{d^4q}{(2\pi)^4}\Phi(-q)A(q,p)\Phi(p)\ , \end{aligned} \tag{4.43}$$

with:

$$A(q,p) = (2\pi)^3\delta^{(3)}(\underline{p}-\underline{q})\begin{pmatrix} 0 & p^2-m^2 \\ p^2-m^2 & -D_2 \end{pmatrix}\left(\pi\delta(p_0-q_0)+\frac{\mathbf{P}\ ie^{-it_0(p_0-q_0)}}{p_0-q_0}\right) \tag{4.44}$$

where $\mathbf{P}$ indicates the principal value of the integral of Equation 4.43. The two-point function will then just be the inverse operator to A with the appropriate boundary conditions, i.e. it will be the Green's function G for such an operator – as standard. Ignoring for a moment boundary conditions (i.e. extending the time countour to $-\infty$ for simplicity), in Fourier domain this is given by:

$$G(q,p) = (2\pi)^4\delta^{(4)}(p-q)\begin{pmatrix} \frac{D_2}{(p^2-m^2)^2} & \frac{1}{p^2-m^2} \\ \frac{1}{p^2-m^2} & 0 \end{pmatrix}\ . \tag{4.45}$$

Of course, this must be accompanied by the appropriate recipe to go around poles in the complex plane for all of these propagators. In MSR, response variables have causal dependence with the real field, meaning that the $\phi\tilde{\phi}$ correlator is of retarded form (it is non-zero only if the field *precedes* the response variable), whilst $\phi\tilde{\phi}$ is the advanced Green's function. This means that, naturally, the MSR path integral implies the mod-squared retarded prescription for the diagonal $\phi\phi$ propagator, in agreement with what we derived in the previous subsection.

4.3.4 Propagators with IR cutoff

Let's insert the Fourier representation of the retarded propagator in Equation 4.29:

$$\mathcal{C}(x,y|t_0) = D_2 \int_{t_0}^{\infty} dz_0 \int d^3z \int \frac{d^4p}{(2\pi)^4} \int \frac{d^4k}{(2\pi)^4} \frac{e^{-ip(x-z)}e^{-ik(y-z)}}{\left[(p_0+i\epsilon)^2 - E(\underline{p})^2\right]\left[(k_0+i\epsilon)^2 - E(\underline{k})^2\right]} \,. \tag{4.46}$$

Now, let's focus on the z_0 integration first:

$$\int_{t_0}^{\infty} dz_0 e^{iz_0(p_0+k_0)} = e^{i(p_0+k_0)t_0}\left(\pi\delta(p_0+k_0) + i\frac{\mathbf{P}}{k_0+p_0}\right), \tag{4.47}$$

It would be tempting to use at this point the Kramers-Kronig relation

$$\mathbf{P}\frac{1}{x} = \lim_{\epsilon\to 0}\frac{1}{x+i\epsilon} + i\pi\delta(x) \tag{4.48}$$

and remove a delta-function. Unfortunately, this would lead down the line to a p_0 pole in the integrand without a definite $i\epsilon$ prescription, so we refrain from doing it and evaluate the two components separately. The spatial z integral trivially gives a delta-function on momenta:

$$\int d^3z e^{-iz(p+k)} = (2\pi)^3\delta(\underline{p}+\underline{k}). \tag{4.49}$$

Performing the integrals over k and combining we obtain (see Appendix B for more details):

$$\mathcal{C}(x,y|t_0) = \mathcal{C}_\infty + \Delta\mathcal{C}, \tag{4.50}$$

where

$$\mathcal{C}_\infty = D_2 \int \frac{d^4p}{(2\pi)^4} \frac{e^{-ip(x-y)}}{\left[(p_0+i\epsilon)^2 - E(\underline{p})^2\right]\left[(p_0-i\epsilon)^2 - E(\underline{p})^2\right]} \,, \tag{4.51}$$

is the infinite-time contribution, whilst

$$\Delta\mathcal{C} = \frac{D_2}{2}e^{-\epsilon(y_0-t_0)} \int \frac{d^4p}{(2\pi)^4}\frac{1}{E(\underline{p})}\frac{e^{-i\underline{p}.\underline{y}}e^{-ipx}e^{ip_0t_0}}{(p_0+i\epsilon)^2 - E(\underline{p})^2}\left[\frac{e^{-iE(\underline{p})(y_0-t_0)}}{p_0 - i\epsilon + E(\underline{p})} - \frac{e^{iE(\underline{p})(y_0-t_0)}}{p_0 - i\epsilon - E(\underline{p})}\right] \tag{4.52}$$

contains information about finite-times effects.

The integral in Equation 4.51 has a leading $1/\epsilon$ divergence. However, so does Equation 4.52 – in such a way that the two divergent contributions cancel and one is left with a finite term only. Detailed calculations are in Appendix B. We report directly the finite result in terms of oscillatory integrals, namely:

$$\mathcal{C}(x,y|t_0) = \frac{D_2}{8\pi^2}\frac{1}{|\underline{x}-\underline{y}|}\left[2(y^0-t_0)I_1 + I_2 - I_3\right] \,, \tag{4.53}$$

with the oscillatory integrals

$$I_1 = \int_0^\infty dp \frac{p}{E(p)^2} \cos\left(E(p)(x^0 - y^0)\right) \sin(p|\underline{x} - \underline{y}|) \ , \tag{4.54}$$

$$I_2 = \int_0^\infty dp \frac{p}{E(p)^3} \sin\left(E(p)(x^0 - y^0)\right) \sin(p|\underline{x} - \underline{y}|) \ , \tag{4.55}$$

$$I_3 = \int_0^\infty dp \frac{p}{E(p)^3} \sin\left(E(p)(x^0 + y^0 - 2t_0)\right) \sin(p|\underline{x} - \underline{y}|) \ , \tag{4.56}$$

where I_3 is really the same as I_2 – only with different time coordinates. While Equation 4.53 seems to give different weighting to x^0 and y^0, this is a residue of the fact that in the calculations we have assumed $x^0 \geq y^0$ throughout. To get the general expression, it suffices to replace $x^0 \to \text{Max}(x^0, y^0)$ and $y^0 \to \text{Min}(x^0, y^0)$. It further turns out that evaluating the integrals explicitly in the massless case yields a result that is invariant under $x^0 - y^0 \to y^0 - x^0$. It is not clear whether the latter property emerges from a particular symmetry in the dynamics. Stationarity of the process usually implies a time-shift symmetry in the two-point function of the stochastic variable, forcing it to be dependent on the time-difference between two observations only. Here the dynamics is not stationary, and indeed the two-point function does not depend only on Δt, but on their absolute value as well – due to the initial condition breaking the time-shift dynamics at the level of the ensemble trajectories. That is, in stochastic although one might have a time-shift invariant law for the increments, the ensemble properties will feel the non-stationarity and the emergence of a preferred initial time.

Massless field

In the massless case, the integrals simplify greatly and can be computed exactly. This is the case of phenomenological relevance, if we want to think about the scalar waves as a proxy for the tensor gravitational waves. Even if they do acquire a small mass due to renormalisation effects, as suggested in [136], the corrections to the massless result would only act to suppress long-distance correlations. Since we are mainly worried about the short-distance divergences, the massless results will suffice. As we show explicitly in Appendix B, the 2-point function for the massless field is given by:

$$\mathcal{C}(x, y|t_0) = \frac{D_2}{16\pi} \left(\frac{y^0 + x^0 - 2t_0}{|\underline{x} - \underline{y}|} - 1 \right) \Theta(-s_{xy}^2) \Theta(x^0 + y^0 - 2t_0 - |\underline{x} - \underline{y}|) \ , \tag{4.57}$$

which indeed matches the result obtained by convolution of the Green's function, computed in Subsection 4.3.1. Again, it is finite and well-behaved modulo the contact divergence at $x \to y$, that is to be handled as usual in field theory – as a distribution acting on regular functions. The IR divergence that we have removed with the definition of the initial state at finite coordinate time t_0 is recovered as we send $t_0 \to -\infty$

4.3.5 Energy production

While in an expanding universe we expect Hubble friction terms such as those found in Equation 4.5, we here consider Minkowski space without additional friction terms. In this case, we expect the energy of the system to increase with time, in analogy with a simple Brownian particle. Since the Hamiltonian is not the generator of the dynamics there is no reason for it to be conserved.

It is straightforward to show this by referring to Itô's lemma. Let's consider the observable in Equation 4.13, the energy H of the field. By applying Itô's lemma we obtain:

$$\dot{H} = \int d^3x \left(\sqrt{D_2}\pi(x)\xi(x) + \frac{1}{2} D_2 \delta(0) \right) \ , \tag{4.58}$$

where the deterministic contributions to the chain rule have cancelled each others (the Klein-Gordon equation itself is energy-preserving), and only diffusion effects survive. Using that the expectation value of the noise process vanishes, we finally obtain that the energy increases linearly with time in a deterministic fashion:

$$H = \frac{D_2 c^5 V}{2G} \delta(0) \Delta t \ , \tag{4.59}$$

where we have reintroduced factors of c and Δt is the time elapsed from the initial condition. Again, this matches Equation 4.24, the thermal state result, where the energy would stop growing after $\Delta t \propto 1/\gamma_H$. Much like for the energy of the thermal state, the δ-divergence is due to the infinite number of modes in the system that are being excited. The energy of a quantum scalar field has a similar contact divergence, even if constant in time. In the case of effective theories with a natural breakdown scale, it can be simply dealt with by introducing a UV cutoff Λ. If instead we wish to consider fundamental CQ field theories, the resolution of this divergences becomes more subtle – and likely requires renormalisation of the coupling constants of the theory.

A note of caution. Naively, one would expect that each mode with spatial momentum p contributes with $1/p^2$ to the total energy of the field at a certain fixed t time slice, since the two-point function ϕ^2 in momentum space scales like $1/p^4$. However (assuming for simplicity that the total energy of the field equipartitions between the time and spatial derivatives, as it does in the thermal state):

$$\begin{aligned}\mathbb{E}[H(\Delta t)] &\sim \int d^3x\ \mathbb{E}[\nabla\phi(\underline{x}).\nabla\phi(\underline{x})] \\ &\sim \int d^3p\ p^2\mathbb{E}[\phi(p,\Delta t)\phi(-p,\Delta t)] \\ &\sim \int d^3p\ p^2\frac{\Delta t}{p^2}\ .\end{aligned} \tag{4.60}$$

From the second to the third line, we have used the leading Δt contribution to the two-point function of the field *after* integrating over p_0, given the initial state (see Appendix B). Hence, each mode will contribute equally to the energy, with an amplitude that increases linearly with the time of diffusion. The total energy of the field relates therefore to the total volume of reciprocal space spanned by the modes of the theory. Indeed, assuming a cutoff energy scale Λ, we have:

$$H = \frac{D_2 c^5 V}{2G}\Lambda^3\Delta t\ , \tag{4.61}$$

in agreement with Equation 4.59.

Comparison to the quantum case

The divergent energy production we observe in the classical stochastic field theory shares a lot of similarities with its better-known counterpart, an open quantum field theory. To see this, consider the following representation of the Fokker-Planck evolution in Equation 4.8 (with no friction)

$$\frac{\partial P}{\partial t} = \{H, P\} + \frac{D_2}{2}\int d^3x\{\phi,\{\phi,P\}\} \tag{4.62}$$

This can also be used to compute the diffusion in energy via the "Heisenberg representation"

$$\frac{dH}{dt} = \frac{D_2}{2}\int d^3x\{\phi,\{\phi,H\}\} \tag{4.63}$$

which gives the linear in time energy increase proportional the contact divergence found in Equation 4.59. Whilst this is just a different representation of Itô's lemma, it is cosmetically very similar to the computation in the quantum case.

Indeed, a similar contact divergence appears in the energy production of the quantum scalar field, owing to the presence of modes with arbitrarily high energy. To see this, consider the following Lindblad equation for scalar fields

$$\frac{\partial \hat{\sigma}}{\partial t} = -i\left[\hat{H}, \hat{\sigma}\right] - \frac{D_0}{2}\int d^3x \, [\phi, [\phi, \hat{\sigma}]] \tag{4.64}$$

for the density matrix $\hat{\sigma}$ and Lindblad operators given by the scalar field operators ϕ [185, 186]. The similarity with the classical evolution is beyond cosmetic – in fact as the Lindblad operators are linear in the field, the quantum dynamics can be mapped exactly to our classical diffusive evolution in a similar fashion as what done in Section 3.3 for the one-dimensional oscillator. In particular, when computing the evolution of the Hamiltonian under the non-unitary evolution, one obtains a similar contact divergence in the heating rate to the one we find [43]. In the quantum field theory this is famously problematic, since it corresponds to an infinite production rate of bosons [186], as can be seen by deriving the time evolution for the bosonic number operator in the Heisenberg representation of the Lindblad dynamics. Of course, the energy production here is a result of the fact that the generator of the dynamics for this QFT model is specifically not the Hamiltonian, and the theory is therefore non-unitary.

4.3.6 Exact mode solution

Whilst the path-integral techniques discussed above are very general and can be applied to a variety of settings, the evolution of the probability distribution for the stochastic Klein-Gordon field can be computed exactly, mode by mode. To see this, introduce the following Fourier mode decomposition for the field and its conjugate momentum

$$\phi(\underline{x}, t) = \int \frac{d^3k}{(2\pi)^3}\phi_k(t)e^{i\underline{k}.\underline{x}} \, , \qquad \pi_\phi(\underline{x}, t) = \int \frac{d^3k}{(2\pi)^3}\pi_k(t)e^{i\underline{k}.\underline{x}} \, , \tag{4.65}$$

where for ease of notation we defined $f(\underline{k}, t) \equiv f_k(t)$. Similarly, let's introduce the mode expansion for the noise field

$$\xi(\underline{x}, t) = \int \frac{d^3k}{(2\pi)^3}\xi_k(t)e^{i\underline{k}.\underline{x}} \, , \tag{4.66}$$

it is straightforward to see that the noise moments imply

$$\mathbb{E}[\xi_k(t)\xi_{k'}(t')] = D\delta(t-t')\delta^{(3)}(\underline{k} + \underline{k}') \, . \tag{4.67}$$

Then, plugging in Equations 4.65 and 4.66 into the first order (frictionless) stochastic equations given by Equation 2.14, we find that the equations neatly separate into mode for mode, giving

$$\dot{\phi}_k = \pi_k \qquad \dot{\pi}_k = -E_k^2 \phi_k + \xi_k \ . \tag{4.68}$$

These are a tower of simple, independent, two-dimensional (degenerate) Ornstein-Ulhenbeck (OU) processes. OU processes are Gaussian-preserving, and the evolution of the moments of the probability distribution can be computed exactly. For simplicity, we take the mean to be zero, since it can be easily re-introduced (it just follows a solution to the Klein-Gordon equation with appropriate initial conditions). Then, consider each independent mode to be sampled from an initial mean-zero Gaussian distribution (we have assumed throughout that the initial state is a δ-function, which can be trivially recovered as its zero-variance limit)

$$P_k(\Phi_k, 0) = \frac{1}{2\pi\sqrt{\det[C_k(0)]}} \exp\left(-\frac{1}{2}\Phi_k^T C_k^{-1}(0)\Phi_k\right) \ . \tag{4.69}$$

The evolution equation preserve the mean-zero *and* the Gaussianity of the state, meaning that the only non-trivial degree of freedom to be solved for is the covariance matrix for the field and momentum of each mode. Note that here we have introduced the "field vector" $\Phi_k = (\phi_k, \pi_k)$. It is a standard result that for a OU process

$$d\Phi_k = \Theta_k \Phi_k \ dt + \Sigma \ dW_t \ , \tag{4.70}$$

where Θ and Σ are constant (field-independent) matrices, the covariance of the mean-subtracted process evolves following the time-dependent Lyapunov equation:

$$dC_k = d\mathbb{E}[\Phi_k \Phi_k^T] = d\mathbb{E}[d\Phi_k \Phi_k^T + \Phi_k d\Phi_k^T + d\Phi_k d\Phi_K^T] \tag{4.71}$$

$$= (\Theta_k C_k + C_k \Theta_k^T + \Sigma\Sigma^T)dt \ , \tag{4.72}$$

where the $(d\Phi_k)^2$ term has to be kept in the variation by Itô's lemma. By matching with the mode equations of motion in Equation 4.68, we can see that the evolution equations for the elements of the covariance matrix are given by

$$\dot{C}_{k,\phi\phi} = 2C_{k,\pi,\phi} \tag{4.73}$$

$$\dot{C}_{k,\pi\pi} = -2E_k^2 C_{k,\pi,\phi} + D \tag{4.74}$$

$$\dot{C}_{k,\pi\phi} = C_{k,\pi,\pi} - E_k^2 C_{k,\phi\phi} \ , \tag{4.75}$$

which can be solved exactly

$$C_{k,\phi\phi}(t) = \frac{C_{k,\phi\phi}(0)}{2}\left(1+\cos(2E_k t)\right) + \frac{C_{k,\pi\pi}(0)}{2E_k^2}\left(1-\cos(2E_k t)\right) + \left(C_{k,\pi\phi}(0) - \frac{D}{4E_k^2}\right)\sin(2E_k t) + \frac{D}{2E_k^2}t \ , \tag{4.76}$$

$$C_{k,\pi\pi}(t) = \frac{C_{k,\pi\pi}(0)}{2}\left(1+\cos(2E_k t)\right) + \frac{E_k^2 C_{k,\phi\phi}(0)}{2}\left(1-\cos(2E_k t)\right) - \left(E_k C_{k,\pi\phi}(0) - \frac{D}{4E_k}\right)\sin(2E_k t) + \frac{D}{2}t \ , \tag{4.77}$$

$$C_{k,\pi\phi}(t) = \left(C_{k,\pi\phi}(0) - \frac{D}{4E_k^2}\right)\cos(2E_k t) - \frac{1}{2}\left(C_{k,\phi\phi}(0) - \frac{C_{k,\pi\pi}(0)}{E_k}\right)\sin(2E_k t) + \frac{D}{4E_k^2} \ . \tag{4.78}$$

As per the now clear theme of this section, variances grow linearly in time mode by mode, both for the field and their conjugate momenta – and therefore so does the energy of the Klein-Gordon solution. By combining the evolution of the probability distribution mode per mode it is straightforward to reconstruct the time evolution of every initial Gaussian probability distribution over field space.

4.3.7 Implications for CQ gravity

Validity as a model of hybrid gravity

When considering linearised perturbation on a flat metric, i.e.:

$$g_{\mu\nu} = \eta_{\mu\nu} + h_{\mu\nu} \ , \qquad |h_{\mu\nu}| \ll 1 \ , \tag{4.79}$$

Einstein's equations in the harmonic gauge reduce to the statement that each component of the trace-subtracted metric follows a massless Klein-Gordon equation sourced by the stress-tensor of matter [187]:

$$\Box \bar{h}_{\mu\nu} = -16\pi G_N T_{\mu\nu} \ . \tag{4.80}$$

In vacuum, the scalar mode of the metric perturbations can be gauged away, with the only physical degrees of freedom being the two polarisations of the gravitational waves. When dynamical matter is present, however, the story is more complicated – the non-relativistic limit of the scalar mode maps to the Newtonian potential sourced by the matter distribution. For

anisotropic matter, there are two independent scalar modes that are gauge-invariant – related to the cosmological Bardeen potentials. These gauge-invariant scalar modes are not dynamical but are rather fixed by constraints equation (the Bianchi identities) [188]. The same is true for the gauge-invariant vector degrees of freedom, which are non-radiative and can in general be gauged away. Further, in cosmological background, they decay with the expansion, becoming irrelevant [188]. The only gauge-invariant mode that is indeed dynamical and follows a wave-like equation is still the transverse-traceless tensor mode – i.e. the two degrees of freedom associated with gravitational waves [187].

The identification of gauge-invariant modes in CQ theories is currently an open problem [135], meaning that we do not currently know whether physical scalar modes lack wave-like propagation as in GR – or have them as in scalar-tensor theories of gravities (in the case, for example, that the fundamental white noise process is a scalar random field). At any rate, we can consider the scalar stochastic wave equation as a toy model for Equation 4.80 where we ignore the tensorial structure of the polarisation of the modes. In this spirit, the stochastic scalar corresponds to the classical sector of CQ Nordström gravity – which does correctly give the Newtonian limit of the theory. Moreover, even if it may lack a concrete connection to CQ gravity itself, scalar fields coupled with Yukawa interactions do give rise to a $1/r$ potential, another reason why the stochastic KG field can be instructive as a simple toy model to understand the qualitative behaviour of a classical-quantum theory of gravity at least in the non-relativistic limit [174].

Moving away from the issue of constraints and physical degrees of freedom, the linearised description on flat space is guaranteed to break down as soon as the ratio between the typical size of the fluctuations and the background metric functions is larger than unity. As it is well-known from the theory of stochastic process, the solution to the stochastic wave equation in 3 spatial dimensions is highly irregular, meaning that in itself the effective linear theory breaks down immediately at short scales, where non-linear terms such as those found in [126] would therefore become important. Fortunately, non-linearities have been shown to cure the irregularity of the stochastic KG equation [189, 175]. These complexities aside, we can think of the stochastic Klein-Gordon field as providing a playground to understand some of the low-energy phenomenology of hybrid gravity theories, without much of the complexities that arise

from gauge redundancy and non-linearities that are necessary features of a complete theory.

Large forces on test masses in the linear theory

We now show how the stochastic fluctuations of the scalar field affects the motion of test particles interacting with it. Whether quantum fluctuations induce stochastic motion of a particle (sourcing and responding to the field) has been addressed in multiple studies [190, 191, 192, 59]. The result is highly sensitive on whether the field is in the vacuum or thermal state, and on the localisation of the particle interacting with the field. However, generally the effect is absent when the field is in the vacuum state and becomes important only at high temperatures [192, 59, 60]. As we see now, the converse is true for the classical stochastic fluctuations.

For a back-of-the-envelope estimation of the forces acting solid extended objects, let's treat the test mass as a classical constant density ρ sphere of diameter R. In the case of quantum particles, we will consider them localised within their Compton wavelength, i.e. $R = \lambda_c/2$. Then, in the Yukawa model, the particle responds to spatial gradients of the field. In particular, ignoring backreaction effects (i.e. radiation-reaction forces), the force on the test particle is simply given by:

$$F_i = -\rho \int d^3x \; \Theta\left(R - r\right) \partial_i \phi \; , \tag{4.81}$$

where r is the radial coordinate of the 3D cartesian system with origin at the center of the spherical mass. On average, ϕ vanishes and so does $\partial_i \phi$, meaning that the force on the particle induced by the stochastic fluctuations is zero on expectation in any specific direction. However, the norm of the vector itself has non-zero expectation. Indeed:

$$\mathbb{E}[F^2] = \mathbb{E}[F_i F^i] = \rho^2 \int d^3x \int d^3y \; \Theta\left(R - r_x\right) \Theta\left(R - r_y\right) \mathbb{E}[\partial_i \phi \partial_j \phi] \tag{4.82}$$

Extracting the two-point function of the spatial gradient of the field is straightforward – it suffices to take the spatial gradient of $\mathcal{C}$ by linearity of the expectation value. The complete expression is cumbersome – see Appendix B. For simplicity, we assume the timescale of the experiment is much shorter than the total time of the evolution of the system T, meaning $x^0 + y^0 - 2t_0 \approx 2T$. In the non-relativistic limit, the expression simplifies to:

$$\mathbb{E}[\partial_i \phi(x) \partial^i \phi(y)] = \frac{D_2 T}{2} \delta^{(3)}(\underline{x} - \underline{y}). \tag{4.83}$$

Again, this maps nicely to the equilibrium 2-point function, Equation 4.22. Then:

$$\mathbb{E}[F^2] = c^5 D_2 T \rho^2 V_M = \frac{D_2 T M^2 c^5}{V_M} \ , \tag{4.84}$$

where M is the mass of the particle, V_M its volume and we have re-introduced factors of c (and G, which does not appear as it is already implicitly included in the dimensionless diffusion coefficient). As measured by a device which coarse-grains the observation on a time-scale t_c, the centre of mass of the particle evolves as:

$$M\ddot{z}^i = F^i + f^i(t) \ , \tag{4.85}$$

where $\underline{F}$ is the sum of any external force acting on the particle, whilst $f^i(t)$ is a stochastic force obeying:

$$\mathbb{E}[f^i(t)] = 0 \ , \qquad \mathbb{E}[f^i(t) f^j(t')] = \frac{c^5 M^2 D_2 T}{4\pi R^3} t_c \ \delta^{ij} \delta(t - t') \ , \tag{4.86}$$

where we have defined $T = 0$ to be t_0, the initial time of diffusion of the scalar field, and have weighted the δ-function by t_c, the time scale associated with the spatial averaging.

First, let's consider the potential effect this would have had on one of the $M \approx 1$ Kg free-falling test masses in the LISA Pathfinder Technology Package, the ESA technology demonstration mission for the future gravitational wave detector LISA. The test masses used were objects of radius $R \approx 5 \times 10^{-2}$ m [193]. LISA Pathfinder results are quoted with respect to the variance in the relative acceleration spectral density of the masses – where the maximum frequency to which the experiment is sensitive is $\omega_* = 1/t_c \approx 1$ Hz. Being the effective force δ-correlated in time and space, the two masses are acted upon by uncorrelated random forces – and the spectral density of the acceleration variance of the test mass has flat frequency profile. Then:

$$\sigma^2_{aa}(\omega) = D_2 \times 10^{62} \ \mathrm{m^2 s^{-4} Hz} \ \lessapprox 10^{-30} \ \mathrm{m^2 s^{-4} Hz} \ . \tag{4.87}$$

Under this model, the accumulation over cosmological times of scalar stochastic wave would provide a formidable bound on the diffusion coefficient of the CQ theory:

$$D_2 \lessapprox 10^{-92} \ . \tag{4.88}$$

Coherence experiments on spatial superpositions currently lower bound the dimensionless diffusion coefficient by $D_2 \gtrapprox 10^{-63}$ [194] by the decoherence-diffusion trade-off, meaning that

the model would be ruled out by experiments. As mentioned earlier, this back-of-the-envelope estimation of the induced force by the stochastic fluctuations is not to be taken at face value as a good proxy for the predictions on tabletop experiments – both because scalar waves are not necessarily expected in CQ gravity, but most importantly because the linearised model cannot be trusted at short scales, where its irregular solution can in principle be cured by the self-interaction of the gravitational field. Yet, it is a strong indication that, unless renormalisation greatly reduces the size of the fluctuations in the UV by several orders of magnitude, CQ gravity can be experimentally tested with current technology.

The force induced by the fluctuations can be very large indeed. Another way to see why CQ gravity is in danger of being falsified unless the stochastic fluctuations are greatly reduced in the UV, is to consider their effects on subatomic particles. For example, consider the force on an electron-sized particle:

$$\bar{F} \approx \sqrt{D_2} \times 10^{19} \text{ N} , \tag{4.89}$$

which can be used set an order of magnitude bound on D_2. A good benchmark is the stability of Rydberg atoms, atoms in which the outermost electron is pushed to very excited radial states (i.e. the principal quantum number of the radial wavefunction n is very large, up to $n \approx 700$ [195]). In these case, the force that keeps the electron bound is of the order:

$$F_R \approx 10^{-19} \text{ N} , \tag{4.90}$$

meaning that, for these atoms to exist, the diffusion coefficient needs to be extremely small, i.e. $D_2 \lessapprox 10^{-76}$ – still violating the decoherence-diffusion trade-off. If the diffusion coefficient were larger than this, the nucleus and the elctrons would each feel a force in an uncorrelated direction of the typical size of the force that keeps the electron bound, meaning that the latter would be stripped out of its orbit immediately.

Heating

Recall, we found that with a cutoff scale Λ, the average energy density produced after evolving for T is given by:

$$H = \frac{D_2 c^5 V}{2G} \Lambda^3 T . \tag{4.91}$$

Comparing the observed energy density of the Universe with the one of the non-dissipative scalar after evolving for a Hubble time can be used to give a combined order of magnitude estimate of $D_2\Lambda^3$ in a hybrid classical-quantum theory of gravity. In particular, this has to be a negligible percentage of the critical energy density of the Universe ρ_c. Therefore, taking the cutoff scale to be $\Lambda \equiv 1/A\ell_P$ (where A is a dimensionless number and ℓ_P the Planck scale):

$$\frac{H}{V}\frac{1}{\rho_c} \ll 1 \implies \frac{D_2}{A^3} \ll \frac{H_0^3\ell_P^3}{4\pi c^3} \approx 10^{-184} \,, \tag{4.92}$$

meaning that either the diffusion coefficient of the theory is vanishingly small, or the cutoff scale of the theory is significantly above the Planck scale. From decoherence experiments we know the diffusion coefficient needs to be larger than $D_2 \geq 10^{-63}$, meaning that if the fluctuations gravitate the cutoff needs to be above the Planck length by at least 40 orders of magnitude, an unreasonably large scale. This observation mirrors the cosmological constant problem in QFT [83], with the twist that here the excess energy is in the classical fluctuations in the gravitational degrees of freedom themselves – other than the quantum matter field. The other distinct feature is that the classical energy density scales as $T\Lambda^3$, whilst the Lorentz invariant QFT vacuum requires Λ^4. Again, it needs to be seen whether a complete CQ theory of gravity resolves this issue through the non-linearities in the gravitational field.

4.4 Summary of the main results

In this chapter, we explored the stochastic KG equation. We began with a review of the classical Klein-Gordon thermal field, and the damped stochastic KG equation, for which the thermal state is a fixed point. We then removed friction, and discussed the non-dissipative system – which corresponds to the classical sector of the CQ scalar Yukawa theory. We first computed the two-point function of the field and showed it has a $1/r$ scaling for spacelike separated points – with the intensity of the covariance increasing linearly with the time elapsed from the initial slice. We similarly showed that the energy of the field grows linearly with time – though with an infinite rate if no UV cutoff exists. This is related to the infinite energy of the field itself, due to the contact divergence. We concluded by showing that the fluctuations have measurable physical effects. Indeed, we computed the induced force on a test-particle of finite size, showing that it is isotropic but has non-zero mean – and can lead to large accelerations on test masses

of the size of those planned for LISA.

Chapter 5

Phantom dark matter

5.1 Introduction

In this chapter, we study the stochastic Friedmann–Lemaître–Robertson–Walker (FLRW) Universe, probing the cosmological consequences of such stochasticity when modelled as a source in Einstein's field equations. Other proposals in which the metric field in cosmological settings is coupled to a stochastic source have been put forward over the years, such as the everpresent Lambda [196] and models motivated by unimodular gravity [197, 198]. We diverge from those approaches both in interpretation and implementation, due to the hypothesis of the gravitational degrees of freedom being *fundamentally* classical. This strongly constrains the form of the moments of the probability distribution of the noise field. Our starting point is that the dynamics needs to be completely positive, norm preserving and linear in the probability density to preserve the statistical interpretation of the probability density. This forces the dynamics to be of the form of [50, 51], where the statistics of the noise field cannot depend on the quantum states.

In standard GR, the set of algebraic relations known as the *constraint equations*, which the gravitational state has to satisfy at all times, arise as a consistency condition for diffeomorphism invariance. Further, the classical equations of motion guarantee that if the system is initialised on the constraint surface, it remains on it. This is no longer necessarily true in a stochastic theory. The generators of the diffeomorphisms become stochastic, and the GR constraint can be violated without necessarily breaking diffeomorphism invariance [135], a point we shall return

to in Subsection 8.2.3.

In our model, we find that the equations of motion evolve the Hamiltonian constraint C_H off the $C_H = 0$ surface even on average, with a positive drift term. Violation of the constraint can behave in an identical manner to cold (i.e. pressureless) dark matter, an effect previously discussed (with a different motivation) by [199, 200] and further explored in [201, 202]. In general however, the constraint violations can lead to the appearance of both positive and negative energy density. The main result of the present paper is to show that cosmological diffusion provides a natural mechanism to drive the system off the constraint surface *positively on average*, a necessary condition for the constraint violation to appear as if it were cold dark matter. Following from this, we find several other results. Starting from plausible assumptions about the dependence of diffusion rate on horizon scale, we calculate the amount of phantom cold dark matter that is produced. We find that the resulting density depends only on the dimensionless coupling constant of the theory, and the number of e-folds during radiation domination, with the phantom cold dark matter being produced primarily at the end of the inflationary phase. Next, we find that shortly after inflation production halts. We then highlight how the combination of tabletop experiments and cosmological data can provide non-trivial tests for the model we discuss.

5.2 Stochastization of Einstein's equations

The dynamics of any theory that describes a classical metric interacting with quantum matter without quantising the gravitational theory must be irreversible. In this chapter, we do not need the full CQ formalism as we assume quantum degrees of freedom to be fully decohered (and therefore classicalised) on cosmological scales. Rather, we look at a stochastic modification of Einstein's field equations (EFEs), since the irreversibility of continuous and Markovian hybrid dynamics translates into an equation of motion for the classical system sourced by a background white noise field ξ, irrespective of the state of the quantum system. The classical sector of canonical CQ gravity, Equation 2.68, corresponds to the Hamiltonian gravitational equations

sourced by a Gaussian stochastic scalar that satisfies:

$$\begin{aligned}\mathbb{E}[\xi(x,t)] &= 0 \ , \\ \mathbb{E}[\xi(x,t)\xi(x',t')] &= \frac{D_2}{\sqrt{h}N} D(x,t,x',t') \ ,\end{aligned} \tag{5.1}$$

where the expectation value is to be considered across realisations. Here, D_2 is the diffusion coefficient, and D is a function which encodes the correlation in the noise tensor between spacetime points. N and h, the lapse function and the determinant of the spatial metric, will be defined shortly, but their appearance is required for covariance. To preserve covariance, we also adopt the local kernel:

$$D(x,t,x',t') = \delta(x-x',t-t') \tag{5.2}$$

as the natural choice. We give an explicit example of how ξ can be constructed to be a scalar using standard tools from stochastic calculus in Section 5.2.2.

In this chapter, we work in the Arnowitt–Deser–Misner (ADM) formalism [129]. Therefore, we induce the following 3+1 decomposition of the metric:

$$g_{00} = -N^2 + h^{ij}N_iN_j \ , \qquad g_{0i} = N_i \ , \qquad g_{ij} = h_{ij}. \tag{5.3}$$

Here, h_{ij} is the spatial metric on the chosen foliation, while N and N^i (called the lapse function and shift vector respectively) tell us how the three geometry is embedded in the 4-dimensional manifold. The canonical equations of motion for gravity, with minimal coupling to the noise process, are given by:

$$\dot{h}_{ij} = \{h_{ij}, H_{\rm GR}\} + \{h_{ij}, H_{\rm m}\} \ , \tag{5.4}$$

$$\dot{\pi}^{ij} = \{\pi^{ij}, H_{\rm GR}\} + \{\pi^{ij}, H_{\rm m}\} + N\sqrt{h}h^{ij}\xi \ , \tag{5.5}$$

where π_{ij} is the conjugate momentum of the 3-metric and an overhead dot means differentiation with respect to coordinate time t. Moreover, $H_{\rm GR}$ and $H_{\rm m}$ are the gravity and matter Hamiltonian respectively, with $\{\cdot,\cdot\}$ being the Poisson brackets. We do not add a stochastic term to the evolution equation for h_{ij} in order to yield a geometry that is differentiable. The dimensionless coupling constant of the stochasticity is given by $G_N\sqrt{D_2/c^3}$, where we have momentarily re-introuced factors of c.

The third term in Equation 5.5 is the simplest stochastic term we can add that has the right transformation properties (i.e. it is a spatial 2-tensor density with weight -1 which

also transforms as a scalar density of weight -1 under time reparametrisations), under the assumption that the fundamental driving term is a scalar. This is equivalent to a noise tensor with the Wheeler-DeWitt metric (Equation 2.71) with large negative β as covariance tensor. The same modification can be obtained starting from the gravitational theory with action $S = S_{EH} + S_M$, made up of an Einstein-Hilbert gravitational term and matter term respectively, by adding a contribution that minimally couples the stochastic field to the metric:

$$S_{\mathrm{N}} = \int \mathrm{d}^4x\sqrt{g}\xi \ . \tag{5.6}$$

Then, deriving the equations of motion as usual, one arrives at Equation 5.5. Integrals such as those in Equation 5.6 require careful treatment, since ξ is nowhere integrable in the standard sense. As usual, we intend them in the Itô sense.

Any other stochastic term would amount to a derivative coupling between the noise field and the spacetime metric, rather than a standard stochastic source to the gravitational field. Nonetheless, at the level of the effective cosmological diffusion, we consider a noise kernel beyond the minimally coupled one, to understand the dependence of our result on the modelling choices. As we will see, the qualitative result remains the same – only quantitative predictions change.

Due to covariance, in standard GR the equations of motion are supplemented by the vanishing of the Hamiltonian and momentum constraints, C_H and C_P^i respectively:

$$C_H \equiv \mathcal{H} + N^2\sqrt{h}T^{00} \approx 0 \ , \tag{5.7}$$

$$C_P^i \equiv \mathcal{H}^i - N\sqrt{h}h^{ij}T_{0j} \approx 0 \ , \tag{5.8}$$

where $\approx$ indicates that such algebraic relations hold only on-shell. Here, $\mathcal{H}$ and $\mathcal{H}^i$ are functionals of the gravitational phase space variables h_{ij} and π_{ij} only. The role of constraints in CQ theory has been explored in detail in [135], and we will further explore the relation between constraints and covariance in stochastic theories in Subsection 8.2.3.

5.2.1 Stochastic FLRW

We now focus on Friedmann-Lemaître-Robertson-Walker universes. As usual, we impose spatial isotropy and homogeneity, picking the gauge $N^i = 0$ to have these symmetries manifest in the

3-metric. The spatial metric h_{ij} must then be of the form:

$$\begin{aligned} \mathrm{d}\ell^2 &= h_{ij}\mathrm{d}x^i\mathrm{d}x^j \\ &= a^2(t)\left(\frac{1}{1-kr^2}\mathrm{d}r^2 + r^2\mathrm{d}\Omega^2\right) \ , \end{aligned} \tag{5.9}$$

where $\mathrm{d}\Omega^2$ is the metric on S_2, whilst $a(t)$ is the so-called scale factor, a dimensionless function controlling the time-dependent "radius" of the Universe. On the other hand, k is the Gaussian curvature of the space for $a(t) = 1$, and, in our convention, has units of inverse area. Later, we consider early time cosmology with an inflationary phase. Since inflation washes out any spatial curvature, we will restrict our attention to flat spatial slices ($k = 0$) for simplicity. We will however treat the general case for as long as useful. Homogeneity also requires that the lapse N has no spatial dependence. Up to the choice of lapse function, the 4-metric has then the form:

$$\mathrm{d}s^2 = -N(t)^2\mathrm{d}t^2 + a^2(t)\left(\frac{1}{1-kr^2}\mathrm{d}r^2 + r^2\mathrm{d}\Omega^2\right) \ . \tag{5.10}$$

For comoving pressureless dust, the stress tensor is given by:

$$\begin{aligned} T_{\mu\nu} &= (1+w)\rho\ u_\mu u_\nu + w\rho\ g_{\mu\nu} \\ &= N^2(t)\rho\ \delta_{\mu 0}\delta_{\nu 0} + w\rho\ g_{\mu\nu}, \end{aligned} \tag{5.11}$$

where ρ is the energy density of matter and w the equation of state parameter. We have used the fact that the appropriately normalised 4-velocity u^μ of a comoving fluid is given by:

$$u^\mu = \frac{1}{N}(1,0,0,0) \ . \tag{5.12}$$

By plugging in the FLRW metric in the Einstein-Hilbert action, one can show that the mini-superspace (the configuration space of GR when restricting to homogeneous metrics) Hamiltonian is given by:

$$H_{\mathrm{GR}} = -N\left(\frac{2\pi G_N}{3}\frac{\pi_a^2}{a} + \frac{3}{8\pi G_N}\frac{k}{a}\right) \ . \tag{5.13}$$

Here, we have used the definition of π_a as the conjugate momentum of a:

$$\pi_a = \frac{\partial \mathcal{L}_{\mathrm{EH}}}{\partial \dot{a}} = -\frac{3}{4\pi G_N}\frac{\dot{a}a}{N}, \tag{5.14}$$

which is related to the conjugate momentum of the homogeneous 3-metric itself via $\pi^{ij} = \delta^{ij}\pi_a/6a$. Now, taking the trace of the ADM equations of motion, we obtain the cosmological

evolution equations:

$$\dot{a} = -\frac{4\pi G_N}{3} N \frac{\pi_a}{a} \tag{5.15}$$

$$\dot{\pi}_a = -\frac{2\pi G_N}{3} N \frac{\pi_a^2}{a^2} + N 3 w a^2 \rho + N \frac{3}{8\pi G_N} k + N a^2 \bar{\xi} \ , \tag{5.16}$$

up to numerical prefactors in the coupling to the noise which can always be absorbed into the diffusion coefficient. Here, we have also included the effect of curvature for completeness. Moreover, we have forced the noise process to be homogeneous in space.

We have assumed that the local noise can be represented by the global random field $\bar{\xi}$, which has to obey the following statistics:

$$\mathbb{E}[\bar{\xi}(t), \bar{\xi}(t')] = \frac{\bar{D}_2(a)}{N} \delta(t - t') \ . \tag{5.17}$$

We explain how $\bar{\xi}$ can be obtained from the local stochastic field in Subsection 5.2.3. The homogeneous diffusion coefficient $\bar{D}_2(a)$ is, in principle, an arbitrary functional of the scale factor which encodes how one translates the local theory into the homogeneous one. The factor of inverse lapse is needed for time reparametrisation invariance as we discuss in Section 5.2.2.

In GR, the Hamiltonian constraint provides an initial condition for the state:

$$C_H = \frac{2\pi G_N}{3} \frac{\pi_a^2}{a} - \rho a^3 + \frac{3}{8\pi G_N} \frac{k}{a} \approx 0 \ , \tag{5.18}$$

where we have made the effect of the curvature k explicit. The set of relations given by Equation 5.15 (without noise) and Equation 5.18 is completely equivalent to Friedmann's equations.

In this chapter, we discuss the consequences of a dynamical violation of the constraint. It is, therefore, natural to question whether one is allowed at all to use the constraint as an initial condition in such a model. In fact, we show that inflation washes out any initial deviation from the constraint, making the ambiguity in the initial state essentially irrelevant. A point that will be important later is that comoving pressureless dust enters the equations of the system only through the Hamiltonian constraint.

Since we do not couple matter and the stochastic field directly, we leave the equations of motion for the fluid unchanged with respect to the standard treatment. Fundamentally, one can understand the system as being described by the following action:

$$S = S_{\mathrm{EH}} + S_{\mathrm{N}} + S_{\mathrm{BK}} \ , \tag{5.19}$$

where S_{BK} is the Brown-Kuchař action [203], which provides the Langrangian formulation of a perfect fluid, whilst S_{EH} is the Einstein-Hilbert action and S_{N} is the stochastic term defined by Equation 5.6. Consequently, one finds that covariant conservation of the stress-energy tensor associated with the fluid ($\nabla_\mu T^\mu_\nu = 0$) still holds. Therefore, the energy density of the fluid dilutes with the scale factor as usual:

$$\rho = \rho_0 a^{-3(1+w)} \ , \tag{5.20}$$

with ρ_0 being the value of the energy density for unit scale factor. The stochastic field pumps energy only into the gravitational sector.

5.2.2 Noise and time reparametrisation

To study the evolution of the constraint under the modified equations of motion, we need to specify the white noise ξ in terms of Wiener processes. Recall that a Wiener process (or, equivalently, Brownian motion) W_t is an almost surely continuous stochastic process with Gaussian increments distributed as:

$$\Delta W = W_t - W_{t'} \sim \mathcal{N}(0, t - t') \ . \tag{5.21}$$

Schematically, the infinitesimal difference of a Wiener process $\mathrm{d}W_t$ is of order $\mathcal{O}(\sqrt{\mathrm{d}t})$, a statement made precise via Itô's lemma. In the physics community, it is standard to define the white noise field as the distributional derivative of Brownian motion [204], i.e:

$$\xi \sim \frac{\mathrm{d}W_t}{\mathrm{d}t} \ . \tag{5.22}$$

However, ξ so defined fails to be a scalar under time reparametrisation (it is a density of weight 1/2), which can be seen from dimensional analysis. The generalisation needed is readily given by:

$$\xi \equiv \frac{\mathrm{d}W_t}{\mathrm{d}t} \to \xi \equiv \frac{1}{N}\frac{\mathrm{d}W_{\int N \mathrm{d}t}}{\mathrm{d}t} = \frac{1}{\sqrt{N}}\frac{\mathrm{d}W_t}{\mathrm{d}t} \tag{5.23}$$

which has the required transformation properties and inherits from the Wiener process the statistics postulated in Equation 5.17 as we now show.

After a monotonic redefinition of time $u = g(t)$, we have that $\mathrm{d}W_t$ can be expressed in terms of a Wiener process with respect to the new time u as:

$$\mathrm{d}W_{u=g(t)} = \sqrt{\dot{g}}\ \mathrm{d}W_t \ . \tag{5.24}$$

This can be understood both from the scaling property of a Wiener process and from Itô's lemma ($\mathrm{d}W_t \sim \sqrt{\mathrm{d}t}$). The stochastic integral:

$$\int \Sigma[N]\mathrm{d}W_t \tag{5.25}$$

is left invariant under such a transformation if Σ to transforms under time reparametrisation as:

$$\Sigma' = \frac{1}{\sqrt{\dot{g}}}\Sigma \ . \tag{5.26}$$

Hence, we need Σ to be a scalar density in time of weight $w = 1/2$. In this form, it is immediate to see that the choice $\Sigma[N] = \sqrt{N}$ gives the desired transformation property. The invariant stochastic integral takes the form:

$$\int \sqrt{N_t}\mathrm{d}W_t = \int \xi N \mathrm{d}t \ , \tag{5.27}$$

where the derivative of the Wiener process has to be understood in a distributional sense.

We can now trivially extract the moments that the stochastic field inherits from the following properties of the Wiener process:

$$\mathbb{E}[W_t] = 0 \ , \qquad \mathbb{E}[W_t W_s] = \min(s,t) \ , \tag{5.28}$$

which, as we now show, lead to:

$$\mathbb{E}[\xi(t)] = 0 \ , \qquad \mathbb{E}[\xi(t)\xi(t')] = \frac{1}{N(t)}\delta(t,t'). \tag{5.29}$$

First, consider the definition of ξ as a distributional derivative of the Wiener process acting on some test function ϕ:

$$\begin{aligned} \xi[\phi] &= \int_0^\infty \xi(t)\phi(t)N(t)\mathrm{d}t \\ &= -\int_0^\infty W(t)\frac{\mathrm{d}}{\mathrm{d}t}\left(\sqrt{N(t)}\phi(t)\right)\mathrm{d}t \ . \end{aligned} \tag{5.30}$$

Then:

$$\begin{aligned} \mathbb{E}[\xi[\phi]] &= -\int_0^\infty \mathbb{E}[W(t)]\frac{\mathrm{d}}{\mathrm{d}t}\left(\sqrt{N(t)}\phi(t)\right)\mathrm{d}t = 0 \\ &= \int_0^\infty \mathbb{E}[\xi(t)]\phi(t)N(t)\mathrm{d}t \ , \end{aligned} \tag{5.31}$$

yielding $\mathbb{E}[\xi] = 0$. For the variance, start from:

$$\begin{aligned}
\mathbb{E}[\xi[\phi]^2] &= \int_0^\infty \int_0^\infty \mathbb{E}[W(t)W(t')] \frac{\mathrm{d}}{\mathrm{d}t}\left(\sqrt{N(t)}\phi(t)\right) \mathrm{d}t \frac{\mathrm{d}}{\mathrm{d}t'}\left(\sqrt{N(t')}\phi(t')\right) \mathrm{d}t' \\
&= \int_0^\infty \int_0^\infty \min(t,t') \frac{\mathrm{d}}{\mathrm{d}t}\left(\sqrt{N(t)}\phi(t)\right) \mathrm{d}t \frac{\mathrm{d}}{\mathrm{d}t'}\left(\sqrt{N(t')}\phi(t')\right) \mathrm{d}t' \\
&= \int_0^\infty \frac{\mathrm{d}}{\mathrm{d}t}\left(\sqrt{N(t)}\phi(t)\right) \left[\int_0^t \sqrt{N(t')}\phi(t')\mathrm{d}t'\right] \mathrm{d}t \\
&= \int_0^\infty \int_0^\infty \delta(t,t')\sqrt{N(t)}\phi(t)\sqrt{N(t')}\phi(t') \ \mathrm{d}t'\mathrm{d}t
\end{aligned} \tag{5.32}$$

.

However, we also have:

$$\mathbb{E}[\xi[\phi]^2] = \int_0^\infty \int_0^\infty \mathbb{E}[\xi(t)\xi(t')] \ \phi(t)\phi(t')N(t)N(t') \ \mathrm{d}t\mathrm{d}t', \tag{5.33}$$

and comparing the two we obtain the claimed variance for the noise process, up to an arbitrary scale D_2.

5.2.3 Renormalising the diffusion coefficient

In order to establish the relation between the local diffusion coefficient and the global parameter $\bar{D}_2(a)$ a procedure to flow to the long-wavelength regime is needed. At present, we do not have a rigorous procedure for performing this renormalisation. Differing procedures could lead to a different scaling of the diffusion with the scale factor. Therefore, we will treat D_2 as a general function of a for as long as possible.

Nonetheless we can commute the spatial averaging and time evolution for a well-motivated estimate of the background evolution of the universe (as is common in standard cosmological calculations). Just as the mean energy density enters the equations of motion for a FLRW Universe, we take the spatial average value of the noise for its realisation at time t to be the stochastic source in the global Einstein's equations. Therefore, we interpret $\bar{\xi}$ as the average of the local random field given by Equation 5.1 over a spatial domain on the spacelike constant t hypersurface. We essentially adopt the standard assumption in cosmology that the inhomogeneous Universe can be approximated as homogeneous and isotropic to leading order [205]. This should be an acceptable approximation as long as the typical size of the local fluctuations is

much smaller than the average energy density of the matter sourcing the homogeneous evolution. Additional work will be required to address whether it is possible to derive formally that such an effective dynamics is valid in the IR (long-wavelength) limit.

Working in the separate-universe approximation [206], we imagine the scale factor as assigned to a finite-sized patch of the Universe. To turn the noise field homogeneous, we define:

$$\bar{\xi}_\Sigma(t) = \frac{\int_\Sigma d^3x\sqrt{g}\xi}{\int_\Sigma d^3x\sqrt{g}} \ , \tag{5.34}$$

where Σ is the spatial region over which we average the noise, introducing a long-distance IR cutoff $R_{\rm IR}$ over which we trust the homogeneous description. Trivially we still have $\mathbb{E}[\xi_\Sigma(t)] = 0$, whereas:

$$\mathbb{E}[\bar{\xi}_\Sigma(t), \bar{\xi}_\Sigma(t')] = \frac{D_2}{N\int_\Sigma d^3x\sqrt{g(x)}}\delta(t-t') \ . \tag{5.35}$$

We thus see that when flowing to a model in which local noise becomes averaged noise, D_2 needs to be renormalised by the volume of the region over which we average, as expected from the central limit theorem. The renormalisation scheme then boils down to choosing the spatial domain over which to average; we now present two natural options that lead to very different late-time behaviour.

One natural choice for $R_{\rm IR}$ in FLRW cosmologies is the comoving Hubble radius $R_{\rm IR} = 1/aH$, i.e. averaging over the spatial region that is in causal contact over the current e-fold of cosmological evolution. This leads to an effective variance that scales as the inverse of the Hubble volume:

$$\mathbb{E}[\bar{\xi}_\Sigma(t), \bar{\xi}_\Sigma(t')] = \frac{3}{4\pi}\frac{D_2}{N}H^3\delta(t-t') \ . \tag{5.36}$$

Imagine now that we work in the low-noise limit, meaning that the stochastic trajectories are well approximated to leading order by the deterministic evolution. In an inflationary early-Universe phase the Hubble parameter is constant ($H(t) = H_I$) and so the variance, too, remains constant. During matter and radiation domination, however, the situation changes radically as the Hubble parameter falls with time following $H \propto t^{-1}$ in both eras. Consequently, the effective noise gets damped significantly as the Universe expands. This is, effectively, a consequence of the causal horizon of the patch expanding after inflation. Indeed, more and more modes re-enter the horizon and contribute to the effective cosmological noise, which converges to the average value with vanishing variance by the central limit theorem. Of course, this is only true at

the cosmological level, meaning that the inhomogeneous perturbations still follow a stochastic evolution.

An alternative spatial averaging scheme in which the stochastic term remains relevant at late times is to adopt the choice of $R_{\rm IR}$ being some fixed comoving radius $R_{\rm IR} = R/a$. This way, we obtain:

$$\mathbb{E}[\bar{\xi}_\Sigma(t), \bar{\xi}_\Sigma(t')] = \frac{3}{4\pi R^3}\frac{D_2}{N}\delta(t-t') \ . \tag{5.37}$$

This appears less motivated than the previous choice of averaging over a horizon volume, but we include it as a possibility in the absence of a fully principled approach at present. From now on, we drop the subscript Σ from the noise field.

5.3 Phantom CDM from constraint violation

5.3.1 Violation of the deterministic Hamiltonian constraint

In standard GR, the constraint equations are satisfied at all times. However, using Itô's lemma, we can see how the constraint evolves on-shell once noise is introduced.

We derive here the evolution of the constraint

$$C_H = \frac{2\pi G_N}{3}\frac{\pi_a^2}{a} - \rho a^3 \ . \tag{5.38}$$

on the stochastic trajectories given by

$$\dot{a} = -\frac{4\pi G_N}{3} N \frac{\pi_a}{a} \tag{5.39}$$

$$\dot{\pi}_a = -\frac{2\pi G_N}{3} N \frac{\pi_a^2}{a^2} + N 3 w a^2 \rho + N \frac{3}{8\pi G_N} k + N a^2 \bar{\xi} \ , \tag{5.40}$$

$$\rho = \rho_0 a^{-3(1+w)} \ , \tag{5.41}$$

i.e. with conservation of energy enforced in the matter sector. We allow:

$$\mathbb{E}[\xi(t)] = 0 \ , \qquad \mathbb{E}[\xi(t), \xi(t')] = \frac{D_2(a)}{N}\delta(t,t') \ , \tag{5.42}$$

with the diffusion having a general dependence on the scale factor. It is always possible to rescale ξ as

$$\xi = \sqrt{D_2(a,\pi_a)}\bar{\zeta} = \sqrt{D_2(a)}\frac{1}{\sqrt{N}}\frac{\mathrm{d}W_t}{\mathrm{d}t} \tag{5.43}$$

such that we make the scaling of the noise with the fundamental degree of freedom a manifest in the equations of motion (keeping, however, $\bar{\zeta}$ a scalar under time-parametrisation since we have not extracted the dependence on N).

Using Itô's lemma, is then immediate to check that up to $\mathcal{O}(\mathrm{d}t)$:

$$\begin{aligned}\mathrm{d}C_H &= \frac{\partial C_H}{\partial a}\mathrm{d}a + \frac{\partial C_H}{\partial \pi_a}\mathrm{d}\pi_a + \frac{1}{2}\frac{\partial^2 C_H}{\partial \pi_a^2}\mathrm{d}\pi_a^2 \\ &= -\frac{2\pi G_N}{3}\frac{\pi_a^2}{a^2}\mathrm{d}a + \frac{4\pi G_N}{3}\frac{\pi_a}{a}\mathrm{d}\pi_a + \frac{2\pi G_N}{3}\frac{1}{a}\mathrm{d}\pi_a^2 \\ &= \frac{4\pi G_N}{3}a\pi_a\sqrt{ND_2(a,\pi_a)}\mathrm{d}W_t + D_2(a,\pi_a)\frac{2\pi G_N}{3}a^3 N\mathrm{d}t\ ,\end{aligned} \tag{5.44}$$

Only terms proportional to D_2 appear since the deterministic equations preserve the constraint – all the drift terms cancel each other. Using the definition of the reparametrisation invariant white noise field and $D_2(a,\pi_a) = 3D_2H^3/4\pi$, we obtain

$$\dot{C}_H = D_2(a)\frac{2\pi G_N}{3}Na^3 + \frac{4\pi G_N}{3}N\pi_a a\bar{\xi}\ . \tag{5.45}$$

The Hamiltonian constraint $C_H \approx 0$ is therefore broken by the stochastic dynamics. The second term causes diffusion of C_H around zero, as expected. The first term is an anomalous drift that can be understood via Itô's lemma. This "second order force" pushes the average value of the constraint away from zero, meaning that C_H is not conserved even on average. Equation 5.45 is the first result of this chapter. From it, we can immediately see that the constraint violation will, on average, be positive. Previous work has considered the role of constraints in classical-quantum theories [207, 135], and whether the constraints of the deterministic part of the dynamics can be violated without breaking covariance. Here, we focus on the phenomenological implications of such a result.

The positive constraint violation is connected with entropy production in the state, since the average constraint depends on the variance of the conjugate momentum. The probability distribution of momenta begins sharply peaked by assumption in the initial conditions, but diffuses in time through stochastic kicks which increase the entropy of the classical distribution. This is formally equivalent to the heating up of a Brownian particle without friction, and it is fundamentally connected to the irreversibility of the Fokker-Planck equation governing the evolution of the probability distribution over states.

5.3.2 Phantom CDM

Now we consider what effects departing from the Hamiltonian constraint has upon the observable properties of the Universe. Consider first a matter dominated Universe for simplicity. When averaging over the Hubble horizon, the noise term drops out at late times from the equations of motion and the system reduces to standard GR, since $H \to 0$. During the early phases of the cosmological evolution, however, the system might have accumulated a non-trivial violation of the deterministic constraint δC.

In such a low-noise regime, a violation of the Hamiltonian constraint evolves as "phantom" extra pressureless dust in the system. To see this, first note that the deterministic Friedmann equations preserve the value of the constraint even when off-shell; consequently, the constraint value C_H is frozen in time once the noise becomes subdominant. The constraint equation reads:

$$\frac{2\pi G_N}{3}\frac{\pi_a^2}{a} - \rho a^3 = C_H, \tag{5.46}$$

where ρ is the total matter density. An observer who infers the expansion history in such a universe assuming that it is governed by GR would attempt to absorb the non-zero value of C_H into this total matter density. For a multi-component fluid, ρ can be re-written as

$$\rho a^3 = \sum_i \rho_i a^{-3w_i} \ , \tag{5.47}$$

meaning that C_H can be absorbed into an effective $w_i = 0$ component. Therefore, the state with violation of the constraint C_H corresponds to a standard FLRW geometry with effective dust energy density $\rho_{\mathrm{eff},0} = \rho_{\mathrm{m},0} + C_H$, where $\rho_{\mathrm{m},0}$ is the energy density of the physical dust when the scale factor a is unity.

A similar observation has been made in [199, 200] and studied in detail in [201, 202], motivated by the classical limit of quantum gauge theories. In [200] a simple argument is presented for why constraint violations appear like dust, even in inhomogeneous spacetimes. To recap the argument, consider Einstein's equations in covariant form:

$$G^\mu_\nu = 8\pi G_N \tilde{T}^\mu_\nu \ , \tag{5.48}$$

where the (i, j) sector corresponds to the ADM equations of motion, whilst the $(0, \mu)$ is related to constraints. Since we are considering the small-noise regime, we take the spatial part of

Einstein's equations is to be satisfied exactly, whilst we allow for the constraints to be violated. Then, we have

$$G^i_j = 8\pi G_N T^i_j \ , \tag{5.49}$$

while

$$G^0_\mu = 8\pi G_N T^0_\mu + 8\pi G_N C^0_\mu \ , \tag{5.50}$$

where T^μ_ν is the visible matter stress tensor, whilst C^μ_ν is the constraint violation. This is the situation we will encounter soon after inflation, when the state has diffused away from the $C_H \approx 0$ surface on average in the positive direction, while $C_i \approx 0$ is still guaranteed from homogeneity and isotropy. For renormalisation schemes that lead to a H^n scaling for the diffusion coefficient, the post-inflationary stochastic dynamics is suppressed due to averaging the fluctuations over an increasingly larger spatial volume whenever $n \geq 3$, as we show shortly. It includes the case we focus on, namely the one where the averaging happens over the Hubble horizon. It is important to point out that, other than the $n = 3$ and $n = 0$ cases, we are not aware of any renormalisation schemes that will lead that general behaviour. We include the general n result for completeness – it is possible, for example, that a non-minimal noise coupling could lead with such a scaling for the diffusion coefficient when flowing from the local to the global theory.

A strong constraint on how C^μ_ν varies in spacetime now arises from the combination of the Bianchi identities and the conservation of stress-energy of the true fluid source. Indeed, by looking at the LHS of Equation 5.48, we have

$$\nabla_\nu G^\nu_\mu = 0 \implies \nabla_\nu (T^\nu_\mu + C^\nu_\mu) = 0 \ . \tag{5.51}$$

Imposing covariant conservation of the matter stress tensor, we end up with the requirement:

$$\nabla_\mu C^\mu_\nu = 0 \tag{5.52}$$

which, alongside $C^i_j = 0$, implies that the constraint violations evolve exactly like a matter perturbation with $w = 0$, even in highly inhomogeneous limits. For completeness, we show now that the same exact statement can be derived by using the spatial components of Einstein's equations and covariant conservation of the visible matter in linear perturbation theory, although the argument given above is more general.

5.4 Inhomogeneous evolution

Consider a homogeneous cosmology with small perturbations. Expanding the metric to linear order as $g_{\mu\nu} = g^{(0)}_{\mu\nu} + \epsilon h_{\mu\nu}$, where ϵ is a small parameter and $g^{(0)}_{\mu\nu}$ satisfies the background Friedmann's equations sourced by a homogeneous perfect fluid $T^{(0)}$ with density ρ and equation of state parameter w. For simplicity, we consider a single background fluid, but the argument is insensitive to this assumption. The homogeneous background evolution is allowed to be off the constraint surface by C_H. The metric perturbations solve the standard linearised equations for cosmological perturbations. For simplicity, consider the cosmological perturbations in Newtonian gauge:

$$\begin{aligned} \mathrm{d}s^2 = a^2(\tau)\Big[&- \left(1 + 2\epsilon\phi(k,\tau)e^{ik^i x_j}\right)\mathrm{d}\tau^2 \\ &+ \left(1 - 2\epsilon\psi(k,\tau)e^{ik^i x_j}\right)\delta_{ij}\mathrm{d}x^i\mathrm{d}x^j\Big] \ , \end{aligned} \tag{5.53}$$

where we have expanded the metric functions in Fourier modes and have assumed $k = 0$ for the background solution. These metric perturbations are sourced by small inhomogeneous perturbations in the matter density. For a comoving perfect fluid, these are given by:

$$\begin{aligned} \delta T^0_0 &= \epsilon\delta\rho \ , \\ \delta T^0_i &= \frac{\epsilon}{a}(1+w)\rho\delta U_i \ , \\ \delta T^i_j &= -\epsilon w\delta\rho \ \delta^i_j \ , \end{aligned} \tag{5.54}$$

where $\delta\rho$ is the perturbation in energy density in the matter field, whilst δU^i is the relative velocity of the fluid perturbations with respect to the comoving frame. Similarly, the inhomogeneous perturbations to the global constraint violation read:

$$\begin{aligned} \delta C^0_0 &= \epsilon\delta C \ , \\ \delta T^0_i &= \frac{\epsilon}{a}C_H\delta C_i \ , \\ \delta C^i_j &= 0 \ \delta^i_j \ , \end{aligned} \tag{5.55}$$

i.e. they cosmetically appear as pressureless matter violation ($w = 0$). To make the analogy precise, however, one needs to check that the evolution itself is identical to that of matter. As we now show, this can be derived just by using the spatial components of Einstein's equations and covariant conservation of the visible matter.

By computing the variation of the Einstein's tensor to linear order in ϵ and matching terms order by order in an ϵ expansion, one obtains on top of the background Friedmann equations the linearised equations for the perturbations:

$$4\pi G_N a^2(\delta\rho + \delta C_H) = -k^2\psi - 3\mathcal{H}(\psi' + \mathcal{H}\phi) \tag{5.56}$$

$$4\pi G_N a(1+w)\rho(\delta U_i + \delta C_i = -ik_i(\psi' + \mathcal{H}\phi) \tag{5.57}$$

$$4\pi G_N a^2 w\delta\rho\ \delta^i_j = \left[\psi'' + \mathcal{H}(2\psi+\phi)' + (2\mathcal{H}' + \mathcal{H}^2)\phi - \frac{1}{2}k^2(\phi-\psi)\right]\delta^j_j - \frac{1}{2}(\phi-\psi)k_i k_j\ , \tag{5.58}$$

where k^2 is the squared euclidean norm of k, $\mathcal{H} = a'/a$ and we indicate differentiation with respect of conformal time with a prime. Again, we have here ignored the noise terms due to CQ effects. The absence of anisotropic stress, as in standard cosmological perturbation theory, forces the two scalar metric functions to be equal to each other ($\psi = \phi$), reducing the equations of motion to:

$$4\pi G_N a^2(\delta\rho + \delta C_H) = -k^2\phi - 3\mathcal{H}(\phi' + \mathcal{H}\phi) \tag{5.59}$$

$$4\pi G_N a\left[(1+w)\rho\delta U_i + C_H\delta C_i\right] = -ik_i(\phi' + \mathcal{H}\phi) \tag{5.60}$$

$$4\pi G_N a^2 w\delta\rho = \left[\phi'' + \mathcal{H}(2\phi+\phi)' + (2\mathcal{H}' + \mathcal{H}^2)\phi\right]\ , \tag{5.61}$$

from which we see that δC acts as a matter perturbation and δC_i as the velocity of the effective fluid. Since we minimally couple the noise of gravity, we can take the stress-tensor of visible matter to be covariantly conserved, which implies:

$$\delta\rho' = -3\mathcal{H}(1+w)\delta\rho - (1+w)\rho(ik_i\delta U_i - 3\phi') \tag{5.62}$$

$$\frac{1}{a^4}\left(a^5(1+w)\rho\ ik_i\delta U^i\right)' = wk^2\delta\rho + (1+w)k^2\rho\phi. \tag{5.63}$$

It is now a matter of simple algebra to show that also δC and δC^i, on shell, obey identical relations with $w = 0$. It will be useful to use Friedmann equations, which correspond to:

$$\mathcal{H}^2 - \mathcal{H}' = 4\pi G_N a^2\left[(1+w)\rho + C_H\right]\ . \tag{5.64}$$

To derive the induced evolution equation for δC, we simply differentiate Equation 5.59 with respect to conformal time and substitute back Equations 5.60, 5.61, 5.62 and 5.64 to obtain:

$$\delta C' = -3\mathcal{H}^2\delta C - C_H\left(ik_i\delta C^i - 3\phi'\right)\ . \tag{5.65}$$

This indeed matches Equation 5.62 with $w = 0$. Similarly, taking both the time and spatial derivative of Equation 5.60 and using the field equations of motion in Equation 5.61 and 5.63 together with Friedmann's equation, we obtain for the momentum constraint violation

$$\frac{1}{a^4}\left(a^5 C_H \; ik_i \delta C^i\right)' = k^2 C_H \phi \; . \tag{5.66}$$

Therefore, we see explicitly that, even at the inhomogeneous level, small constraint violations in the zero-noise limit behave exactly as pressureless dust perturbations with average energy density C_H. Indeed, the linearised inhomogeneous Hamiltonian constraint violation δC acts as energy density perturbations, whilst the violation to the momentum constraint δC^i plays the role of the peculiar velocity of the phantom fluid.

5.4.1 Production during inflation

In order for the constraint violation to play the role of CDM, C_H needs to be on average positive and in agreement with the dark matter density inferred from observations. We find that an inflationary phase of the early-Universe can drive the Universe to the desired state, albeit with a density that is highly uncertain. To see why, we return to the homogeneous model in the separate Universe approximation. Consider the ADM equations of motion for a FLRW Universe with Lambda domination instead

$$\dot{a} = -\frac{4\pi G_N}{3}\frac{\pi_a}{a} \tag{5.67}$$

$$\dot{\pi}_a = -\frac{2\pi G_N}{3}\frac{\pi_a^2}{a^2} + \frac{3}{2\pi G_N} a^2 \Lambda_I + a^2 \bar{\xi} \; . \tag{5.68}$$

This is an effective approximation to the inflationary state, which reproduces the main feature we are interested in for the generation of constraint violation – a shrinking horizon – without the need of modelling the evolution of a dynamical (slow-rolling) inflationary field. Whilst a more complete description of the dynamics can quantitatively change the results we obtain here due to the fact that the Hubble parameter is not *exactly* constant in slow-roll inflation, but rather slowly decreasing, at this stage we are only interested in producing an order of magnitude estimation for the phantom dark matter energy density produced. Further, as we will shortly see, the early stage of radiation-domination causes an order 1 enhancement of the phantom CDM produced in inflation anyways – every corrections due to appropriate modelling of the

inflaton field and the reheating stage can be interesting refinements, but won't significantly change the main result.

The stochastic field acts as a random fluctuation to the dark energy term. Note that we have chosen Λ_I to have the geometric units of m^{-2} and picked the renormalisation scheme for D_2 where we average over the Hubble horizon:

$$\bar{D}_2(a) = \frac{3}{4\pi} D_2 H^3. \tag{5.69}$$

We can further rescale $\bar{\xi}$ to make the dependence of the variance explicit:

$$\bar{\xi} = \sqrt{D_2 H^3}\bar{\zeta} \tag{5.70}$$

This way, $\bar{\zeta}$ has units of $\mathrm{m}^{-1/2}$ and moments:

$$\mathbb{E}[\bar{\zeta}(t)] = 0 \ , \qquad \mathbb{E}[\bar{\zeta}(t), \bar{\zeta}(t')] = \frac{1}{N}\delta(t - t') \ , \tag{5.71}$$

with the units of the diffusion coefficient D_2 being

$$[D_2] = \mathrm{kg}^2\,\mathrm{s}\,\mathrm{m}^{-3} = [G_N]^{-2}\,[c]^3, \tag{5.72}$$

where we have momentarily reintroduced factors of c for completeness.

If the standard deviation of the stochastic kicks is much smaller than the energy density that drives inflation, then $\sqrt{D_2} G_N \ll 1$. One can accordingly approximate the inflationary evolution as the deterministic exponential expansion:

$$a(t) = \tilde{a} e^{H_I t} \ , \tag{5.73}$$

with $\tilde{a}$ the initial value of the scale factor at inflation and $H_I = \sqrt{\Lambda_I/3}$ the value of the Hubble parameter (which, in this approximation, remains constant during the inflationary period). Then, the evolution of the constraint is given by:

$$\begin{aligned} \dot{C}_H &= \frac{3 D_2 G_N}{8\pi} a^3 H^3 + \frac{4\pi G_N}{3} \pi_a a \sqrt{D_2 H^3}\bar{\zeta} \\ &= \frac{3 D_2 G_N}{8\pi} \tilde{a}^3 e^{3H_I t} H_I^3 - H_I \tilde{a}^3 e^{3H_I t} \sqrt{\frac{3}{4\pi} D_2 H_I^3}\bar{\zeta} \ . \end{aligned} \tag{5.74}$$

We take inflation to last from $t_0 = 0$ to reheating at t_I, corresponding to $N_I = \ln[a(t_I)/a(0)]$ e-folds of expansion. The evolution of the expectation value of C_H from the beginning of inflation

can be readily integrated (recalling that $\bar{\zeta}$ has zero mean) to give:

$$\begin{aligned}\bar{C}_I = \mathbb{E}[C_H(t_I)] &= C_{H,0} + \frac{3D_2G_N}{8\pi}\tilde{a}^3H_I^3\int_0^{t_I} e^{3H_It'}\mathrm{d}t' \\ &= C_{H,0} + \frac{D_2G_N}{8\pi}\tilde{a}^3H_I^2\left(e^{3H_It_I}-1\right) \\ &\sim \frac{D_2G_N}{8\pi}\tilde{a}^3H_I^2e^{3H_It_I} = \frac{D_2G_N}{8\pi}a_I^3H_I^2\ ,\end{aligned} \tag{5.75}$$

where $C_{H,0}$ is an arbitrary initial violation of the constraint at the beginning of inflation, a_I is the value of the scale factor at the end of inflation and in the last line we have taken the large N_I limit. This shows that, if the inflationary phase lasts long enough, any initial violation of the constraint becomes negligible and we would be left at reheating with a positive average violation C_H. Combined with the previous result, that constraint violations act as pressureless dust, this shows that phantom cold dark matter can arise dynamically in a CQ theory of gravity.

A natural question to ask is what variation around the mean one can expect for C_H under the above assumptions. For this calculation, we take $C_{H,0} = 0$ since it is so easily swamped by the dynamically-generated constraint violation. First, consider:

$$\mathbb{E}[C_H^2] = \bar{C}_I^2 + \frac{3D_2H_I^5}{4\pi}\tilde{a}^6\int_0^{t_I}\int_0^{t_I} e^{3H_It'}e^{3H_It''}\mathbb{E}[\bar{\zeta}(t')\bar{\zeta}(t'')]\mathrm{d}t'\mathrm{d}t''\ . \tag{5.76}$$

Imposing Equation 5.36 one obtains:

$$\begin{aligned}\sigma_I^2 &= \mathbb{E}[C_H^2(t_I)] - \bar{C}_I^2\ , \\ &= D_2\tilde{a}^6\frac{H_I^4}{8\pi}\left(e^{6H_It_I}-1\right) \\ &\sim \frac{1}{8\pi}D_2\tilde{a}^6H_I^4e^{6H_It_I} = \frac{1}{8\pi}D_2a_I^6H_I^4\ ,\end{aligned} \tag{5.77}$$

where again we have taken the large e-folds limit. Finally, one can evaluate the ratio between the standard deviation and the mean to be:

$$\frac{\sigma_I}{\bar{C}_I} = \frac{\sqrt{8\pi}}{\sqrt{D_2}G_N}\ , \tag{5.78}$$

independent of the number of e-folds during or after inflation.

The above results are derived assuming renormalization via averaging over a Hubble volume, such that the effective diffusion rate scales with H^3. For generality, we also report the result for a renormalisation procedure that leads to a polynomial scaling of arbitrary degree n with the

Hubble parameter H. From dimensional analysis, cosmic diffusion scaling with H^n is related to the local diffusion coefficient by:

$$\bar{D}_2 = \frac{3}{4\pi} D_2 H^n L^{n-3} \ , \tag{5.79}$$

up to numerical factors, where L is some length scale needed for dimensional consistency. Under this general scaling the average constraint violation accumulated during inflation in the large e-fold limit is given by:

$$\bar{C}_{I,n} \simeq \frac{D_2 G_N}{8\pi} a_I^3 H_I^{n-1} L^{n-3} \ . \tag{5.80}$$

Similarly, the variance amounts to:

$$\sigma^2_{I,n} \simeq \frac{D_2}{8\pi} a_I^6 H_I^{n+1} L^{n-3} \ , \tag{5.81}$$

meaning that the normalised variations have typical size:

$$\frac{\sigma_{I,n}}{\bar{C}_{I,n}} = \frac{\sqrt{8\pi}}{\sqrt{D_2} G_N} \left(H_I L\right)^{\frac{3-n}{2}} \ . \tag{5.82}$$

For $n = 3$ we indeed recover our previous result.

5.4.2 Radiation domination and beyond

In standard cosmological models, once inflation ends, the universe reheats into a radiation domination phase. During radiation domination, the violation of the Hamiltonian constraint continues to accumulate. Since the comoving Hubble radius expands during radiation domination, one has the additional complication that patches which have different stochastic realisations during inflation now enter causal contact, necessitating an inhomogeneous calculation.

However, the rate of change for C_H depends cubically on H when averaging over a horizon patch. H drops linearly with time during radiation domination, so phantom cold dark matter is generated significantly only in the first few e-folds of radiation domination, where one can still work in the separate Universe approximation. By the time significant inhomogeneities enter the horizon, the noise has effectively decoupled from the evolution of the scale factor. From there on, we can treat the Universe as satisfying the standard Friedmann equations, with the density (and density fluctuations) of phantom cold dark matter already determined. As the universe

later evolves out of radiation domination and into matter domination, this picture continues to hold since H only decreases.

To evaluate the phantom cold dark matter produced during the early stages of radiation domination, we can repeat the same calculation as before, now assuming that the zeroth order evolution in the scale factor is given by:

$$a(t) = a_I \sqrt{2H_I t + 1} \ , \tag{5.83}$$

where we have matched both the scale factor and the Hubble parameter at the end of inflation with the respective quantities at the beginning of radiation domination. Also, we are re-shifting time such that radiation domination runs from $t = 0$ to $t = t_R$. We indicate with $\bar{C}_R$ the average violation of the Hamiltonian constraint accumulated during radiation domination:

$$\begin{aligned} \bar{C}_R &= \frac{D_2 G_N}{2} a_I^3 \int_0^{t_R} \left(H \sqrt{2H_I t' + 1} \right)^3 \mathrm{d}t' \\ &= \frac{D_2 G_N}{2} a_I^3 H_I^3 \int_0^{t_R} \left(2H_I t' + 1 \right)^{-3/2} \mathrm{d}t' \\ &= \frac{D_2 G_N}{2} a_I^3 H_I^2 \left(1 - \frac{1}{\sqrt{2H_I t_R + 1}} \right) \\ &\sim \frac{D_2 G_N}{2} a_I^3 H_I^2 = 3 \bar{C}_I \ . \end{aligned} \tag{5.84}$$

Note that in the last line we have dropped the t_R-dependent term since we have taken the large N_R limit for radiation domination as well. As expected, most of the phantom matter density is accumulated in the first few e-folds of radiation domination. That leads to a factor of 3 enhancement with respect to what was generated during inflation, i.e.:

$$\frac{\bar{C}_R}{\bar{C}_I} = 3 \ . \tag{5.85}$$

We can similarly calculate the growth in the size of the fluctuations during radiation domination. The variance of the violation is given by:

$$\begin{aligned} \sigma_R^2 &= a_I^6 D_2 H_I^2 \int_0^{t_R} \int_0^{t_R} H^3 \mathbb{E}[\bar{\zeta}(t') \bar{\zeta}(t'')] \times \\ &\qquad \times \sqrt{2H_I t' + 1} \sqrt{2H_I t'' + 1} \mathrm{d}t' \mathrm{d}t'' \\ &= \frac{3}{4\pi} a_I^6 H_I^5 D_2 \frac{t_R}{2H_I t_R + 1} \\ &\sim \frac{3}{8\pi} a_I^6 H_I^4 D_2 = 3\sigma_I^2 \ . \end{aligned} \tag{5.86}$$

The total final variance is additive, since the noise is uncorrelated in time. Therefore:

$$\sigma^2 = \sigma_I^2 + \sigma_R^2 \tag{5.87}$$

Hence, at the end of radiation domination, the density contrast in $\bar{C}_H$ is given by:

$$\frac{\sigma}{\bar{C}_H} = \frac{\sqrt{\sigma_I^2 + \sigma_R^2}}{\bar{C}_I + \bar{C}_R} = \frac{1}{2}\frac{\sigma_I}{\bar{C}_I} = \frac{3}{\sqrt{8\pi}}\frac{1}{\sqrt{D_2}G_N} \ . \tag{5.88}$$

Since we have been working in the limit of $\sqrt{D_2}G_N \ll 1$, σ_I would be much greater than the average violation; i.e. fluctuations in the density of phantom cold dark matter are larger than the overall density, leading to negative densities in some regions. At first sight this is a major problem, since measurement of the CMB temperature fluctuations show $\delta T/T \ll 1$, which, in standard cosmology, is a quantity related to the density contrast $\delta\rho/\rho$ of matter. However, Equation 5.88 is not the quantity that we expect to observe in the CMB itself, because it is strongly dominated by fluctuations on microscopic scales (in the order of the comoving horizon scale at the end of inflation). Indeed, there are even more extreme fluctuations that have been averaged over to write down an effective homogeneous theory. The evolution of these microscopic scales is beyond the scope of this chapter, but we continue to work on the assumption that cosmological effects will see an effective density averaged over relevant scales. If this is the case, the variance in the phantom dark matter density will be drastically dampened by a factor given by the averaging volume, yielding a positive energy density with very small perturbations around the mean.

Returning to the mean density, we should consider the effect of our renormalisation choice on the result. For general polynomial scaling with H, the average constraint violation accumulated during radiation domination is:

$$\bar{C}_R = \frac{D_2 G_N H_I^{n-1} L^{n-3}}{2}\frac{(2H_I t_r + 1)^{\frac{5-2n}{2}} - 1}{5-2n}a_I^3 \ . \tag{5.89}$$

Whilst for inflation different n trivially translated into different scaling of the final result with H_I, in radiation domination the situation is more complex, due to the dynamical nature of the Hubble parameter. Indeed, the accumulation of constraint violation continues long into radiation domination unless $n \geq 3$. This would pose severe issues for interpreting the stochastic effects as phantom cold dark matter, since the gravitating density would vary while baryon acoustic waves propagated through the early universe, likely violating CMB constraints [208].

5.4.3 Estimating the amount of phantom dark matter

The energy scale of inflation, the e-folds of inflationary expansion and the averaged diffusion coefficient of the theory determine the amount of phantom dark matter generated. To check whether observational bounds on the cosmological density parameters can rule out such a mechanism for dark matter generation, we compute the density parameter of phantom dark matter today given that we generate phantom dark matter with average energy density $\bar{C}_H$ in the early stages of radiation domination. As usual, we define the density parameter of an energy species i as:

$$\Omega_i = \frac{\rho_i}{\rho_c} \ , \tag{5.90}$$

where $\rho_c = 3H_0^2/8\pi G_N$ is the critical energy density. Then:

$$\Omega_c(a) = \frac{8\pi G_N \bar{C}_H a^{-3}}{3H_0^2} = \frac{4\pi}{9} D_2 G_N^2 \frac{H_I^2}{H_0^2}\frac{a_I^3}{a^3} \ , \tag{5.91}$$

which, assuming N, P and M e-folds of inflation, radiation domination and matter domination respectively, reduces to:

$$\Omega_c(a) = \frac{4\pi D_2 G_N^2}{9c^3}\frac{H_I^2}{H_0^2} e^{-3(M+P)} \ , \tag{5.92}$$

where we have momentarily reintroduced factors of c. The e-folds of inflation naturally drop from the expression since the generation of dark matter and its dilution due to the expansion of the Universe have opposite scaling with the scale factor a. However, H_I/H_0 is completely determined once M and P are known. Indeed, at the end of radiation domination we have:

$$H_R = H_I e^{-2P} \ , \tag{5.93}$$

whilst from the beginning of matter domination to today the Hubble parameter evolves to:

$$H_0 = H_R e^{-3M/2} = H_I e^{-\frac{4P+3M}{2}} \ . \tag{5.94}$$

Plugging this back into Equation 5.92 we have that the e-folds of matter domination also drop from the expression, leaving:

$$\Omega_c(a) = \frac{4\pi D_2 G_N^2}{9c^3} e^P \ . \tag{5.95}$$

The phantom cold dark matter density thus depends only on the dimensionless coupling constant $D_2 G^2/c^3$ and P, the number of e-folds of radiation domination, meaning that it is in

principle determined by existing cosmological constraints and laboratory limits on diffusion. P is constrained by the ratio of the temperature at matter-radiation equality ($z_{eq} = 3400$) and at the temperature after reheating, which in turn is related to the inflationary energy (often taken to be GUT scale). Minimal models of inflation usually constrain $P \approx 55$, following from bounds on the inflation energy scale given by CMB data [208].

Table-top experiments currently bound the value of the diffusion coefficient to $D_2 G_N^2 \lessapprox 10^{-43}$ (in natural units) in the case the fluctuations have no effective mass [209]. Relating the diffusion at the energy scales of table-top experiments, to the higher energy scale of inflation requires, other than the averaging procedure already described and the renormalisation of D_2 that accompanies it, a careful consideration of the RG flow of the stochastic theory at different energy scales [136]. Since the theory can be related to quadratic gravity which is asymptotically free, the coupling constant $D_2 G_N^2$ is expected to run [210, 211, 212, 213, 136]. The stochastic fluctuations may also have an effective mass [136], which can also suppress fluctuations at lower energy scales. These topics are still active area of research, and most of the questions are still open, meaning that we cannot currently perform that mapping reliably. The best we can do at the moment is to use current bounds on the diffusion coefficient from table-top experiments and assume that they trivially apply in Equation 5.92, in order to showcase how the combination of cosmological observations and table-top experiments can provide a powerful stress-test for classical-quantum theories of gravity.

Assuming $P = 55$ e-folds of radiation domination, we obtain $\Omega_c \approx 10^{-19}$ as the density parameter of phantom dark matter today, saturating the quoted upper bound for the diffusion coefficient. In order to obtain an Ω_c of order unity, one would require, still with $P = 55$, a diffusion coefficient of $D_2 G_N^2 \approx 10^{-25}$, several orders of magnitudes above this bound. Saturating the experimental bounds on D_2, instead, one would require $P = 100$ e-folds of radiation domination. Were the bounds on the diffusion coefficient derived in Chapter 4 apply even when one considers refinement to the linear model, the situation would worsen further – the mechanism here described would virtually not contribute at all to the observed dark matter budget under standard models of inflation.

However, a similar disclaimer as for the results in Chapter 4 is in order. This back-of-the-envelope calculation has to be taken lightly since, as discussed above, flowing the local theory

to the IR cosmology consistently is a non-trivial step, currently a work in progress. Still, if, like in the case we have discussed, $\bar{C}_H$ turns out to be very small, then one cannot rule out hybrid gravity since CDM can always be included as a bona fide matter component in the Universe. The upshot would be that the cosmological departure from the constraint would be very hard to detect, and the homogeneous cosmology is well approximated by deterministic GR models even if spacetime is indeed fundamentally classical. If instead precise measurement of H_I, P and D_2 lead to a larger-than-observed amount of phantom CDM, one would rule out CQ theories that do not preserve the deterministic constraints of GR. Indeed, even though the GR constraint violation is a natural consequence of the model we have considered, one can expect that non-minimal models exist in which the constraints are satisfied exactly at the level of trajectories. We describe such an option in Section 5.5.1. In general, however, the expectation is that such dynamics require a modification of the equations of motion even at the level of the deterministic drift, which makes them less desirable. In the middle of these two extremes is the possibility that phantom CDM is produced with the correct density to account for cosmological CDM; however, the calculations above show that this would imply a fine-tuned relationship between P and D_2.

5.5 Summary of the main results

In this chapter, we have shown that a natural consequence of the stochasticity is the violation of the deterministic constraints of GR. We argued why in the low-noise limit, such a constraint violation acts as an effective pressureless dust both in the homogeneous and inhomogeneous treatment. Then, we presented a mechanism by which, during inflation, the integrated effect of the stochasticity leads to a constraint violation that is, on average, positive. This provides one of the missing ingredients needed to show that such an effect could imitate the cosmological fingerprint of cold dark matter.

We discussed how, for a natural choice of renormalisation scheme in which the homogeneous global noise is related to the local one by averaging across the Hubble horizon, the phantom matter generation stops a few e-folds after inflation, since the effective diffusion coefficient drops as H^3. This is a necessary condition for this mechanism to produce phantom cold

dark matter that is consistent with CMB constraints. Shortly after the beginning of radiation domination, the cosmological noise becomes negligible and the evolution is adequately captured by the standard Friedmann's equations with phantom CDM on cosmological scales. The average density of the phantom matter follows a simple relation that depends on the horizon-scale diffusion coefficient, the energy scale of inflation and the number of e-folds of expansion of the Universe. Improving existing constraints on H_I, the number of e-folds of inflation and the inferred CDM density will in turn put tight constraints on D_2.

5.5.1 Imposing the constraint

The deviation from the deterministic constraint is not necessarily a sign that the stochastic theory is inconsistent. Still, a natural question is whether one can come up with any modification to the evolution process that conserves the deterministic constraint. This has been done for a stochastic extension to the geodesic equation, where the associated Dirac constraint corresponds to the mass shell condition $p^2 = -m^2$. A Lorentz covariant diffusion equation was derived from first principle in [7] and matched with the causal set theory-motivated Lorentz invariand diffusion equation dubbed as the "swerves equation" [214, 215]. In order to preserve the mass-shell condition *exactly* at the level of trajectory, a diffusion-dependent drift term had to be added.

It turns out that, for the stochastic cosmological model, there are two possible modifications that will lead to that result. The first one is coupling the noise to the matter system, breaking covariant conservation of energy-momentum for matter. We can see this with a bottom-up approach. Assume that the energy density is allowed to evolve via under a general SDE:

$$\mathrm{d}\rho = \mu(a, \pi_a, \rho)\mathrm{d}t + \sigma(a, \pi_a, \rho)\mathrm{d}W_t \ . \tag{5.96}$$

We can then *require* that the constraint is satisfied and work out what the evolution law for ρ needs to be. Using Itô's lemma once more, we get:

$$\begin{aligned}
\mathrm{d}C_H &= \frac{\partial C_H}{\partial a}\mathrm{d}a + \frac{\partial C_H}{\partial \pi_a}\mathrm{d}\pi_a + \frac{1}{2}\frac{\partial^2 C_H}{\partial \pi_a^2}\mathrm{d}\pi_a^2 + \frac{\partial C_H}{\partial \rho}\mathrm{d}\rho \\
&= -\left(\frac{2\pi G}{3}\frac{\pi_a^2}{a^2} + 3\rho a^2\right)\mathrm{d}a + \frac{4\pi G}{3}\frac{\pi_a}{a}\mathrm{d}\pi_a - a^3\mathrm{d}\rho + \frac{4\pi G}{3}\frac{1}{a}\mathrm{d}\pi_a^2 \\
&= -a^3\mathrm{d}\rho + 4\pi G\rho a\pi_a N\mathrm{d}t + \frac{4\pi G}{3}a\pi_a\sqrt{ND_2}\mathrm{d}W_t + D_2\frac{2\pi G}{3}a^3 N\mathrm{d}t + \mathcal{O}(\mathrm{d}t\ \mathrm{d}W_t) \ .
\end{aligned} \tag{5.97}$$

Requiring this to vanish amounts to setting:

$$\mu(a, \pi_a, \rho) = -\frac{4\pi G}{3}\left(3\frac{\pi_a}{a^2}N + \frac{D_2}{2}N\right) \tag{5.98}$$

$$\sigma(a, \pi_a, \rho) = -\frac{4\pi G}{3}\frac{\pi_a}{a^2}\sqrt{ND_2}\ , \tag{5.99}$$

meaning

$$\mathrm{d}\rho = \frac{4\pi G}{3}\left(3\frac{\pi_a}{a^2}\rho + \frac{D_2}{2}\right)N\mathrm{d}t + \frac{4\pi G}{3}\frac{\pi_a}{a^2}\sqrt{ND_2}\mathrm{d}W_t\ . \tag{5.100}$$

Of course, for $D_2 = 0$ this recovers the deterministic evolution for matter.

The other approach is to make the evolution of a stochastic instead. Here, we work under the assumption that the deterministic drift should not be changed as we still want the canonical gravitational equations of motion to be satisfied on average for every value of D_2. Therefore, we allow only for a diffusion term in a:

$$\mathrm{d}a = -\frac{4\pi G}{3}N\frac{\pi_a}{a}\mathrm{d}t + \sigma_a(a, N)\mathrm{d}W_t\ . \tag{5.101}$$

By repeating the same procedure as above we find that by picking:

$$\sigma_a = \frac{a^3}{\pi_a}\sqrt{N} \tag{5.102}$$

the induced drift term in the evolution of the constraint cancels, meaning that the constraint is satisfied on average (but not at the level of trajectories). However, stochasticity in a directly means that the definition of the conjugate momentum breaks dowm.

Part II

Braneworld holography

Chapter 6

Braneworld holography

Semi-classical gravity remains a useful proxy to study quantum effects in gravity from the perspective of a macroscopic observer. In this context, quantum fields live in a classical dynamical spacetime where the combined system is characterized by the semi-classical Einstein equations [216, 217]

$$G_{\mu\nu}(g) + \Lambda g_{\mu\nu} = 8\pi G_N \langle T^{\rm QFT}_{\mu\nu} \rangle \ . \tag{6.1}$$

Here, we allow a general cosmological constant Λ – but we will shortly restrict to the case of asymptotically de Sitter Universe ($\Lambda > 0$). As briefly discussed in Subsection 1.2.1, the right-hand side $\langle T^{\rm QFT}_{\mu\nu} \rangle$ is the expectation value of the *renormalized* stress-energy tensor of the quantum field theory in some quantum state $|\Psi\rangle$. Semi-classical gravity should be viewed as an approximation and only valid in a certain regime. Indeed, the semi-classical approximation fails near the Planck scale as at this level quantum gravity effects become important, such that Equation 6.1 can no longer be trusted. Further, the semi-classical field equations are not expected to be valid for generic quantum states $|\Psi\rangle$, e.g., macroscopic superpositions [218].

Even in its regime of validity, solutions to semi-classical gravity, particularly black holes, are difficult to study consistently. In this chapter we review the main ideas behind *braneworld holography*, an approach motivated by the AdS/CFT correspondence to solve the backreaction problem exactly. In fact, as we see shortly, we won't be solving Equation 6.1, but a semiclassical gravity theory with higher-derivative corrections in d spacetime dimensions

$$G_{ij} + \Lambda_d g_{ij} + (\text{higher-curvature}) = 8\pi G_d \langle T^{\rm CFT}_{ij} \rangle_{\rm planar} \ . \tag{6.2}$$

with the matter being specifically a conformal field theory (i.e. matter fields invariant under the conformal group).

At first glance it would appear that the braneworld has only complicated the situation with its higher-derivative corrections: solving the induced field equations in Equation 6.2 requires solving the problem of backreaction in a complex higher-derivative theory of gravity. The computational advantage of braneworld holography, however, is that the semi-classical induced brane theory has an equivalent bulk description in terms of classical AdS_{d+1} gravity coupled to a brane obeying Israel junction conditions. Thus, exact spacetimes solving the classical bulk field equations with brane boundary conditions automatically correspond to exact solutions to the semi-classical brane equations of motion, Equation 6.2. Holographic braneworlds thus provide a means to exactly study the problem of backreaction without having to explicitly solve semi-classical field equations. In particular, classical AdS_{d+1} black holes which localize on an end-of-the-world (ETW) brane are conjectured to precisely map to black holes in d-dimensions, including all orders of quantum backreaction [113], i.e., 'quantum' black holes.

The primary purpose of this chapter (and the next) is to review the state of the art regarding such holographic quantum black holes – and then present in detail a novel solution uncovered using the braneworld approach. Emphasis is given to a particular class of analytic black holes which localize on an AdS_4 braneworld, first uncovered by Emparan, Horowitz and Myers [219, 220], corresponding to three-dimensional quantum black holes [113, 221, 219, 5]. These braneworld black holes lead to an important observation: backreaction can lead to the existence of black holes where there were none before. That is, famously, there are no black hole solutions in vacuum to classical Einstein gravity in three-dimensions with positive or vanishing cosmological constant. Rather, the geometry of a point mass in Mink_3 or dS_3 is described as a conical defect without a black hole horizon [222, 223]; Schwarzschild-dS_3, for example, is a conical defect with a single cosmological horizon but no black hole horizon. Quantum corrections due to backreaction alter the three-dimensional geometry in such a way that a black hole horizon is induced, leading to a type of (quantum) censorship of conical singularities. Meanwhile, classical black holes do exist in three-dimensional Einstein gravity with a negative cosmological constant [224, 225], a consequence of the tendency for gravitational collapse afforded by the negatively curved geometry. Nonetheless, in such contexts backreaction yields behavior strik-

ingly different from their classical counterparts. Unfortunatley, for phenomenologically relevant 4-dimensional black holes, the braneworld approach we describe here – using a brane judiciously placed in a bulk C-metric geometry to derive quantum-corrected solution – is inapplicable (due to the absence of a 5-dimensional generalisation to the C-metric). We discuss this in more detail in Chapter 8.

This chapter contains the following. We begin with a quick review of the classical Kerr-dS$_3$ geometry, a conical singularity with a cosmological horizon. Then, we perturbatively compute the backreaction in the geometry, showing that to leading order the corrections imply a $1/r$ term in the metric – suggesting that backreaction might set up a black hole horizon to "censor" the conical singularity. However, the correction due to a simple conformally coupled scalar is Planckian in size – meaning that it can't be trusted, as it pertains to the regime where semiclassical gravity itself breaks down. We then take a step back, and introduce the general braneworld construction. We start by using holographic renormalisation to derive the theory induced by the bulk on the ETW brane, followed by a detailed discussion why the AdS/CFT correspondence implies that the metric on the brane is to be interpreted as encoding all the backreaction effects from a quantum CFT. As we will see, such corrections are in generally macroscopic. Indeed, the typical associated lengthscale is the Planck length enhanced by a factor proportional to the central charge of the CFT – which is generally taken to be large in holographic setups.

6.1 Black holes and backreaction in 3D: a perturbative analysis

6.1.1 Three-dimensional black holes and conical defects

In vacuum general relativity, black holes tend to disappear when lowering the dimension of spacetime from four to three. This can be understood at the level of dimensional analysis. If the only dimensionful parameter is three-dimensional Newton's constant G_3, then introducing a massive object of mass M does not introduce an additional length scale needed to characterize a black hole horizon solely in terms of its mass; indeed, $G_3 M$ is dimensionless. Since we have set $c = 1$, mass has dimensions of inverse length while G_3 has dimensions of length. In fact, a massive point particle in flat $(2+1)$-dimensional general relativity is a conical defect, with

angular deficit $\delta = 2\pi(1 - \sqrt{1 - 8G_3M})$ and a conical singularity at the origin [222]. Moreover, while a cosmological constant Λ will introduce another length scale, this alone is not sufficient to have a black hole horizon. Gravitational attraction is also required.

To elaborate, there are black holes in asymptotically AdS_3. Namely, the Bañados-Teitelboim-Zanelli (BTZ) black hole [224, 225]

$$ds^2 = -N(r)dt^2 + N^{-1}(r)dr^2 + r^2(d\phi + N_\phi dt)^2 \,, \tag{6.3}$$

with lapse and shift metric functions

$$N(r) \equiv -8G_3M + \frac{r^2}{L_3^2} + \frac{(4G_3J)^2}{r^2} \,, \quad N_\phi \equiv -\frac{4G_3J}{r^2} \,, \tag{6.4}$$

for mass M and spin J. The roots of the lapse,

$$r_\pm^2 = \frac{L_3^2}{2}\left[8G_3M \pm \sqrt{(8G_3M)^2 - \left(\frac{8G_3J}{L_3}\right)^2}\right] \,, \tag{6.5}$$

characterize the outer (r_+) and inner/Cauchy (r_-) horizons, with $r_+ \geq r_- \geq 0$, assuming $ML_3 \geq J > 0$ to avoid naked singularities. The reason we can interpret the BTZ metric as a 'black hole' is because the negatively curved geometry of AdS_3 provides an innate geometric tendency for gravitational collapse (see, e.g., [226]). Alternatively, there are no black holes in dS_3; the positively curved dS_3 background leads to an inability for collapse. Consequently, a point mass in dS_3, is described by a conical defect [223] with a single cosmological horizon.

To see this latter point, consider the Kerr-dS_3 metric. The line element formally takes the same form as Equation 6.3 except now with lapse and shift functions

$$N(r) \equiv 1 - 8G_3M - \frac{r^2}{R_3^2} + \frac{(4G_3J)^2}{r^2} \,, \quad N_\phi \equiv +\frac{4G_3J}{r^2} \,, \tag{6.6}$$

where R_3 denotes the dS_3 length scale and '+' sign in N_ϕ is convention. Next, introduce dimensionless parameters $\gamma \equiv r_+/R_3$ and $\alpha \equiv -4G_3J/\gamma R_3 = ir_-/R_3$, where $r_\pm$ are

$$r_\pm^2 = \frac{R_3^2}{2}\left[(1 - 8G_3M) \pm \sqrt{(1 - 8G_3M)^2 - \left(\frac{8G_3J}{R_3}\right)^2}\right] \,, \tag{6.7}$$

with only a single positive root, r_+, identified as the cosmological horizon. Then, the coordinate transformation [223, 227, 5]

$$\tilde{t} = \gamma t + \alpha R_3 \phi \,, \quad \tilde{\phi} = \gamma\phi - \alpha t/R_3 \,, \quad \tilde{r}/R_3 = \sqrt{\frac{(r/R_3)^2 + \alpha^2}{\gamma^2 + \alpha^2}} \tag{6.8}$$

brings the Kerr-dS$_3$ geometry into an empty dS$_3$ form, i.e.,

$$ds^2 = -\left(1 - \frac{\tilde{r}^2}{R_3^2}\right) d\tilde{t}^2 + \left(1 - \frac{\tilde{r}^2}{R_3^2}\right)^{-1} d\tilde{r}^2 + \tilde{r}^2 d\tilde{\phi}^2 \, . \tag{6.9}$$

Here, however, the coordinates $(\tilde{t}, \tilde{\phi})$ do not have the same periodicity as standard dS$_3$, where $(t, r, \phi) \sim (t, r, \phi + 2\pi)$. Rather,

$$(\tilde{t}, \tilde{\phi}) \sim (\tilde{t} + 2\pi R_3 \alpha, \tilde{\phi} + 2\pi\gamma) \, . \tag{6.10}$$

Hence, Kerr$-$dS$_3$ is a conical defect geometry with angular deficit $\delta = 2\pi(1 - \gamma)$.

The thermodynamics of the cosmological horizon is straightforward to work out (see [228])

$$\begin{aligned} m &= \gamma^2 - \alpha^2 \, , \quad J = -\frac{\alpha\gamma R_3}{4G_3} \, , \quad \Omega_c = -\frac{\alpha}{\gamma R_3} \, , \\ T_c &= \frac{\gamma^2 + \alpha^2}{2\pi\gamma R_3} \, , \quad S_{\rm BH} = \frac{2\pi r_c}{4G_3} = \frac{2\pi R_3 \gamma}{4G_3} \, , \end{aligned} \tag{6.11}$$

satisfying the first law

$$dM = -T_c dS_{\rm BH} + \Omega_c dJ \, , \tag{6.12}$$

where $m = 1 - 8G_3 M$. Moreover, the system obeys the following Smarr relation

$$0 = -T_c S_{\rm BH} + \Omega_c J - 2PV_c \, , \tag{6.13}$$

where $P = -\frac{\Lambda}{8\pi G_3} = -\frac{1}{8\pi G_3 R_3^2}$ is a thermodynamic pressure and $V_c = \pi r_c^2$ the conjugate thermodynamic volume. If we allow for variations to the dynamical pressure, the above first law is extended to include a $+V_c dP$ term.

It is worth pointing out that the AdS$_3$ geometry in Equation 6.3 is not always a black hole. For $8G_3 M < 0$, the geometry is a conical defect, taking the form of empty AdS$_3$ (the line element in Equation 6.9 with Wick rotation $R_3 = -iL_3$), with the same periodicity as Equation 6.10, where now $\alpha \equiv r_+/L_3$ and $\gamma \equiv 4G_3 iJ/L_3$. In particular, when $J = 0$, the states with $-1 < 8G_3 M < 0$ correspond to conical defects with angular deficit $\delta = 2\pi(1 - \sqrt{-8G_3 M})$, while for $8G_3 M < -1$ the geometry has a conical excess; at $8G_3 M = -1$, the BTZ geometry is exactly empty AdS$_3$. Further, when $8G_3 M < 0$ (for arbitrary J) the metric components are well-defined everywhere, i.e., there is no horizon and the conical singularity at $r = 0$ is 'naked'.

6.1.2 Perturbative backreaction in Kerr-dS$_3$

Another way to introduce a dimensionful parameter is to allow for quantum effects. Namely, for $\hbar \neq 0$, there exists the three-dimensional Planck length $L_{\rm P} = \hbar G_3$ (though there is no notion of Planck mass in three-dimensions). The question then is whether such quantum effects can modify the classical three-dimensional geometry so as to induce a (black hole) horizon when there was none before.

Evidence of this comes from perturbatively solving the semi-classical Einstein equations (Equation 6.1) for a conformally coupled scalar field Φ [229, 230, 231, 232, 233, 97, 219, 5], characterized by the action

$$I = \frac{1}{16\pi G_3}\int d^3x\sqrt{-g}\,[R-2\Lambda] - \frac{1}{2}\int d^3x\sqrt{-g}\left[(\nabla\Phi)^2 + \frac{1}{8}R\Phi^2\right] . \tag{6.14}$$

In such a set-up, the first step is to determine the renormalized stress tensor $\langle T_{\mu\nu}\rangle$.

The energy-momentum tensor for Φ is found by varying the matter action

$$T_{\mu\nu} \equiv -\frac{2}{\sqrt{-g}}\frac{\delta I_\Phi}{\delta g^{\mu\nu}} = \frac{3}{4}\nabla_\mu\Phi\nabla_\nu\phi - \frac{1}{4}g_{\mu\nu}(\nabla\Phi)^2 - \frac{1}{4}\Phi\nabla_\mu\nabla_\nu\Phi + \frac{1}{4}g_{\mu\nu}\Phi\Box\Phi + \frac{1}{8}G_{\mu\nu}\Phi^2 . \tag{6.15}$$

We will be interested in the case when $G_{\mu\nu} = -g_{\mu\nu}\Lambda$, where $\Lambda = \frac{1}{R_3^2}$ and $R = 6/R_3^2$. Upon invoking the scalar equation of motion,

$$\left(\Box - \frac{1}{8}R\right)\Phi = 0 , \tag{6.16}$$

it follows that the stress-energy tensor is both traceless and conserved.

Below we compute the renormalized quantum stress-energy tensor $\langle T_{\mu\nu}\rangle$ of the free scalar field. We do this in two steps, primarily following the techniques developed for the BTZ black hole and conical AdS$_3$ [229, 233, 97], extending the analysis in [219]. First we determine the Green function of the conical dS$_3$ defect geometry in Equation 6.9 related to Kerr-dS$_3$ using the method of images. The method of images is a technique for obtaining the Green's function $G(x,x')$ on a quotient space by summing the Green's function $G_0(x,\Lambda_n x')$ of the covering space over all group elements Λ_n whose action leaves x' invariant in the quotient space [234]. We then use point-splitting to compute the renormalized $\langle T_{\mu\nu}\rangle$.

Green function in conical dS_3

We begin with the Green function $G(x, x')$ of pure dS_3 which solves the scalar field equations of motion in Equation 6.16. Imposing transparent boundary conditions, the Green function is [235, 231]

$$G(x, x') = \frac{1}{4\pi} \frac{1}{|x - x'| - i\epsilon} \,, \tag{6.17}$$

where $|x-x'| \equiv \sqrt{(x-x')^a (x-x')_a}$ is the chordal or geodesic distance between x and x' in the four-dimensional embedding space $\mathbb{R}^{1,3}$. Here the $i\epsilon$ is needed to define the contact divergences of the Green's function in distributional sense [235]. However, for simplicity of notation, we will drop it from now onwards. We choose transparent boundary conditions because the holographic computation naturally selects these boundary conditions. More generically, the Green function solving the scalar field equation of motion is $4\pi G(x, x') = (|x - x'|)^{-1} + \lambda(|x + x'|)^{-1}$, where λ is a parameter related to the boundary conditions one imposes; transparent ($\lambda = 0$), Dirichlet ($\lambda = -1$) and Neumann ($\lambda = 1$). The embedding coordinates $x^a = (X_1, X_2, T_1, T_2)^T$ for empty dS_3 are

$$T_1 = \sqrt{\tilde{r}^2 - R_3^2} \cosh(\tilde{t}/R_3) \,, \quad T_2 = \sqrt{\tilde{r}^2 - R_3^2} \sinh(\tilde{t}/R_3) \,, \quad X_1 = \tilde{r} \cos\tilde{\phi} \,, \quad X_2 = \tilde{r} \sin\tilde{\phi} \,, \tag{6.18}$$

obeying $-T_1^2 + T_2^2 + X_1^2 + X_2^2 = R_3^2$, and where the metric $ds^2 = -dT_1^2 + dT_2^2 + dX_1^2 + dX_2^2$ yields empty dS_3 in static patch coordinates. Moreover, it is easy to verify

$$\left(\Box - \frac{3}{4R_3^2} \right) G_{dS_3}(x, x') = 0 \tag{6.19}$$

for $x \neq x'$, with the chordal distance being

$$\begin{aligned} |x - x'| &= [-(T_1 - T_1')^2 + (T_2 - T_2')^2 + (X_1 - X_1')^2 + (X_2 - X_2')^2]^{1/2} \\ &= \left[2R_3^2 + 2\sqrt{\tilde{r}^2 - R_3^2}\sqrt{\tilde{r}'^2 - R_3^2} \cosh\left(\frac{\tilde{t} - \tilde{t}'}{R_3} \right) - 2\tilde{r}\tilde{r}' \cos(\tilde{\phi} - \tilde{\phi}') \right]^{1/2} . \end{aligned} \tag{6.20}$$

To construct the Green function $G_{CdS_3}(x, x')$ for the conical defect spacetime in Equation 6.9 we use the method of images, exploiting the fact the conical defect geometry is an orbifold due to discrete identifications of dS_3. Namely, the Green function is given by summing over the distinct images under the action respecting the periodicity conditions in Equation 6.10. In particular, identified points are related by an element $H \in SO(1, 3)$ on the embedding space

coordinates in Equation 6.18, except where now $\tilde{\phi} \sim \tilde{\phi} + 2\pi\gamma$ and $\tilde{t} \sim \tilde{t} + 2\pi\alpha'$, where we defined $\alpha' = R_3\alpha$ in Equation 6.10 for notational convenience. Explicitly,

$$H(\gamma, \alpha') = \begin{pmatrix} \cos(2\pi\gamma) & \sin(2\pi\gamma) & 0 & 0 \\ -\sin(2\pi\gamma) & \cos(2\pi\gamma) & 0 & 0 \\ 0 & 0 & \cosh(2\pi\alpha') & -\sinh(2\pi\alpha') \\ 0 & 0 & -\sinh(2\pi\alpha') & \cosh(2\pi\alpha') \end{pmatrix} . \tag{6.21}$$

For integer n we observe $H^n(\gamma, \alpha') = H(n\gamma, n\alpha')$. When $\alpha = 0$, we recover the identification matrix for static dS_3 related to the Schwarzschild-dS_3 solution [219].

The Green function $G_{CdS_3}(x, x')$ for the conical defect spacetime in Equation 6.9 then follows using the method of images, where one sums over all distinct images of a point obtained by the embedding space identification:

$$G_{CdS_3}(x, x') = \frac{1}{4\pi} \sum_{n \in I} G_{dS_3}(x, H^n x') = \frac{1}{4\pi} \sum_{n \in I} \frac{1}{|x - H^n x'|} , \tag{6.22}$$

with

$$\begin{aligned} |x - H^n x'| = \Bigg[& 2\sqrt{\tilde{r}^2 - R_3^2}\sqrt{\tilde{r}'^2 - R_3^2} \cosh\left(\frac{\tilde{t} - \tilde{t}' + 2\pi n\alpha}{R_3}\right) \\ & - 2\tilde{r}\tilde{r}' \cos\left(\tilde{\phi} - \tilde{\phi}' + 2\pi n\gamma\right) + 2R_3^2 \Bigg]^{1/2} . \end{aligned} \tag{6.23}$$

The summation range $I \subset \mathbb{Z}$ depends on the number of distinct images, and is related to the nature of the identification matrix H. For the case of the Kerr-dS geometry, the identification matrix in Equation 6.21 will act transitively on $\mathbb{R}^{1,3}$ such that there are a countably infinite number of distinct images, i.e., $I = \mathbb{Z}$. By contrast, in the limit of vanishing rotation $\alpha = 0$, the identification matrix H becomes cyclic, such that there are a finite number of distinct images, $N - 1$, where N is the smallest positive integer such that $H^N = 1$. This implies γ is a rational number, which without loss of generality can be set to $\gamma = 1/N$. The cyclic property is broken for the Kerr-dS_3 identification matrix due to the lower block matrix. An analogous story carries over for rotating BTZ and (static or rotating) conical AdS_3 [233, 97]. Notably, at this stage, upon the Wick rotation

$$\ell_3 = iR_3 , \qquad J \to -J , \qquad r_\pm \to -ir_\pm^{\mathrm{BTZ}} \tag{6.24}$$

one recovers the scalar field Green function in conical AdS_3 [233], however, Wick rotating the identification matrix in Equation 6.21 does not yield the appropriate identification matrix for conical AdS_3 or the rotating BTZ.

Renormalized quantum stress-tensor

The renormalized quantum stress tensor $\langle T_{\mu\nu} \rangle$ is obtain from $G(x, x')$ using the point-splitting method [236, 229, 95, 233]. Specifically,

$$\langle T_{\mu\nu}(x) \rangle = \lim_{x' \to x} \left(\frac{3}{4} \nabla^x_\mu \nabla^{x'}_\nu G - \frac{1}{4} g_{\mu\nu} g^{\alpha\beta} \nabla^x_\alpha \nabla^{x'}_\beta G - \frac{1}{4} \nabla^x_\mu \nabla^x_\nu G + \frac{1}{16 R_3^2} g_{\mu\nu} G \right) . \tag{6.25}$$

Here $G(x, x') = G_{\mathrm{CdS}_3}(x, x')$ is the Green function in Equation 6.22, the metric $g_{\mu\nu}$ is a function of the spacetime point x, ∇^x_μ denotes a covariant derivative with respect to x, and $\nabla^{x'}_\mu$ denotes a derivative with respect to the point x'. Moreover, the coincident limit $x \to x'$ amounts to evaluating the resulting expression at $x' = x$. Note that while normally the renormalization of the stress tensor is difficult, here we simply subtract off the divergent $n = 0$ contribution in the image sum in the coincident limit.

To evaluate each component of the renormalized stress tensor in the conical defect background, we use the fact $G(x, x')$ is a symmetric biscalar, while its covariant derivatives are bitensors. Thus, we invoke a generalization of Synge's theorem for bitensors [236]:

$$\lim_{x' \to x} (\nabla^{x'}_\mu A_{\alpha_1}) = \nabla^x_\mu \lim_{x' \to x} (A_{\alpha_1}) - \lim_{x' \to x} (\nabla^x_\mu A_{\alpha_1}) , \tag{6.26}$$

where A_{α_1} is a bivector with equal weight at both x and x', whose coincidence limit exists. Consequently, applying Equation 6.26 (Synge's rule) to the quantum stress tensor in Equation 6.25 we have:

$$\begin{aligned} \langle T_{\mu\nu}(x) \rangle = \frac{3}{4} \left[\nabla^x_\nu \lim_{x' \to x} (\nabla^x_\mu G) - \lim_{x' \to x} (\nabla^x_\nu \nabla^x_\mu G) \right] - \frac{1}{4} g_{\mu\nu} g^{\alpha\beta} \left[\nabla^x_\beta \lim_{x' \to x} (\nabla^x_\alpha G) - \lim_{x' \to x} (\nabla^x_\beta \nabla^x_\alpha G) \right] \\ + \lim_{x' \to x} \left(-\frac{1}{4} \nabla^x_\mu \nabla^x_\nu G + \frac{1}{16 R_3^2} g_{\mu\nu} G \right) . \end{aligned} \tag{6.27}$$

To clarify,

$$\nabla^x_\nu \lim_{x' \to x} (\nabla^x_\mu G) = \partial^x_\nu \left(\lim_{x' \to x} \partial^x_\mu G \right) - \Gamma^\rho_{\nu\mu} \left(\lim_{x' \to x} \partial^x_\rho G \right) , \tag{6.28}$$

where the coincident limit is taken before evaluating the ∂^x_ν derivative. Meanwhile,

$$\lim_{x'\to x}(\nabla^x_\nu\nabla^x_\mu G) = \lim_{x'\to x}(\partial^x_\mu\partial^x_\nu G - \Gamma^\rho{}_{\mu\nu}\partial_\rho G)\ , \tag{6.29}$$

where the limit $x \to x'$ is taken at the end.

Evaluating the quantum stress-tensor in Equation 6.27 in the defect geometry of Equation 6.9 and performing the inverse coordinate transformation of Equation 6.8 to return to (t, r, ϕ) coordinates yields,

$$\begin{aligned}
\langle T^t_t\rangle &= \frac{1}{8\pi}\sum_{n=1}^{\infty}\frac{(4r^2[(\beta_+^2+\beta_-^2)b_n - 3a_n] + 2R_3^2 g_n)c_n - 3\beta_+\beta_- e_n[8r^2 + (\beta_-^2-\beta_+^2)R_3^2]}{(\beta_+^2+\beta_-^2)^2 d_n(r)^{5/2}}\ ,\\
\langle T^r_r\rangle &= \frac{1}{16\pi}\sum_{n=1}^{\infty}\frac{c_n}{d_n(r)^{3/2}}\ ,\\
\langle T^\phi_\phi\rangle &= -\frac{1}{8\pi}\sum_{n=1}^{\infty}\frac{(4r^2[3\bar{a}_n - (\beta_+^2+\beta_-^2)b_n] + 2R_3^2\bar{g}_n)c_n - 3\beta_+\beta_- e_n[8r^2 + (\beta_-^2-\beta_+^2)R_3^2]}{(\beta_+^2+\beta_-^2)^2 d_n(r)^{5/2}}\ ,\\
\langle T^t_\phi\rangle &= -\frac{3R_3}{8\pi}\sum_{n=1}^{\infty}\frac{\beta_+\beta_- c_n[4r^2(c_n-4) - R_3^2 a_n] + e_n[4r^2(\beta_+^2-\beta_-^2) + 2\beta_-^2\beta_+^2 R_3^2]}{(\beta_+^2+\beta_-^2)^2 d_n(r)^{5/2}}\ ,\\
\langle T^\phi_t\rangle &= -\frac{3}{8\pi R_3}\sum_{n=1}^{\infty}\frac{\beta_+\beta_- c_n[4r^2(c_n-4) - R_3^2 a_n] + e_n[4r^2(\beta_+^2-\beta_-^2) - R_3^2(\beta_+^4+\beta_-^4)]}{(\beta_+^2+\beta_-^2)^2 d_n(r)^{5/2}}\ .
\end{aligned} \tag{6.30}$$

Here we introduced parameters $\beta_+ \equiv 2\gamma$ and $\beta_- \equiv 2\alpha'/R_3$ and defined

$$a_n = 2\left[\beta_-^2\sin^2\left(\frac{n\pi\beta_+}{2}\right) + \beta_+^2\sinh^2\left(\frac{n\pi\beta_-}{2}\right)\right]\ , \tag{6.31}$$

$$\bar{a}_n = 2\left[\beta_+^2\sin^2\left(\frac{n\pi\beta_+}{2}\right) + \beta_-^2\sinh^2\left(\frac{n\pi\beta_-}{2}\right)\right]\ , \tag{6.32}$$

$$b_n \equiv 2\left[\sinh^2\left(\frac{n\pi\beta_-}{2}\right) + \sin^2\left(\frac{\pi n\beta_+}{2}\right)\right]\ . \tag{6.33}$$

$$c_n \equiv 2 + \cos(\pi n\beta_+) + \cosh(\pi n\beta_-)\ , \tag{6.34}$$

$$e_n \equiv 2\sin(n\pi\beta_+)\sinh(n\pi\beta_-)\ , \tag{6.35}$$

$$g_n \equiv \beta_-^2(\beta_+^2 - 2\beta_-^2)\sin^2\left(\frac{n\pi\beta_+}{2}\right) - \beta_+^2(\beta_-^2 - 2\beta_+^2)\sinh^2\left(\frac{n\pi\beta_-}{2}\right)\ , \tag{6.36}$$

$$\bar{g}_n \equiv \beta_+^2(\beta_+^2 - 2\beta_-^2)\sinh^2\left(\frac{n\pi\beta_-}{2}\right) - \beta_-^2(\beta_-^2 - 2\beta_+^2)\sin^2\left(\frac{n\pi\beta_+}{2}\right)\ , \tag{6.37}$$

and with denominator

$$d_n(r) \equiv \frac{4R_3^2}{\beta_+^2+\beta_-^2}\left[\beta_-^2\sin^2\left(\frac{n\pi\beta_+}{2}\right)-\beta_+^2\sinh^2\left(\frac{\pi n\beta_-}{2}\right)+2R_3^{-2}r^2b_n\right], \tag{6.38}$$

We have already removed the divergent $n=0$ contribution. Note that we recover components of the renormalized stress-tensor for a free conformally coupled scalar field in conical AdS_3 [97] upon the Wick rotations $R_3 \to -iL$ and $\beta_- \to i\beta_-$. To arrive at these expressions we used the summation symmetry over negative and positive integers $n \in \mathbb{Z}$ such that $\sum_{n\in\mathbb{Z}/\{0\}} f_n = \frac{1}{2}\sum_{n=1}^{\infty}(f_n + f_{-n})$, where $f_{-n} = \pm f_n$ depending on each summand f_n. For example, $\langle T^{\tilde{r}}_{\tilde{t}}\rangle$ has a numerator $\sin^2(n\pi\gamma)\sinh(2\pi n\alpha'/R_3)$ which is eliminated under the sum symmetry between positive and negative integers. This symmetry eliminates all mixed components with $\tilde{r}$.

To compare to the holographic stress-tensor in Chapter 7 it is useful to define

$$r_n \equiv d_n^{1/2}\,, \quad d_n = r^2 d_n^{(1)} + R_3^2 d_n^{(2)}\,, \tag{6.39}$$

with

$$d_n^{(1)} = \frac{8b_n}{(\beta_+^2+\beta_-^2)}\,, \quad d_n^{(2)} = \frac{4}{\beta_+^2+\beta_-^2}\left[\beta_-^2\sin^2\left(\frac{n\pi\beta_+}{2}\right)-\beta_+^2\sinh^2\left(\frac{\pi n\beta_-}{2}\right)\right], \tag{6.40}$$

so as to suggestively write the stress-tensor

$$\begin{aligned}
\langle T^t_{\ t}\rangle &= \frac{1}{8\pi}\sum_{n=1}^{\infty}\frac{1}{r_n^3}\left(A_n+\frac{\tilde{A}_n}{r_n^2}\right), \quad \langle T^r_{\ r}\rangle = \frac{1}{16\pi}\sum_{n=1}^{\infty}\frac{c_n}{r_n^3}, \quad \langle T^\phi_{\ \phi}\rangle = -\frac{1}{8\pi}\sum_{n=1}^{\infty}\frac{1}{r_n^3}\left(B_n+\frac{\tilde{A}_n}{r_n^2}\right),\\
\langle T^t_{\ \phi}\rangle &= -\frac{3R_3}{8\pi}\sum_{n=1}^{\infty}\frac{1}{r_n^3}\left(E_n+\frac{\tilde{E}_n}{r_n^2}\right), \quad \langle T^\phi_{\ t}\rangle = -\frac{3}{8\pi R_3}\sum_{n=1}^{\infty}\frac{1}{r_n^3}\left(E_n+\frac{F_n}{r_n^2}\right),
\end{aligned} \tag{6.41}$$

where

$$\begin{aligned}
A_n &\equiv \frac{A'_n}{r_n^2}\,, \quad A'_n = \frac{(4r^2[(\beta_+^2+\beta_-^2)b_n - 3a_n] + 2R_3^2 g_n)c_n}{(\beta_+^2+\beta_-^2)^2}\,,\\
B_n &\equiv \frac{B'_n}{r_n^2}\,, \quad B'_n = \frac{(4r^2[3\bar{a}_n - (\beta_+^2+\beta_-^2)b_n] + 2R_3^2\bar{g}_n)c_n}{(\beta_+^2+\beta_-^2)^2}\,,\\
E_n &\equiv \frac{E'_n}{r_n^2}\,, \quad E'_n = \frac{\beta_+\beta_- c_n[4r^2(c_n-4) - R_3^2 a_n]}{(\beta_+^2+\beta_-^2)^2}\,,\\
\tilde{A}_n &= -\frac{3\beta_+\beta_- e_n[8r^2 + (\beta_-^2-\beta_+^2)R_3^2]}{(\beta_+^2+\beta_-^2)^2}\,,\\
\tilde{E}_n &= \frac{e_n[4r^2(\beta_+^2-\beta_-^2) + 2\beta_-^2\beta_+^2 R_3^2]}{(\beta_+^2+\beta_-^2)^2}\,, \quad F_n = \frac{e_n[4r^2(\beta_+^2-\beta_-^2) - R_3^2(\beta_+^4+\beta_-^4)]}{(\beta_+^2+\beta_-^2)^2}\,.
\end{aligned} \tag{6.42}$$

Quantum-corrected geometry

With the renormalized quantum stress-tensor at hand, let us proceed and compute the quantum corrections to Kerr-dS$_3$ by solving the three-dimensional semi-classical Einstein equations

$$G_{\mu\nu} + \frac{1}{R_3^2} g_{\mu\nu} = 8\pi G_3 \langle T_{\mu\nu} \rangle \tag{6.43}$$

perturbatively in $L_{\rm P}$. Our strategy closely follows the AdS$_3$ analysis presented in [97]. Our starting point is the general form of the stationary (rotating) balck hole:

$$ds^2 = N(r)^2 f(r) dt^2 + \frac{dr^2}{f(r)} + r^2 (d\theta + k(r) dt)^2 \ , \tag{6.44}$$

where k, f and N are the functions to be determined. Expanding to linear order in L_p

$$\begin{aligned} N(r) &= N_0(r) + L_P N_1(r) + \mathcal{O}(L_P^2) \ , \\ f(r) &= f_0(r) + + L_P f_1(r) + \mathcal{O}(L_P^2) \ , \\ k(r) &= k_0(r) + L_P k_1(r) + \mathcal{O}(L_P^2) \ . \end{aligned} \tag{6.45}$$

Note that, in our units, the 0th order metric functions are dimensionless. Formally, the expansion is valid only when the dimensionless ratio $|h_{\mu\nu}/g_{\mu\nu}| \ll 1$, where $g_{\mu\nu}$ is the leading order term and $h_{\mu\nu}$ the corrections. However, we here explicitly pull out factors of L_P, since as we'll see is the relevant scale for the corrections – this makes the corrected metric functions appropriately dimensionful. Heuristically, the expansion should be intended to be in powers of L_P/ℓ_M, where ℓ_M is the length scale associated with the energy density of the matter fields. We substitute these expressions back into the left hand side of Equation 6.43 and match order by order in L_P with the expectation value for the stress energy tensor. At $\mathcal{O}(L_P^0)$ we obtain

$$N_0 = 1 \ , \quad f_0 = m - \frac{r^2}{R_3^2} + \frac{J^2}{4r^2} \ , \quad k_0 = \frac{J}{2r^2} \ , \tag{6.46}$$

recovering the Kerr-dS$_3$ metric of Equation 6.6, to a minor redefinition of the constants of integration J. Note that we have also made the choice of a vanishing shift vector at infinity, which sets a third integration constant to zero.

At linear order in L_P, we solve the differential equations for the linear corrections to the Kerr metric using that we have computed the stress-tensor to linear order in L_P. It is helpful to use the traceless property of the perturbative stress energy tensor,

$$\langle T_{tt} \rangle = f_0^2 \langle T_{rr} \rangle - \left(\frac{1}{R_3^2} - \frac{m}{r^2} \right) \langle T_{\phi\phi} \rangle + \frac{J}{r^2} \langle T_{t\phi} \rangle \ . \tag{6.47}$$

Going through the algebra and requiring the corrections to go to zero for vanishing stress energy tensor, we eventually find

$$\begin{aligned} N_1(r) &= \frac{8\pi G_3}{L_P}\int dr\left(2r\langle T_{rr}\rangle + \frac{\langle T_{\phi\phi}\rangle}{rf_0}\right), \\ f_1(r) &= \int dr\left[-2f_0N_1' + \left(\frac{2m}{r}+\frac{J^2}{r^3}\right)N_1 + \frac{2}{r^3}\int dr\left(-2mrN_1 + \frac{8\pi G_3}{L_P}r^3 f_0\langle T_{rr}\rangle\right)\right], \\ Jk_1 &= f_1 + 2f_0N_1 + 2\int rdr\left(\frac{2N_1(r)}{R_3^2} - f_0\frac{8\pi G_3}{L_P}\langle T_{rr}\rangle\right). \end{aligned} \tag{6.48}$$

Substituting in Equation 6.30 and integrating, we obtain

$$N_1(r) = \frac{R_3^2}{2(\beta_+^2+\beta_-^2)}\sum_{n=1}^{\infty}\frac{a_nc_n - 2\beta_+\beta_-e_n}{b_nr_n^3}\ , \tag{6.49}$$

$$f_1(r) = \sum_{n=1}^{\infty}\frac{4h_n(r)(a_nc_n - 2\beta_+\beta_-e_n) - c_nr_n^4(\beta_+^2+\beta_-^2)^3}{64r^2(\beta_+^2+\beta_-^2)b_n^2r_n^3}\ , \tag{6.50}$$

$$k_1(r) = -\frac{R_3}{8r^2}\sum_{n=1}^{\infty}\frac{(\beta_+^2-\beta_-^2)e_n + \beta_+\beta_-c_n(c_n-4)}{b_n^2r_n}\ . \tag{6.51}$$

with

$$h_n \equiv (4r^2 - R_3\beta_+^2)(4r^2+R_3^2\beta_-^2)b_n + (\beta_+^2+\beta_-^2)\left(4r^2 - \frac{(\beta_-^2-\beta_-^2)R_3^2}{2}\right)d_n\ . \tag{6.52}$$

Since $f_1 \sim 1/r$ as $r\to\infty$, the correction to the blackening factor does resemble the 4D Schwarzschild-like contribution that emerges from the holographic calculations. However, as this derivation can only be accomplished to linear order in $L_{\rm P}$, a limit of the perturbative approach, we cannot justify these quantum corrections induce a black hole horizon; one must consider higher order corrections. The 'horizon' radius, however, is proportional to the Planck length, the scale when quantum gravitational effects are expected to become important. Consequently, the above perturbative semi-classical analysis cannot be trusted, and we are not able to conclude the backreacted geometry results in a genuine horizon. This is not to say semi-classical backreaction will always result in Planckian-sized horizons. Indeed, both gravitational and quantum effects are in play: a large $c\gg 1$ number of conformally coupled scalars results in a combined quantum effect $\propto c\hbar$ which may gravitate to yield semi-classical black holes, i.e., those with horizon radius $\sim Gc\hbar = cL_{\rm P}\gg L_{\rm P}$, for which quantum gravity effects may be safely neglected. To verify this, the backreaction problem of a large number of fields must be non-linearly accounted for, and, thus far, perturbative methods have been unable accomplish this

consistently. Braneworld holography provides a framework for which the backreaction problem due to a large-c holographic conformal field theory can be exactly solved.

6.2 Braneworld holography and quantum black holes

The perturbative analysis above suggests semi-classical backreaction due to quantum fields can lead to the appearance of a black hole horizon when there was none before. Due to the limitations of the perturbative approach, however, the observation is cursory at best. Since the perturbative correction to the classical geometry is on the order of the Planck scale we cannot definitively argue a black horizon appears. Only if there are a large-c number of quantum fields present would this conclusion be plausible. The only known framework where a solution with these requirements can be consistently achieved is braneworld holography, where one innately works in a large-c limit. Below we summarize the relevant aspects of holographic braneworlds.

6.2.1 AdS/CFT dictionary and holographic renormalization

The AdS/CFT correspondence [101], in its strongest form, describes a duality between a theory of gravity and conformal field theory at the level of their partition functions, summarized by Gubser, Klebanov, Polyakov and Witten (GKPW) [237, 238]

$$\left\langle e^{-\int_{\partial\mathcal{M}} \mathcal{O}\phi_{(0)}} \right\rangle_{\text{CFT}} = Z_{\text{grav}}[\phi_{(0)}]|_{\mathcal{M}} \, . \tag{6.53}$$

On the right-hand side we have the gravitational partition function of a bulk field Φ over an asymptotically $d+1$-dimensional AdS spacetime $\mathcal{M}$, with conformal boundary $\partial\mathcal{M}$, and $\phi_{(0)}$ is the fixed boundary value of the bulk field Φ. On the left-hand side is the generating functional for the dual d-dimensional CFT living on $\partial\mathcal{M}$, where $\mathcal{O}$ is the field theory operator dual to the bulk field. Taking variations with respect to $\phi_{(0)}$ and then setting $\phi_{(0)} = 0$, one can obtain correlation functions of $\mathcal{O}$, sourced by $\phi_{(0)}$. This equivalence of partition functions in Equation 6.53 is often dubbed the standard AdS/CFT dictionary, and, at least formally, defines a model of non-perturbative quantum gravity.

One of the essential features of the AdS/CFT correspondence is that it can probe strongly coupled field theories on a non-dynamical background using weakly coupled, classical (super)gravity. This is because, typically, the holographic field theories are non-abelian gauge

theories with gauge group of rank N and 't Hooft coupling λ, where, at large-N and $\lambda \gg 1$ (the planar-diagram limit) the dynamics are effectively classical, with $\mathcal{O}(1/N)$ corrections in the dual field theory corresponding to bulk gravity quantum corrections $\mathcal{O}(G_N)$. A concrete realization of AdS/CFT duality is that of $\mathcal{N} = 4$ super-Yang-Mills theory, a superconformal field theory, which is dual to type IIB string theory on $\mathrm{AdS}_5 \times S^5$, where the 't Hooft coupling λ controls curvature scale of AdS_5 whilst the string coupling is $g_s \sim N^{-1}$. In the large-N limit, stringy interactions are thus suppressed and $\lambda \gg 1$ forces curvatures to be small, such that the string theory may be replaced by an effectively classical gravity.

More generally, the dual field theory degrees of freedom are encoded in the central charge c, which, for known holographic theories scale with N, i.e., $c \sim N^{\alpha}$ for positive, real α. Thus, the large-c limit coincides with the classical limit in the bulk, and the right-hand side of the dictionary in Equation 6.53 may be approximately given by a sum over classical saddles $\{\Phi_i\}$

$$\lim_{c\to\infty} \left\langle e^{-\int_{\partial\mathcal{M}} \mathcal{O}\phi_{(0)}} \right\rangle_{\mathrm{CFT}} = \sum_i e^{-I_{\mathrm{grav}}^{\text{on-shell}}[\Phi_i]} \,, \tag{6.54}$$

where each field configuration Φ_i is a solution to the bulk classical gravity equations of motion subject to the prescribed boundary conditions. A particular case of interest is to turn off all sources $\phi_{(0)}$ except those the boundary value of the bulk metric. In such an event, at large-c, it is consistent to turn off all bulk fields except the metric, such that the bulk is described by a pure theory of gravity, often taken to be the Einstein-Hilbert action.

Holographic renormalization

The standard dictionary in Equation 6.53, however, requires special care in regards to divergences. Indeed, even at tree-level – Equation 6.54 – the gravity partition function exhibits long distance infrared (IR) divergences, which correspond to ultraviolet (UV) divergences in the CFT correlation functions. These divergences may be removed via holographic renormalization, a prescription that adds appropriate local counterterms [108, 109, 110, 111, 112] in a minimal subtraction scheme. Whilst there is in principle freedom in choosing specific finite terms – corresponding to different renormalisation schemes – the nature of the local divergent terms is universal, meaning that there is no ambiguity in the action we shortly derive for the brane theory. The local finite scheme-dependent terms can be added, beyond minimal subtraction,

to match specific CFT data if needed [239]. Since it will become relevant momentarily, let us outline the holographic renormalization procedure – see the appendices in [4] for further details.

Consider a bulk asymptotically AdS_{d+1} spacetime $\mathcal{M}$ of curvature scale L_{d+1} and cosmological constant $\Lambda_{d+1} = -d(d-1)/2L_{d+1}^2$, governed by classical Einstein gravity

$$I_{\text{bulk}} = \frac{1}{16\pi G_{d+1}} \int_{\mathcal{M}} d^{d+1}x\sqrt{-\hat{g}}\left(\hat{R} - 2\Lambda_{d+1}\right) + \frac{1}{8\pi G_{d+1}} \int_{\partial\mathcal{M}} d^d x\sqrt{-h}K \ . \tag{6.55}$$

Here G_{d+1} is the $d+1$-dimensional Newton's constant, $\hat{g}_{ab}$ is the metric endowed on $\mathcal{M}$, and K in the Gibbons-Hawking York (GHY) boundary term is the trace of the extrinsic curvature of the boundary submanifold $\partial\mathcal{M}$ endowed with induced metric h_{ij}. Working in the large-c, planar-diagram limit, the bulk gravity theory has a dual holographic description in terms of a CFT_d living on the asymptotic conformal boundary $\partial\mathcal{M}$.

Asymptotically, the bulk AdS spacetime can be cast in Fefferman-Graham gauge [240], such that near the boundary

$$ds^2 = \hat{g}_{ab}dx^a dx^b = L_{d+1}^2\left(\frac{d\rho^2}{4\rho^2} + \frac{1}{\rho}g_{ij}(x,\rho)dx^i dx^j\right) \ , \tag{6.56}$$

where the d-dimensional metric has the expansion $g_{ij}(x,\rho) = g_{ij}^{(0)}(x) + \rho g_{ij}^{(2)}(x) + ... + \rho^{d/2} g_{ij}^{(d)}(x)$. The conformal boundary is located at $\rho = 0$. By perturbatively solving the bulk Einstein's equations, the higher-order metric coefficients $g_{ij}^{(k>0)}(x)$ may be cast covariantly in terms of the metric $g_{ij}^{(0)}$ and derivatives thereof.

On-shell, the bulk action in Equation 6.55 has IR divergences at $\rho = 0$. To isolate and regulate these divergences, introduce an IR cutoff $\rho = \epsilon$, for $\epsilon \ll 1$, near the asymptotic boundary, and integrate over bulk coordinate ρ between $\epsilon < \rho < \rho_c$, where $\rho_c > \epsilon$ is some constant.

See Figure 6.1 for an illustration. This procedure produces a regulated bulk action,

$$I_{\text{bulk}}^{\text{reg}} = \frac{1}{16\pi G_{d+1}}\left[\int_{\rho>\epsilon} d^{d+1}x\sqrt{-\hat{g}}\left(\hat{R} - 2\Lambda_{d+1}\right) + 2\int_{\rho=\epsilon} d^d x\sqrt{-h}K\right] \ . \tag{6.57}$$

Using the perturbative expansion for $g_{ij}(x,\rho)$, the regulated action in Equation 6.57 may be divided into a contribution I_{div} which diverges in the limit $\epsilon \to 0$, and a finite contribution I_{fin}

$$I_{\text{bulk}}^{\text{reg}} = I_{\text{div}} + I_{\text{fin}} \ . \tag{6.58}$$

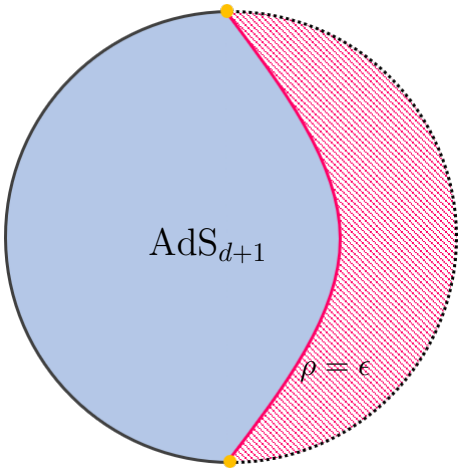

Figure 6.1: **Holographic regularization**. A constant timeslice of empty AdS$_{d+1}$. An IR cutoff surface is introduced at $\rho = \epsilon$ (thick, red line). The regulated action follows from integrating out the bulk radial coordinate from $\epsilon < \rho < \rho_c$. As $\epsilon \to 0$, the cutoff surface recedes to the AdS boundary.

Schematically, the IR divergent contribution is

$$I_{\rm div} = \frac{L_{d+1}}{16\pi G_{d+1}} \int d^d x \sqrt{g_{(0)}} \left[\epsilon^{-d/2} a_{(0)} + \epsilon^{-d/2+1} a_{(2)} + ... + \epsilon^{-1} a_{(d-2)} - \log \epsilon a_{(d)} \right] , \qquad (6.59)$$

with coefficients $a_{(0)}, a_{(2)}, ...$ that are covariant combinations of $g^{(0)}_{ij}$ and its derivatives. In terms of the boundary metric h_{ij}, it may be cast as

$$I_{\rm div} = \frac{L_{d+1}}{16\pi G_{d+1}} \int_{\partial \mathcal{M}} d^d x \sqrt{-h} \left[\frac{2(d-1)}{L^2_{d+1}} + \frac{R}{(d-2)} + \frac{L^2_{d+1}}{(d-2)^2(d-4)} \left(R^2_{ij} - \frac{dR^2}{4(d-1)} \right) + ... \right] \qquad (6.60)$$

where the ellipsis indicates higher-curvature and higher-derivative contributions (see, e.g., [108, 112, 241, 242]). The finite contribution $I_{\rm fin} \sim \mathcal{O}(\epsilon^0) + \mathcal{O}(\epsilon)...$ survives the $\epsilon \to 0$ limit, though it will also typically include higher-curvature terms. Its interpretation will be given momentarily.

At this stage the renormalized action is obtained by minimal subtraction,

$$I^{\rm ren}_{\rm bulk} = \lim_{\epsilon \to 0} (I^{\rm reg}_{\rm bulk} + I_{\rm ct}) , \qquad (6.61)$$

where a local counterterm action has been introduced, $I_{\rm ct} = -I_{\rm div}$, to precisely cancel the IR divergences. Then, via the standard AdS/CFT dictionary, variations with respect to the metric h_{ij} of the renormalized action yields the quantum expectation value of the stress-tensor of the holographic CFT,

$$\langle T^{\rm CFT}_{ij} \rangle = \lim_{\epsilon \to 0} \left(- \frac{2}{\sqrt{\hat{g}(x,\rho)}} \frac{\delta I^{\rm ren}_{\rm bulk}}{\delta \hat{g}^{ij}(x,\epsilon)} \right) \equiv - \frac{2}{\sqrt{h}} \frac{\delta W_{\rm CFT}[h]}{\delta h^{ij}} , \qquad (6.62)$$

such that the renormalized bulk action is identified with the quantum effective action of the CFT, $W_{\text{CFT}}[h]$. Thus, at leading order, the finite action I_{fin} characterizes the CFT.

6.2.2 Braneworld holography

In braneworld holography [243], the bulk IR cutoff surface $\partial\mathcal{M}$ is instead replaced by a d-dimensional (ETW) Randall-Sundrum [99, 105] or Karch-Randall [106, 107] brane $\mathcal{B}$ at a small fixed distance away from the boundary. Hence, the physical space is cutoff at the ETW brane and there are no longer IR divergences to be removed. For simplicity, assume the brane is purely tensional, having an action

$$I_\tau = -\tau \int_{\mathcal{B}} d^d x \sqrt{-h}\,, \tag{6.63}$$

where τ is the brane tension. Since a portion of the bulk has been removed, to complete the space, a second copy of AdS_{d+1} with a brane is sewn to the first cutoff geometry along the cutoff surface (see Figure 6.2). This surgical procedure leads to a discontinuity in the extrinsic curvature K_{ij} across the junction. The Israel junction conditons [244] relate this discontinuity to the brane stress-tensor S_{ij} via

$$\Delta K_{ij} - h_{ij}\Delta K = 8\pi G_{d+1} S_{ij} = -8\pi G_{d+1}\tau h_{ij}\ , \tag{6.64}$$

where $\Delta K_{ij} = K^+_{ij} - K^-_{ij}$ denoting the difference between the extrinsic curvature across either '+' and '−' sides of the brane (here we take $K^+_{ij} = -K^-_{ij}$ such that $\Delta K_{ij} = 2K_{ij}$), and the last equality follows from taking the metric h_{ij} variation of the brane action in Equation 6.63, i.e., $S_{ij} \equiv -\frac{2}{\sqrt{-h}}\frac{\delta I_\tau}{\delta h^{ij}}$. Thus, the location of the brane in the completed space is determined by the junction conditions in Equation 6.64, which in the present case amounts to tuning the brane tension τ.

Moreover, unlike the metric on the AdS boundary, the brane metric is dynamical, governed by a holographically induced higher-curvature theory of gravity coupled to matter. Precisely, the induced brane theory is found by adding the bulk theory in Equation 6.55 to the brane action in Equation 6.63. Integrating out the bulk up to the ETW brane $\mathcal{B}$, as in holographic regularization, leads to an effective induced theory with action I

$$I \equiv I_{\text{Bgrav}}[\mathcal{B}] + I_{\text{CFT}}[\mathcal{B}]\,. \tag{6.65}$$

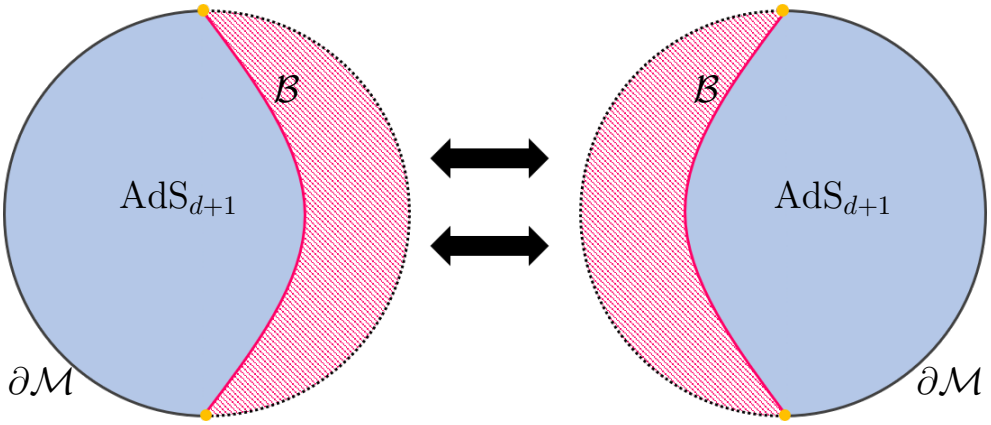

Figure 6.2: **Braneworld surgery.** Replace the IR cutoff surface with an end-of-the-world (Karch-Randall) brane $\mathcal{B}$ (thick, red line), excising the shaded region from the bulk spacetime. To complete the space, two copies of the spacetime are glued along $\mathcal{B}$ making the brane double-sided. A BCFT_d lives on the AdS_{d+1} boundary $\partial\mathcal{M}$ and is coupled to a defect CFT_{d-1} where $\mathcal{B}$ intersects the AdS boundary (yellow dot). The induced brane theory is characterized by a specific higher-derivative gravity coupled to a CFT_d with a UV cutoff.

The brane gravity theory is (cf. [245, 242])

$$\begin{aligned} I_{\mathrm{Bgrav}} &= 2I_{\mathrm{div}} + I_\tau \\ &= \frac{1}{16\pi G_d}\int_{\mathcal{B}} d^d x\sqrt{-h}\left[R - 2\Lambda_d + \frac{L_{d+1}^2}{(d-4)(d-2)}\left(R_{ij}^2 - \frac{dR^2}{4(d-1)}\right) + \cdots\right], \end{aligned} \tag{6.66}$$

where the factor of two accounts for integrating out the bulk on both sides of the brane, and the ellipsis corresponds to higher curvature densities, entering with higher powers of L_{d+1}^2. So far the higher-derivative contributions have been computed up to quintic order in curvature for arbitrary d, and sextic order for $d = 3$ [242]. In principle, these results could be extended to arbitrary order, even though the calculations might be practically prohibitive. Here G_d represents the effective brane Newton's constant induced from the bulk

$$G_d = \frac{d-2}{2L_{d+1}} G_{d+1}\,, \tag{6.67}$$

and $\Lambda_d = -(d-1)(d-2)/2L_d^2$ is an effective brane cosmological constant with an induced curvature scale L_d

$$\frac{1}{L_d^2} = \frac{2}{L_{d+1}^2}\left(1 - \frac{4\pi G_{d+1} L_{d+1}}{d-1}\tau\right). \tag{6.68}$$

As written, it has been assumed the brane has a negative cosmological constant such that the bulk theory is coupled to a Karch-Randall brane [106]. When coupled to a Randall-Sundrum brane, the brane cosmological constant can be tuned to be positive or zero, as will be considered later.

Due to the presence of higher-derivative terms in Equation 6.66, the brane theory of gravity is in general 'massive' since a massive graviton bound state will localize on the brane [106]. This brane graviton mass, however, will become negligible for a brane very near the boundary. Further, general higher-derivative theories of gravity are often sick since they are typically accompanied by ghosts. In the present case, however, provided the series of higher-derivative terms is not truncated, the brane theory is not expected to inherit these usual pathologies since the starting bulk theory and the procedure of integrating out bulk degrees of freedom are not pathological

The action $I_{\rm CFT}[\mathcal{B}]$, meanwhile, describes the CFT theory, now living on the brane, and corresponds to the finite contribution to the regulated bulk action upon integrating out the bulk. To see this, note that upon integrating out the bulk degrees of freedom on both sides of the brane we have

$$I \equiv 2I^{\rm reg}_{\rm bulk} + I_\tau \ . \tag{6.69}$$

Then add and subtract the $2I_{\rm div}$, giving

$$I \equiv (2I_{\rm div} + I_\tau) + (2I^{\rm reg}_{\rm bulk} - 2I_{\rm div}) \ , \tag{6.70}$$

where the first term in parentheses is recognized as $I_{\rm Bgrav}$. The second term is simply $2I_{\rm fin} \equiv I_{\rm CFT}$, which, to leading order in the cutoff ϵ, is identified with the quantum effective action of the CFT, $I_{\rm CFT} = W_{\rm CFT} + \mathcal{O}(\epsilon)$. In most cases of interest, we work in the limit that ϵ is small, i.e., when the brane is close to the (now fictitious) AdS_{d+1} boundary, such that the matter on the brane has an approximate description as a large-c holographic CFT. Roughly speaking, a portion of the conformal AdS_{d+1} boundary has been pushed into the bulk, such that the dual CFT_d is now residing on the brane – however, at a cost. Since the brane represents an IR cutoff surface, the CFT has a UV cutoff [246, 247]. The cutoff, from the perspective of the boundary $g^{(0)}_{ij}$ metric, is denoted by ϵ, while from the induced brane metric $h_{ij} = (L^2_{d+1}/\epsilon)g^{(0)}_{ij}$ the UV cutoff of the CFT is $\delta_{\rm UV} = L_{d+1}$.

6.2.3 Holographic quantum black holes: a conjecture

Two equivalent ways to interpret the theory given by Equation 6.65 are as follows. From the bulk perspective, I characterizes a theory of a $(d+1)$-dimensional system with dynamics ruled by Einstein gravity coupled to an end-of-the-world brane obeying appropriate boundary conditions. Meanwhile, from the brane perspective I represents a specific higher-curvature gravity in d dimensions coupled to a large-c cutoff CFT that backreacts on the brane metric h_{ij}. The tower of higher-order derivative terms to the Einstein-Hilbert contribution represent quantum-corrections induced by the backreaction of the CFT_d. We refer to this higher-derivative tower as 'corrections' because in most cases of interest one treats the brane action as an effective theory, thereby assuming $L_d \gg L_{d+1}$ and guaranteeing the higher-derivative terms are suppressed by at least $\mathcal{O}(L_{d+1}^2/L_d^2)$. Equally, $L_{d+1}^2/L_d^2 \sim \epsilon$, and thus the gravitational brane action is recognized as an expansion in small ϵ. Moreover, from the brane perspective, the short-distance UV cutoff of the CFT_d goes like L_{d+1} such that the higher-derivative terms also correspond to an expansion in the UV cutoff. Consistency between these two viewpoints implies solutions to the classical bulk equations satisfying proper brane boundary conditions exactly correspond to solutions to the semi-classical field equations on the brane. Therefore, the classical $(d+1)$-dimensional geometry encodes the entire series of quantum-corrections to the d-dimensional brane geometry, accounting for all orders in backreaction. Thus, holographic braneworlds provide a distinct computational advantage: rather than directly solving a complicated semi-classical theory of gravity, one may instead solve simpler classical gravitational field equations in one dimension higher.

This philosophy, combined with the observation [248] that the $\sim 1/r^3$ corrections to the four-dimensional Newtonian potential due to massive Kaluza-Klein modes in the Randall-Sundrum model precisely coincide with corrections induced by one-loop quantum effects of the graviton propagator [249], suggests braneworld black holes from the brane perspective are quantum-corrected geometries. These insights in part motivated Emparan, Fabbri and Kaloper [113] to make the following conjecture:

Conjecture: Classical black holes which localize on a brane in AdS_{d+1} exactly map to d-dimensional quantum-corrected black holes including all orders of backreaction.

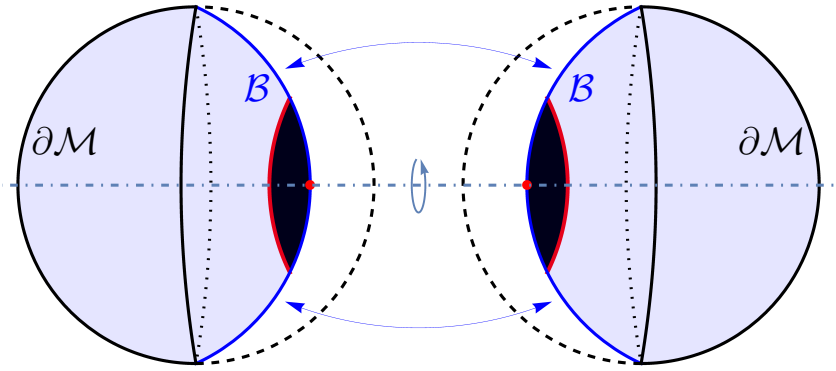

Figure 6.3: **Braneworld black hole.** The bulk white region is excised down to the brane $\mathcal{B}$ (blue line), and glued to a copy of itself. A bulk black hole with an event horizon (red line) is intersected by (depicted here, Karch-Randall) brane, inducing a horizon on the brane.

Such quantum-corrected black holes are dubbed 'quantum' black holes, though, technically are solutions to the semi-classical theory induced on the brane. An illustration is given in Figure 6.3.

Explicit tests of this proposal include the exact localized AdS_4 braneworld black holes discovered by Emparan, Horowitz, and Myers [219, 220], with their projection onto the brane being reinterpreted as three-dimensional quantum black holes. The exact static (neutral) quantum black holes receive the same modifications to their geometry as suggested by the (non-holographic) perturbative analysis summarized in Section 6.1. The rotating and charged holographic quantum black holes, meanwhile, do not match exactly to the non-holographic perturbatively-corrected counterparts (cf. [229, 97, 5, 250, 6]), although they share the qualitative behaviour. In particular, perturbative backreaction to the rotating BTZ black hole or Kerr-dS_3 solution due to a conformally coupled scalar field leads to a more complicated radial dependence than that of a holographic CFT and a quantum stress-tensor.

Before moving on to the next chapter where we analyze an exact quantum-corrected three-dimensional black holes, it is worth briefly commenting on the status of the proposal [113] in higher and lower dimensions. For brane dimensions $d \geq 4$, the most physically relevant case being $d = 4$, there are still no known exact stationary solutions (see [251] for a review of analytic and numerical braneworld black holes). In fact, there is a no-go theorem [252] which alleges the exterior geometry on the brane in $d \geq 4$ cannot be static. The lack of exact solutions

makes identifying the specific state of the CFT$_d$ more difficult. In [113, 253], for $d \geq 4$, it was qualitatively argued the obstruction to having static quantum black holes can be understood as a consequence of backreaction due to Hawking effects, such that any black hole that localizes on the brane must evaporate. However, static braneworld black holes in higher-dimensions have been found numerically, e.g., [254, 255, 256, 257, 258, 259], and the qualitative argument was shown to have flaws [256].

Lastly, let us make some general remarks about static black holes localized on the brane. First, a brane with non-vanishing tension is an accelerated trajectory with respect to the bulk, i.e., the brane does not undergo geodesic motion. Thus, a black hole which localizes on the brane is in an accelerating frame; likewise for any observer glued to the brane. Next, a static black hole stuck to the brane will neither eat the brane or slide off it. The reason is as follows [260]. To be static, the brane intersects the black hole orthogonally, otherwise the black hole would grow by eating the brane. Indeed, a black hole will grow if $T_{ij}k^ik^j > 0$ in the background, for null generator of the horizon k^i. A black hole thus remains static when $T_{ij}k^ik^j = 0$. Since the brane stress tensor is proportional to the induced metric, the static condition translates to $k^ik_i = 0$, i.e., the k^i lies entirely on the brane, which occurs when the radial direction orthogonal to the black hole is tangent to the brane. Consequently, the brane bends to remain orthogonal to the black hole if the latter is being pulled off the brane (by, say, another black hole in the bulk). Thus, a static black hole localized on the brane experiences a restoring force due to the tension of the brane and does not slide off. Evaporating black holes, on the other hand, eventually slide off the brane.

Chapter 7

Quantum Kerr de Sitter

In this chapter we use braneworld holography to find an exact quantum-corrected rotating black hole in dS_3, a non-trivial extension of [219]. Our starting point, as in [221], is the rotating AdS_4 C-metric, however, coupled to an asymptotically dS_3 Randall-Sundrum brane. As a solution to the bulk Einstein equations, we are guaranteed the brane geometry is an exact solution to the full semi-classical theory given by Equation 6.66, in the planar limit of the CFT, resulting in the quantum Kerr-dS (qKdS) black hole.

An outline of the chapter is as follows. In Section 7.1 we summarily review elements of the 4-dimensional C-metric in AdS space, the bulk solution at the basis of our braneworld construction. Section 7.2 is primarily devoted to the geometric construction of the qKdS black hole, where include an analysis of each of its Nariai, extremal, and ultracold limits, and compute the renormalized stress-tensor of the holographic CFT. A detailed account of the horizon thermodynamics is instead given in Section 7.3.

7.1 Elements of the AdS C-metric

The AdS_4 C-metric is a solution to Einstein's equation with negative cosmological constant, arising from a particular rescaling of the Plebanski-Demianski solution [261]:

$$ds^2 = \frac{1}{A^2(x-y)^2}\left[H(y)dt^2 - \frac{dy^2}{H(y)} + \frac{dx^2}{G(x)} + G(x)d\phi^2\right] , \tag{7.1}$$

with

$$H(y) = -\lambda + ky^2 - 2mAy^3 , \quad G(x) = 1 + kx^2 - 2mAx^3 , \tag{7.2}$$

and $k = +1, 0, -1$ which will determine the topology of the horizon of the black hole solutions when they exist. The parameters A and m can be thought of as acceleration and mass, respectively, while λ is related to the cosmological constant. Indeed, the bulk Ricci tensor satisfies $\hat{R}_{AB} = -(3/L_4^2)\hat{g}_{AB}$ where $L_4 \equiv (A\sqrt{\lambda+1})^{-1}$ sets the scale for the bulk cosmological constant. Maintaining a negative cosmological constant in the bulk requires $\lambda > -1$, however, as summarized below, various ranges of λ describe different asymptotic brane geometries.

The overall factor $(x-y)^{-2}$ in Equation 7.1 implies the point $y = x$ is infinitely far away from points $y \neq x$ (the point $y = x$ corresponds to the asymptotic AdS_4 geometry). A curvature singularity is located at $y = -\infty$, which is hidden behind one of the horizons. To maintain a 'mostly plus' Lorentzian signature requires $G(x) \geq 0$, restricting the range of x.

Each zero of $H(y)$ corresponds to a Killing horizon associated with the time translation Killing vector ∂_t. Meanwhile, the zeros of $G(x)$ correspond to an axis for the rotation symmetry ∂_ϕ, i.e., for $\xi^a = \partial^a_\phi$, then $\xi^2 \sim G(x)$, vanishing at a zero of $G(x)$. For a range of values of mA and k, there will be three distinct real zeros. Explicitly, the cubic $G(x) = -2mAx^3 + kx^2 + 1 = 0$ can be solved by introducing $x = z - \frac{k}{3}$ and express in depressed form, $z^3 + pz + q = 0$, with $p = -\frac{k^2}{12(mA)^2}$ and $q = -\frac{[2k^3+27(4mA)^2]}{27(2mA)^3}$, such that the discriminant is $\Delta \equiv -(4p^3 + 27q^2) = -\frac{k^3+27(mA)^2}{4(mA)^4}$. When $\Delta > 0$, then $G(x)$ will have three distinct real roots, while if $\Delta < 0$ then $G(x)$ will have one real root and two complex roots. For example, for $\lambda = 0$ and $k = -1$, then $G(x)$ will have three distinct roots $x_0 < x_2 < 0 < x_1$ provided $0 < mA < \frac{1}{3\sqrt{3}}$ [219]. The three roots to $G(x)$, $\{x_0, x_1, x_2\}$, each lead to a distinct conical singularity. One singularity can be removed via

$$\phi \sim \phi + \Delta\phi \,, \quad \Delta\phi = \frac{4\pi}{|G'(x_i)|} \,, \tag{7.3}$$

where x_i is one of the zeros. Once the period of ϕ has been fixed in this way, say at $x = x_1$, then ϕ cannot be readjusted to eliminate the remaining conical singularities at $x = x_0, x_2$. Thus, in general there will be a conical singularity along the axis $x = x_i$ with deficit angle

$$\delta = \frac{4\pi}{G'(x_i)} - \Delta\phi \,, \tag{7.4}$$

which can be interpreted as a cosmic string with tension $\tau_{cs} = \delta/8\pi$. Note that it is this feature which leads one to interpret the C-metric as a single or pair of accelerating black holes. For example, for a single black hole, a cosmic string attaches at one pole in the background

and the black hole, suspending it away from the center of the spacetime, thereby inducing its acceleration (for a detailed analysis on the interpretation of the C-metric, see [262]). This acceleration leads to an additional acceleration horizon, analogous to a Rindler horizon, and an equilibrium thermodynamic description [220] (see also [263]).

We are interested in introducing a brane into the AdS_4 spacetime. Generally there will be a discontinuity in the extrinsic curvature $K_{ij}[h]$ across the brane which, via the Israel junction conditions (equations of motion for the brane), is related to the stress-tensor introduced by the brane. In the four-dimensional case at hand, where the brane action is purely tensional, the junction conditions are

$$\Delta K_{ij} - h_{ij}\Delta K^k_{\ k} = 8\pi G_4 \tau h_{ij} \ , \tag{7.5}$$

where $\Delta K_{ij} = K^+_{ij} - K^-_{ij} = 2K_{ij}$ and $S_{ij} = -\tau h_{ij}$. Therefore, the tension can be seen as a parameter which fixes the location of the brane $\mathcal{B}$. In the case of the C-metric, a natural choice for the location of $\mathcal{B}$ is the surface $x = 0$ since it is *umbilic*. To see this, note that the unit normal to the brane at $x = 0$ is $n^i_x = A\epsilon(x-y)\sqrt{G(x)}\partial^i_x$, where $\epsilon = \pm 1$ corresponds to the orientation of the normal; here we take $\epsilon = +1$ since $x = 0$ is a timelike hypersurface. The non-vanishing components of $K_{ij} = \nabla_i n_j$ obey $K_{ij} = -Ah^{(x)}_{ij}$, with $h^{(x)}_{ij}$ being the induced metric along the $x = 0$ brane. Comparing to the Israel junction conditions we identify the brane tension as

$$\tau = \frac{A}{2\pi G_4} \ . \tag{7.6}$$

Similarly, the $y = 0$ hypersurface is umbilic. Indeed, with unit normal $n^i_y = A\epsilon(x-y)\sqrt{H(y)}\partial^i_y$, then $K_{ij} = -A\epsilon\sqrt{-\lambda}h^{(y)}_{ij}$, where $h^{(y)}_{ij}$ is the induced metric at $y = 0$.

To gain some intuition for the brane construction, it is helpful to consider the simplifying case when $mA = 0$. One can then move to a coordinate frame showing the geometry is locally AdS_4 where the brane itself has a three-dimensional cosmological constant $\Lambda_3 = -\lambda$ [220]. Thus, the sign of λ denotes different constant curvature slicings of AdS_4. There are three distinct cases: **(1)** $\lambda = 0$, a flat slicing. In this case one must choose $k = \pm 1$, where for $k = -1$ the coordinate t is timelike everywhere; **(2)** $-1 < \lambda < 0$, leads to a three-dimensional de Sitter slicing. One must select $k = -1$ to have dS_3 in static patch coordinates and cosmological horizons, and **(3)** $\lambda > 0$, an AdS_3 slicing where the three different values of k distinguish three distinct slicings of AdS_3: global coordinates ($k = -1$), the massive BTZ black hole ($k = +1$),

and the massless BTZ black hole ($k = 0$). The flat ($\lambda = 0$) solution was studied in [219] while the AdS_3 slicings were analyzed in [220].

Adding rotation

Let us now briefly review the rotating AdS_4 C-metric, following the conventions of [220]. The line element is

$$ds^2 = \frac{1}{A^2(x-y)^2}\left[\frac{H(y)}{\Sigma(x,y)}(dt + ax^2 d\phi)^2 - \frac{\Sigma(x,y)}{H(y)}dy^2 + \frac{\Sigma(x,y)}{G(x)}dx^2 + \frac{G(x)}{\Sigma(x,y)}(d\phi - ay^2 dt)^2\right], \tag{7.7}$$

with metric functions

$$\begin{aligned} H(y) &= -\lambda + ky^2 - 2mAy^3 - a^2y^4\,, \quad \Sigma(x,y) = 1 + a^2x^2y^2 \\ G(x) &= 1 + kx^2 - 2mAx^3 + a^2\lambda x^4\,. \end{aligned} \tag{7.8}$$

As in the static case, this spacetime is obeys $\hat{R}_{AB} = -3/L_4^2 \hat{g}_{AB}$ with the same scale L_4. When $m \neq 0$, there is a curvature singularity when $1/y^2\Sigma(x,y) = 0$, i.e., when both $y \to -\infty$ and $x = 0$, which may be recognized as the standard ring singularity familiar to Kerr black holes.

The zeros x_i of $G(x)$ now correspond to fixed orbits of the rotational Killing vector

$$\xi = \partial_\phi - ax_i^2\partial_t\,. \tag{7.9}$$

Indeed, the vector ∂_ϕ^μ no longer has vanishing norm at $x = x_i$, while ξ does. Avoiding a conical defect at, say, $x = x_1$ requires one identify points along the integral curves of this Killing vector with an appropriate period, amounting to coordinate transformation $\tilde{t} = t + ax_1^2\phi$, where angular variable ϕ has the same period as Equation 7.3. To see this, expand the relevant portion of the metric in Equation 7.7 near a zero of $G(x)$. Without loss of generality, consider the slice $y = 0$, where, up to the conformal factor

$$ds^2 \approx -\lambda(dt + ax_i^2 d\phi)^2 + \frac{dx^2}{G'(x_i)(x - x_i)} + G'(x_i)(x - x_i)d\phi^2\,. \tag{7.10}$$

Aside from the first term, the (x, ϕ) sector takes the same form as in the non-rotating case, from which the periodicity of ϕ is given by Equation 7.3. Including rotation, however, this would not be the correct periodicity for ϕ. The situation is remedied with the coordinate transformation

$\tilde{t} = t + ax_i^2\phi$, such that, at $x = x_i$, then $d\tilde{t} = (dt + ax_i^2 d\phi)$. Similarly, at the roots y_i of $H(y)$, the Killing vector $\zeta = \partial_t + ay_i^2\partial_\phi$ becomes null, defining horizons with angular velocity $\Omega = ay_i^2$.

The brane is again placed at $x = 0$ since this surface remains umbilic. Indeed, for space-like unit normal $n_x^i = A(x-y)\sqrt{G(x)/\Sigma(x,y)}\partial_x^i$, the extrinsic curvature again satisfies $K_{ij} = -Ah_{ij}^{(x)}$ at $x = 0$. Similarly, the $y = 0$ hypersurface, with unit normal $n_y^i = A\epsilon(x-y)\sqrt{H(y)/\Sigma(x,y)}\partial_y^i$, obeys $K_{ij} = (-A\epsilon\sqrt{-\lambda})h_{ij}^{(y)}$.

Due to the periodicity in ϕ, notice that along the orbit ξ the coordinate t is shifted: via $t = \tilde{t} - ax_1^2\phi$ and $\tilde{t} \sim \tilde{t}$, then $t \sim t - ax_1^2\Delta\phi$. Consequently, this introduces a rotation of frames in the asymptotic limit; namely, introducing radial coordinate $\rho = -y^{-1}$ and performing the coordinate transformation $(t, y, \phi) \to (\tilde{t}, \rho, \phi)$, the $h_{\tilde{t}\phi}$ component of the brane metric at $x = 0$ will grow as ρ^2 and not as a constant [220]. To remove this undesired asymptotic growth, one further shifts $\phi = \tilde{\phi} + C\tilde{t}$ for a judiciously chosen constant to remove the ρ^2 growth in the coordinate frame $(\tilde{t}, \rho, \tilde{\phi})$. To place the brane metric in more canonically normalized coordinates, one further rescales coordinates $\tilde{t}$ and $\tilde{\phi}$ and redefines the radial coordinate ρ.

7.2 Bulk and brane geometry

7.2.1 The qSdS black hole

Let's begin by reviewing quickly the static quantum-corrected Schwarzschild-de Sitter black hole, first derived in [264].

Consider the four-dimensional static AdS_4 C-metric

$$ds^2 = \frac{\ell^2}{(\ell + xr)^2}\left[-H(r)dt^2 + \frac{dr^2}{H(r)} + r^2\left(\frac{dx^2}{G(x)} + G(x)d\phi^2\right)\right] , \tag{7.11}$$

with metric functions $H(r)$ and $G(x)$

$$H(r) = 1 - \frac{r^2}{R_3^2} - \frac{\mu\ell}{r} , \qquad G(x) = 1 - x^2 - \mu x^3 . \tag{7.12}$$

Note, we have changed convention for convenience. Now, our conventions primarily follow [221], however, with $\kappa = +1$ and set $\ell_3^2 = -R_3^2$ such that the brane we eventually introduce is a dS_3 brane of radius R_3. The cases $\kappa = 0$ or $\kappa = -1$ exclude the possibility of a dS_3 brane, since the roots of $H(r)$ do not represent a cosmological horizon in those cases. To move from the form

of the C-metric in Equation 7.1 to the one in Equation 7.11, one identifies

$$\lambda = \frac{\ell^2}{\ell_3^2} \,, \quad A = \frac{1}{\ell} \,, \quad k = -\kappa \,, \quad 2mA = \mu \,, \quad y = \frac{-\ell}{r}$$

and further rescale $t \to t/\ell$. The real, positive parameter ℓ is equal to the (inverse) acceleration. Meanwhile, $\mu > 0$ is interpreted to be a mass parameter of the four-dimensional black hole. The AdS_4 length scale L_4 is related to the parameters R_3 and ℓ via

$$L_4^{-2} = \ell^{-2} \left[1 - \left(\frac{\ell}{R_3} \right)^2 \right] \,. \tag{7.13}$$

For $L_4^2 > 0$ such that the bulk cosmological constant is negative, we require $R_3^2 > \ell^2$.

Following the construction of [219, 220], a Randall-Sundrum brane with tension τ and action given by Equation 6.63) is placed at the umbilic $x = 0$ surface, resulting in a tension

$$\tau = \frac{1}{2\pi G_4 \ell} \,. \tag{7.14}$$

As explained in Section 7.1, the tension may be read off from the Israel junction conditions which determine the location of the brane, such that tuning the tension corresponds to changing the position of the brane. Further, recall that the brane effectively cuts off the bulk space. For a dS braneworld, we keep only the $x > 0$ portion of the bulk, eliminating all but one of the roots of $G(x)$, which we denote as x_1. This root corresponds to an axis for the rotational Killing symmetry ∂_ϕ resulting in a conical singularity at $x = x_1$, and is removed via the identification

$$\phi \sim \phi + \Delta\phi \,, \quad \Delta\phi = \frac{4\pi}{|G'(x_1)|} = \frac{4\pi x_1}{3 - x_1^2} \,. \tag{7.15}$$

To complete the space, we perform surgery by cutting the bulk at $x = 0$, keeping only the range $0 \leq x \leq x_1$, where there are no conical singularities, and glue a second copy along $\mathcal{B}$ to complete the space. See Figure 7.1 for an illustration.

The geometry induced on the brane at $x = 0$ will result in a metric in (t, r, ϕ)-coordinates which has a conical deficit angle due to the identification in Equation 7.15. To respect regularity in the bulk, one thus rescales coordinates $(t, r, \phi) \to (\bar{t}, \bar{r}, \bar{\phi})$, where $t = \eta\bar{t}$, $r = \eta^{-1}\bar{r}$, and $\phi = \eta\bar{\phi}$, and $2\pi\eta \equiv \Delta\phi$, such that $\bar{\phi}$ is periodic in 2π, and results in the geometry [264]

$$ds^2_{\text{qSdS}} = -H(\bar{r})d\bar{t}^2 + H^{-1}(\bar{r})d\bar{r}^2 + \bar{r}^2 d\bar{t}^2 \,, \quad H(\bar{r}) = 1 - 8\mathcal{G}_3 M - \frac{\ell F(M)}{\bar{r}} - \frac{\bar{r}^2}{R_3^2} \,. \tag{7.16}$$

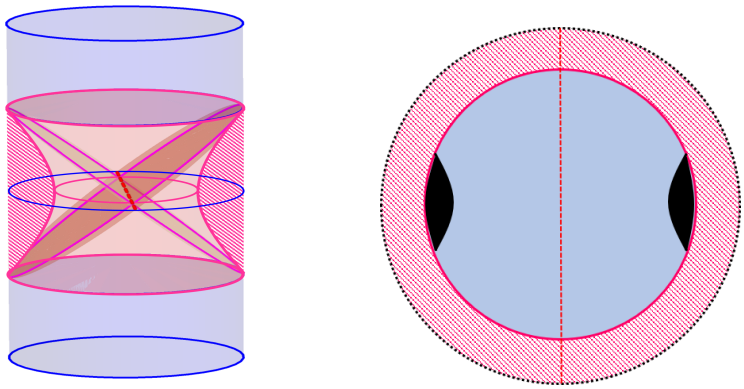

Figure 7.1: **Left:** Bulk AdS_4 with a de Sitter$_3$ brane. The brane is represented as a (magenta) hyperboloid. The bulk region up to the brane ($x < 0$, dashed magenta region) is excluded. To complete the construction, we glue a second copy along the two-sided brane. Cosmological horizons on the dS brane corresponds to the bulk acceleration horizons intersecting the brane (red dashed line). **Right:** Constant t-time slice of a single AdS_4 cylinder with a de Sitter brane (thick red circle) containing black holes. The coordinates cover only half of the disk, containing only a single black hole and cosmological horizon, where the other half is obtained via an appropriate analytic continuation.

This is the three-dimensional quantum Schwarzschild-de Sitter black hole. Depending on the size of $\ell F(M)$, there exist two positive roots to $H(\bar{r}) = 0$, denoted $\bar{r}_+$ and $\bar{r}_c$, the black hole and cosmological horizon, respectively. From the bulk perspective, the cosmological horizon on the brane arises due to the brane intersecting the acceleration horizon of the bulk black hole. Moreover, here the mass M of the brane black hole and the form factor $F(M)$ are

$$8\mathcal{G}_3 M \equiv 1 - \frac{4x_1^2}{(3-x_1^2)^2}\,, \quad F(M) \equiv \frac{8(1-x_1^2)}{(3-x_1^2)^3}\,, \tag{7.17}$$

with renormalized Newton's constant $\mathcal{G}_3 \equiv L_4 G_3/\ell$. To arrive at the expression for $F(M)$, the parameter μ is treated as being "derived" from $G(x_1) = 0$, such that $x_1 \in (0, 1]$, where $x_1 = 1$ coincides with $\mu = 0$ [221].

We can think of the metric in Equation 7.16 as a semi-classical black hole because it is an exact solution to the holographically induced theory of gravity

$$I = \frac{1}{16\pi G_3}\int_{\mathcal{B}} d^3x\sqrt{-h}\left[R - \frac{2}{L_3^2} - L_4^2\left(R_{ij}^2 - \frac{3}{8}R^2\right) + ...\right] + I_{\text{CFT}}\,, \tag{7.18}$$

with semi-classical equations of motion

$$8\pi G_3\langle T_{ij}^{\mathrm{CFT}}\rangle = G_{ij} + \frac{h_{ij}}{L_3^2} \tag{7.19}$$
$$+\ell^2\left[4R_i^{\ k}\tilde{R}_{jk} - \frac{9}{4}RR_{ij} - \Box R_{ij} + \frac{1}{4}\nabla_i\nabla_j R + \frac{1}{2}h_{ij}\left(\frac{13}{8}R^2 - 3R_{kl}^2 + \frac{1}{2}\Box R\right)\right] + \dots .$$

The CFT stress-energy tensor sources the effective three-dimensional gravity theory such that backreaction is accounted for by $\langle T_{ij}^{\mathrm{CFT}}\rangle$. Here we work in the limit where the effective three-dimensional theory obeys $L_4 \ll L_3$, or, equivalently, $\ell \sim L_4$ such that ℓ/R_3 is taken to be a small expansion parameter. Thus, the higher curvature terms in the action are multiplied by higher powers of ℓ, where, from the brane perspective, ℓ captures the strength of backreaction. Hence, the higher-derivative corrections can be understood as a series of corrections due to semi-classical backreaction. In the limit of small backreaction, moreover, $L_3^2 \approx R_3^2$ while the central charge $c \equiv L_4^2/G_4$ of the CFT_3 satisfies $2cG_3 = L_4 \approx \ell$. Therefore, for fixed c, gravity becomes weak on the brane as $\ell \to 0$ such that there is no backreaction due to the CFT. Lastly, $\ell \approx 2cL_{\mathrm{P}}$, where $L_{\mathrm{P}} = G_3$ is the Planck length (since we set $\hbar = 1$). The limit of vanishing backreaction looks singular from the bulk perspective, since keeping R_3 finite would then require $L_4 \to 0$. Instead take the limit $L_4 \to 0$ while rescaling the bulk metric by a factor L_4^2, then the brane is pushed to the boundary and gravitational dynamics on the brane is turned off, while still keeping a non-trivial state of the non-backreacting CFT_3 [264].

Returning to the qSdS geometry in Equation 7.16, we see that the $\ell F(M)/\bar{r}$ contribution characterizes quantum-corrections to the classical SdS_3 solution. Since $\ell \approx 2cL_{\mathrm{P}}$ and $c \gg 1$, as required by holography, the qSdS is not a Planck-sized black hole, but rather has a horizon much larger than the Planck length. Further, the renormalized Newton's constant $\mathcal{G}_3$ given by Equation 7.17 takes into account the modification of the definition of mass due to the higher curvature corrections [221]. Finally, we emphasize that analyzing the semi-classical Einstein's equations for a free conformally coupled scalar results in the metric in Equation 7.16 to leading order in L_{P} [264]. In principle, any correction (even if Planckian) is significant with respect to the background geometry, as it corresponds to *generating* a bona-fide horizon, rather than expanding an existing geometric feature. However, the corrections need to be super-Planckian in order for them to be meaningful, and not be relevant only at scales where the semiclassical approximation breaks down in the first place – with quantum gravity effects expected to play

a key role instead.

7.2.2 The qKdS black hole

We now describe the main novel result of this chapter, the quantum Kerr-de Sitter black hole. Analogous to the rotating quantum BTZ black hole [221], our starting point is the rotating AdS_4 C-metric, describing accelerating Kerr-AdS_4 black holes and has the line element

$$ds^2 = \omega^2\left(-\frac{H(r)}{\Sigma}(dt - ax^2 d\phi)^2 + \frac{\Sigma}{H(r)}dr^2 + r^2\left[\frac{\Sigma}{G(x)}dx^2 + \frac{G(x)}{\Sigma}\left(d\phi + \frac{a}{r^2}dt\right)^2\right]\right) \tag{7.20}$$

with metric functions

$$H(r) = 1 - \frac{r^2}{R_3^2} - \frac{\mu\ell}{r} + \frac{a^2}{r^2}\,, \quad G(x) = 1 - x^2 - \mu x^3 - \frac{a^2}{R_3^2}x^4\,, \tag{7.21}$$

$$\omega^2 = \frac{\ell^2}{(\ell + xr)^2}\,, \quad \Sigma = 1 + \frac{a^2x^2}{r^2}\,. \tag{7.22}$$

Here a is a parameter encoding the rotation of the bulk black hole (the angular momentum per unit mass), and in the limit $a = 0$ we recover the static C-metric in Equation 7.11. Evaluating the bulk Kretschmann scalar invariant $\hat{R}^{abcd}\hat{R}_{abcd}$, there is a curvature singularity when $r^2\Sigma = r^2 + a^2x^2 = 0$, i.e., when both $r = 0$ and $x = 0$. This is the familiar ring singularity in Kerr black holes. This is clarified when one moves to coordinates where $x = \cos\theta$, such that the singularity lies at the $\theta = \pi/2$ edge of the $r = 0$ disk.

Despite rotation, the $x = 0$ hypersurface remains umbilic, obeying $K_{ij} = -\ell^{-1}h_{ij}$, and is thus a natural location to place the de Sitter brane. The geometry on the brane is

$$ds^2|_{x=0} = -H(r)dt^2 + H^{-1}(r)dr^2 + r^2\left(d\phi + \frac{a}{r^2}dt\right)^2\,. \tag{7.23}$$

Since the rotating C-metric in Equation 7.20 is a solution to the bulk Einstein equations, we are guaranteed the brane geometry is a solution to the induced theory of gravity given by Equation 6.66. However, at this stage it would be naive to interpret this solution as the quantum Kerr-dS_3 black hole. This is because we have not yet accounted for bulk regularity conditions, which will affect more than just the periodicity of the angular variable ϕ. In fact, we know the 'naive metric' in Equation 7.23 does not capture all of the correct features because the ring singularity lives on the brane, yet the above metric does not have a ring singularity at $r = 0$ but rather a standard curvature singularity. We will see momentarily how the ring singularity makes an appearance.

Bulk regularity

Notice that the Killing vector ∂_ϕ no longer has vanishing norm at a zero x_i of $G(x)$. Rather, the Killing vector

$$\xi^b = \partial^b_\phi + a x_i^2 \partial^b_t \,, \tag{7.24}$$

obeys $\xi^2|_{x_i} = 0$. Avoiding conical defects at $x = x_i$ requires us to identify points along the integral curves of the vector given by Equation 7.24 with an appropriate period. To determine the correct periodicity, consider the rotating C-metric in Equation 7.20 near a zero $x = x_i$ such that $G(x) \sim G'(x_i)(x - x_i)$, as explained in Section 7.1. Removal of a conical singularity at $x = x_i$ requires one simultaneously perform the coordinate transformation $\tilde{t} = t - a x_i^2 \phi$ together with the same periodicity condition on ϕ as Equation 7.15. Specifically, singling out the smallest positive root $x = x_1$, then

$$\phi \sim \phi + \Delta\phi \,, \quad \Delta\phi = \frac{4\pi}{|G'(x_1)|} = \frac{4\pi x_1}{3 - x_1^2 + \tilde{a}^2} \,, \tag{7.25}$$

where to arrive to the second equality we recast the parameter μ in terms of x_1

$$\mu = \frac{1 - x_1^2 - \tilde{a}^2}{x_1^3} \,, \quad \tilde{a} \equiv \frac{a x_1^2}{R_3} \,. \tag{7.26}$$

Thus, identifying points along the orbits of ξ^b are made on surfaces of constant

$$\tilde{t} \equiv t - a x_1^2 \phi \,. \tag{7.27}$$

The remaining zeros $x_i \neq x_1$ are dealt with by cutting off the bulk spacetime at $x = 0$, and gluing to a second region such that the complete space is comprised of a bulk region with $x \in [0, x_1]$, leaving a space which is free of conical singularities at $x = x_i$.

Returning to the naive geometry at $x = 0$ given by Equation 7.23, consider the asymptotic limit $r \to \infty$. The metric is asymptotic to 'rotating dS_3', where the $dtd\phi$ component grows like a constant. Unfortunately, the coordinates are not canonically normalized due to the periodicity in ϕ in Equation 7.25. In fact, since points along orbits of Equation 7.24 are identified, the periodicity in ϕ as Equation 7.25 returns one to a different point in time t: from Equation 7.27, we see that with $\tilde{t} \sim \tilde{t}$ then $t \sim t + 2\pi\eta a x_1^2$, where $\eta \equiv \Delta\phi/2\pi$. This means we cannot just rescale coordinates $(t, r, \phi) \to (\bar{t}, \bar{r}, \bar{\phi})$ as done in the static case for Equation 7.16. Additionally, the periodicity alters the asymptotic form of the metric such that the $dtd\phi$ grows as r^2, which would

seem to imply a diverging angular momentum. To see this, perform the following coordinate transformation in the brane geometry given by Equation 7.23 $t \to \tilde{t} + ax_1^2\tilde{\phi}$ and $\phi \to \tilde{\phi}$. Then, it is straightforward to show for large r the $h_{\tilde{t}\tilde{\phi}}$ component of the geometry diverges as r^2.

We can remedy the situation by changing coordinates (t, ϕ) to $(\tilde{t}, \tilde{\phi})$ where $t = \tilde{t} + ax_1^2\tilde{\phi}$ and $\phi = \tilde{\phi} + C\tilde{t}$ for some constant C. In the asymptotic limit, the $\tilde{t} - \tilde{\phi}$ component of the naive brane metric in Equation 7.23 will have go as

$$h_{\tilde{t}\tilde{\phi}} = \left(C + \frac{ax_1^2}{R_3^2}\right) r^2 + (a - ax_1^2 + Ca^2x_1^2) + \mathcal{O}(1/r) \ . \tag{7.28}$$

Judiciously, we choose $C \equiv -ax_1^2/R_3^2 = -\tilde{a}/R_3$ to eliminate the r^2 divergence. Making this choice deals with the undesired asymptotic growth, however, $\tilde{\phi}$ is still not periodic in 2π. This is now easily resolved by a simple rescaling, $\tilde{t} = \eta\bar{t}$ and $\tilde{\phi} = \eta\bar{\phi}$, such that the transformation

$$t = \eta(\bar{t} + \tilde{a}R_3\bar{\phi}) \ , \quad \phi = \eta\left(\bar{\phi} - \frac{\tilde{a}}{R_3}\bar{t}\right) \ , \tag{7.29}$$

puts the brane geometry in a more canonical form. Inverting the transformation in Equation 7.29,

$$\bar{t} = \frac{1}{\eta(1+\tilde{a}^2)}(t - \tilde{a}R_3\phi) \ , \quad \bar{\phi} = \frac{1}{\eta(1+\tilde{a}^2)}\left(\phi + \frac{\tilde{a}}{R_3}t\right) \ , \tag{7.30}$$

we see the Killing vectors ∂_t and ∂_ϕ transform as

$$\partial_t = \frac{1}{\eta(1+\tilde{a}^2)}\left(\partial_{\bar{t}} + \frac{\tilde{a}}{R_3}\partial_{\bar{\phi}}\right) \ , \quad \partial_\phi = \frac{1}{\eta(1+\tilde{a}^2)}\left(\partial_{\bar{\phi}} - \tilde{a}R_3\partial_{\bar{t}}\right) \ . \tag{7.31}$$

Consequently, now the rotational Killing vector in Equation 7.24 is $\xi^b = \eta^{-1}\partial_{\bar{\phi}}$.

With the coordinate change in Equation 7.29, the brane metric does not quite have the canonical asymptotic form of a rotating de Sitter black hole. We still need to redefine the radial coordinate r. Following [221], let

$$r^2 \equiv \frac{\bar{r}^2 - r_s^2}{(1+\tilde{a}^2)\eta^2} \ , \quad r_s = -\frac{R_3\tilde{a}\eta}{x_1}\sqrt{2 - x_1^2} = -\frac{2\tilde{a}R_3\sqrt{2-x_1^2}}{3 - x_1^2 + \tilde{a}^2} \ . \tag{7.32}$$

Altogether, the geometry on the brane in the canonically normalized coordinates $(\bar{t}, \bar{r}, \bar{\phi})$ is

$$\begin{aligned} ds^2|_{x=0} = &-\left(\eta^2\left(1 - \tilde{a}^2 + \frac{4\tilde{a}^2}{x_1^2}\right) - \frac{\bar{r}^2}{R_3^2} - \frac{\mu\ell\eta^2}{r}\right) d\bar{t}^2 \\ &+ \left(\eta^2\left(1 - \tilde{a}^2 + \frac{4\tilde{a}^2}{x_1^2}\right) - \frac{\bar{r}^2}{R_3^2} - \frac{\mu\ell(1+\tilde{a}^2)^2\eta^4 r}{\bar{r}^2} + \frac{R_3^2\tilde{a}^2\mu^2x_1^2\eta^4}{\bar{r}^2}\right)^{-1} d\bar{r}^2 \\ &+ \left(\bar{r}^2 + \frac{\mu\ell\tilde{a}^2R_3^2\eta^2}{r}\right) d\bar{\phi}^2 + R_3\tilde{a}\mu x_1\eta^2\left(1 + \frac{\ell}{x_1 r}\right)(d\bar{\phi}d\bar{t} + d\bar{t}d\bar{\phi}) \ , \end{aligned} \tag{7.33}$$

where we have kept both r and $\bar{r}$ when convenient.

7.2.3 Black hole on the brane

Let us now scrutinize the brane geometry in Equation 7.33. First, we identify the mass M as

$$8\mathcal{G}_3 M \equiv 1-\eta^2\left(1-\tilde{a}^2+\frac{4\tilde{a}^2}{x_1^2}\right)=1-\frac{4[x_1^2-\tilde{a}^2(x_1^2-4)]}{(3-x_1^2+\tilde{a}^2)^2}\,, \tag{7.34}$$

where $\mathcal{G}_3 \equiv L_4 G_3/\ell$ is the 'renormalized' three-dimensional Newton's constant [221]. Since the brane theory is generally three-dimensional Einstein-de Sitter gravity plus higher-derivative corrections, we do not have a generic Komar-like mass integral in which we compute M. Rather, here we have identified the mass as the subleading constant term in $h_{\overline{tt}}$, as done in Einstein-de Sitter gravity, and used $\mathcal{G}_3$ to encompass all of the higher-derivative corrections entering at order ℓ^2 in the brane action in Equation 7.18 [265]. The expression is not terribly transparent, but the mass of the black hole depends implicitly, via $\tilde{x}_1$, on μ. As we will see later, this is exactly the parameter that controls the expectation value of the backreacting energy of the quantum field. Similarly, we have identified the three-dimensional angular momentum J to be

$$4\mathcal{G}_3 J \equiv -R_3\tilde{a}\mu x_1\eta^2=\frac{4R_3\tilde{a}(x_1^2+\tilde{a}^2-1)}{(3-x_1^2+\tilde{a}^2)^2}\,, \tag{7.35}$$

where again the renormalized Newton's constant plays the role of accounting for higher-derivative corrections to the angular momentum. Importantly, notice M and J depend on $\tilde{a}^2$ and x_1^2, and the parameter ℓ does not make an explicit appearance.

We emphasize, at this stage, the mass M given by Equation 7.34 and angular momentum J in Equation 7.35 are identifications. Justification for this, in part, comes from the fact that these quantities satisfy a first law of thermodynamics, as we demonstrate in the next section. Essentially, as argued in [113] the mass of the black hole on the brane is identified as the mass of the bulk black hole intersecting the brane. A feature distinguishing AdS and dS braneworld constructions is how the mass Equation 7.34 coincides with a conserved charge. This is because asymptotically dS spacetimes do not have a boundary which makes providing an invariant notion of conserved charges more difficult. From the brane perspective, one could compute conserved charges, for example, by calculating the Brown-York quasi-local stress tensor on slices at past and future infinity [266]. The mass found should then coincide with the mass of the bulk black hole intersecting the brane at $I^{\pm}$. In practice this is difficult, however, because the theory on the brane is a complicated higher-order theory of gravity, a context in which

defining conserved charges is also a subtle matter (AdS braneworld models encounter the same subtlety in this regard). Alternatively, one can use the method developed in [267], which does not require entering an asymptotic region. It would be worthwhile to explore this question and verify the mass identified in the first law coincides with an invariant conserved charge.

With the substitutions given by Equation 7.34 and Equation 7.35, the brane geometry in Equation 7.33 takes the form

$$\begin{aligned} ds^2_{\text{qKdS}} = &-\left(1-8\mathcal{G}_3 M-\frac{\bar{r}^2}{R_3^2}-\frac{\mu\ell\eta^2}{r}\right)d\bar{t}^2 \\ &+\left(1-8\mathcal{G}_3 M-\frac{\bar{r}^2}{R_3^2}+\frac{(4\mathcal{G}_3 J)^2}{\bar{r}^2}-\frac{\mu\ell(1+\tilde{a}^2)^2\eta^4 r}{\bar{r}^2}\right)^{-1}d\bar{r}^2 \\ &+\left(\bar{r}^2+\frac{\mu\ell\tilde{a}^2R_3^2\eta^2}{r}\right)d\bar{\phi}^2-4\mathcal{G}_3 J\left(1+\frac{\ell}{x_1 r}\right)(d\bar{\phi}d\bar{t}+d\bar{t}d\bar{\phi})\,. \end{aligned} \tag{7.36}$$

Since the metric in Equation 7.36 is an *exact* solution to the full semi-classical theory of gravity on the brane, we refer to the three-dimensional spacetime as the quantum Kerr-dS$_3$ black hole (qKdS). We say 'black hole' because, as we describe below, this geometry possesses both an inner and outer black hole horizon, shrouding a ring singularity, and a cosmological horizon. We say 'quantum' because it includes all orders of semi-classical backreaction due to the CFT, where terms in the metric proportional to $\mu\ell$ are understood to be quantum corrections to the classical Kerr-dS$_3$ conical defect. Justification of this terminology will be given when we compute the renormalized CFT stress-tensor $\langle T_{ij}^{\text{CFT}}\rangle$.

Before we analyze the brane geometry given by Equation 7.36 in more detail, there are a few special limits to consider. First, clearly, when the rotation $a \to 0$, then $J = 0$ and the geometry reduces to the static metric in Equation 7.16, the quantum Schwarzschild-de Sitter black hole [219]. Next, in the limit of vanishing backreaction $\ell \to 0$, in which the gravitational effects of the cutoff CFT are suppressed (where $\mathcal{G}_3 \to G_3$), the metric in Equation 7.36 takes the form of the classical Kerr-dS$_3$ conical defect spacetime (see Section 6.1.1). Thirdly, when the parameter μ in Equation 7.26 vanishes, i.e., $x_1 = \sqrt{1-\tilde{a}^2}$, then both $M = J = 0$, resulting in the empty dS$_3$ geometry. The mass M will also be zero when $x_1 = \sqrt{9-\tilde{a}^2}$. When this is the case, $J \neq 0$ and $\mu \neq 0$,

$$4\mathcal{G}_3 J = \frac{32\tilde{a}R_3}{(6-2\tilde{a}^2)^2}\,, \quad \mu = \frac{512\tilde{a}R_3}{(\tilde{a}^2-9)^3(\tilde{a}^2-3)^2}\,, \tag{7.37}$$

and we can think of the brane geometry as quantum rotating dS$_3$.

Horizons and closed timelike curves

While the metric given by Equation 7.36 is in the correct canonically normalized coordinates $(\bar{t}, \bar{r}, \bar{\phi})$, in what follows we will perform calculations in the naive background (t, r, ϕ) of Equation 7.23, and perform the appropriate coordinate transformation. This is largely done for convenience, but also because both metrics share nearly all of the same qualitative features.

In the static case, roots of $H(r)$ correspond to the Killing horizons of the Killing vector ∂_t. With rotation, the Killing vector

$$\zeta^b = \partial_t - \frac{a}{r_i^2}\partial_\phi \tag{7.38}$$

becomes null at roots r_i of $H(r)$. Define the function $Q(r) \equiv r^2 H(r)$. Since $Q(r)$ is a quartic polynomial in r, it will generally have either four, two, or zero real roots. Here we focus on the case when there are four real roots, which we will see later enforces conditions on the physical parameters a and μ. The three positive roots to $Q(r)$ are the cosmological horizon r_c, the outer black hole horizon r_+ and inner black hole horizon r_-, obeying $r_- \leq r_+ \leq r_c$. The fourth root, r_n, is negative and resides behind the singularity at $r = 0$. Using $H(r_c) = 0$, and $H(r_\pm) = 0$, we can express

$$\begin{aligned} R_3^2 &= r_c^2 + r_+^2 + r_c r_+ + r_-(r_c + r_+ + r_-) \,, \\ \mu\ell &= \frac{(r_c + r_+)(r_c + r_-)(r_+ + r_-)}{r_c^2 + r_+^2 + r_c r_+ + r_-(r_c + r_+ + r_-)} \,, \\ a^2 &= \frac{r_c r_+ r_-(r_c + r_+ + r_-)}{r_c^2 + r_+^2 + r_c r_+ + r_-(r_c + r_+ + r_-)} \,. \end{aligned} \tag{7.39}$$

The blackening factor $H(r)$ factorizes as

$$H(r) = \frac{1}{R_3^2 r^2}(r_c - r)(r - r_+)(r - r_-)(r + r_c + r_+ + r_-) \,. \tag{7.40}$$

The limit $r_- \to 0$ coincides with $a = 0$, while $r_+ = r_- = 0$ corresponds to $\mu \to 0$, resulting in the Kerr-dS$_3$ geometry with a single cosmological horizon. Let us point out now that, whilst the roots $r_\pm$ are strictly "quantum" – in the sense that they would not be at all present if the backreaction of the quantum field was not accounted for – the location of the other two horizons as well suffers a correction due to the quantum stress tensor. Moreover, the four roots need not be all distinct. When they coincide, we obtain interesting limiting geometries – which we further explore in Section 7.2.4.

Since the black hole is stationary, the positive roots r_i to $H(r)$ correspond to rotating horizons with rotation Ω_i,

$$\Omega_i \equiv \frac{a}{R_3^2}\frac{(x_1^2 r_i^2 - R_3^2)}{(r_i^2 + a^2 x_1^2)} \,, \tag{7.41}$$

where we used the transformations in Equation 7.31, to express ζ^b and define $\bar{\zeta}^b$

$$\bar{\zeta}^b \equiv \frac{\eta(1+\tilde{a}^2)}{\left(1+\frac{a^2 x_1^2}{r_i^2}\right)}\zeta^b = \partial_{\bar{t}}^b + \Omega_i \partial_{\bar{\phi}}^b \,. \tag{7.42}$$

Further, relative to $\bar{\zeta}^b$, the surface gravity κ_i associated with each horizon r_i is given by

$$\kappa_i = \frac{\eta(1+\tilde{a}^2)}{\left(r_i^2 + a^2 x_1^2\right)}\frac{r_i^2}{2}|H'(r_i)| = \frac{\eta(1+\tilde{a}^2)}{\left(r_i^2 + a^2 x_1^2\right)}\frac{1}{2R_3^2 r_i}|R_3^2 \mu \ell r_i - 2r_i^4 - 2a^2 R_3^2| \,, \tag{7.43}$$

where we used the definition $\bar{\zeta}^b \nabla_b \bar{\zeta}^c = \kappa \bar{\zeta}^c$. Explicitly,

$$\begin{aligned}
\kappa_c &= -\frac{\eta(1+\tilde{a}^2)}{2R_3^2\left(r_c^2 + a^2 x_1^2\right)}(r_c - r_+)(r_c - r_-)(r_+ + r_- + 2r_c) \,, \\
\kappa_+ &= \frac{\eta(1+\tilde{a}^2)}{2R_3^2\left(r_+^2 + a^2 x_1^2\right)}(r_c - r_+)(r_+ - r_-)(r_c + r_- + 2r_+) \,, \\
\kappa_- &= -\frac{\eta(1+\tilde{a}^2)}{2R_3^2\left(r_-^2 + a^2 x_1^2\right)}(r_c - r_-)(r_+ - r_-)(r_c + r_+ + 2r_-) \,.
\end{aligned} \tag{7.44}$$

Notice the cosmological horizon surface gravity κ_c vanishes when $r_c = r_+$ or $r_c = r_-$, and similarly for the other surface gravities. We explore these extremal limits momentarily. When $r_- \to 0$, i.e., vanishing rotation, we recover the surface gravities of the cosmological horizon and black hole horizon of the qSdS black hole [219]. Additionally, in the limit of vanishing backreaction, then $r_\pm \to 0$ such that $\kappa_\pm \to 0$.

As mentioned previously, in the naive coordinates of Equation 7.23, a computation of the Kretschmann scalar reveals a curvature singularity at $r = 0$. In the canonically normalized coordinates of Equation 7.36, $r = 0$ corresponds $\bar{r} = r_s$, corresponding to a ring singularity, and is endowed from the bulk black hole solution. Moreover, near the ring singularity there exists the possibility of closed timelike curves. Relative to the canonically normalized metric in Equation 7.36, the norm of the axial Killing vector $\partial_{\bar{\phi}}$ is

$$\partial_{\bar{\phi}}^2 = h_{\bar{\phi}\bar{\phi}} = \bar{r}^2 + \frac{\mu \ell \tilde{a}^2 R_3^2 \eta^2}{r} \,. \tag{7.45}$$

Thus, for sufficiently small and negative r, the vector $\partial_{\bar{\phi}}$ becomes timelike, the orbits of which are closed curves around the rotation axis. However, unlike the rotating qBTZ black hole, these closed timelike curves do not become naked.

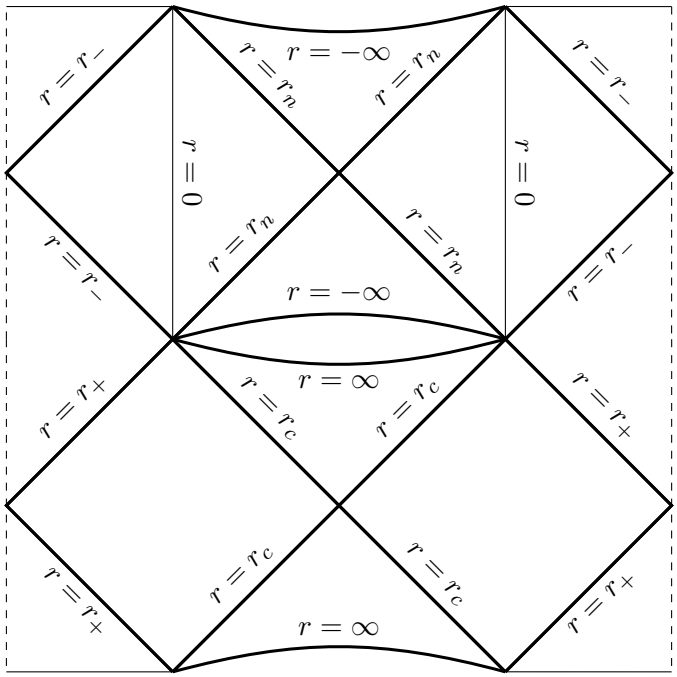

Figure 7.2: Penrose diagram of a neutral quantum Kerr black hole in dS_3. Shown here is the global structure with periodic identifications made along constant $\bar{t}$ hypersurfaces. The diagram has infinite extent in the vertical directions while the dashed edges are identified.

When all of the roots to $Q(r)$ are distinct, then standard methods [268] lead to a maximal extension of the quantum Kerr-dS_3 black hole. Generally, the resulting conformal diagram is infinite in extent and is nearly identical to the Kruskal extension of the classical four-dimensional Kerr-dS black hole. The aforementioned closed timelike curves may be eliminated by an appropriate periodic identification [269], such that constant $\bar{t}$ hypersurfaces are closed and span two black hole regions with opposite spin, cutting through intersections of $r = r_c$ and $r = r_+$ (see Figure 7.2 for a diagram).

Ergoregions

As with classical Kerr-de Sitter spacetimes, the qKdS black hole has a stationary limit surface and two ergoregions associated with the outer black hole and cosmological horizons. Explicitly, the time-translation Killing vector ∂_t in the naive metric has the norm $\mathcal{N}$

$$\mathcal{N} = -H(r) + \frac{a^2}{r^2} \,. \tag{7.46}$$

Clearly, at the outer and cosmological horizons, where $H = 0$, then ∂_t is spacelike. The locus of points where $\mathcal{N} = 0$ yields a stationary limit surface, satisfying $r(R_3^2 - r^2) = R_3^2\mu\ell$. Since there exist regions in between the outer and cosmological horizons where ∂_t is timelike, there are two ergoregions, where an observer is forced to move in the direction of rotation of the outer black hole horizon or cosmological horizon (the black hole and cosmological ergoregions, respectively). With the appearance of ergoregions, one can in principle examine the Penrose process of energy extraction in the qKdS solution in morally the same way as a classical four-dimensional Kerr-de Sitter black hole (see, e.g., [270]). At least for small backreaction, it is expected the Penrose process in the cosmological ergoregion is not possible.

7.2.4 Extremal, Nariai, ultracold, and lukewarm limits

As with the four-dimensional Kerr-de Sitter black hole, the quantum Kerr-dS$_3$ has a number of limiting geometries. Specifically, (i) extremal or 'cold' limit, where $r_+ = r_-$; (ii) rotating Nariai limit, where $r_c = r_+$; (iii) the 'ultacold' limit where $r_c = r_+ = r_-$, and (iv) the 'lukewarm' limit, where the surface gravities $\kappa_c = \kappa_+$. Below we summarize each of these limiting geometries and briefly explore their features, leaving the details to Appendix C. Our analysis primarily follows [269], and for simplicity, we work with the naive metric (t, r, ϕ) of Equation 7.23 except when stated otherwise.

Extremal black hole: $r_+ = r_-$

The extremal black hole corresponds to when the outer and inner black hole horizons coincide. In this limit the surface gravity of the outer horizon $\kappa_+ = 0$, and, correspondingly the Hawking temperature T_+ of the black hole vanishes, i.e., the black hole is 'cold'. Moreover, parameters a^2 and $\mu\ell$ may be cast as

$$a^2 = r_+^2 - \frac{3r_+^4}{R_3^2}\,, \quad \mu\ell = 2r_+ - \frac{4r_+^3}{R_3^2}\,. \tag{7.47}$$

In the extremal limit the global structure of the spacetime changes because now the (double) black hole horizon moves to an infinite proper distance away from all other portions of the geometry, such that the black hole interior is inaccessible from the rest of the spacetime.

In the near horizon limit of extremal qKdS, we can no longer express the metric in coordinates (t, r, ϕ) as they become singular. Rather, we perform a coordinate transformation analogous to [271, 272]

$$r = r_+ + \lambda\rho \ , \quad t = \frac{\tau}{\lambda} \ , \quad \phi = \varphi - \frac{a\tau}{r_+^2\lambda} \ , \tag{7.48}$$

where upon taking $\lambda \to 0$ we find

$$ds^2_{\text{ex}} = \Gamma\left(-\hat{\rho}^2 d\hat{\tau}^2 + \frac{d\hat{\rho}^2}{\hat{\rho}^2}\right) + r_+^2\left(d\varphi + k\hat{\rho}d\hat{\tau}\right)^2 \ , \tag{7.49}$$

with

$$\Gamma = \frac{r_+^2}{1 - 6r_+^2/R_3^2} \ , \quad k = -\frac{2aR_3^2}{r_+(R_3^2 - 6r_+^2)} \ . \tag{7.50}$$

This is the near horizon extremal Kerr (NHEK) geometry for the quantum-corrected Kerr-dS$_3$. Formally it has the same structure as the NHEK region of four-dimensional Kerr-(A)dS spacetimes, and has the form of a fibered product of AdS$_2$ and the circle. As such, following [272], the isometry group is $\text{SL}(2,\mathbb{R}) \times U(1)$.

Notice from Equation 7.47 that $a = 0$ when $r_+ = 0$ or $r_+ = R_3/\sqrt{3}$, which, respectively, corresponds to $\mu\ell = 0$ or $\mu\ell = 2R_3/3\sqrt{3}$. The latter is simply the Nariai limit of the quantum Schwarzschild-de Sitter black hole [219], which we explore in more detail below.

Rotating Nariai black hole: $r_c = r_+$

The Nariai solution occurs when the cosmological and outer black hole horizons coincide $r_c = r_+ \equiv r_{\text{N}}$. Then

$$a^2 = \frac{r_{\text{N}}^2}{R_3^2}(R_3^2 - 3r_{\text{N}}^2) \ , \quad (\mu\ell)_{\text{N}} = \frac{2r_{\text{N}}}{R_3^2}(R_3^2 - 2r_{\text{N}}^2) \ . \tag{7.51}$$

Notice when $a = 0$ we recover $r_{\text{N}} = R_3/\sqrt{3}$ and $(\mu\ell)_{\text{N}} = 2R_3/3\sqrt{3}$, the Nariai limit of the static Schwarzschild-de Sitter black hole. Physically, the Nariai black hole is the largest black hole which may fit inside the cosmological horizon, saturating at μ_{N}. Moreover, the rotating Nariai black hole is generally larger than the static Nariai solution, analogous to how the charged Nariai black hole is larger than the neutral geometry.

The blackening factor $H(r)$ vanishes when $r = r_{\text{N}}$ making the (t, r, ϕ) coordinate system incompatible in describing the Nariai geometry. Thus, introduce coordinates [269]

$$r = r_{\text{N}} + \epsilon\rho \ , \quad t = \frac{\Gamma\hat{\tau}}{\epsilon} \ , \quad \phi = \varphi - \frac{a}{r_{\text{N}}^2\epsilon}\tau \ . \tag{7.52}$$

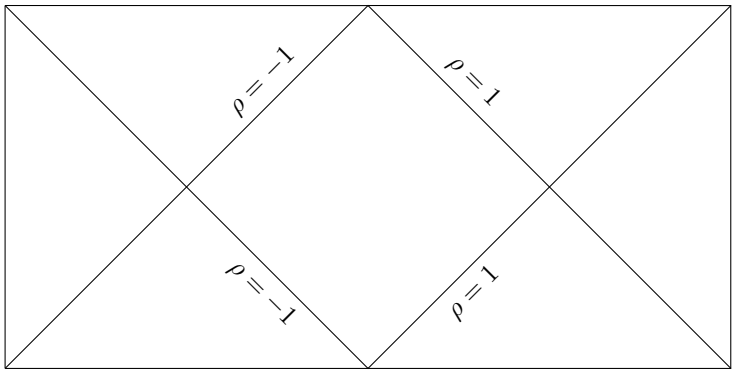

Figure 7.3: Penrose diagram of the Nariai qKdS black hole. The black hole and cosmological horizons are located at $\rho = -1$ and $\rho = 1$, respectively, and are in thermal equilibrium at a non-zero temperature. Clearly there is a finite proper distance between the two horizons. Future and past infinity $\mathcal{I}^{\pm}$ are located at $\rho = \infty$, while the past and future black hole singularities correspond to $\rho = -\infty$. The left and right sides of the diagram are identified.

and send $\epsilon \to 0$ such that the naive geometry in Equation 7.23 becomes

$$ds_{\rm N}^2 = \Gamma \left(-(1-\rho^2) d\hat{\tau}^2 + \frac{d\rho^2}{(1-\rho^2)} \right) + r_{\rm N}^2 \left(d\varphi + k\rho d\hat{\tau} \right)^2 \ , \tag{7.53}$$

where

$$\Gamma = \frac{R_3^2 r_{\rm N}^2}{6r_{\rm N}^2 - R_3^2} \ , \quad k = -\frac{2aR_3^2}{r_{\rm N}(6r_{\rm N}^2 - R_3^2)} \ . \tag{7.54}$$

Hence, the Nariai limit of the qKdS black hole has the product structure of dS_2 fibered over a circle, written here in static patch coordinates, and has the isometry group $U(1) \times \mathrm{SL}(2, \mathbb{R})$. When $a = 0$, then $\Gamma = R_3^2/3$, leading to the non-rotating Nariai metric [273, 274, 275] with product geometry $\mathrm{dS}_2 \times S_2$. A static patch observer is restricted to the region $\rho \in (-1, 1)$, where $\rho = -1$ corresponds to the black hole horizon and $\rho = +1$ the cosmological horizon, at a finite proper distance apart. To draw the Penrose diagram (see Figure 7.3) it is useful to switch to global coordinates [276]

$$\begin{aligned} \tan(\eta/2) &= \tanh\left(\frac{1}{2} \sinh^{-1}(\sqrt{1-\rho^2} \sinh\hat{\tau}) \right) \\ \cos\psi &= \rho(\cosh^2\hat{\tau} - \rho^2 \sinh^2\hat{\tau})^{-1/2} \\ \chi &= \varphi + \frac{k}{2} \log\left(\frac{\sin(\eta+\psi)}{\sin(\eta-\psi)} \right) \ , \end{aligned} \tag{7.55}$$

such that

$$ds^2_{\rm N} = \Gamma\left(\frac{-d\eta^2 + d\psi^2}{\cos^2\eta}\right) + r^2_{\rm N}(d\chi + k\tan\eta d\psi)^2 \ , \tag{7.56}$$

where $\psi \sim \psi + 2\pi$ and $\eta \in (-\pi/2, \pi/2)$ cover the all of the dS_2 portion.

Naively, when $r_c = r_+$ the surface gravities given by Equation 7.43 of the cosmological and black hole horizons vanish, $\kappa_c = \kappa_+ = 0$. However, in the Nariai geometry given by Equation 7.53, the two horizons are in thermal equilibrium at a non-zero temperature $T_{\rm N}$. We will return to this in Section 7.3.

Ultracold black hole: $r_c = r_+ = r_-$

The ultracold black hole is the limit when all of the horizons coincide, namely, $r_c = r_+ = r_- \equiv r_{uc}$. The form of the metric can be found directly from the Nariai geometry in Equation 7.53. Since the Nariai geometry becomes singular when $r_{\rm N} = r_-$, the coordinates $(\rho, \hat{\tau})$ require an appropriate rescaling

$$\rho = \sqrt{\frac{2r_{\rm uc} - \delta}{R_3}}X \ , \quad \tau = \sqrt{\frac{R_3}{2r_{\rm uc} - \delta}}\frac{R_3 r_{\rm uc}}{4}T \ , \tag{7.57}$$

where $\tau = \Gamma\hat{\tau}$, and subsequently take the limit $\delta \to 2r_{\rm uc}$. The resulting geometry is

$$ds^2_{\rm uc} = \frac{R_3 r_{\rm uc}}{4}(-dT^2 + dX^2) + r^2_{\rm uc}\left(d\varphi - \frac{2aX}{r^3_{\rm uc}}dT\right)^2 \ . \tag{7.58}$$

This geometry is of the form of a fibered product of two-dimensional Minkowski space over a circle. Via an appropriate coordinate transformation (see [269]), the ultracold solution can also be expressed as a fibered product of two-dimensional Rindler space and a circle. In the limit of vanishing rotation there is no ultracold solution, but rather a static Nariai black hole.

Lukewarm black hole: $\kappa_c = \kappa_+$

As with all Kerr-de Sitter black holes, the quantum Kerr-dS_3 has a lukewarm limit. This occurs when the surface gravities of the cosmological and outer black hole horizons coincide at a value different from the surface gravity of the Nariai black hole. Notably, the geometry is non-singular in (t, r, ϕ) coordinates. Thermodynamically speaking, this spacetime is another example of where the black hole and cosmological horizon are in thermal equilibrium. We will

return to this limit in Section 7.3, however, in Appendix C we find its limiting form in the naive brane geometry.

Before moving on, we point out that the special limits of the quantum Kerr-dS$_3$ black hole has qualitatively similar features to dS$_3$ black hole solutions to topologically massive gravity, cf. [277, 278, 279]. Indeed, the asymptotically warped dS$_3$ black hole (obtained from discrete global identifications of warped dS$_3$) has a Nariai limit whose $U(1)\times U(1)$ isometry is enhanced to a $\mathrm{SL}(2,\mathbb{R})\times U(1)$ isometry group. It would be interesting to understand the relation between quantum dS$_3$ black holes and warped dS$_3$ black holes in more detail.

7.2.5 Holographic conformal matter stress-tensor

We have been referring to the geometry on the brane given by Equation 7.36 as a quantum black hole since, via the holographic dictionary, it is a solution to the semi-classical equations of motion i Equation 7.19 to all orders in backreaction. Let us now justify this claim and solve for the expectation value of the CFT stress-energy tensor $\langle T_{ij}\rangle$ sourcing the black hole.

Following [221], we decompose $\langle T^i_{\ j}\rangle = \langle T^i_{\ j}\rangle_0 + \ell^2\langle T^i_{\ j}\rangle_2 + ...$ in increasing powers of ℓ^2. Specifically, the leading order contribution is

$$8\pi G_3\langle T^i_{\ j}\rangle_0 = R^i_{\ j} - \frac{1}{2}\delta^i_{\ j}\left(R - \frac{2}{R_3^2}\right) , \tag{7.59}$$

while the $\mathcal{O}(\ell^2)$ contribution is

$$\begin{aligned} 8\pi G_3\langle T^i_{\ j}\rangle_2 = {} & 4R^{ik}R_{jk} - \Box R^i_{\ j} - \frac{9}{4}RR^i_{\ j} + \frac{1}{4}\nabla^i\nabla_j R \\ & + \frac{1}{2}\delta^i_{\ j}\left(\frac{13}{8}R^2 - 3R^2_{kl} + \frac{1}{2}\Box R - \frac{1}{2R_3^4}\right) . \end{aligned} \tag{7.60}$$

It proves is more computationally convenient to determine $\langle T_{ij}\rangle$ in the naive metric of Equation 7.23 and then transform into the $(\bar{t},\bar{r},\bar{\phi})$ than working directly with the metric in Equation 7.36. Thus, in the naive background we find the only non-vanishing components of the stress-tensor are

$$\begin{aligned} \langle T^t_{\ t}\rangle_0 = \langle T^r_{\ r}\rangle_0 = -\frac{1}{2}\langle T^\phi_{\ \phi}\rangle_0 = \frac{1}{16\pi G_3}\frac{\mu\ell}{r^3} , \\ \langle T^\phi_{\ t}\rangle_0 = -\frac{1}{16\pi G_3}\frac{3\mu\ell a}{r^5} , \end{aligned} \tag{7.61}$$

and, for completeness,

$$\begin{aligned}
\langle T^t_{\ t}\rangle_2 &= -\frac{\mu\ell}{32\pi G_3 R_3^2 r^7}\left[90a^2R_3^2 - 11r^4 + R_3^2 r(18r - 19\mu\ell)\right] \ , \\
\langle T^r_{\ r}\rangle_2 &= -\frac{\mu\ell}{32\pi G_3 R_3^2 r^7}\left[r^4 + 30a^2R_3^2 + R_3^2 r(6r - 7\mu\ell)\right] \ , \\
\langle T^\phi_{\ \phi}\rangle_2 &= -\frac{\mu\ell}{32\pi G_3 R_3^2 r^7}\left[10r^4 - 120a^2R_3^2 - R_3^2 r(24r - 29\mu\ell)\right] \ , \\
\langle T^t_{\ \phi}\rangle_2 &= -\frac{3a\mu\ell}{2\pi G_3 r^5} \ , \\
\langle T^\phi_{\ t}\rangle_2 &= -\frac{3a\mu\ell}{32\pi G_3 R_3^2 r^9}\left[23r^4 - 70a^2R_3^2 - R_3^2 r(30r - 32\mu\ell)\right]
\end{aligned} \tag{7.62}$$

Notice that while $\langle T^i_{\ i}\rangle_0 = 0$, as one would expect for a CFT stress-tensor, we see $\langle T^i_{\ i}\rangle_2 = -3(\mu\ell)^2/32\pi G_3 r^6$. A non-termminating trace at higher order powers is a consequence of the fact that the CFT on the brane has an ultraviolet cutoff. Indeed, the Weyl anomaly (and hence the sporious trace at the quantum level for CFTs) is absent in odd space-time dimensions [280], meaning that if a non-zero contribution to the trace appears must have its origin in an explicit breaking of the conformal symmetry. Such a breaking is a consequence of the IR cutoff in the bulk (the brane that cuts AdS space), which is dual to a UV cutoff in the CFT on brane itself [113].

Transforming to the $(\bar{t}, \bar{r}, \bar{\phi})$ coordinates

$$\langle T^{\bar{i}}_{\ \bar{j}}\rangle = \Lambda^{\bar{i}}_{\ i}\Lambda^{j}_{\ \bar{j}}\langle T^i_{\ j}\rangle \ , \quad \Lambda^{\bar{i}}_{\ j} \equiv \frac{\partial \bar{x}^i}{\partial x^j} = \frac{1}{\eta(1+\tilde{a}^2)}\begin{pmatrix} 1 & 0 & -\tilde{a}R_3 \\ 0 & r\sqrt{\frac{1+\tilde{a}^2}{r^2-r_s^2}} & 0 \\ -\frac{\tilde{a}}{R_3} & 0 & 1 \end{pmatrix} \ , \tag{7.63}$$

we find the leading order contribution to the stress-tensor is

$$\begin{aligned}
\langle T^{\bar{t}}_{\ \bar{t}}\rangle_0 &= \frac{\mu\ell}{16\pi G_3(1+\tilde{a}^2)r^3}\left(1 - 2\tilde{a}^2 + \frac{3\tilde{a}^2R_3^2}{x_1^2r^2}\right) \ , \\
\langle T^{\bar{r}}_{\ \bar{r}}\rangle_0 &= \frac{\mu\ell}{16\pi G_3 r^3} \ , \\
\langle T^{\bar{\phi}}_{\ \bar{\phi}}\rangle_0 &= -\frac{\mu\ell}{16\pi G_3(1+\tilde{a}^2)r^3}\left(2 - \tilde{a}^2 + \frac{3\tilde{a}^2R_3^2}{x_1^2r^2}\right) \ , \\
\langle T^{\bar{t}}_{\ \bar{\phi}}\rangle_0 &= \frac{3\mu\ell\tilde{a}R_3}{16\pi G_3(1+\tilde{a}^2)r^3}\left(1 + \frac{\tilde{a}^2R_3^2}{x_1^2r^2}\right) \ , \\
\langle T^{\bar{\phi}}_{\ \bar{t}}\rangle_0 &= \frac{3\mu\ell\tilde{a}}{16\pi G_3(1+\tilde{a}^2)R_3r^3}\left(1 - \frac{R_3^2}{x_1^2r^2}\right) \ ,
\end{aligned} \tag{7.64}$$

where recall r is given in Equation 7.32. In what follows it suffices to only study the stress-tensor to this order and therefore we do not include the cumbersome expressions of $\langle T^{\bar{i}}_{\bar{j}} \rangle$ at higher orders in ℓ. Notice these components are equivalent to the stress-tensor of the CFT in the rotating quantum BTZ black hole upon the simultaneous Wick rotations $\ell_3 \to iR_3$ and $\tilde{a} \to i\tilde{a}$.

For practical purposes, we can view the black hole as being characterized by $R_3, x_1^2, \tilde{a}$ and ℓ. Notably, the mass M in Equation 7.34 and angular momentum J given by Equation 7.35 do not explicitly depend on ℓ, they only depend on ℓ through the renormalized Newton's constant $\mathcal{G}_3$. Moreover, at least with respect to the leading order components of the stress-tensor in Equation 7.64, the parameter ℓ only appears in the overall prefactor. Combining these two observations indicates $\langle T^i_j \rangle_0$ depends on backreaction only through $\mathcal{G}_3$. This is no longer the case at higher orders, however, as can be gleaned from the $\mathcal{O}(\ell^2)$ contributions in Equation 7.62.

In the static case, the quantum SdS black hole given by Equation 7.16, the dependence of the stress-tensor on the mass was entirely captured by a single function $F(M)$ given by Equation 7.17 [219],

$$\langle T^{\bar{i}}_{\bar{j}} \rangle_0^{\text{qSdS}} = \frac{1}{16\pi G_3} \frac{\ell F(M)}{\bar{r}^3} \text{diag}(1, 1, -2) \, . \tag{7.65}$$

Unfortunately this is not possible when rotation is included: the dependence of the stress-tensor on M and J cannot be characterized solely by a single function $F(M, J)$. However, as in [221], we instead identify $F(M, J)$ with the leading contribution at large $\bar{r}$. Precisely, consider $\langle T^{\bar{t}}_{\bar{t}} \rangle_0$ at large r,

$$\langle T^{\bar{t}}_{\bar{t}} \rangle_0 = \frac{\mu \ell}{16\pi G_3 \bar{r}^3} \sqrt{1 + \tilde{a}^2} \eta^3 (1 - 2\tilde{a}^2) + \mathcal{O}(\bar{r}^{-5}) \, , \tag{7.66}$$

where we used $r \approx \bar{r}/\sqrt{1 + \tilde{a}^2}\eta$. We thus define

$$F(M, J) \equiv \mu \eta^3 \sqrt{1 + \tilde{a}^2}(1 - 2\tilde{a}^2) = \frac{8\sqrt{1 + \tilde{a}^2}(1 - 2\tilde{a}^2)}{(3 - x_1^2 + \tilde{a}^2)^3}(1 - x_1^2 - \tilde{a}^2) \, , \tag{7.67}$$

such that for large $\bar{r}$

$$\langle T^{\bar{t}}_{\bar{t}} \rangle_0 \approx \frac{1}{16\pi G_3} \frac{\ell F(M, J)}{\bar{r}^3} \, , \tag{7.68}$$

and similarly for the other components of the stress-tensor in Equation 7.64. Notice $F(M, J)$ will vanish when $\mu = 0$ (i.e., $a^2 = 1 - x_1^2$), the empty dS_3 solution, or when $\tilde{a}^2 = 1/2$, and it reduces to the $F(M)$ in Equation 7.17 for the static solution when $\tilde{a} = 0$.

It is worth repeating there are two perspectives to interpret the solution on the brane and the parameters defining the background. From the bulk viewpoint, the solution is naturally characterized by L_4, ℓ, μ and a. Meanwhile, from the point of view of the brane, the natural quantities parameterizing the solution include the radius R_3 fixing the scale of the brane geometry, cG_3, $\mathcal{G}_3 M$, and $\mathcal{G}_3 J$. The cutoff length of the three-dimensional effective theory is $L_4 = cL_{\rm P}$, such that for large c, this cutoff is much larger than the Planck length, where quantum gravity effects dominate. Thus, the 'quantum' black holes constructed here, as described in the introduction, are much larger than the Planck length. Hence, our solution can be viewed as a valid solution to the problem of semi-classical backreaction.

Comparison to perturbative backreaction

It is illustrative to compare the holographic stress-tensor in Equation 7.64 to the renormalized quantum stress-tensor due to perturbative backreaction of a free conformally coupled scalar field in conical Kerr-dS$_3$. We presented those results in Section 6.1.2, but they are summarized below for convenience:

$$\begin{aligned}
\langle T^t_{\ t}\rangle &= \frac{L_{\rm P}}{8\pi G_3}\sum_{n=1}^{\infty}\frac{1}{r_n^3}\left(A_n + \frac{\tilde{A}_n}{r_n^2}\right)\,,\\
\langle T^r_{\ r}\rangle &= \frac{L_{\rm P}}{16\pi G_3}\sum_{n=1}^{\infty}\frac{c_n}{r_n^3}\,,\\
\langle T^\phi_{\ \phi}\rangle &= -\frac{L_{\rm P}}{8\pi G_3}\sum_{n=1}^{\infty}\frac{1}{r_n^3}\left(B_n + \frac{\tilde{A}_n}{r_n^2}\right)\,,\\
\langle T^t_{\ \phi}\rangle &= -\frac{3R_3 L_{\rm P}}{8\pi G_3}\sum_{n=1}^{\infty}\frac{1}{r_n^3}\left(E_n + \frac{\tilde{E}_n}{r_n^2}\right)\,,\\
\langle T^\phi_{\ t}\rangle &= -\frac{3L_{\rm P}}{8\pi G_3 R_3}\sum_{n=1}^{\infty}\frac{1}{r_n^3}\left(E_n + \frac{F_n}{r_n^2}\right)\,.
\end{aligned} \tag{7.69}$$

Here the denominator $r_n \equiv \sqrt{r^2 d_n^{(1)} + R_3^2 d_n^{(2)}}$ with

$$\begin{aligned}
d_n^{(1)} &= \frac{16}{(\beta_+^2+\beta_-^2)}\left[\sinh^2\left(\frac{n\pi\beta_-}{2}\right) + \sin^2\left(\frac{\pi n\beta_+}{2}\right)\right]\,,\\
d_n^{(2)} &= \frac{4}{(\beta_+^2+\beta_-^2)}\left[\beta_-^2\sin^2\left(\frac{n\pi\beta_+}{2}\right) - \beta_+^2\sinh^2\left(\frac{\pi n\beta_-}{2}\right)\right]\,.
\end{aligned} \tag{7.70}$$

The remaining coefficients $A_n, \tilde{A}_n, c_n$, etc., are cumbersome to write here, but explicitly given in Section 6.1.2 and satisfy $A_n + \frac{c_n}{2} - B_n = 0$. Moreover, the parameters $\beta_+ \equiv 2r_c/R_3$ and

$\beta_- = -8G_3 J/r_c$ are related to the periodicity of coordinates in t and ϕ, respectively, where r_c is the cosmological horizon radius. The infinite sum arises from using the method of images to determine the appropriate Green function solving the scalar equation of motion, where, unlike the Schwarzschild-dS$_3$ case [219], there are a countably infinite number of distinct images.

Comparing to the holographic stress-tensor in Equation 7.64, we notice the tensor components share a similar structure. In particular, coefficients aside, the two sets of tensors have a comparable radial dependence, comparing the $\bar{r}$ dependence in Equation 7.64 and r_n above. Of course, once the infinite sums are performed, the radial dependence in Equation 7.69 is sufficiently more complicated than its holographic counterpart. Likewise, substituting in the explicit expressions of $\beta_\pm$ results in expressions with cumbersome dependence on M and J. This is in contrast to the static case explored in [219], where the radial dependence in either the holographic or perturbative methods was the same, going as $1/\bar{r}^3$ in Equation 7.65. In summary, due to the complicated radial dependence, with non-zero rotation the result of a holographic CFT backreacting on the geometry is far simpler than that of a single conformally coupled scalar field. Indeed, the holographic stress-tensor given by Equation 7.64 is clearly non-singular everywhere outside of the ring singularity at $r = 0$. This is far less obvious looking at the perturbative stress-tensor.

Moreover, the complicated radial dependence in the perturbative backreaction in Equation 7.69 lead to far more complicated quantum corrections to the Kerr-dS$_3$ geometry, a result from solving the three-dimensional semi-classical Einstein equations

$$G_{\mu\nu} + \frac{1}{R_3^2} g_{\mu\nu} = 8\pi G_3 \langle T_{\mu\nu} \rangle \tag{7.71}$$

perturbatively in $L_{\rm P}$. Leaving the details to Appendix 6.1.2, we expand the metric ansatz

$$ds^2 = N(r)^2 f(r) dt^2 + \frac{dr^2}{f(r)} + r^2 (d\theta + k(r) dt)^2 \tag{7.72}$$

to linear order in $L_{\rm P}$ such that

$$N(r) = N_0(r) + L_{\rm P} N_1(r) \ , \quad f(r) = f_0(r) + + L_{\rm P} f_1(r) \ , \quad k(r) = k_0(r) + L_{\rm P} k_1(r) \ . \tag{7.73}$$

At $\mathcal{O}(L_{\rm P}^0)$ we recover the classical Kerr-dS$_3$ geometry, while perturbatively solving the semi-classical Einstein equations yields

$$N_1(r) = \frac{R_3^2}{2(\beta_+^2 + \beta_-^2)} \sum_{n=1}^{\infty} \frac{a_n c_n - 2\beta_+ \beta_- e_n}{b_n r_n^3} \ , \tag{7.74}$$

$$f_1(r) = \sum_{n=1}^{\infty} \frac{4h_n(r)(a_n c_n - 2\beta_+\beta_- e_n) - c_n r_n^4(\beta_+^2+\beta_-^2)^3}{64r^2(\beta_+^2+\beta_-^2)b_n^2 r_n^3} \ , \tag{7.75}$$

$$k_1(r) = -\frac{R_3}{8r^2}\sum_{n=1}^{\infty} \frac{(\beta_+^2-\beta_-^2)e_n + \beta_+\beta_- c_n(c_n-4)}{b_n^2 r_n} \ . \tag{7.76}$$

with coefficients a_n, b_n etc. are presented in Section 6.1.2. Clearly, the terms to linear order in $L_{\rm P}$ are more cumbersome than the quantum corrected geometry due to the holographic stress-tensor. However, $f_1 \sim 1/r$ as $r \to \infty$, i.e. the correction to the blackening factor does resemble the 4D Schwarzschild-like contribution that emerges from the holographic calculations.

7.3 Thermodynamics of quantum Kerr-dS$_3$ black holes

Here we analyze the thermodynamics of the quantum Kerr-dS black hole. As with the geometry, there are two perspectives to view the thermodynamics of the system: the thermodynamics of the classical bulk black hole, and the thermodynamics of the quantum black hole on the brane. Due to the holographic construction, the formulae we derive in either perspective appear the same, however, with conceptually different interpretations. Since the parent solution is well understood, we begin with the thermodynamics of the bulk.

7.3.1 Bulk thermodynamics

The C-metric in Equation 7.20 is known to describe a uniformly accelerating black hole or a pair of such black holes, whose acceleration is mediated by a cosmic string. Since the bulk black hole is accelerating it is natural to wonder whether it is sensible to study the thermodynamics of accelerating black holes. It is worth emphasizing that while the black hole is accelerating, it is nonetheless stationary, having a time-translation Killing symmetry ∂_t. Moreover, the black hole(s) are held fixed at a proper distance away from the acceleration horizon. Consequently, the black hole has a sensible thermodynamic interpretation (see, e.g., [263]), having a well-defined temperature and entropy.

When analyzing the thermodynamics, it is useful to introduce the parameters [221]

$$z \equiv \frac{R_3}{r_i x_1} \ , \quad \nu \equiv \frac{\ell}{R_3} \ , \quad \alpha \equiv \frac{a x_1}{R_3} = \frac{\tilde{a}}{x_1} \ , \tag{7.77}$$

where r_i is a positive real root of the bulk blackening factor $H(r)$, representing each horizon of braneworld black hole. We can express x_1, μ and r_i solely in terms of these parameters,

$$\begin{aligned} x_1^2 &= \frac{1+\nu z^3}{z^2[1+\nu z+\alpha^2 z(z+\nu)]}\,, \\ r_i^2 &= R_3^2\frac{1+\nu z+\alpha^2 z(z+\nu)}{1+\nu z^3}\,, \\ \mu x_1 &= \frac{(z^2-1)(1+\alpha^2(1+z^2))}{1+\nu z^3}\,. \end{aligned} \tag{7.78}$$

The first expression is found by solving $H(r_i)=0$ for x_1^2, from which the other two relations readily follow. Moreover, the bare and renormalized Newton's constants are

$$G_4 = 2L_4 G_3 = \frac{2G_3\ell}{\sqrt{1-\nu^2}}\,, \quad \mathcal{G}_3 = \frac{L_4}{\ell}G_3 = \frac{G_3}{\sqrt{1-\nu^2}}\,. \tag{7.79}$$

The limit of vanishing backreaction now coincides with small ν, and we take $\nu^2<1$, which guarantees the bulk is asymptotically AdS_4. Using the parameters in Equation 7.78, we can recast the mass M in Equation 7.34 and angular momentum J in Equation 7.35

$$M = \frac{1}{8G_3}\sqrt{1-\nu^2}\frac{(z^2-1)[1+\alpha^2(1+z^2)][9z^2-1+8\nu z^3+\alpha^2(9z^4-1+8\nu z^3)]}{(3z^2-1+2\nu z^3+\alpha^2(1+4\nu z^3+3z^4))^2}\,, \tag{7.80}$$

$$J = \frac{\alpha R_3}{G_3}\sqrt{1-\nu^2}\frac{z(z^2-1)[1+\alpha^2(1+z^2)]\sqrt{(1+\nu z^3)(1+\nu z+\alpha^2 z(z+\nu))}}{(3z^2-1+2\nu z^3+\alpha^2(1+4\nu z^3+3z^4))^2}\,. \tag{7.81}$$

As described in the previous section, the canonically normalized Killing vector $\bar{\zeta}^b = \partial_{\bar{t}}^b + \Omega_i \partial_{\bar{\phi}}$ in Equation 7.42 generates rotating horizons at the positive roots r_i with rotation Ω_i given by Equation 7.41, now expressed as

$$\Omega_i = \frac{\alpha}{R_3}\frac{(z^2-1)\sqrt{(1+\nu z^3)(1+\nu z+\alpha^2 z(z+\nu))}}{z(1+\nu z)(1+\alpha^2(1+z^2))}\,. \tag{7.82}$$

Additionally, the surface gravity κ_i in Equation 7.43 relative to $\bar{\zeta}^b$ yields a temperature $T_i = \kappa_i/2\pi$,

$$T_i = \frac{1}{2\pi R_3}\frac{(z^2(1+\nu z)+\alpha^2(1+2\nu z^3+z^4))|(2+3\nu z-\nu z^3+\alpha^2(4z^2+\nu z(z^4+3)))|}{z(1+\nu z)(1+\alpha^2(1+z^2))(3z^2-1+2\nu z^3+\alpha^2(1+3z^4+4\nu z^3))}\,. \tag{7.83}$$

We will deal with absolute value more carefully in the next section.

Lastly, the bulk horizon entropy is given by the Bekenstein-Hawking area formula

$$\begin{aligned} S^{(4)}_{\rm BH} &= \frac{\text{Area}(r_i)}{4G_4} = \frac{2}{4G_4}\int_0^{2\pi} d\bar{\phi}\int_0^{x_1} dx \frac{r_i^2\ell^2}{(\ell+r_i x)^2}\eta\left(1+\frac{a^2x_1^2}{r_i^2}\right) \\ &= \frac{\pi}{G_4}\frac{\eta\ell x_1(r_i^2+a^2x_1^2)}{(\ell+r_i x_1)} \\ &= \frac{\pi R_3}{G_3}\frac{\sqrt{1-\nu^2}z(1+\alpha^2(1+z^2))}{(3z^2-1+2\nu z^3+\alpha^2(1+3z^4+4\nu z^3))} \ . \end{aligned} \tag{7.84}$$

Altogether, the mass, angular momentum, angular velocity, temperature and entropy constitute the thermodynamics of the rotating AdS_4 bulk black hole. In the $\alpha = 0$ limit, one recovers the thermodynamics of the static AdS_4 bulk [219]. One may derive the bulk thermodynamics using a canonical partition function by evaluating the on-shell bulk gravity action via an appropriate modification of the presentation given in [281]. Additionally, by explicit computation it is straightforward to verify

$$\partial_z M - T_i\partial_z S^{(4)}_{\rm BH} - \Omega_i\partial_z J = 0 \ , \quad \partial_\alpha M - T_i\partial_\alpha S^{(4)}_{\rm BH} - \Omega_i\partial_\alpha J = 0 \ , \tag{7.85}$$

such that the bulk system obeys the first law

$$dM = T_i dS^{(4)}_{\rm BH} + \Omega_i dJ \ , \tag{7.86}$$

for all values of the parameters, including any value of the brane tension, as controlled by ν.

7.3.2 Semi-classical thermodynamics on the brane

From the brane perspective, the thermodynamics of the classical bulk system doubles as the thermodynamics of the quantum de Sitter black hole. It is worth mentioning that, even without accounting for backreaction, de Sitter thermodynamics is more subtle than their flat or AdS space counterparts. Firstly, this is because de Sitter space lacks an asymptotic region to introduce boundary conditions which fix thermoodynamic data to define a thermal ensemble. Moreover, the first law of cosmological horizons [268] comes with a minus sign which begs how the thermodynamics of the dS static patch should be understood. In what follows, we ignore these subtleties, though it would be interesting to return to them in the future, adapting the quasi-local approach developed in [282, 283] (see also [284, 285]). These approaches derive the first law of thermodynamics for de Sitter horizons by using an auxiliary non-dynamical "York"

boundary to specify the appropriate thermodynamic ensemble. This is in principle straightforward on the brane, although it is not obvious what the dual description of such a boundary in the bulk is. One can expect it to be some co-dimension 2 surface in AdS that induces the appropriate co-dimension 1 boundary term on the brane, but how to choose it remains unclear at this stage. The biggest complication, however, is to extend the quasi-local approach to spacetimes solving higher-curvature theories of gravity – a possible route is to make use of the covariant phase-space formalism which has been successful in generalising the horizon entropy formula for higher-derivative Lagrangians [286].

Thermodynamics with multiple horizons

The quantum de Sitter black hole comes with three horizons which are generally at different temperatures. Consequently, each horizon generally has its own thermodynamics, satisfying its own first laws, as we now show. The mass, angular momentum, and angular velocity given by Equations 7.80, 7.81, 7.82 of the quantum black hole all take the same form in terms of parameters in Equation 7.77. The temperature in Equation 7.83 encodes the temperature of each horizon of the quantum black hole, where we remind the reader the outer and inner black hole horizons correspond to the outer and inner bulk black hole horizons localized on the brane, while the cosmological horizon arises from the bulk acceleration horizon intersecting the brane. To distinguish each horizon, it is useful to slightly modify the notation for z via $z_c = R_3/r_c x_1$ and $z_\pm = R_3/r_\pm x_1$ to denote the cosmological and black hole horizons, respectively. Then, from the surface gravities given by Equation 7.44

$$T_c = T_i(z_c)\ , \quad T_+ = -T_i(z_+)\ , \quad T_- = T_i(z_-)\ , \tag{7.87}$$

where we used $r_- < r_+ < r_c$ such that $z_- > z_+ > z_c$. Consequently, the black hole horizon is generally hotter than the cosmological horizon, $T_c < T_+$, such that the system is not in thermal equilibrium; an observer located between the cosmological and (outer) black hole horizon is in a system characterized by two temperatures. There are three special cases, where the horizons degenerate, when the outer black hole and cosmological horizons are in thermal equilibrium, as we explore below.

The most notable difference between the bulk and brane black hole thermodynamics is the interpretation of the entropy given by Equation 7.84. On the brane, this entropy $S^{(4)}_{\rm BH}$ is equal

to the sum of gravitational entropy and the entanglement entropy of the holographic CFT [221]. Thus, the bulk entropy is identified with the generalized entropy on the brane $S^{(3)}_{\text{gen}}$,

$$S^{(4)}_{\text{BH}} = S^{(3)}_{\text{gen}} = S^{(3)}_{\text{grav}} + S^{(3)}_{\text{CFT}} \, . \tag{7.88}$$

This relation is exact to all orders in semi-classical backreaction codified by ν. The gravitational entropy is computed using Wald's entropy functional [286],

$$S_{\text{Wald}} = -2\pi \int_{\mathcal{H}} dA \frac{\partial \mathcal{L}}{\partial R^{abcd}} \epsilon_{ab}\epsilon_{cd} \, , \tag{7.89}$$

where $dA = d^{d-2}x\sqrt{q}$ is the codimension-2 area element of the bifurcate horizon $\mathcal{H}$, with $q_{ab} = h_{ab} + n_a n_b - u_a u_b$ being the induced metric, for spacelike and timelike unit normals n_a and u_a, respectively. The binormal $\epsilon_{ab} = (n_a u_b - n_b u_a)$ satisfies $\epsilon^2 = -1$, and we define $(d-1)$-dimensional metric in directions orthogonal to the horizon. Moreover, $\mathcal{L}$ refers to the Lagrangian density defining the theory. With respect to the induced theory of gravity on the brane given by Equation 7.18, the gravitational entropy is

$$S^{(3)}_{\text{grav}} = \frac{1}{4G_3} \int_{\mathcal{H}} dx\sqrt{q} \left[1 + \ell^2 \left(\frac{3}{4}R - g^{ab}_{\perp} R_{ab} \right) + \mathcal{O}(\ell^4/R_3^6) \right] \, . \tag{7.90}$$

We see higher-curvature corrections to entropy enter at order ℓ^2, such that the dominant contribution to the entropy at leading order in backreaction is the three-dimensional Bekenstein-Hawking entropy

$$S^{(3)}_{\text{BH}} = \frac{1}{4G_3} \int_{\mathcal{H}} dx\sqrt{q} = \frac{2\pi r_i \eta}{4G_3} \left(1 + \frac{a^2 x_1^2}{r_i^2} \right) = \frac{1+\nu z}{\sqrt{1-\nu^2}} S^{(3)}_{\text{gen}} \, . \tag{7.91}$$

Therefore, the Bekenstein-Hawking entropy includes semi-classical backreaction effects.

Formally, the matter entropy $S^{(3)}_{\text{CFT}}$ is given by the difference

$$S^{(3)}_{\text{CFT}} = S^{(3)}_{\text{gen}} - S^{(3)}_{\text{grav}} \, . \tag{7.92}$$

Notably, the matter entropy enters at linear order in ν,

$$S^{(3)}_{\text{CFT}} \approx S^{(3)}_{\text{gen}} - S^{(3)}_{\text{BH}} = -\nu z S^{(3)}_{\text{BH}} \, , \tag{7.93}$$

in contrast with the higher-curvature contributions to the gravitational entropy which enter at order ν^2. Recall that the central charge $c = L_4^2/G_4 \approx \nu R_3/2G_3$, such that $S^{(3)}_{\text{CFT}}$ is proportional

to c. As in the quantum BTZ case [221], generally the matter entropy will be dominated by entanglement across the horizon(s) in CFT states with large Casimir effects.

Interpreting $S^{(4)}_{\rm BH}$ as the generalized entropy of the quantum black hole, the bulk first law in Equation 7.86 leads to a semi-classical first law for each horizon

$$dM = T_+ dS^{(3)}_{\text{gen},+} + \Omega_+ dJ \ , \tag{7.94}$$

$$dM = -T_c dS^{(3)}_{\text{gen},c} + \Omega_c dJ \ , \tag{7.95}$$

$$dM = -T_- dS^{(3)}_{\text{gen},-} + \Omega_- dJ \ , \tag{7.96}$$

where $\Omega_c = \Omega_i(z_c)$ and $\Omega_\pm = \Omega_i(z_\pm)$ are the angular speeds of the cosmological and black hole horizons. Combining the first two first laws yields

$$0 = T_+ dS^{(3)}_{\rm gen} + T_c dS^{(3)}_{\rm gen} + (\Omega_+ - \Omega_-) dJ \ . \tag{7.97}$$

Our first law is consistent with the semi-classical first laws for static two-dimensional (A)dS black holes in [284, 287]. Notice the minus sign in the first law of the cosmological horizon remains even in the quantum-backreacted geometry. Consequently, adding positive energy into the static patch reduces the total entropy of the system, with the entropy of pure dS being maximal, such that de Sitter black holes behave as instantons constraining the states of the original de Sitter degrees of freedom (cf. [288, 289, 290]).

At this stage, there are two limits of interest. The first is the quantum de Sitter limit, at $z = 1$ or $\mu = 0$, and, consequently,

$$M = J = \Omega_i = 0 \ , \tag{7.98}$$

$$S^{(3)}_{\rm gen} = \frac{2\pi R_3}{4G_3} \frac{\sqrt{1-\nu^2}}{1+\nu} \ , \quad T_c = \frac{1}{2\pi R_3} \ , \tag{7.99}$$

where we see the temperature of the quantum dS_3 cosmological horizon is the same as classical

dS_3. Second, when backreaction vanishes $\nu \to 0$, then $z_\pm \to \infty$ since $r_\pm \to 0$ and we have

$$\begin{aligned}
M &= \frac{1}{8G_3}\frac{(z^2-1)(1+\alpha^2(1+z^2))(9z^2-1+\alpha^2(9z^4-1))}{(3z^2-1+\alpha^2(1+3z^4))^2}\,, \\
J &= \frac{\alpha R_3}{G_3}\frac{z(z^2-1)(1+\alpha^2(1+z^2))\sqrt{1+\alpha^2 z^2}}{(3z^2-1+\alpha^2(1+3z^4))^2}\,, \\
\Omega_c &= \frac{\alpha(z^2-1)\sqrt{1+\alpha^2 z^2}}{R_3 z(1+\alpha^2(1+z^2))}\,, \\
T_c &= \frac{1}{2\pi R_3}\frac{2(1+2\alpha^2 z^2)(z^2+\alpha^2(1+z^4))}{z(3z^2-1+\alpha^2(1+3z^4))(1+\alpha^2(1+z^2))}\,, \\
S_c &= \frac{\pi R_3}{G_3}\frac{z(1+\alpha^2(1+z^2))}{(3z^2-1+\alpha^2(1+3z^4))}\,,
\end{aligned} \tag{7.100}$$

where it is understood that here $z = z_c$. It is straightforward to show the resulting thermodynamics reproduces that of the classical Kerr-dS_3 (see Section 6.1.1), namely,

$$S^{(3)}_{\text{gen}}|_{\nu=0} = \frac{\pi R_3}{4G_3}\left(\sqrt{(1-8G_3M)+i\frac{8G_3J}{R_3}}+\sqrt{(1-8G_3M)-i\frac{8G_3J}{R_3}}\right) = S_{\text{KdS}_3}\,, \tag{7.101}$$

where we used the relation $\sqrt{x+iy}+\sqrt{x-iy} = 2\sqrt{x+\sqrt{x^2+y^2}}/\sqrt{2}$.

Thermodynamics of degenerate horizons

As described in Section 7.2, the quantum Kerr black hole has special limits where two or more horizons become degenerate. Of interest are the extremal ($r_+ = r_-$), Nariai ($r_c = r_+$), and lukewarm ($T_c = T_+$) geometries. The extremal black hole is one with a vanishing temperature, $T_{\text{ext}} = 0$. Naively, the Nariai black hole will have a vanishing temperature, however, in its near horizon geometry, the temperature of the black hole and cosmological horizon will be in thermal equilibrium at a non-zero temperature T_{N}. The precise form of the temperature can be found, for example, by removing the conical singularity in the Euclideanized section of the (naive) Nariai geometry in Equation 7.53, given via the Wick rotation $\hat{\tau} \to i\hat{\tau}_E$ and $a \to ia_E$, resulting in $T_{\text{N}} = (2\pi\sqrt{\Gamma})^{-1}$.

To connect to the canonical geometry, we relate the Nariai radii r_{N} and $\bar{r}_{\text{N}}$ via Equation 7.32. Lastly, the lukewarm limit occurs when the outer black hole and cosmological horizons are in thermal equilibrium at a temperature different from the Nariai temperature. Though the resulting expression is cumbersome and not very illustrative, the precise temperature can be solved for explicitly by setting $T_+ = T_c$ (using the surface gravities in Equation 7.44) and

following the method described in Appendix C. The lukewarm temperature is proportional to $(r_c - r_+)/2\pi R_3^2$, with $r_c \neq r_+$.

7.4 Summary of the main results

In this chapter we used braneworld holography to construct a three-dimensional quantum-corrected Kerr-de Sitter black hole exactly accounting for backreaction effects due to a conformal field theory. By stark contrast, there are no de Sitter black holes in three-dimensions, only conical defect geometries with a single cosmological horizon. Thus, semi-classical backreaction alters the defect geometry so as to induce inner and outer black hole horizons, which hide a ring singularity, sharing many qualitative features with the classical four-dimensional Kerr-de Sitter solution. With three horizons, we uncovered the extremal, Nariai, and 'ultracold' limits of the semi-classical black hole, which appear as fibered products of a circle and AdS_2, dS_2, or two-dimensional Minkowski space, respectively.

Moreover, the thermodynamics of the classical bulk black hole, described by the rotating AdS_4 C-metric, has a dual interpretation on the brane as thermodynamics of the semi-classical Kerr-dS_3 black hole. Specifically, the standard first law of thermodynamics in the bulk becomes a semi-classical first law, where the four-dimensional Bekenstein-Hawking area-entropy is identified with the three-dimensional generalized entropy, given by the sum of the Wald entropy due to higher curvature corrections, and the matter entropy of the CFT. In essence, we have derived the semi-classical generalization of the first law of cosmological horizons of Gibbons and Hawking [268]. As in the classical four-dimensional Kerr-dS solution, the limiting geometries of the quantum Kerr-dS black hole give rise to scenarios of thermal equilibrium, including the Nariai and lukewarm limits where the temperatures of the cosmological and outer black hole horizons coincide. Therefore, quantum-corrections greatly enrich the thermodynamic structure of three-dimensional de Sitter solutions.

Part III

Closing remarks

Chapter 8

Closing Remarks

In this thesis, we have discussed two parallel approaches to the problem of backreaction of quantum degrees of freedom on classical ones. The first one, CQ dynamics, assumes fundamental classicality of the classical degree of freedom in the model – an assumption that requires any such physical system to feature both diffusion and decoherence effects. However, the scope of the hybrid formalism is transversal –it can be used to describe any model of classical-quantum interaction both as a fundamental and effective level. In this thesis, we mainly focused on the application of CQ ideas on the problem of gravitational backreaction, in order to explore the recent proposal of a consistent theory of fundamentally classical gravity. The second approach we discussed – braneworld holography – is instead a novel method that can be used to compute the backreaction of quantum fields on an effectively classical geometry using the AdS/CFT correspondence.

8.1 Summary of the main results

We now briefly summarise the main results presented in the thesis, before discussing natural extensions to the work and long-term objectives for both research directions.

CQ steady state

In Chapter 3 we studied a simple system of coupled classical-quantum oscillators with classical friction. We showed that the CQ evolution flows to a unique steady state by relying on standard

results in the theory of stochastic processes, and computed the two-point functions with respect to such a hybrid state. We showed that the steady state becomes thermal in the high-diffusion regime. We also derived the phase-space representation of CQ dynamics by performing the Wigner-Moyal transform of the hybrid generator. We showed that for harmonic potentials the dynamics exactly maps to a Fokker-Planck equation with diffusion in both the classical and quantum phase-space.

Stochastic gravity

In Chapter 4 we studied the classical stochastic Klein-Gordon equation to understand the potential phenomenology of linearised CQ gravity. We showed how to regularise the divergences in the Fourier-space integrals for the two-point function of the stochastic field. We used them to compute the non-equilibrium covariances for the field and compared them with the standard thermal Klein-Gordon results. We concluded by discussing the issue of infinite energy production and that a stochastic scalar can induce large forces on test particles. If these results hold up when considering a spin-2 massless field (rather than the spin-0 model we considered), CQ gravity would risk of running afoul of experiments.

In Chapter 5 we similarly studied the effects of a stochastic driving term in the cosmological FLRW equations. We discovered that, whilst a time reparametrisation-invariant stochastic model can be constructed, the dynamics naturally breaks the Hamiltonian constraints of General Relativity in an inflationary epoch. In the later stages of radiation-domination and matter-domination, the stochasticity decouples from the evolution of the scale factor and we would be left with a positive on average amount of constraint violation. We showed that such a constraint violation, in the current cosmological era, would have the same effect as cold dark matter.

Quantum rotating black hole in dS_3

In Chapter 7 we used braneworld holography to uncover a novel solution to the (higher-curvature) semiclassical Einstein's equations. We found that backreaction on the (2+1)-dimensional rotating conical defect in de Sitter space induces two black-hole horizons – one inner and one outer, much like the 4-dimensional Kerr black hole. This quantum Kerr-de Sitter black hole has a ring-singularity and an ergoregion. We derived the generalised laws of black hole mechanics

for the system, including higher-curvature corrections and contribution due to the backreacting matter. We compared our exact result with the perturbative solutions to the standard semiclassical Einstein's equation, with the source being a single conformally coupled scalar.

8.2 Outlook

8.2.1 Oscillators and CQ thermodynamics

The main novel result in Chapter 3 is that classical friction can be enough for minimal hybrid system to reach a steady state, even though it might not be an equilibrium state in general. Whilst thermal states in CQ models have been recently studied in detail [162], much can still be said on non-equilibrium states. In particular, the hybrid oscillator would be a good toy model to study properties of hybrid systems that do not satisfy detailed balance. A first objective would be to derive the generalised fluctuation relations for CQ non-equilibrium thermodynamics and compute the entropy production in the system [291].

Both classical and quantum thermal equilibrium and the fluctuation-dissipation relations can be shown to be associated with particular symmetries of the respective path-integral actions. A key step towards a complete understanding of CQ thermodynamics would be to show that such an equivalence exists for hybrid systems as well, deriving the fluctuation-dissipation relations from first principles in the process [292]. Another interesting avenue would be to make contact between quantum and hybrid thermodynamics, deriving the latter as a special case of the former – possibly integrating out some environment a la Caldera-Leggett [293].

8.2.2 Field theory

The results of Chapter 4 pave the way for a more rigorous exploration of CQ field theory, which can take many interesting directions.

Linearised CQ gravity: A natural one is to go beyond stochastic scalar fields, and study a CQ model of a classical spin-2 field interacting with quantum matter – i.e. the full linearised CQ gravity. This necessarily requires, however, the understanding of covariance in stochastic processes. Developing such a model is a crucial step in the formulation of a fundamental CQ

theory of gravity, with obvious applications to the theory of cosmological perturbations. The derivation of CQ predictions for the cosmic microwave background and gravitational wave background would be obvious objectives. They would provide formidable tests for hybrid theories of gravity – and possibly assess the proposal that stochastic fluctuations in the gravitational field can act as cold dark matter [3, 209].

CQ renormalisation: Another natural direction is to study the renormalisation properties of the CQ scalar Yukawa theory. The path-integral formulation of CQ gravity is expected to be free of the renormalisation issues that plague Einstein's gravity due to the analogies with the quadratic gravity action[136], whose quantum theory is known to be renormalisable [294]. Nonetheless, no explicit renormalisation analysis has ever been performed on a CQ field theory – the scalar Yukawa model seems the ideal playground to approach the problem by building on known results for classical statistical field theory and open QFT [295, 184]. A fundamental question is whether the renormalisation group can preserve the decoherence-diffusion trade-off, the crucial consistency condition of CQ theories. Moreover, as we discussed at length when estimating the induced forces from the classical stochastic fluctuations on extended object, it is important to address whether self-interaction vertices (either from non-linearities in the classical equations or induced from quantum backreaction) can indeed curb the irregularity of the free stochastic wave equation – inspired by some existing formal results [176, 189].

CQ field theory as effective: Finally, CQ theories have been shown to emerge as effective theories when the partial classical limit of a bipartite quantum system [78, 296] is taken. Extending this result to the case of field theories is crucial to understand better the regime of validity of the semiclassical Einstein's equations [68, 66], and of CQ models as *effective* theories of semiclassical gravity. This is in the spirit of including both decoherence and diffusion effects, going beyond the stochastic corrections to the semiclassical Eisntein's equations that are considered in the formalism of stochastic gravity [80].

8.2.3 CQ Cosmology

In Chapter 5 we explored the cosmological implications of a potential fundamental classicality of the gravitational field. Many fundamental questions on CQ gravity arose in the process, indicating natural future steps for investigations on CQ gravity and cosmology.

Diffeomorphisms and constraints in CQ: The model presented in Chapter 5 allows for the violation of the constraints of general relativity. As mentioned in the introduction, constraints are a necessary condition for covariance in the deterministic theory. In the Hamiltonian ADM formulation, they are required for the series of three-dimensional spatial geometries to be embeddable into a (3+1)-dimensional spacetime. However, in a stochastic theory the role of constraints is more subtle and their violation should not be taken to indicate loss of covariance, but rather that the constraint was formulated ignoring the existence of the stochastic field. Indeed, the two approaches typically used to derive constraints [134, 133] in the deterministic theory fail here. The Dirac procedure is not applicable as the Hamiltonian is not the generator of the dynamics, a point already made in [207]. The expectation is that the concept of the constraint needs modifying for random systems, similarly to what happens for Noether's theorem [297, 298, 299]. Moreover, deriving the constraints by demanding that the hypersurface deformation algebra closes [133], yields no constraints in minisuperspace since the algebra is trivial. Of course, the situation is more complex when considering the full local theory, as discussed in [207]. Our construction is indeed valid only as a description within a preferred frame, the cosmological one, since spacetime looks homogeneous and isotropic only within a specific set of coordinates. These, adapted to the symmetries of the problem, are effectively provided by the perfect fluid sourcing the geometry. It is only in these coordinates that we can identify a consistent low-noise regime on late-time spatial hypersurfaces. On a different, arbitrary, foliation of spacetime, the homogeneous description breaks down and a more refined analysis is needed.

An interesting playground for such an exploration is the so-called second order differential geometry [300], a coordinate invariant formulation of stochastic processes on manifolds that has been shown to be useful in characterising global charges in random processes. It would be interesting to approach the problem of constraints taking inspiration from the geometric perspective given by the covariant phase-space formalism [301].

Cosmological tests on the quantumness of spacetime This work sets the basis for the study of the cosmological consequences of theories where gravity is classical and, therefore, fundamentally stochastic. The main objective of this line of work is to try to establish predictions that may help test such theories in the near future, possibly proving observationally

the necessity of quantising the gravitational theory. CQ theories of gravity predict that the amount of diffusion in the gravitational system is lower-bounded by the typical decoherence rate of superposition in the quantum matter degrees of freedom. As explored in detail in [65], table-top experiments can lower-bound the diffusion in the metric and squeeze the theory from both sides. Here, we find that cosmological measurements can also provide easily accessible data that can also constrain the amount of diffusion allowed, on a very different scale. When integrated over long times, the stochastic force can cause the gravitational system to diverge significantly from its deterministic trajectory. In particular, we have seen that if CDM can be understood by the mechanism presented in its article, its abundance would be entirely fixed by the parameters of the early-Universe model.

A key step towards using cosmological data to constrain the value of the diffusion coefficient in stochastic theories of gravity is studying the inhomogeneous evolution. This is key to reconstruct clear predictions for the observed Universe and especially the CMB; we know the separate-universe approximation is not really self-consistent, since the shrinking horizon during inflation partitions the universe into multiple causally-disconnected regions. The resulting inhomogeneous modes will re-enter the horizon following reheating, and their subsequent evolution can only be handled via an inhomogeneous calculation. Furthermore, whilst the homogeneous noise at late times goes to zero, locally the dynamics is still stochastic, meaning that late-time evolution might still differ from standard deterministic calculations. Altogether, moving away from the homogeneous model is fundamental in order to extract the power spectrum of the perturbations imprinted on the CMB that the stochastic theory predicts. This will ultimately provide a powerful stress-test for CQ theories of gravity, since there is a plethora of strong observational constraints that the stochastic theory will have to reproduce [149].

8.2.4 Comparison with other models of stochastic gravity

The motivation behind the models in Chapters 4 and 5 is that stochasticity in the classical gravitational degrees of freedom is a necessary consequence of a theory that describes classical and quantum systems with non-trivial interaction in a consistent manner. In particular, it follows once the physical requirements of complete positivity, trace preservation and linearity are imposed at the level of the master equation, which is the evolution equation of the hybrid

state [50, 51]. While this specific motivation has emerged over the past few years, having some randomness in the evolution equations for the gravitational field is not a new proposal, with stochastic evolution equations put forward mainly as effective theories. Here we give a brief overview of some of these approaches and how they differ from our analysis.

Cosmetically, the closest approach to our own comes from the formalism of "stochastic gravity" [80]. Its objective is to include quantum fluctuations when calculating backreaction effects in semiclassical gravity. In stochastic gravity, the stochastic tensor $\xi_{\mu\nu}$ represents the quantum fluctuations of the field that sources the metric and is therefore not a fundamental white noise process. Indeed, the moments of the random field match those of the stress energy tensor of the QFT. Stochastic gravity is governed by the Einstein-Langevin equations

$$G_{\mu\nu} = 8\pi G \left(\langle T_{\mu\nu} \rangle + \xi_{\mu\nu} \right), \tag{8.1}$$

and aims to include corrections to the semiclassical Einstein's equations, with which it partially shares the regime of validity (i.e. when the fluctuation in the stress-energy tensor of the quantum system are small with respect to the mean). This condition is commonly probed by the Kuo-Ford criterion [66]. Indeed, even though stochastic gravity can improve on the semiclassical Einstein's equation by including both the quantum fluctuations of the matter fields and the induced one of the gravitational field [68], the expectation value in Equation 8.1 leads to a breakdown in causality unless the theory is modified in some way [302, 303] due to the non-linearity in the density matrix, much like in the standard semiclassical Einstein's equations. As such, stochastic gravity can only be treated as an effective theory. This is also true for the other proposals of stochastic theories of gravity that modify Einstein's equations by adding a random gravitational constant G instead [304, 305].

Causal set theory and unimodular gravity also motivate some models of effective spacetime diffusion. In the everpresent Lambda proposal [196], the stochasticity in the cosmological constant comes from the causal set interpretation of Λ being the conjugate variable to the local spacetime volume, a stochastic variable. In unimodular gravity (often considered the continuum limit of causal set theory) the motivation of having a stochastic evolution of spacetime comes from violation of the conservation of the matter stress-energy tensor instead, which is allowed by the theory [197, 198].

8.3 Braneworld

The braneworld construction we outlined in chapters 6 and 7 is versatile and can used in a variety of future studies. Some of them are listed below.

Other three-dimensional quantum black holes: Here we focused on neutral rotating quantum de Sitter black holes. It is natural to ask whether other types of three-dimensional quantum black holes are possible using a similar braneworld construction. Recently, a charged quantum BTZ solution in has been found [250], and we have extended the results to the case of a charged de Sitter black hole, simply by starting from the charged AdS_4 C-metric. Although there is no need for counterterms for the Maxwell field in AdS_4 [109, 306], a Maxwell action is nevertheless generated on a brane at finite distance in the bulk, further modifying the geometry of the quantum black hole [307]. Similarly, starting from the accelerating Taub-NUT AdS_4 black hole, one would conceivably find a quantum Taub-NUT black hole on the brane. Altogether, via suitable modifications to the AdS_4 C-metric, one could develop a catalog of charged, rotating, Taub-NUT quantum (A)dS black holes in three-dimensions.

A further generalization would be to consider quantum black holes with scalar hair. One way to do this is to consider bulk Einstein gravity in addition to a conformally coupled scalar field. Black hole solutions to this theory have a rich history, dating back to Bekenstein [308, 309], including exact generalizations of the charged C-metric [310] and Plebanski-Demianski family of metrics [311].

Higher dimensional quantum black holes: The quantum Kerr-dS_3 black hole is another example of an exact description of a localized three-dimensional black hole in a Randall-Sundrum braneworld, belonging to the class of the solutions uncovered in [220, 219] (see also [312], where the brane tension was detuned from the bulk acceleration). It is natural to wonder whether one can construct higher-dimensional quantum black holes in a similar fashion. Extrapolating from the four-dimensional bulk models, holographic considerations predict backreaction due to conformal fields is expected to similarly induce quantum corrections to the geometry. For example, a semi-classical four-dimensional brane black hole would include a $\ell\mu/r^2$ correction to the standard $1/r$ gravitational potential, a behavior inherited from its parent AdS_5 black hole.

Thus far, however, there are no known exact quantum black holes in higher dimensions. This

is because finding static brane localized black holes in higher dimensions has proven challenging, both analytically and numerically (for a review, see [251]). The essential feature of the four-dimensional C-metric which is exploited is that there is a natural location to place the brane, at $x = 0$, where the Israel-junction conditions are automatically satisfied. A higher-dimensional analog of the C-metric exuding this feature is not known to exist [313], making the construction of exact quantum black holes difficult. Perhaps numerical techniques together with the large-D approximation of bulk Einstein gravity, as was recently accomplished to describe evaporating brane black holes [259], can be adapted to construct exact quantum black holes in higher-dimensions.

8.4 Closing remarks

The problem of backreaction of quantum matter on a classical spacetime has a rich history. It had the virtue of highlighting many conceptual subtleties that were originally overlooked – from what part of the quantum stress-tensor actually gravitates, to the possibility of coupling consistently classical and quantum degrees of freedom. In this thesis, we have presented two modern outlooks on the problem, albeit coming from largely different motivations and technical tools. Both promise to enrich our understanding of classical-quantum interaction, in gravitational physics and beyond. Braneworlds have the potential of allowing us to explore quantum corrections to classical solutions to GR without resorting to numerical analysis or perturbative solutions. On the other hand, CQ offers an appealing route to test the quantum nature of the gravitational field not by measuring directly subtle quantum effects – but by contradiction. Studying theories of fundamentally classical gravity interacting with quantum matter can allow us to understand how to test the decoherence-diffusion trade-off, a key requirement for spacetime not to be quantum mechanical.

Even though the starting point are vastly different, braneworlds and CQ do not need to be perpendicular approaches. In fact, CQ provides a completion of the standard semiclassical toolkit even for effective theories. Whilst in that case the decoherence-diffusion trade-off does not need to hold, in principle a semiclassical model should include both decoherence and diffusion effects, especially due to the coarse-graining that is performed on the "classical" system.

Holography has historically been about unitary quantum theories, but in recent years decoherence, open evolution and measurements have been discussed (e.g. [314, 315, 316]). It would be interesting to explore whether the semiclassical limit of the AdS/CFT correspondence can be made to account explicitly for these effects.

Bibliography

[1] Emanuele Panella. Classical-quantum oscillators as diffusive processes in phase space. 2025.

[2] Jonathan Oppenheim and Emanuele Panella. Diffusion in the stochastic klein-gordon equation. 2025.

[3] Jonathan Oppenheim, Emanuele Panella, and Andrew Pontzen. Emergence of phantom cold dark matter from spacetime diffusion, 2024. URL https://arxiv.org/abs/2407.13820.

[4] Emanuele Panella, Juan F. Pedraza, and Andrew Svesko. Three-dimensional quantum black holes: a primer. 7 2024.

[5] Emanuele Panella and Andrew Svesko. Quantum kerr-de sitter black holes in three dimensions. *Journal of High Energy Physics*, 2023(6), June 2023. ISSN 1029-8479. doi:10.1007/jhep06(2023)127. URL http://dx.doi.org/10.1007/JHEP06(2023)127.

[6] Ana Climent, Robie A. Hennigar, Emanuele Panella, and Andrew Svesko. Nucleation of charged quantum de-sitter$_3$ black holes, 2024. URL https://arxiv.org/abs/2410.02375.

[7] Emma Albertini, Arad Nasiri, and Emanuele Panella. Stochastic dark matter: Covariant Brownian motion from Planckian discreteness. *Phys. Rev. D*, 111(2):023514, 2025. doi:10.1103/PhysRevD.111.023514.

[8] John C. Tully. Molecular dynamics with electronic transitions. *The Journal of Chemical*

Physics, 93(2):1061–1071, 07 1990. ISSN 0021-9606. doi:10.1063/1.459170. URL https://doi.org/10.1063/1.459170.

[9] John C. Tully. Mixed quantum–classical dynamics. *Faraday Discuss.*, 110:407–419, 1998. doi:10.1039/A801824C. URL http://dx.doi.org/10.1039/A801824C.

[10] Seth Lloyd. Coherent quantum feedback. *Phys. Rev. A*, 62:022108, Jul 2000. doi:10.1103/PhysRevA.62.022108. URL https://link.aps.org/doi/10.1103/PhysRevA.62.022108.

[11] Björn Annby-Andersson, Faraj Bakhshinezhad, Debankur Bhattacharyya, Guilherme De Sousa, Christopher Jarzynski, Peter Samuelsson, and Patrick P. Potts. Quantum fokker-planck master equation for continuous feedback control. *Physical Review Letters*, 129(5), July 2022. ISSN 1079-7114. doi:10.1103/physrevlett.129.050401. URL http://dx.doi.org/10.1103/PhysRevLett.129.050401.

[12] M. A. Lichnerowicz and M. A. Tonnelat, editors. *Proceedings, Les théories relativistes de la gravitation : actes du colloque international (Relativistic Theories of Gravitation): Royaumont, France, June 21-27, 1959*, Paris, 1962. CNRS. URL https://inspirehep.net/files/145765ed9caf7dd14944b9099f5f2ed2.

[13] Iwao Sato. An attempt to unite the quantum theory of wave field with the theory of general relativity. *Science reports of the Tohoku University 1st ser. Physics, chemistry, astronomy*, 33(1):30–37, 1950.

[14] Bryce S. DeWitt. New directions for research in the theory of gravitation, 1953.

[15] Nicolas Gisin. Stochastic quantum dynamics and relativity. *Helv. Phys. Acta*, 62(4): 363–371, 1989.

[16] Claudia de Rham and Andrew J. Tolley. Causality in curved spacetimes: The speed of light and gravity. *Physical Review D*, 102(8), October 2020. ISSN 2470-0029. doi:10.1103/physrevd.102.084048. URL http://dx.doi.org/10.1103/PhysRevD.102.084048.

[17] Dean Rickles and Cécile M. DeWitt. *The Necessity of Gravitational Quantization*. Max-Planck-Gesellschaft zur Förderung der Wissenschaften, 2011. ISBN 978-3-945561-29-4. doi:10.34663/9783945561294-30.

[18] Yakir Aharonov and Daniel Rohrlich. *Quantum Paradoxes: Quantum Theory for the Perplexed*. WILEY-VCH Verlag GmbH & Co. KGaA, Weinheim, 2005. ISBN 9783527403912. doi:10.1002/9783527619115. URL https://doi.org/10.1002/9783527619115.

[19] Bryce S. DeWitt. Definition of Commutators via the Uncertainty Principle. *Journal of Mathematical Physics*, 3(4):619–624, 07 1962. ISSN 0022-2488. doi:10.1063/1.1724265. URL https://doi.org/10.1063/1.1724265.

[20] Kenneth Eppley and Eric Hannah. The necessity of quantizing the gravitational field. *Foundations of Physics*, 7(1):51–68, 1977. doi:10.1007/BF00715241. URL https://doi.org/10.1007/BF00715241.

[21] Adrian Kent. Simple refutation of the eppley-hannah argument. *arXiv preprint arXiv:1807.08708*, 2018.

[22] J. Caro and L. L. Salcedo. Impediments to mixing classical and quantum dynamics. *Phys. Rev. A*, 60:842–852, Aug 1999. doi:10.1103/PhysRevA.60.842. URL https://link.aps.org/doi/10.1103/PhysRevA.60.842.

[23] Wayne Boucher and Jennie Traschen. Semiclassical physics and quantum fluctuations. *Phys. Rev. D*, 37:3522–3532, Jun 1988. doi:10.1103/PhysRevD.37.3522. URL https://link.aps.org/doi/10.1103/PhysRevD.37.3522.

[24] Viqar Husain, Irfan Javed, Sanjeev S. Seahra, and Nomaan X. Motivating semiclassical gravity: a classical-quantum approximation for bipartite quantum systems, 2023. URL https://arxiv.org/abs/2306.01060.

[25] I. V. Aleksandrov. The Statistical Dynamics of a System Consisting of a Classical and a Quantum Subsystem. *Zeitschrift Naturforschung Teil A*, 36(8):902–908, August 1981. doi:10.1515/zna-1981-0819.

[26] E. C. G. Sudarshan. Interaction between classical and quantum systems and the measurement of quantum observables. *Pramana*, 6(3):117–126, 1976. doi:10.1007/BF02847120. URL https://doi.org/10.1007/BF02847120.

[27] Viktor Ivanovych Gerasimenko. Dynamical equations of quantum-classical systems. *Theoretical and Mathematical Physics*, 50(1):49–55, 1982.

[28] Raymond Kapral and Giovanni Ciccotti. Mixed quantum-classical dynamics. *The Journal of chemical physics*, 110(18):8919–8929, 1999.

[29] Arlen Anderson. Quantum backreaction on" classical" variables. *Physical review letters*, 74(5):621, 1995.

[30] Michael JW Hall and Marcel Reginatto. Interacting classical and quantum ensembles. *Physical Review A*, 72(6):062109, 2005.

[31] Philippe Blanchard and Arkadiusz Jadczyk. On the interaction between classical and quantum systems. *Physics Letters A*, 175(3-4):157–164, 1993.

[32] Ph. Blanchard and A. Jadczyk. Event-enhanced quantum theory and piecewise deterministic dynamics. *Annalen der Physik*, 507(6):583–599, 1995. doi:https://doi.org/10.1002/andp.19955070605. URL https://onlinelibrary.wiley.com/doi/abs/10.1002/andp.19955070605.

[33] Lajos Diosi. Quantum dynamics with two planck constants and the semiclassical limit. 1995. URL https://arxiv.org/abs/quant-ph/9503023.

[34] Lajos Diósi and Jonathan J Halliwell. Coupling classical and quantum variables using continuous quantum measurement theory. *Physical review letters*, 81(14):2846, 1998.

[35] Lajos Diósi. The gravity-related decoherence master equation from hybrid dynamics. *Journal of Physics: Conference Series*, 306(1):012006, 2011. doi:10.1088/1742-6596/306/1/012006. URL https://dx.doi.org/10.1088/1742-6596/306/1/012006.

[36] D Kafri, J M Taylor, and G J Milburn. A classical channel model for gravitational decoherence. *New Journal of Physics*, 16(6):065020, 2014. doi:10.1088/1367-2630/16/6/065020. URL https://dx.doi.org/10.1088/1367-2630/16/6/065020.

[37] Antoine Tilloy and Lajos Diósi. Sourcing semiclassical gravity from spontaneously localized quantum matter. *Phys. Rev. D*, 93:024026, Jan 2016. doi:10.1103/PhysRevD.93.024026. URL https://link.aps.org/doi/10.1103/PhysRevD.93.024026.

[38] Antoine Tilloy and Lajos Diósi. Principle of least decoherence for newtonian semiclassical gravity. *Phys. Rev. D*, 96:104045, Nov 2017. doi:10.1103/PhysRevD.96.104045. URL https://link.aps.org/doi/10.1103/PhysRevD.96.104045.

[39] Philip Pearle. Combining stochastic dynamical state-vector reduction with spontaneous localization. *Phys. Rev. A*, 39:2277–2289, Mar 1989. doi:10.1103/PhysRevA.39.2277. URL https://link.aps.org/doi/10.1103/PhysRevA.39.2277.

[40] G. C. Ghirardi, A. Rimini, and T. Weber. Unified dynamics for microscopic and macroscopic systems. *Phys. Rev. D*, 34:470–491, Jul 1986. doi:10.1103/PhysRevD.34.470. URL https://link.aps.org/doi/10.1103/PhysRevD.34.470.

[41] Stephen L Adler and Todd A Brun. Generalized stochastic schrödinger equations for state vector collapse. *Journal of Physics A: Mathematical and General*, 34(23):4797, 2001.

[42] Angelo Bassi and GianCarlo Ghirardi. Dynamical reduction models. *Physics Reports*, 379 (5):257–426, 2003. ISSN 0370-1573. doi:https://doi.org/10.1016/S0370-1573(03)00103-0. URL https://www.sciencedirect.com/science/article/pii/S0370157303001030.

[43] Tom Banks, Leonard Susskind, and Michael E. Peskin. Difficulties for the Evolution of Pure States Into Mixed States. *Nucl. Phys. B*, 244:125–134, 1984. doi:10.1016/0550-3213(84)90184-6.

[44] Matteo Carlesso, Angelo Bassi, Paolo Falferi, and Andrea Vinante. Experimental bounds on collapse models from gravitational wave detectors. *Physical Review D*, 94(12):124036, 2016.

[45] Sandro Donadi, Kristian Piscicchia, Catalina Curceanu, Lajos Diósi, Matthias Laubenstein, and Angelo Bassi. Underground test of gravity-related wave function collapse. *Nature Physics*, 17(1):74–78, 2021.

[46] Stephen L Adler. Lower and upper bounds on csl parameters from latent image formation and igm heating. *Journal of Physics A: Mathematical and Theoretical*, 40(12): 2935, mar 2007. doi:10.1088/1751-8113/40/12/S03. URL https://dx.doi.org/10.1088/1751-8113/40/12/S03.

[47] Frederick Karolyhazy. Gravitation and quantum mechanics of macroscopic objects. *Il Nuovo Cimento A (1965-1970)*, 42(2):390–402, 1966.

[48] Lajos Diósi. Models for universal reduction of macroscopic quantum fluctuations. *Physical Review A*, 40(3):1165, 1989.

[49] Roger Penrose. On gravity's role in quantum state reduction. *General relativity and gravitation*, 28(5):581–600, 1996.

[50] Jonathan Oppenheim. A postquantum theory of classical gravity? *Phys. Rev. X*, 13: 041040, Dec 2023. doi:10.1103/PhysRevX.13.041040. URL https://link.aps.org/doi/10.1103/PhysRevX.13.041040.

[51] Jonathan Oppenheim, Carlo Sparaciari, Barbara Šoda, and Zachary Weller-Davies. The two classes of hybrid classical-quantum dynamics. 2022.

[52] Thomas D. Galley, Flaminia Giacomini, and John H. Selby. Any consistent coupling between classical gravity and quantum matter is fundamentally irreversible. *Quantum*, 7:1142, October 2023. ISSN 2521-327X. doi:10.22331/q-2023-10-16-1142. URL https://doi.org/10.22331/q-2023-10-16-1142.

[53] Leon Rosenfeld. On quantization of fields. *Nuclear Physics*, 40:353–356, 1963.

[54] Matvei Bronstein. Republication of: Quantum theory of weak gravitational fields. *General Relativity and Gravitation*, 44(1):267–283, 2012. doi:10.1007/s10714-011-1285-4. URL https://doi.org/10.1007/s10714-011-1285-4.

[55] Marc H. Goroff and Augusto Sagnotti. The Ultraviolet Behavior of Einstein Gravity. *Nucl. Phys. B*, 266:709–736, 1986. doi:10.1016/0550-3213(86)90193-8.

[56] Sougato Bose, Anupam Mazumdar, Gavin W Morley, Hendrik Ulbricht, Marko Toroš, Mauro Paternostro, Andrew A Geraci, Peter F Barker, MS Kim, and Gerard Milburn. Spin entanglement witness for quantum gravity. *Physical review letters*, 119(24):240401, 2017.

[57] Chiara Marletto and Vlatko Vedral. Gravitationally induced entanglement between two massive particles is sufficient evidence of quantum effects in gravity. *Physical review letters*, 119(24):240402, 2017.

[58] Belinda Pang and Yanbei Chen. Quantum interactions between a laser interferometer and gravitational waves. *Physical Review D*, 98(12), December 2018. ISSN 2470-0029. doi:10.1103/physrevd.98.124006. URL http://dx.doi.org/10.1103/PhysRevD.98.124006.

[59] Maulik Parikh, Frank Wilczek, and George Zahariade. The Noise of Gravitons. *Int. J. Mod. Phys. D*, 29(14):2042001, 2020. doi:10.1142/S0218271820420018.

[60] Daniel Carney, Manthos Karydas, and Allic Sivaramakrishnan. Response of interferometers to the vacuum of quantum gravity. 9 2024.

[61] Ludovico Lami, Julen S. Pedernales, and Martin B. Plenio. Testing the quantumness of gravity without entanglement. *Physical Review X*, 14(2), May 2024. ISSN 2160-3308. doi:10.1103/physrevx.14.021022. URL http://dx.doi.org/10.1103/PhysRevX.14.021022.

[62] Daniel Carney, Valerie Domcke, and Nicholas L. Rodd. Graviton detection and the quantization of gravity. *Physical Review D*, 109(4), February 2024. ISSN 2470-0029. doi:10.1103/physrevd.109.044009. URL http://dx.doi.org/10.1103/PhysRevD.109.044009.

[63] Serhii Kryhin and Vivishek Sudhir. Distinguishable consequence of classical gravity on quantum matter. *Phys. Rev. Lett.*, 134:061501, Feb 2025. doi:10.1103/PhysRevLett.134.061501. URL https://link.aps.org/doi/10.1103/PhysRevLett.134.061501.

[64] Daniel Carney, Philip C E Stamp, and Jacob M Taylor. Tabletop experiments for quantum gravity: a user's manual. *Classical and Quantum Gravity*, 36(3):034001, jan 2019. doi:10.1088/1361-6382/aaf9ca. URL https://dx.doi.org/10.1088/1361-6382/aaf9ca.

[65] Jonathan Oppenheim, Carlo Sparaciari, Barbara Šoda, and Zachary Weller-Davies. Gravitationally induced decoherence vs space-time diffusion: testing the quantum nature of gravity. *Nature Communications*, 14(1):7910, 2023. doi:10.1038/s41467-023-43348-2. URL https://doi.org/10.1038/s41467-023-43348-2.

[66] Chung-I Kuo and L. H. Ford. Semiclassical gravity theory and quantum fluctuations. *Physical Review D*, 47(10):4510–4519, May 1993. ISSN 0556-2821. doi:10.1103/physrevd.47.4510. URL http://dx.doi.org/10.1103/PhysRevD.47.4510.

[67] Isaac Layton, Jonathan Oppenheim, and Zachary Weller-Davies. A healthier semiclassical dynamics. *Quantum*, 8:1565, 2024. doi:10.22331/q-2024-12-16-1565.

[68] Shahnewaz Ahmed, Caroline Lima, and Eduardo Martín-Martínez. Semiclassical gravity beyond coherent states. *Journal of High Energy Physics*, 2024(1):1, 2024. doi:10.1007/JHEP01(2024)001. URL https://doi.org/10.1007/JHEP01(2024)001.

[69] Andrew Eberhardt, Alvaro Zamora, Michael Kopp, and Tom Abel. The classical field approximation of ultra light dark matter: quantum breaktimes, corrections, and decoherence, 2023. URL https://arxiv.org/abs/2310.07119.

[70] A. B. Klimov, I. Sainz, and J. L. Romero. Truncated Wigner approximation as non-positive Kraus map. *Phys. Scripta*, 95(7):074006, 2020. doi:10.1088/1402-4896/ab8d53.

[71] Andreas Albrecht, Pedro Ferreira, Michael Joyce, and Tomislav Prokopec. Inflation and squeezed quantum states. *Phys. Rev. D*, 50:4807–4820, Oct 1994. doi:10.1103/PhysRevD.50.4807. URL https://link.aps.org/doi/10.1103/PhysRevD.50.4807.

[72] Jonathan Braden, Matthew C. Johnson, Hiranya V. Peiris, Andrew Pontzen, and Silke Weinfurtner. New semiclassical picture of vacuum decay. *Phys. Rev. Lett.*, 123:031601,

Jul 2019. doi:10.1103/PhysRevLett.123.031601. URL https://link.aps.org/doi/10.1103/PhysRevLett.123.031601.

[73] M. J. Steel, M. K. Olsen, L. I. Plimak, P. D. Drummond, S. M. Tan, M. J. Collett, D. F. Walls, and R. Graham. Dynamical quantum noise in trapped bose-einstein condensates. *Phys. Rev. A*, 58:4824–4835, Dec 1998. doi:10.1103/PhysRevA.58.4824. URL https://link.aps.org/doi/10.1103/PhysRevA.58.4824.

[74] Christopher D. Mink and Michael Fleischhauer. Collective radiative interactions in the discrete truncated wigner approximation. *SciPost Physics*, 15(6), December 2023. ISSN 2542-4653. doi:10.21468/scipostphys.15.6.233. URL http://dx.doi.org/10.21468/SciPostPhys.15.6.233.

[75] Alice Sinatra, Carlos Lobo, and Yvan Castin. The truncated wigner method for bose-condensed gases: limits of validity and applications1. *Journal of Physics B: Atomic, Molecular and Optical Physics*, 35(17):3599, 2002. doi:10.1088/0953-4075/35/17/301. URL https://dx.doi.org/10.1088/0953-4075/35/17/301.

[76] Fabio van Dissel and George Zahariade. Semiclassical backreaction: A qualitative assessment. *Phys. Rev. D*, 111(6):065008, 2025. doi:10.1103/PhysRevD.111.065008.

[77] Toma Yoneya, Kazuya Fujimoto, and Yuki Kawaguchi. Path-integral formulation of truncated wigner approximation for bosonic markovian open quantum systems. *Annals of Physics*, 479:170072, August 2025. ISSN 0003-4916. doi:10.1016/j.aop.2025.170072. URL http://dx.doi.org/10.1016/j.aop.2025.170072.

[78] Isaac Layton and Jonathan Oppenheim. The classical-quantum limit. *PRX Quantum*, 5:020331, May 2024. doi:10.1103/PRXQuantum.5.020331. URL https://link.aps.org/doi/10.1103/PRXQuantum.5.020331.

[79] Eanna E. Flanagan and Robert M. Wald. Does back reaction enforce the averaged null energy condition in semiclassical gravity? *Phys. Rev. D*, 54:6233–6283, Nov 1996. doi:10.1103/PhysRevD.54.6233. URL https://link.aps.org/doi/10.1103/PhysRevD.54.6233.

[80] Bei Lok Hu and Enric Verdaguer. Stochastic gravity: Theory and applications. *Living Reviews in Relativity*, 11(1):3, 2008. doi:10.12942/lrr-2008-3. URL https://doi.org/10.12942/lrr-2008-3.

[81] Marco Baldovin, Angelo Vulpiani, Andrea Puglisi, and Antonio Prados. Derivation of a langevin equation in a system with multiple scales: The case of negative temperatures. *Physical Review E*, 99(6), June 2019. ISSN 2470-0053. doi:10.1103/physreve.99.060101. URL http://dx.doi.org/10.1103/PhysRevE.99.060101.

[82] Xiangjun Xing. A rigorous foundation for stochastic thermodynamics via the microcanonical ensemble, 2025. URL https://arxiv.org/abs/2506.23604.

[83] Steven Weinberg. The cosmological constant problem. *Rev. Mod. Phys.*, 61:1–23, Jan 1989. doi:10.1103/RevModPhys.61.1. URL https://link.aps.org/doi/10.1103/RevModPhys.61.1.

[84] Varun Sahni and Alexei A Starobinsky. The case for a positive cosmological -term. *International Journal of Modern Physics D*, 09(04):373–443, August 2000. ISSN 1793-6594. doi:10.1142/s0218271800000542. URL http://dx.doi.org/10.1142/S0218271800000542.

[85] Ya. B. Zeldovich and Alexei A. Starobinsky. Particle production and vacuum polarization in an anisotropic gravitational field. *Zh. Eksp. Teor. Fiz.*, 61:2161–2175, 1971.

[86] Leonard Parker and S. A. Fulling. Adiabatic regularization of the energy-momentum tensor of a quantized field in homogeneous spaces. *Phys. Rev. D*, 9:341–354, Jan 1974. doi:10.1103/PhysRevD.9.341. URL https://link.aps.org/doi/10.1103/PhysRevD.9.341.

[87] Robert M. Wald. The Back Reaction Effect in Particle Creation in Curved Space-Time. *Commun. Math. Phys.*, 54:1–19, 1977. doi:10.1007/BF01609833.

[88] Adrian del Rio. The backreaction problem for black holes in semiclassical gravity. *General Relativity and Gravitation*, 57(2):30, 2025. doi:10.1007/s10714-025-03352-x. URL https://doi.org/10.1007/s10714-025-03352-x.

[89] H. Epstein, V. Glaser, and A. Jaffe. Nonpositivity of the energy density in quantized field theories. *Il Nuovo Cimento (1955-1965)*, 36(3):1016–1022, 1965. doi:10.1007/BF02749799. URL https://doi.org/10.1007/BF02749799.

[90] Matt Visser. Gravitational vacuum polarization. ii. energy conditions in the boulware vacuum. *Physical Review D*, 54(8):5116–5122, October 1996. ISSN 1089-4918. doi:10.1103/physrevd.54.5116. URL http://dx.doi.org/10.1103/PhysRevD.54.5116.

[91] Noah Graham and Ken D. Olum. Achronal averaged null energy condition. *Phys. Rev. D*, 76:064001, Sep 2007. doi:10.1103/PhysRevD.76.064001. URL https://link.aps.org/doi/10.1103/PhysRevD.76.064001.

[92] S. M. Christensen and S. A. Fulling. Trace anomalies and the hawking effect. *Phys. Rev. D*, 15:2088–2104, Apr 1977. doi:10.1103/PhysRevD.15.2088. URL https://link.aps.org/doi/10.1103/PhysRevD.15.2088.

[93] Alexei A Starobinsky. A new type of isotropic cosmological models without singularity. *Physics Letters B*, 91(1):99–102, 1980.

[94] Luis P. Chimento and Norberto A. Zuccalá. Self-consistent solutions of the semi-classical einstein equations with cosmological constant and perfect fluid. *Astrophysics and Space Science*, 201(2):341–345, 1993. doi:10.1007/BF00627205. URL https://doi.org/10.1007/BF00627205.

[95] Tarun Souradeep and Varun Sahni. Quantum effects near a point mass in (2 + 1)-dimensional gravity. *Physical Review D*, 46(4):1616–1633, August 1992. ISSN 0556-2821. doi:10.1103/physrevd.46.1616. URL http://dx.doi.org/10.1103/PhysRevD.46.1616.

[96] Harald H Soleng. Inverse square law of gravitation in (2 + 1)-dimensional space–time as a consequence of casimir energy. *Physica Scripta*, 48(6):649–652, December 1993. ISSN 1402-4896. doi:10.1088/0031-8949/48/6/002. URL http://dx.doi.org/10.1088/0031-8949/48/6/002.

[97] Marc Casals, Alessandro Fabbri, Cristián Martínez, and Jorge Zanelli. Quantum-corrected rotating black holes and naked singularities in (2+1) dimensions. *Physical Review D*, 99

(10), May 2019. ISSN 2470-0029. doi:10.1103/physrevd.99.104023. URL http://dx.doi.org/10.1103/PhysRevD.99.104023.

[98] Nima Arkani-Hamed, Savas Dimopoulos, and G. R. Dvali. The Hierarchy problem and new dimensions at a millimeter. *Phys. Lett. B*, 429:263–272, 1998. doi:10.1016/S0370-2693(98)00466-3.

[99] Lisa Randall and Raman Sundrum. An Alternative to compactification. *Phys. Rev. Lett.*, 83:4690–4693, 1999. doi:10.1103/PhysRevLett.83.4690.

[100] Kris Pardo, Maya Fishbach, Daniel E. Holz, and David N. Spergel. Limits on the number of spacetime dimensions from gw170817. *Journal of Cosmology and Astroparticle Physics*, 2018(07):048–048, July 2018. ISSN 1475-7516. doi:10.1088/1475-7516/2018/07/048. URL http://dx.doi.org/10.1088/1475-7516/2018/07/048.

[101] Juan Martin Maldacena. The Large N limit of superconformal field theories and supergravity. *Adv. Theor. Math. Phys.*, 2:231–252, 1998. doi:10.4310/ATMP.1998.v2.n2.a1.

[102] Gerard 't Hooft. Dimensional reduction in quantum gravity. *Conf. Proc. C*, 930308: 284–296, 1993.

[103] Leonard Susskind and John Uglum. Black hole entropy in canonical quantum gravity and superstring theory. *Phys. Rev. D*, 50:2700–2711, 1994. doi:10.1103/PhysRevD.50.2700.

[104] Veronika E. Hubeny, Donald Marolf, and Mukund Rangamani. Hawking radiation from AdS black holes. *Class. Quant. Grav.*, 27:095018, 2010. doi:10.1088/0264-9381/27/9/095018.

[105] Lisa Randall and Raman Sundrum. A Large mass hierarchy from a small extra dimension. *Phys. Rev. Lett.*, 83:3370–3373, 1999. doi:10.1103/PhysRevLett.83.3370.

[106] Andreas Karch and Lisa Randall. Locally localized gravity. *JHEP*, 05:008, 2001. doi:10.1088/1126-6708/2001/05/008.

[107] Andreas Karch and Lisa Randall. Open and closed string interpretation of SUSY CFT's on branes with boundaries. *JHEP*, 06:063, 2001. doi:10.1088/1126-6708/2001/06/063.

[108] Per Kraus, Finn Larsen, and Ruud Siebelink. The gravitational action in asymptotically AdS and flat space-times. *Nucl. Phys. B*, 563:259–278, 1999. doi:10.1016/S0550-3213(99)00549-0.

[109] Roberto Emparan, Clifford V. Johnson, and Robert C. Myers. Surface terms as counterterms in the AdS / CFT correspondence. *Phys. Rev. D*, 60:104001, 1999. doi:10.1103/PhysRevD.60.104001.

[110] Sebastian de Haro, Sergey N. Solodukhin, and Kostas Skenderis. Holographic reconstruction of space-time and renormalization in the AdS / CFT correspondence. *Commun. Math. Phys.*, 217:595–622, 2001. doi:10.1007/s002200100381.

[111] Kostas Skenderis. Lecture notes on holographic renormalization. *Class. Quant. Grav.*, 19:5849–5876, 2002. doi:10.1088/0264-9381/19/22/306.

[112] Ioannis Papadimitriou and Kostas Skenderis. AdS / CFT correspondence and geometry. *IRMA Lect. Math. Theor. Phys.*, 8:73–101, 2005. doi:10.4171/013-1/4.

[113] Roberto Emparan, Alessandro Fabbri, and Nemanja Kaloper. Quantum black holes as holograms in ads braneworlds. *Journal of High Energy Physics*, 2002(08):043–043, August 2002. ISSN 1029-8479. doi:10.1088/1126-6708/2002/08/043. URL http://dx.doi.org/10.1088/1126-6708/2002/08/043.

[114] RF Pawula. Rf pawula, phys. rev. 162, 186 (1967). *Phys. Rev.*, 162:186, 1967.

[115] G. G. Batrouni, H. Kawai, and Pietro Rossi. Coordinate independent formulation of the langevin equation. *J. Math. Phys.*, 27:1646, 1986. doi:10.1063/1.527396.

[116] Kiyosi Itô. On a formula concerning stochastic differentials. *Nagoya Mathematical Journal*, 3:55–65, 1951. doi:DOI: 10.1017/S0027763000012216. URL https://www.cambridge.org/core/product/CA39C46B3829C055DBD1BF839BA0E140.

[117] N. G. van Kampen. Itô versus stratonovich. *Journal of Statistical Physics*, 24(1):175–187, 1981. doi:10.1007/BF01007642. URL https://doi.org/10.1007/BF01007642.

[118] Massimo D'Elia, Kurt Langfeld, and Biagio Lucini. *Stochastic Methods in Scientific Computing*. Numerical Analysis and Scientific Computing Series. CRC Press LLC, 4 2024. doi:10.1201/9781315156156.

[119] P. C. Martin, E. D. Siggia, and H. A. Rose. Statistical dynamics of classical systems. *Phys. Rev. A*, 8:423–437, Jul 1973. doi:10.1103/PhysRevA.8.423. URL https://link.aps.org/doi/10.1103/PhysRevA.8.423.

[120] L. Onsager and S. Machlup. Fluctuations and irreversible processes. *Phys. Rev.*, 91: 1505–1512, Sep 1953. doi:10.1103/PhysRev.91.1505. URL https://link.aps.org/doi/10.1103/PhysRev.91.1505.

[121] Xinze Zhang and Yong Li. Onsager-machlup functional and large deviation principle for stochastic hamiltonian systems, 2025. URL https://arxiv.org/abs/2503.13932.

[122] D. E. Evans and J. T. Lewis. Dilations of Dynamical Semigroups. *Commun. Math. Phys.*, 50:219–227, 1976. doi:10.1007/BF01609402.

[123] J. L. Gaona-Reyes, D. G. A. Altamura, and A. Bassi. Theoretical limits of protocols for distinguishing different unravelings, 2025. URL https://arxiv.org/abs/2502.19268.

[124] Kurt Jacobs. *Quantum Measurement Theory and its Applications*. Cambridge University Press, Cambridge, 2014. ISBN 9781107025486. doi:DOI: 10.1017/CBO9781139179027. URL https://www.cambridge.org/core/product/120E32FFBEBF6EE0F6EC6F84D51DC907.

[125] Jonathan Oppenheim and Zachary Weller-Davies. Path integrals for classical-quantum dynamics. 2023. URL https://arxiv.org/abs/2301.04677.

[126] Jonathan Oppenheim and Zachary Weller-Davies. Covariant path integrals for quantum fields back-reacting on classical space-time. 2023. URL https://arxiv.org/abs/2302.07283.

[127] Jonathan Oppenheim, Andrea Russo, and Zachary Weller-Davies. Diffeomorphism invariant classical-quantum path integrals for Nordström gravity. *Phys. Rev. D*, 110(2):024007, 2024. doi:10.1103/PhysRevD.110.024007.

[128] Lajos Diósi. Classical-quantum hybrid canonical dynamics and its difficulties with special and general relativity. *Phys. Rev. D*, 110:084052, Oct 2024. doi:10.1103/PhysRevD.110.084052. URL https://link.aps.org/doi/10.1103/PhysRevD.110.084052.

[129] R. Arnowitt, S. Deser, and C. W. Misner. Dynamical structure and definition of energy in general relativity. *Phys. Rev.*, 116:1322–1330, Dec 1959. doi:10.1103/PhysRev.116.1322. URL https://link.aps.org/doi/10.1103/PhysRev.116.1322.

[130] Lajos Diósi. Hybrid quantum-classical master equations. *Physica Scripta*, 2014(T163): 014004, 2014. doi:10.1088/0031-8949/2014/T163/014004. URL https://dx.doi.org/10.1088/0031-8949/2014/T163/014004.

[131] R. Penrose. Gravitational collapse: The role of general relativity. *Riv. Nuovo Cim.*, 1: 252–276, 1969. doi:10.1023/A:1016578408204.

[132] Lajos Diosi. A universal master equation for the gravitational violation of quantum mechanics. *Physics letters A*, 120(8):377–381, 1987.

[133] Sergio A Hojman, Karel Kuchař, and Claudio Teitelboim. Geometrodynamics regained. *Annals of Physics*, 96(1):88–135, 1976. doi:https://doi.org/10.1016/0003-4916(76)90112-3. URL https://www.sciencedirect.com/science/article/pii/0003491676901123.

[134] Paul A. M. Dirac. *Lectures on Quantum Mechanics*. Yeshiva University Press, New York, 1967. Belfer Graduate School of Science Monographs Series.

[135] Jonathan Oppenheim and Zachary Weller-Davies. The constraints of post-quantum classical gravity. *Journal of High Energy Physics*, 2022(2):80, 2022. doi:10.1007/JHEP02(2022)080. URL https://doi.org/10.1007/JHEP02(2022)080.

[136] Andrzej Grudka, Jonathan Oppenheim, Andrea Russo, and Muhammad Sajjad. Renormalisation of postquantum-classical gravity. 2024.

[137] Isaac Layton, Jonathan Oppenheim, Andrea Russo, and Zachary Weller-Davies. The weak field limit of quantum matter back-reacting on classical spacetime. *Journal of*

High Energy Physics, 2023(8):163, 2023. doi:10.1007/JHEP08(2023)163. URL https://doi.org/10.1007/JHEP08(2023)163.

[138] Philip D Mannheim and Demosthenes Kazanas. Exact vacuum solution to conformal weyl gravity and galactic rotation curves. *Astrophysical Journal, Part 1 (ISSN 0004-637X), vol. 342, July 15, 1989, p. 635-638. Research supported by the National Academy of Sciences.*, 342:635–638, 1989.

[139] Philip D Mannheim. Are galactic rotation curves really flat? *The Astrophysical Journal*, 479(2):659, 1997.

[140] Philip D Mannheim and James G O'Brien. Fitting galactic rotation curves with conformal gravity and a global quadratic potential. *Physical Review D*, 85(12):124020, 2012.

[141] Bharat Ratra and Michael S. Vogeley. The beginning and evolution of the universe. *Publications of the Astronomical Society of the Pacific*, 120(865):235–265, March 2008. ISSN 1538-3873. doi:10.1086/529495. URL http://dx.doi.org/10.1086/529495.

[142] Alan H. Guth. The Inflationary Universe: A Possible Solution to the Horizon and Flatness Problems. *Phys. Rev. D*, 23:347–356, 1981. doi:10.1103/PhysRevD.23.347.

[143] Daniel Baumann. Tasi lectures on inflation, 2012. URL https://arxiv.org/abs/0907.5424.

[144] Ana Achúcarro et al. Inflation: Theory and Observations. 3 2022.

[145] Andrei D. Linde. A New Inflationary Universe Scenario: A Possible Solution of the Horizon, Flatness, Homogeneity, Isotropy and Primordial Monopole Problems. *Phys. Lett. B*, 108:389–393, 1982. doi:10.1016/0370-2693(82)91219-9.

[146] Juan Garcia-Bellido and David Wands. Metric perturbations in two field inflation. *Phys. Rev. D*, 53:5437–5445, 1996. doi:10.1103/PhysRevD.53.5437.

[147] Andrei D. Linde. Chaotic Inflation. *Phys. Lett. B*, 129:177–181, 1983. doi:10.1016/0370-2693(83)90837-7.

[148] Adam G. Riess et al. Observational evidence from supernovae for an accelerating universe and a cosmological constant. *Astron. J.*, 116:1009–1038, 1998. doi:10.1086/300499.

[149] N. Aghanim et al. Planck 2018 results - vi. cosmological parameters. *Astronomy & Astrophysics*, 641:A6, sep 2020. doi:10.1051/0004-6361/201833910. URL https://doi.org/10.1051%2F0004-6361%2F201833910.

[150] Miao Li, Xiao-Dong Li, Shuang Wang, and Yi Wang. Dark Energy: A Brief Review. *Front. Phys. (Beijing)*, 8:828–846, 2013. doi:10.1007/s11467-013-0300-5.

[151] S. Navas et al. Review of particle physics. *Phys. Rev. D*, 110(3):030001, 2024. doi:10.1103/PhysRevD.110.030001.

[152] A. G. Adame et al. DESI 2024 VI: cosmological constraints from the measurements of baryon acoustic oscillations. *JCAP*, 02:021, 2025. doi:10.1088/1475-7516/2025/02/021.

[153] K. Lodha et al. Desi 2024: Constraints on physics-focused aspects of dark energy using desi dr1 bao data. *Phys. Rev. D*, 111:023532, Jan 2025. doi:10.1103/PhysRevD.111.023532. URL https://link.aps.org/doi/10.1103/PhysRevD.111.023532.

[154] Ali Rida Khalife, Maryam Bahrami Zanjani, Silvia Galli, Sven Günther, Julien Lesgourgues, and Karim Benabed. Review of hubble tension solutions with new sh0es and spt-3g data, 2024. URL https://arxiv.org/abs/2312.09814.

[155] Morgan Hollis. Hints of a physical origin for the s8 tension. *Nature Astronomy*, 8 (4):405–405, 2024. doi:10.1038/s41550-024-02262-3. URL https://doi.org/10.1038/s41550-024-02262-3.

[156] Benoit Famaey and Stacy McGaugh. Modified Newtonian Dynamics (MOND): Observational Phenomenology and Relativistic Extensions. *Living Rev. Rel.*, 15:10, 2012. doi:10.12942/lrr-2012-10.

[157] Indranil Banik, Charalambos Pittordis, Will Sutherland, Benoit Famaey, Rodrigo Ibata, Steffen Mieske, and Hongsheng Zhao. Strong constraints on the gravitational law from

gaia dr3 wide binaries. *Monthly Notices of the Royal Astronomical Society*, 527(3):4573–4615, November 2023. ISSN 1365-2966. doi:10.1093/mnras/stad3393. URL http://dx.doi.org/10.1093/mnras/stad3393.

[158] Dillon Brout et al. The Pantheon+ Analysis: Cosmological Constraints. *Astrophys. J.*, 938(2):110, 2022. doi:10.3847/1538-4357/ac8e04.

[159] Ariane Dekker, Shin'ichiro Ando, Camila A. Correa, and Kenny C. Y. Ng. Warm dark matter constraints using milky way satellite observations and subhalo evolution modeling. *Phys. Rev. D*, 106:123026, Dec 2022. doi:10.1103/PhysRevD.106.123026. URL https://link.aps.org/doi/10.1103/PhysRevD.106.123026.

[160] A. Arbey and F. Mahmoudi. Dark matter and the early Universe: a review. *Prog. Part. Nucl. Phys.*, 119:103865, 2021. doi:10.1016/j.ppnp.2021.103865.

[161] Muhammad Sajjad, Andrea Russo, Maite Arcos, Andrzej Grudka, and Jonathan Oppenheim. A quantum oscillator interacting with a classical oscillator, 2025. URL https://arxiv.org/abs/2403.07479.

[162] Isaac Layton and Harry J. D. Miller. Restoring the second law to classical-quantum dynamics. 4 2025.

[163] A. S. Trushechkin, M. Merkli, J. D. Cresser, and J. Anders. Open quantum system dynamics and the mean force gibbs state. *AVS Quantum Science*, 4(1), March 2022. ISSN 2639-0213. doi:10.1116/5.0073853. URL http://dx.doi.org/10.1116/5.0073853.

[164] Claude Godrèche and Jean-Marc Luck. Characterising the nonequilibrium stationary states of ornstein–uhlenbeck processes. *Journal of Physics A: Mathematical and Theoretical*, 52(3):035002, December 2018. ISSN 1751-8121. doi:10.1088/1751-8121/aaf190. URL http://dx.doi.org/10.1088/1751-8121/aaf190.

[165] E.J. Routh. *A Treatise on the Stability of a Given State of Motion: Particularly Steady Motion*. Adams prize essay. Macmillan and Company, 1877. URL https://books.google.co.uk/books?id=xLQEAAAAYAAJ.

[166] A. Hurwitz. Ueber die bedingungen, unter welchen eine gleichung nur wurzeln mit negativen reellen theilen besitzt. *Mathematische Annalen*, 46(2):273–284, 1895. doi:10.1007/BF01446812. URL https://doi.org/10.1007/BF01446812.

[167] Tzon-Tzer Lu and Sheng-Hua Shiou. Inverses of 2 ×2 block matrices. *Computers & Mathematics with Applications*, 43(1):119–129, 2002. doi:https://doi.org/10.1016/S0898-1221(01)00278-4. URL https://www.sciencedirect.com/science/article/pii/S0898122101002784.

[168] A. ISAR, A. SANDULESCU, and W. SCHEID. Phase space representation for open quantum systems within the lindblad theory. *International Journal of Modern Physics B*, 10(22):2767–2779, October 1996. ISSN 1793-6578. doi:10.1142/s0217979296001240. URL http://dx.doi.org/10.1142/S0217979296001240.

[169] Anton Arnold, Franco Fagnola, and Lukas Neumann. Quantum fokker-planck models: the lindblad and wigner approaches, 2008. URL https://arxiv.org/abs/0806.2984.

[170] Mohammad F. Maghrebi and Alexey V. Gorshkov. Nonequilibrium many-body steady states via keldysh formalism. *Phys. Rev. B*, 93:014307, Jan 2016. doi:10.1103/PhysRevB.93.014307. URL https://link.aps.org/doi/10.1103/PhysRevB.93.014307.

[171] L M Sieberer, M Buchhold, and S Diehl. Keldysh field theory for driven open quantum systems. *Reports on Progress in Physics*, 79(9):096001, August 2016. ISSN 1361-6633. doi:10.1088/0034-4885/79/9/096001. URL http://dx.doi.org/10.1088/0034-4885/79/9/096001.

[172] Wojciech H. Zurek. Decoherence and the transition from quantum to classical – revisited, 2003. URL https://arxiv.org/abs/quant-ph/0306072.

[173] J. M. Sellier, M. Nedjalkov, and I. Dimov. An introduction to applied quantum mechanics in the wigner monte carlo formalism. *Physics Reports*, 577:1–34, 2015. doi:https://doi.org/10.1016/j.physrep.2015.03.001. URL https://www.sciencedirect.com/science/article/pii/S0370157315001982.

[174] Daniel Carney and Akira Matsumura. Classical-quantum scattering. 12 2024.

[175] Robert C. Dalang and Marta Sanz-Solé. HL̈der-sobolev regularity of the solution to the stochastic wave equation in dimension 3, 2005. URL https://arxiv.org/abs/math/0512540.

[176] Dalang Robert C. Conus, Daniel. The non-linear stochastic wave equation in high dimensions. *Electronic Journal of Probability [electronic only]*, 13:629–670, 2008. URL http://eudml.org/doc/232217.

[177] Raluca M. Balan and Ciprian A. Tudor. The stochastic wave equation with fractional noise: A random field approach. *Stochastic Processes and their Applications*, 120(12):2468–2494, 2010. doi:https://doi.org/10.1016/j.spa.2010.08.006. URL https://www.sciencedirect.com/science/article/pii/S0304414910001924.

[178] Joseph I. Kapusta. *Finite Temperature Field Theory*. Cambridge Monographs on Mathematical Physics. Cambridge University Press, Cambridge, 1989. ISBN 978-0-521-35155-3.

[179] David Tong. Statistical field theory. https://www.damtp.cam.ac.uk/user/tong/sft/sft.pdf, 2017. Lecture notes, University of Cambridge, Part III Mathematical Tripos.

[180] *The Early Universe and Observational Cosmology*. Springer Berlin Heidelberg, 2004. ISBN 9783540409182. doi:10.1007/b97189. URL http://dx.doi.org/10.1007/b97189.

[181] Robert C. Dalang and Marta Sanz-Solé. Stochastic partial differential equations, space-time white noise and random fields, 2024. URL https://arxiv.org/abs/2402.02119.

[182] Alexei A. Starobinsky and Jun'ichi Yokoyama. Equilibrium state of a self-interacting scalar field in the de sitter background. *Physical Review D*, 50(10):6357–6368, November 1994. ISSN 0556-2821. doi:10.1103/physrevd.50.6357. URL http://dx.doi.org/10.1103/PhysRevD.50.6357.

[183] G. Scharf. *Finite Quantum Electrodynamics: The Causal Approach, Third Edition*. Dover Books on Physics. Dover Publications, 2014. ISBN 9780486492735. URL https://books.google.co.uk/books?id=zxnqAgAAQBAJ.

[184] Avinash Baidya, Chandan Jana, R Loganayagam, and Arnab Rudra. Renormalization in open quantum field theory. part i. scalar field theory. *Journal of High Energy Physics*, 2017(11):204, 2017. Also, initial work by Poulin and Preskill (unpublished note).

[185] G. C. Ghirardi, R. Grassi, and P. Pearle. Relativistic dynamical reduction models: General framework and examples. *Foundations of Physics*, 20(11):1271–1316, 1990. doi:10.1007/BF01883487. URL https://doi.org/10.1007/BF01883487.

[186] Lajos Diósi. Is there a relativistic gorini-kossakowski-lindblad-sudarshan master equation? *Physical Review D*, 106(5), September 2022. ISSN 2470-0029. doi:10.1103/physrevd.106.l051901. URL http://dx.doi.org/10.1103/PhysRevD.106.L051901.

[187] Robert M. Wald. *General Relativity*. Chicago Univ. Pr., Chicago, USA, 1984. doi:10.7208/chicago/9780226870373.001.0001.

[188] V. Mukhanov. *Physical Foundations of Cosmology*. Cambridge University Press, Oxford, 2005. ISBN 978-0-521-56398-7. doi:10.1017/CBO9780511790553.

[189] Tadahiro Oh, Yuzhao Wang, and Younes Zine. Three-dimensional stochastic cubic nonlinear wave equation with almost space-time white noise. *Stochastics and Partial Differential Equations: Analysis and Computations*, 10(3):898–963, April 2022. ISSN 2194-041X. doi:10.1007/s40072-022-00237-x. URL http://dx.doi.org/10.1007/s40072-022-00237-x.

[190] Gilad Gour and L. Sriramkumar. Will small particles exhibit brownian motion in the quantum vacuum?, 1999. URL https://arxiv.org/abs/quant-ph/9808032.

[191] Hongwei Yu and L. H. Ford. Vacuum fluctuations and brownian motion of a charged test particle near a reflecting boundary. *Physical Review D*, 70(6), September 2004. ISSN 1550-2368. doi:10.1103/physrevd.70.065009. URL http://dx.doi.org/10.1103/PhysRevD.70.065009.

[192] Philip R. Johnson and B. L. Hu. Stochastic theory of relativistic particles moving in a quantum field: Scalar abraham-lorentz-dirac-langevin equation,

radiation reaction, and vacuum fluctuations. *Phys. Rev. D*, 65:065015, Feb 2002. doi:10.1103/PhysRevD.65.065015. URL https://link.aps.org/doi/10.1103/PhysRevD.65.065015.

[193] Michele Armano et al. Lisa pathfinder, 2019. URL https://arxiv.org/abs/1903.08924.

[194] Martijn Janse, Dennis G Uitenbroek, Loek van Everdingen, Jaimy Plugge, Bas Hensen, and Tjerk H Oosterkamp. Current experimental upper bounds on spacetime diffusion. *arXiv preprint arXiv:2403.08912*, 2024.

[195] F B Dunning, J J Mestayer, C O Reinhold, S Yoshida, and J Burgdörfer. Engineering atomic rydberg states with pulsed electric fields. *Journal of Physics B: Atomic, Molecular and Optical Physics*, 42(2):022001, 2009. doi:10.1088/0953-4075/42/2/022001. URL https://dx.doi.org/10.1088/0953-4075/42/2/022001.

[196] Maqbool Ahmed, Scott Dodelson, Patrick B. Greene, and Rafael Sorkin. Everpresent lambda. *Physical Review D*, 69(10), May 2004. ISSN 1550-2368. doi:10.1103/physrevd.69.103523. URL http://dx.doi.org/10.1103/PhysRevD.69.103523.

[197] Alejandro Perez, Daniel Sudarsky, and Edward Wilson-Ewing. Resolving the h0 tension with diffusion. *General Relativity and Gravitation*, 53(1), January 2021. ISSN 1572-9532. doi:10.1007/s10714-020-02781-0. URL http://dx.doi.org/10.1007/s10714-020-02781-0.

[198] Susana J. Landau, Micol Benetti, Alejandro Perez, and Daniel Sudarsky. Cosmological constraints on unimodular gravity models with diffusion. 2022.

[199] Anne-Katherine Burns, David E. Kaplan, Tom Melia, and Surjeet Rajendran. Time evolution in quantum cosmology. 2023.

[200] David E. Kaplan, Tom Melia, and Surjeet Rajendran. The Classical Equations of Motion of Quantized Gauge Theories, Part I: General Relativity. 5 2023.

[201] Roberto Casadio, Leonardo Chataignier, Alexander Yu. Kamenshchik, Francisco G. Pedro, Alessandro Tronconi, and Giovanni Venturi. Relaxation of first-class constraints and

the quantization of gauge theories: from "matter without matter" to the reappearance of time in quantum gravity. 2 2024.

[202] Loris Del Grosso, David E. Kaplan, Tom Melia, Vivian Poulin, Surjeet Rajendran, and Tristan L. Smith. Cosmological Consequences of Unconstrained Gravity and Electromagnetism. 5 2024.

[203] J. David Brown and Karel V. Kuchař. Dust as a standard of space and time in canonical quantum gravity. *Physical Review D*, 51(10):5600–5629, May 1995. ISSN 0556-2821. doi:10.1103/physrevd.51.5600. URL http://dx.doi.org/10.1103/physrevd.51.5600.

[204] Bernt Øksendal. *Space-Time Stochastic Calculus and White Noise*, pages 629–649. Springer International Publishing, Cham URL https://doi.org/10.1007/978-3-031-12244-6_44.

[205] Roy Maartens. Is the universe homogeneous? *Philosophical Transactions of the Royal Society A: Mathematical, Physical and Engineering Sciences*, 369(1957):5115–5137, 2011. doi:10.1098/rsta.2011.0289. URL https://royalsocietypublishing.org/doi/abs/10.1098/rsta.2011.0289.

[206] David Wands, Karim A. Malik, David H. Lyth, and Andrew R. Liddle. A new approach to the evolution of cosmological perturbations on large scales. *Physical Review D*, 62: 043527, 2000. URL https://api.semanticscholar.org/CorpusID:40791120.

[207] Jonathan Oppenheim. The constraints of a continuous realisation of hybrid classical-quantum gravity. manuscript in preparation.

[208] Yashar Akrami, Frederico Arroja, M Ashdown, J Aumont, Carlo Baccigalupi, M Ballardini, Anthony J Banday, RB Barreiro, Nicola Bartolo, S Basak, et al. Planck 2018 results-x. constraints on inflation. *Astronomy & Astrophysics*, 641:A10, 2020.

[209] Jonathan Oppenheim and Andrea Russo. Anomalous contribution to galactic rotation curves due to stochastic spacetime. 2024.

[210] J. Julve and M. Tonin. Quantum Gravity with Higher Derivative Terms. *Nuovo Cim. B*, 46:137–152, 1978. doi:10.1007/BF02748637.

[211] E. S. Fradkin and Arkady A. Tseytlin. Renormalizable Asymptotically Free Quantum Theory of Gravity. *Phys. Lett. B*, 104:377–381, 1981. doi:10.1016/0370-2693(81)90702-4.

[212] Dario Benedetti, Pedro F. Machado, and Frank Saueressig. Asymptotic safety in higher-derivative gravity. *Mod. Phys. Lett. A*, 24:2233–2241, 2009. doi:10.1142/S0217732309031521.

[213] Diego Buccio, John F. Donoghue, Gabriel Menezes, and Roberto Percacci. Physical running of couplings in quadratic gravity. 2024.

[214] Fay Dowker, Joe Henson, and Rafael D. Sorkin. Quantum gravity phenomenology, Lorentz invariance and discreteness. *Mod. Phys. Lett. A*, 19:1829–1840, 2004. doi:10.1142/S0217732304015026.

[215] Lydia Philpott, Fay Dowker, and Rafael D. Sorkin. Energy-momentum diffusion from spacetime discreteness. *Phys. Rev. D*, 79:124047, 2009. doi:10.1103/PhysRevD.79.124047.

[216] N. D. Birrell and P. C. W. Davies. *Quantum Fields in Curved Space*. Cambridge Monographs on Mathematical Physics. Cambridge Univ. Press, Cambridge, UK, 2 1984. ISBN 978-0-521-27858-4, 978-0-521-27858-4.

[217] Robert M. Wald. *Quantum Field Theory in Curved Space-Time and Black Hole Thermodynamics*. Chicago Lectures in Physics. University of Chicago Press, Chicago, IL, 1995. ISBN 978-0-226-87027-4.

[218] Don N Page and C.D. Geilker. Indirect evidence for quantum gravity. *Physical Review Letters*, 47(14):979, 1981.

[219] Roberto Emparan, Gary T. Horowitz, and Robert C. Myers. Exact description of black holes on branes. *JHEP*, 01:007, 2000. doi:10.1088/1126-6708/2000/01/007.

[220] Roberto Emparan, Gary T. Horowitz, and Robert C. Myers. Exact description of black holes on branes. 2. Comparison with BTZ black holes and black strings. *JHEP*, 01:021, 2000. doi:10.1088/1126-6708/2000/01/021.

[221] Roberto Emparan, Antonia Micol Frassino, and Benson Way. Quantum btz black hole. *Journal of High Energy Physics*, 2020(11), November 2020. ISSN 1029-8479. doi:10.1007/jhep11(2020)137. URL http://dx.doi.org/10.1007/JHEP11(2020)137.

[222] Stanley Deser and R. Jackiw. Three-Dimensional Cosmological Gravity: Dynamics of Constant Curvature. *Annals Phys.*, 153:405–416, 1984. doi:10.1016/0003-4916(84)90025-3.

[223] Stanley Deser and R. Jackiw. Three-Dimensional Cosmological Gravity: Dynamics of Constant Curvature. *Annals Phys.*, 153:405–416, 1984. doi:10.1016/0003-4916(84)90025-3.

[224] Maximo Banados, Claudio Teitelboim, and Jorge Zanelli. The Black hole in three-dimensional space-time. *Phys. Rev. Lett.*, 69:1849–1851, 1992. doi:10.1103/PhysRevLett.69.1849.

[225] Maximo Banados, Marc Henneaux, Claudio Teitelboim, and Jorge Zanelli. Geometry of the (2+1) black hole. *Phys. Rev. D*, 48:1506–1525, 1993. doi:10.1103/PhysRevD.48.1506. [Erratum: Phys.Rev.D 88, 069902 (2013)].

[226] S. F. Ross and Robert B. Mann. Gravitationally collapsing dust in (2+1)-dimensions. *Phys. Rev. D*, 47:3319–3322, 1993. doi:10.1103/PhysRevD.47.3319.

[227] Raphael Bousso, Alexander Maloney, and Andrew Strominger. Conformal vacua and entropy in de Sitter space. *Phys. Rev. D*, 65:104039, 2002. doi:10.1103/PhysRevD.65.104039.

[228] Mu-In Park. Statistical entropy of three-dimensional Kerr-de Sitter space. *Phys. Lett. B*, 440:275–282, 1998. doi:10.1016/S0370-2693(98)01119-8.

[229] Alan R. Steif. The Quantum stress tensor in the three-dimensional black hole. *Phys. Rev. D*, 49:585–589, 1994. doi:10.1103/PhysRevD.49.R585.

[230] Kiyoshi Shiraishi and Takuya Maki. Quantum fluctuation of stress tensor and black holes in three dimensions. *Phys. Rev. D*, 49:5286–5294, 1994. doi:10.1103/PhysRevD.49.5286.

[231] Gilad Lifschytz and Miguel Ortiz. Scalar field quantization on the (2+1)-dimensional black hole background. *Phys. Rev. D*, 49:1929–1943, 1994. doi:10.1103/PhysRevD.49.1929.

[232] Cristian Martinez and Jorge Zanelli. Back reaction of a conformal field on a three-dimensional black hole. *Phys. Rev. D*, 55:3642–3646, 1997. doi:10.1103/PhysRevD.55.3642.

[233] Marc Casals, Alessandro Fabbri, Cristián Martínez, and Jorge Zanelli. Quantum dress for a naked singularity. *Phys. Lett. B*, 760:244–248, 2016. doi:10.1016/j.physletb.2016.06.044.

[234] Sung-Won Kim and Kip S. Thorne. Do vacuum fluctuations prevent the creation of closed timelike curves? *Phys. Rev. D*, 43:3929–3947, Jun 1991. doi:10.1103/PhysRevD.43.3929. URL https://link.aps.org/doi/10.1103/PhysRevD.43.3929.

[235] S. J. Avis, C. J. Isham, and D. Storey. Quantum field theory in anti-de sitter space-time. *Phys. Rev. D*, 18:3565–3576, Nov 1978. doi:10.1103/PhysRevD.18.3565. URL https://link.aps.org/doi/10.1103/PhysRevD.18.3565.

[236] S. M. Christensen. Vacuum Expectation Value of the Stress Tensor in an Arbitrary Curved Background: The Covariant Point Separation Method. *Phys. Rev. D*, 14:2490–2501, 1976. doi:10.1103/PhysRevD.14.2490.

[237] S. S. Gubser, Igor R. Klebanov, and Alexander M. Polyakov. Gauge theory correlators from noncritical string theory. *Phys. Lett. B*, 428:105–114, 1998. doi:10.1016/S0370-2693(98)00377-3.

[238] Edward Witten. Anti-de Sitter space and holography. *Adv. Theor. Math. Phys.*, 2:253–291, 1998.

[239] Massimo Bianchi, Daniel Z. Freedman, and Kostas Skenderis. Holographic renormalization. *Nuclear Physics B*, 631(1–2):159–194, June 2002. ISSN 0550-3213. doi:10.1016/s0550-3213(02)00179-7. URL http://dx.doi.org/10.1016/S0550-3213(02)00179-7.

[240] Charles Fefferman and C. Robin Graham. The ambient metric. *Ann. Math. Stud.*, 178:1–128, 2011.

[241] Henriette Elvang and Marios Hadjiantonis. A Practical Approach to the

Hamilton-Jacobi Formulation of Holographic Renormalization. *JHEP*, 06:046, 2016. doi:10.1007/JHEP06(2016)046.

[242] Pablo Bueno, Roberto Emparan, and Quim Llorens. Higher-curvature Gravities from Braneworlds and the Holographic c-theorem. 4 2022.

[243] Sebastian de Haro, Kostas Skenderis, and Sergey N. Solodukhin. Gravity in warped compactifications and the holographic stress tensor. *Class. Quant. Grav.*, 18:3171–3180, 2001. doi:10.1088/0264-9381/18/16/307.

[244] W. Israel. Singular hypersurfaces and thin shells in general relativity. *Nuovo Cim. B*, 44S10:1, 1966. doi:10.1007/BF02710419. [Erratum: Nuovo Cim.B 48, 463 (1967)].

[245] Hong Zhe Chen, Robert C. Myers, Dominik Neuenfeld, Ignacio A. Reyes, and Joshua Sandor. Quantum Extremal Islands Made Easy, Part I: Entanglement on the Brane. *JHEP*, 10:166, 2020. doi:10.1007/JHEP10(2020)166.

[246] Roberto Emparan. Black hole entropy as entanglement entropy: A Holographic derivation. *JHEP*, 06:012, 2006. doi:10.1088/1126-6708/2006/06/012.

[247] Robert C. Myers, Razieh Pourhasan, and Michael Smolkin. On Spacetime Entanglement. *JHEP*, 06:013, 2013. doi:10.1007/JHEP06(2013)013.

[248] M. J. Duff and James T. Liu. Complementarity of the Maldacena and Randall-Sundrum pictures. *Phys. Rev. Lett.*, 85:2052–2055, 2000. doi:10.1088/0264-9381/18/16/310.

[249] M. J. Duff. Quantum corrections to the schwarzschild solution. *Phys. Rev. D*, 9:1837–1839, 1974. doi:10.1103/PhysRevD.9.1837.

[250] Ana Climent, Roberto Emparan, and Robie A. Hennigar. Chemical Potential and Charge in Quantum Black Holes. 4 2024.

[251] Norihiro Tanahashi and Takahiro Tanaka. Black holes in braneworld models. *Prog. Theor. Phys. Suppl.*, 189:227–268, 2011. doi:10.1143/PTPS.189.227.

[252] Marco Bruni, Cristiano Germani, and Roy Maartens. Gravitational collapse on the brane. *Phys. Rev. Lett.*, 87:231302, 2001. doi:10.1103/PhysRevLett.87.231302.

[253] Takahiro Tanaka. Classical black hole evaporation in Randall-Sundrum infinite brane world. *Prog. Theor. Phys. Suppl.*, 148:307–316, 2003. doi:10.1143/PTPS.148.307.

[254] Hideaki Kudoh, Takahiro Tanaka, and Takashi Nakamura. Small localized black holes in brane world: Formulation and numerical method. *Phys. Rev. D*, 68:024035, 2003. doi:10.1103/PhysRevD.68.024035.

[255] Hideaki Kudoh. Six-dimensional localized black holes: Numerical solutions. *Phys. Rev. D*, 69:104019, 2004. doi:10.1103/PhysRevD.70.029901. [Erratum: Phys.Rev.D 70, 029901 (2004)].

[256] A. Liam Fitzpatrick, Lisa Randall, and Toby Wiseman. On the existence and dynamics of braneworld black holes. *JHEP*, 11:033, 2006. doi:10.1088/1126-6708/2006/11/033.

[257] Hirotaka Yoshino. On the existence of a static black hole on a brane. *JHEP*, 01:068, 2009. doi:10.1088/1126-6708/2009/01/068.

[258] Pau Figueras and Toby Wiseman. Gravity and large black holes in Randall-Sundrum II braneworlds. *Phys. Rev. Lett.*, 107:081101, 2011. doi:10.1103/PhysRevLett.107.081101.

[259] Roberto Emparan, Raimon Luna, Ryotaku Suzuki, Marija Tomašević, and Benson Way. Holographic duals of evaporating black holes. *JHEP*, 05:182, 2023. doi:10.1007/JHEP05(2023)182.

[260] Roberto Emparan, Gary T. Horowitz, and Robert C. Myers. Black holes radiate mainly on the brane. *Phys. Rev. Lett.*, 85:499–502, 2000. doi:10.1103/PhysRevLett.85.499.

[261] J. F. Plebanski and M. Demianski. Rotating, charged, and uniformly accelerating mass in general relativity. *Annals Phys.*, 98:98–127, 1976. doi:10.1016/0003-4916(76)90240-2.

[262] J. B. Griffiths, P. Krtous, and J. Podolsky. Interpreting the C-metric. *Class. Quant. Grav.*, 23:6745–6766, 2006. doi:10.1088/0264-9381/23/23/008.

[263] Michael Appels, Ruth Gregory, and David Kubiznak. Thermodynamics of Accelerating Black Holes. *Phys. Rev. Lett.*, 117(13):131303, 2016. doi:10.1103/PhysRevLett.117.131303.

[264] Roberto Emparan, Juan F. Pedraza, Andrew Svesko, Marija Tomašević, and Manus R. Visser. Black holes in ds3. *Journal of High Energy Physics*, 2022(11), November 2022. ISSN 1029-8479. doi:10.1007/jhep11(2022)073. URL http://dx.doi.org/10.1007/JHEP11(2022)073.

[265] Sera Cremonini, James T. Liu, and Phillip Szepietowski. Higher Derivative Corrections to R-charged Black Holes: Boundary Counterterms and the Mass-Charge Relation. *JHEP*, 03:042, 2010. doi:10.1007/JHEP03(2010)042.

[266] Vijay Balasubramanian, Jan de Boer, and Djordje Minic. Mass, entropy and holography in asymptotically de Sitter spaces. *Phys. Rev. D*, 65:123508, 2002. doi:10.1103/PhysRevD.65.123508.

[267] Brian P. Dolan. The definition of mass in asymptotically de Sitter space-times. *Class. Quant. Grav.*, 36(7):077001, 2019. doi:10.1088/1361-6382/ab0bdb.

[268] G. W. Gibbons and S. W. Hawking. Cosmological Event Horizons, Thermodynamics, and Particle Creation. *Phys. Rev. D*, 15:2738–2751, 1977. doi:10.1103/PhysRevD.15.2738.

[269] I. S. Booth and Robert B. Mann. Cosmological pair production of charged and rotating black holes. *Nucl. Phys. B*, 539:267–306, 1999. doi:10.1016/S0550-3213(98)00756-1.

[270] Arindam Bhattacharjee and Muktajyoti Saha. JT gravity from holographic reduction of 3D asymptotically flat spacetime. *JHEP*, 01:138, 2023. doi:10.1007/JHEP01(2023)138.

[271] James M. Bardeen and Gary T. Horowitz. The Extreme Kerr throat geometry: A Vacuum analog of AdS(2) x S**2. *Phys. Rev. D*, 60:104030, 1999. doi:10.1103/PhysRevD.60.104030.

[272] Thomas Hartman, Keiju Murata, Tatsuma Nishioka, and Andrew Strominger. CFT Duals for Extreme Black Holes. *JHEP*, 04:019, 2009. doi:10.1088/1126-6708/2009/04/019.

[273] Hidekazu Nariai. On a new cosmological solution of einstein's field equations of gravitation. *General relativity and gravitation*, 31:963 – 971, 06 1999. doi:10.1023/A:1026602724948.

[274] Paul H. Ginsparg and Malcolm J. Perry. Semiclassical Perdurance of de Sitter Space. *Nucl. Phys. B*, 222:245–268, 1983. doi:10.1016/0550-3213(83)90636-3.

[275] Vitor Cardoso, Oscar J. C. Dias, and Jose P. S. Lemos. Nariai, Bertotti-Robinson and anti-Nariai solutions in higher dimensions. *Phys. Rev. D*, 70:024002, 2004. doi:10.1103/PhysRevD.70.024002.

[276] Dionysios Anninos and Thomas Hartman. Holography at an Extremal De Sitter Horizon. *JHEP*, 03:096, 2010. doi:10.1007/JHEP03(2010)096.

[277] Y. Nutku. Exact solutions of topologically massive gravity with a cosmological constant. *Class. Quant. Grav.*, 10:2657–2661, 1993. doi:10.1088/0264-9381/10/12/022.

[278] Dionysios Anninos. Sailing from Warped AdS(3) to Warped dS(3) in Topologically Massive Gravity. *JHEP*, 02:046, 2010. doi:10.1007/JHEP02(2010)046.

[279] Dionysios Anninos, Sophie de Buyl, and Stephane Detournay. Holography For a De Sitter-Esque Geometry. *JHEP*, 05:003, 2011. doi:10.1007/JHEP05(2011)003.

[280] S. Deser and A. Schwimmer. Geometric classification of conformal anomalies in arbitrary dimensions. *Physics Letters B*, 309(3–4):279–284, July 1993. ISSN 0370-2693. doi:10.1016/0370-2693(93)90934-a. URL http://dx.doi.org/10.1016/0370-2693(93)90934-A.

[281] Hideaki Kudoh and Yasunari Kurita. Thermodynamics of four-dimensional black objects in the warped compactification. *Phys. Rev. D*, 70:084029, 2004. doi:10.1103/PhysRevD.70.084029.

[282] Batoul Banihashemi and Ted Jacobson. Thermodynamic ensembles with cosmological horizons. *JHEP*, 07:042, 2022. doi:10.1007/JHEP07(2022)042.

[283] Batoul Banihashemi, Ted Jacobson, Andrew Svesko, and Manus Visser. The minus sign in the first law of de Sitter horizons. *JHEP*, 01:054, 2023. doi:10.1007/JHEP01(2023)054.

[284] Andrew Svesko, Evita Verheijden, Erik P. Verlinde, and Manus R. Visser. Quasi-local energy and microcanonical entropy in two-dimensional nearly de Sitter gravity. *JHEP*, 08:075, 2022. doi:10.1007/JHEP08(2022)075.

[285] Dionysios Anninos and Eleanor Harris. Interpolating geometries and the stretched dS_2 horizon. *JHEP*, 11:166, 2022. doi:10.1007/JHEP11(2022)166.

[286] Robert M. Wald. Black hole entropy is the Noether charge. *Phys. Rev. D*, 48(8):R3427–R3431, 1993. doi:10.1103/PhysRevD.48.R3427.

[287] Juan F. Pedraza, Andrew Svesko, Watse Sybesma, and Manus R. Visser. Semi-classical thermodynamics of quantum extremal surfaces in Jackiw-Teitelboim gravity. *JHEP*, 12: 134, 2021. doi:10.1007/JHEP12(2021)134.

[288] Edward K. Morvan, Jan Pieter van der Schaar, and Manus R. Visser. On the Euclidean Action of de Sitter Black Holes and Constrained Instantons. 3 2022.

[289] Patrick Draper and Szilard Farkas. de Sitter black holes as constrained states in the Euclidean path integral. *Phys. Rev. D*, 105(12):126022, 2022. doi:10.1103/PhysRevD.105.126022.

[290] Edward K. Morvan, Jan Pieter van der Schaar, and Manus R. Visser. Action, entropy and pair creation rate of charged black holes in de Sitter space. 12 2022.

[291] Claudia L. Clarke and Ian J. Ford. Stochastic entropy production associated with quantum measurement in a framework of markovian quantum state diffusion. *Entropy*, 26(12):1024, November 2024. ISSN 1099-4300. doi:10.3390/e26121024. URL http://dx.doi.org/10.3390/e26121024.

[292] L. M. Sieberer, A. Chiocchetta, A. Gambassi, U. C. Täuber, and S. Diehl. Thermodynamic equilibrium as a symmetry of the schwinger-keldysh action. *Physical Review B*, 92(13), October 2015. ISSN 1550-235X. doi:10.1103/physrevb.92.134307. URL http://dx.doi.org/10.1103/PhysRevB.92.134307.

[293] A. O. Caldeira and A. J. Leggett. Influence of dissipation on quantum tunneling in macroscopic systems. *Phys. Rev. Lett.*, 46:211–214, Jan 1981. doi:10.1103/PhysRevLett.46.211. URL https://link.aps.org/doi/10.1103/PhysRevLett.46.211.

[294] K. S. Stelle. Renormalization of higher-derivative quantum gravity. *Phys. Rev. D*, 16:

953–969, Aug 1977. doi:10.1103/PhysRevD.16.953. URL https://link.aps.org/doi/10.1103/PhysRevD.16.953.

[295] Michael E. Fisher. Renormalization group theory: Its basis and formulation in statistical physics. *Rev. Mod. Phys.*, 70:653–681, Apr 1998. doi:10.1103/RevModPhys.70.653. URL https://link.aps.org/doi/10.1103/RevModPhys.70.653.

[296] Isaac Layton. *Effective theories of classical-quantum dynamics*. PhD thesis, University College London, University Coll. London, 2025.

[297] Tetsuya Misawa. Conserved quantities and symmetries related to stochastic dynamical systems. *Annals of the Institute of Statistical Mathematics*, 51(4):779–802, 1999. doi:10.1023/A:1004095516648. URL https://doi.org/10.1023/A:1004095516648.

[298] S Albeverio and Shao-Ming Fei. A remark on symmetry of stochastic dynamical systems and their conserved quantities. *Journal of Physics A: Mathematical and General*, 28(22): 6363, 1995. doi:10.1088/0305-4470/28/22/012. URL https://dx.doi.org/10.1088/0305-4470/28/22/012.

[299] Jonathan Oppenheim and Benni Reznik. Fundamental destruction of information and conservation laws. 2009. URL https://arxiv.org/abs/0902.2361.

[300] Qiao Huang and Jean-Claude Zambrini. From second-order differential geometry to stochastic geometric mechanics. *Journal of Nonlinear Science*, 33(4), June 2023. ISSN 1432-1467. doi:10.1007/s00332-023-09917-x. URL http://dx.doi.org/10.1007/s00332-023-09917-x.

[301] Joohan Lee and Robert M. Wald. Local symmetries and constraints. *Journal of Mathematical Physics*, 31(3):725–743, 6/20/2025 1990. doi:10.1063/1.528801. URL https://doi.org/10.1063/1.528801.

[302] Nicolas Gisin. Weinberg's non-linear quantum mechanics and supraluminal communications. *Physics Letters A*, 143(1-2):1–2, 1990.

[303] Joseph Polchinski. Weinberg's nonlinear quantum mechanics and the einstein-podolsky-rosen paradox. *Physical Review Letters*, 66(4):397, 1991.

[304] J. W. Moffat. Stochastic gravity. *Physical Review D*, 56(10):6264–6277, November 1997. ISSN 1089-4918. doi:10.1103/physrevd.56.6264. URL http://dx.doi.org/10.1103/PhysRevD.56.6264.

[305] Marco de Cesare, Fedele Lizzi, and Mairi Sakellariadou. Effective cosmological constant induced by stochastic fluctuations of newton's constant. *Physics Letters B*, 760:498–501, 2016. ISSN 0370-2693. doi:https://doi.org/10.1016/j.physletb.2016.07.015. URL https://www.sciencedirect.com/science/article/pii/S0370269316303562.

[306] Andrew Chamblin, Roberto Emparan, Clifford V. Johnson, and Robert C. Myers. Charged AdS black holes and catastrophic holography. *Phys. Rev. D*, 60:064018, 1999. doi:10.1103/PhysRevD.60.064018.

[307] Ana Climent, Robie A. Hennigar, Emanuele Panella, and Andrew Svesko. Nucleation of charged quantum de-Sitter$_3$ black holes. *JHEP*, 05:086, 2025. doi:10.1007/JHEP05(2025)086.

[308] J. D. Bekenstein. Exact solutions of Einstein conformal scalar equations. *Annals Phys.*, 82:535–547, 1974. doi:10.1016/0003-4916(74)90124-9.

[309] J. D. Bekenstein. Black Holes with Scalar Charge. *Annals Phys.*, 91:75–82, 1975. doi:10.1016/0003-4916(75)90279-1.

[310] C. Charmousis, Theodoros Kolyvaris, and E. Papantonopoulos. Charged C-metric with conformally coupled scalar field. *Class. Quant. Grav.*, 26:175012, 2009. doi:10.1088/0264-9381/26/17/175012.

[311] Andres Anabalon and Hideki Maeda. New Charged Black Holes with Conformal Scalar Hair. *Phys. Rev. D*, 81:041501, 2010. doi:10.1103/PhysRevD.81.041501.

[312] Mohamed Anber and Lorenzo Sorbo. New exact solutions on the Randall-Sundrum 2-brane: lumps of dark radiation and accelerated black holes. *JHEP*, 07:098, 2008. doi:10.1088/1126-6708/2008/07/098.

[313] Jiri Podolsky and Marcello Ortaggio. Robinson-Trautman spacetimes in higher dimensions. *Class. Quant. Grav.*, 23:5785–5797, 2006. doi:10.1088/0264-9381/23/20/002.

[314] Shih-Hao Ho, Wei Li, Feng-Li Lin, and Bo Ning. Quantum decoherence with holography. *Journal of High Energy Physics*, 2014(1), January 2014. ISSN 1029-8479. doi:10.1007/jhep01(2014)170. URL http://dx.doi.org/10.1007/JHEP01(2014)170.

[315] Chandan Jana, R. Loganayagam, and Mukund Rangamani. Open quantum systems and schwinger-keldysh holograms. *Journal of High Energy Physics*, 2020(7), July 2020. ISSN 1029-8479. doi:10.1007/jhep07(2020)242. URL http://dx.doi.org/10.1007/JHEP07(2020)242.

[316] Stefano Antonini, Gregory Bentsen, ChunJun Cao, Jonathan Harper, Shao-Kai Jian, and Brian Swingle. Holographic measurement and bulk teleportation. *Journal of High Energy Physics*, 2022(12), December 2022. ISSN 1029-8479. doi:10.1007/jhep12(2022)124. URL http://dx.doi.org/10.1007/JHEP12(2022)124.

Appendix A

Brownian motion

SDEs perspective

As an illustrative example of the results presented here, consider a particle undergoing Brownian motion:

$$\ddot{q} = \xi(t) \ , \tag{A.1}$$

where:

$$\mathbb{E}[\xi(t)] = 0 \ , \qquad \mathbb{E}[\xi(t)\xi(t')] = D\delta(t - t') \ . \tag{A.2}$$

We initialise the state at $t = t_0$ such that $q(t_0) = 0$ and $\dot{q}(t_0) = 0$. Essentially:

$$P(q, \dot{q}, t_0) = \delta(q)\delta(\dot{q}) \ . \tag{A.3}$$

We then let the system evolve following Equation A.1 up to some future time t. The covariance of the stochastic process is then defined as:

$$C(t, s) = \mathbb{E}[q(t), q(s)|q(t_0) = \dot{q}(t_0) = 0] \ . \tag{A.4}$$

Given a realisation of the stochastic field ξ, we can reconstruct the trajectory of the Brownian particle by simply convoluting with the retarded Green's function of the equation of motion:

$$q(t) = \int dt' G_R(t, t')\xi(t')\theta(t' - t_0) \ , \tag{A.5}$$

where the theta function is there to impose the BC's and:

$$G_R(t, t') = \theta(t - t')(t - t') \ . \tag{A.6}$$

Therefore, given the boundary conditions, we simply have (assume $t \geq s$):

$$C(t,s|t_0) = \int_{t_0}^{\infty} d\tau \int_{t_0}^{\infty} d\tau' G_R(t,\tau) G_R(s,\tau') \mathbf{E}[\xi(\tau)\xi(\tau')] \tag{A.7}$$

$$= D \int_{t_0}^{\infty} d\tau \theta(t-\tau)\theta(s-\tau)(t-\tau)(s-\tau) \tag{A.8}$$

Since $t \geq s$, the first θ-function is irrelevant, whilst the second one sets the upper integration limit:

$$C(t,s|t_0) = D \int_{t_0}^{s} d\tau \; G_R(t,\tau) G_R(s,\tau) \tag{A.9}$$

$$= D \int_{t_0}^{s} d\tau (t-\tau)(s-\tau) \tag{A.10}$$

$$= \frac{D}{6}(s-t_0)^2(3t-s-2t_0) \; , \tag{A.11}$$

or, in explicit powers of s:

$$C(t,s) = \frac{D}{6}[-s^3 + 3ts^2 + 3st_0(t_0-2t) + t_0^2(3t-2t_0)] \; . \tag{A.12}$$

The variance, instead:

$$V(t;t_0) \equiv C(t,t;t_0) = \frac{D}{3}(t^3 - 3t_0t^2 + 3t_0^2t - t_0^3) \; . \tag{A.13}$$

Clearly, as $t_0 \to -\infty$ both variance and covariance diverge.

Fourier representation of the propagator

We know derive the same result by performing the convolution in Fourier domain, uncovering the pole prescription of the propagator in the complex plane. Let's begin with the Fourier representation of the retarded propagator. This is given by:

$$G_R(t-s) = \int \frac{d\omega}{2\pi} \mathcal{G}_R(\omega) e^{-i\omega(t-s)} \; , \tag{A.14}$$

where:

$$\mathcal{G}_R(\omega) = \frac{-1}{(\omega + i\epsilon)^2} \; . \tag{A.15}$$

To see this, first note that for $t < s$, the Fourier integral vanishes since the complex contour of integration (closing from above, to make the contribution from the semicircle limit to zero).

For $t > s$, however, the contour encloses the $\omega = -i\epsilon$ pole of order $p = 2$. Using the residue theorem we see:

$$\int \frac{d\omega}{2\pi} \frac{-1}{(\omega + i\epsilon)^2} e^{-i\omega(t-s)} = -i\text{Res}\left[\frac{1}{(\omega + i\epsilon)^2} e^{-i\omega(t-s)}, -i\epsilon\right] \tag{A.16}$$

$$= t - s \tag{A.17}$$

Combining the two time-ordered result we indeed obtain Equation A.5.

Now, let's derive the Fourier representation of $C(t, s)$. To do this, we start from Equation A.8 and substitute the Fourier representation of the retarded propagators:

$$C(t, s|t_0) = D \int_{t_0}^{\infty} d\tau \int_{-\infty}^{\infty} \frac{d\omega}{2\pi} \int_{-\infty}^{\infty} \frac{d\omega'}{2\pi} \frac{1}{(\omega + i\epsilon)^2} \frac{1}{(\omega' + i\epsilon)^2} e^{-i\omega(t-\tau)} e^{-i\omega'(s-\tau)} \tag{A.18}$$

$$= D \int_{-\infty}^{\infty} \frac{d\omega}{2\pi} \int_{-\infty}^{\infty} \frac{d\omega'}{2\pi} \frac{1}{(\omega + i\epsilon)^2} \frac{1}{(\omega' + i\epsilon)^2} e^{-i\omega t} e^{-i\omega' s} \int_{t_0}^{\infty} d\tau e^{i(\omega+\omega')\tau} \tag{A.19}$$

$$= D \int_{-\infty}^{\infty} \frac{d\omega}{2\pi} \int_{-\infty}^{\infty} \frac{d\omega'}{2\pi} \frac{1}{(\omega + i\epsilon)^2} \frac{1}{(\omega' + i\epsilon)^2} e^{-i\omega t} e^{-i\omega' s} \int_{0}^{\infty} d\tau e^{i(\omega+\omega')(\tau+t_0)} \tag{A.20}$$

$$= D \int_{-\infty}^{\infty} \frac{d\omega}{2\pi} \int_{-\infty}^{\infty} \frac{d\omega'}{2\pi} \frac{1}{(\omega + i\epsilon)^2} \frac{1}{(\omega' + i\epsilon)^2} e^{-i\omega(t-t_0)} e^{-i\omega'(s-t_0)} \left(\pi\delta(\omega + \omega') + \mathbf{P}\frac{i}{\omega + \omega'}\right) \tag{A.21}$$

$$= \frac{1}{2} C_{\infty}(t, s) + \Delta C(t, s|t_0) \tag{A.22}$$

Here we have split the integral in the infinite time (the integral involving the delta function kills all the t_0 dependence, and is exactly half of the integral resulting from the $t_0 \to -\infty$ limit) and finite time effects. Note that here $\mathbf{P}$ indicates that the principal value of the integral needs to be extracted for such a pole.

Let's begin with:

$$C_{\infty}(t, s) = D \int_{-\infty}^{\infty} \frac{d\omega}{2\pi} \int_{-\infty}^{\infty} \frac{d\omega'}{2\pi} \frac{1}{(\omega + i\epsilon)^2} \frac{1}{(\omega' + i\epsilon)^2} e^{-i\omega(t-t_0)} e^{-i\omega'(s-t_0)} 2\pi\delta(\omega + \omega') \tag{A.23}$$

$$= D \int_{-\infty}^{\infty} \frac{d\omega}{2\pi} \frac{1}{(\omega + i\epsilon)^2} \frac{1}{(\omega - i\epsilon)^2} e^{-i\omega(t-s)} \tag{A.24}$$

$$= \int_{-\infty}^{\infty} \frac{d\omega}{2\pi} \mathcal{C}_{\infty}(\omega) e^{-i\omega(t-s)} \tag{A.25}$$

where:

$$\mathcal{C}_{\infty}(\omega) = \frac{D}{(\omega + i\epsilon)^2(\omega - i\epsilon)^2} \ . \tag{A.26}$$

Note, this is different from the Feynman mod-squared (FM2) prescription proposed in [136]. In fact, the latter is given by:

$$\mathcal{C}_{\infty}^{\text{mod2}}(\omega) = \frac{D}{(\omega^2 + i\epsilon)(\omega^2 - i\epsilon)} \neq \mathcal{C}_{\infty}(\omega) \ . \tag{A.27}$$

The biggest difference between the two prescriptions is the nature of the poles. The 2-point function obtained as convolution of 2 retarded Green's function (RM2) has two second order poles, whilst the FM2 prescription involves four simple poles.

The finite time effects, instead, are given by:

$$\begin{aligned}\Delta C(t,s|t_0) &= \mathbf{P}\int_{-\infty}^{\infty}\frac{d\omega}{2\pi}\int_{-\infty}^{\infty}\frac{d\omega'}{2\pi}\frac{iD}{(\omega+i\epsilon)^2(\omega'+i\epsilon)^2(\omega+\omega')}e^{-i\omega(t-t_0)}e^{-i\omega'(s-t_0)} \\ &= \frac{1}{2}\int_{-\infty}^{\infty}\frac{d\omega}{2\pi}\mathcal{C}_{\infty}(\omega)e^{-i\omega(t-s)} \\ &\quad - De^{-\epsilon(s-t_0)}\int_{-\infty}^{\infty}\frac{d\omega}{2\pi}\left(i(s-t_0)+\frac{1}{\omega-i\epsilon}\right)\frac{e^{-i\omega(t-t_0)}}{(\omega+i\epsilon)^2(\omega-i\epsilon)}\end{aligned} \tag{A.28}$$

Performing the inverse Fourier transform

Let's begin with the infinite time effects. For $t \geq s$ close below, picking up the double $\omega = -i\epsilon$ pole. Using the residue theorem we get:

$$C_{\infty}(t,s) = \lim_{\epsilon\to 0}\frac{e^{-\epsilon(t-s)}}{4\epsilon^2}\left(t-s+\frac{1}{\epsilon}\right) \ . \tag{A.29}$$

On the other hand:

$$\begin{aligned}De^{-\epsilon(s-t_0)}\int_{-\infty}^{\infty}\frac{d\omega}{2\pi}\left(i(s-t_0)+\frac{1}{\omega-i\epsilon}\right)\frac{1}{(\omega+i\epsilon)^2(\omega-i\epsilon)}e^{-i\omega(t-t_0)} = \\ \lim_{\epsilon\to 0}\frac{De^{-\epsilon(t+s-2t_0)}}{2\epsilon}\left[(s-t_0)\left(t-t_0+\frac{1}{2\epsilon}\right)+\frac{1}{2\epsilon}\left(t-t_0+\frac{1}{\epsilon}\right)\right] \ .\end{aligned} \tag{A.30}$$

Plugging all together and keeping terms up to $\mathcal{O}(\epsilon^0)$ we get:

$$C(t,s|t_0) = \frac{D}{6}(s-t_0)^2(3t-s-2t_0) \ . \tag{A.31}$$

This is indeed the correct solution, and no divergent term survives. Recall, once more, that here $t \geq s$ was assumed.

Appendix B

Integrals in Fourier space

We assume the field (and its conjugate momentum) is initialised on an initial slice t_0 to vanish everywhere, i.e. $\phi(\underline{x}, t_0) = \dot{\phi}(\underline{x}, t_0) = 0$. Then the covariance is given by:

$$\mathcal{C}(x,t;t_0) = D_2 \int_{t_0}^{\infty} dz_0 \int d^3z \int \frac{d^4p}{(2\pi)^4} \int \frac{d^4k}{(2\pi)^4} \frac{e^{-ip(x-z)} e^{-ik(y-z)}}{\left[(p_0+i\epsilon)^2 - E(\underline{p})^2\right]\left[(k_0+i\epsilon)^2 - E(\underline{k})^2\right]} \ . \tag{B.1}$$

Now, let's focus on the z_0 integration first:

$$\int_{t_0}^{\infty} dz_0 e^{iz_0(p_0+k_0)} = e^{i(p_0+k_0)t_0} \int_0^{\infty} d\tau e^{i\tau(p_0+k_0)} = e^{i(p_0+k_0)t_0} \left(\pi\delta(p_0+k_0) + i\frac{\mathbf{P}}{k_0+p_0}\right), \tag{B.2}$$

where the capital $\mathbf{P}$ stands for the *principal value* of the integral for the corresponding pole. The spatial z integral gives:

$$\int d^3z e^{-iz(p+k)} = (2\pi)^3 \delta(\underline{p}+\underline{k}). \tag{B.3}$$

Combining:

$$\mathcal{C}(x,t;t_0) = \frac{1}{2}\mathcal{C}_{\infty} + \bar{\mathcal{C}}, \tag{B.4}$$

where:

$$\begin{aligned} \mathcal{C}_{\infty} &= D_2 \int \frac{d^4p}{(2\pi)^4} \int \frac{d^4k}{(2\pi)^4} \frac{e^{-ipx} e^{-iky}}{\left[(p_0+i\epsilon)^2 - E(\underline{p})^2\right]\left[(k_0+i\epsilon)^2 - E(\underline{k})^2\right]} (2\pi)^4 \delta(p+k) \\ &= D_2 \int \frac{d^4p}{(2\pi)^4} \frac{e^{-ip(x-y)}}{\left[(p_0+i\epsilon)^2 - E(\underline{p})^2\right]\left[(p_0-i\epsilon)^2 - E(\underline{p})^2\right]} \ , \end{aligned} \tag{B.5}$$

whilst:

$$\begin{aligned}\bar{\mathcal{C}} &= iD_2 \int \frac{d^4p}{(2\pi)^4} \int \frac{d^4k}{(2\pi)^4} \frac{e^{-ipx}e^{-iky}}{\left[(p_0+i\epsilon)^2 - E(\underline{p})^2\right]\left[(k_0+i\epsilon)^2 - E(\underline{k})^2\right]} (2\pi)^3 \delta(\underline{p}+\underline{k}) \frac{\mathbf{P}}{p_0+k_0} \\ &= iD_2 \int \frac{d^4p}{(2\pi)^4} \int \frac{dk_0}{2\pi} \frac{e^{i\underline{p}(\underline{x}-\underline{y})}e^{-ip_0x}e^{-ik_0y}}{\left[(p_0+i\epsilon)^2 - E(\underline{p})^2\right]\left[(k_0+i\epsilon)^2 - E(\underline{p})^2\right]} \frac{\mathbf{P}}{p_0+k_0}\end{aligned} \tag{B.6}$$

Infinite-time terms

Let's first compute $\mathcal{C}_\infty$ for the massive KG field corresponding to the retarded mod-squared prescription:

$$\begin{aligned}\mathcal{C}_\infty(x,y) &= D_2 \int \frac{d^4p}{(2\pi)^4} \frac{e^{-ip(x-y)}}{[(p_0-i\epsilon)^2 - E(p)^2][(p_0+i\epsilon)^2 - E(p)^2]} \\ &= D_2 \int \frac{d^4p}{(2\pi)^4} \frac{e^{-ip(x-y)}}{(p_0+i\epsilon+E(\underline{p}))(p_0+i\epsilon-E(\underline{p}))(p_0-i\epsilon+E(\underline{p}))(p_0-i\epsilon-E(\underline{p}))}\end{aligned} \tag{B.7}$$

Throughout we assume the time ordering of the events as $x_0 \geq y_0$. This means that we close the complex contour from below (clockwise) picking up contributions from the poles in the lower-half plane. First, let's integrate over energy:

$$\begin{aligned}&\int_{-\infty}^{+\infty} \frac{dp_0}{2\pi} \frac{e^{-ip_0(x^0-y^0)}}{(p_0+i\epsilon+E(\underline{p}))(p_0+i\epsilon-E(\underline{p}))(p_0-i\epsilon+E(\underline{p}))(p_0-i\epsilon-E(\underline{p}))} \\ &= -i\left[\mathrm{Res}\left(f(p_0), p_0 = E(\underline{p}) - i\epsilon\right) + \mathrm{Res}\left(f(p_0), p_0 = -E(\underline{p}) - i\epsilon\right)\right] \\ &= \frac{-i}{-8i\epsilon E(\underline{p})} e^{-\epsilon(x^0-y^0)} \left[\frac{e^{-iE(\underline{p})(x^0-y^0)}}{E(\underline{p})-i\epsilon} + \frac{e^{-iE(\underline{p})(x^0-y^0)}}{E(\underline{p})+i\epsilon}\right] \\ &= \frac{1}{4\epsilon E(\underline{p})(E(\underline{p})^2+\epsilon^2)} e^{-\epsilon(x^0-y^0)} \left[E(\underline{p})\cos\left(E(\underline{p})(x^0-y^0)\right) + \epsilon \sin\left(E(\underline{p})(x^0-y^0)\right)\right] \ .\end{aligned} \tag{B.8}$$

Moreover, we can integrate the angular coordinates of the 3-momentum:

$$\int_0^{2\pi} d\phi \int_0^{\pi} d\theta \sin\theta \ e^{i\underline{p}(\underline{x}-\underline{y})} = \int_0^{2\pi} d\phi \int_0^{\pi} d\theta \sin\theta \ e^{ip|\underline{x}-\underline{y}|\cos\theta} = 4\pi \frac{\sin(p|\underline{x}-\underline{y}|)}{p|\underline{x}-\underline{y}|}. \tag{B.9}$$

Finally, recall the following limit:

$$\lim_{\epsilon\to 0} \frac{\epsilon}{x^2+\epsilon^2} = \pi\delta(x) \ . \tag{B.10}$$

We can now combine these results to obtain:

$$\begin{aligned}\mathcal{C}_\infty &= \frac{D_2}{8\pi^2}\frac{e^{-\epsilon(x^0-y^0)}}{|\underline{x}-\underline{y}|}\left(\frac{1}{\epsilon}I_1 + I_2\right) \\ &= \frac{D_2}{8\pi^2}\frac{1}{|\underline{x}-\underline{y}|}\left[\left(\frac{1}{\epsilon}-(x^0-y^0)\right)I_1 + I_2 + \pi\frac{(x^0-y^0)^2}{2}I_{\delta 1} - \pi(x^0-y^0)I_{\delta 2}\right] + \mathcal{O}(\epsilon)\end{aligned} \tag{B.11}$$

Here we have defined:

$$I_1 = \int_0^\infty dp \frac{p}{E(p)^2}\cos\big(E(p)(x^0-y^0)\big)\sin(p|\underline{x}-\underline{y}|), \tag{B.12}$$

$$I_2 = \int_0^\infty dp \frac{p}{E(p)^3}\sin\big(E(p)(x^0-y^0)\big)\sin(p|\underline{x}-\underline{y}|) \tag{B.13}$$

$$I_{\delta 1} = \int_0^\infty dp\ \delta(E(p))\ p\cos\big(E(p)(x^0-y^0)\big)\sin(p|\underline{x}-\underline{y}|) = 0, \tag{B.14}$$

$$I_{\delta 2} = \int_0^\infty dp\ \delta(E(p))\ \frac{p}{E(p)}\sin\big(E(p)(x^0-y^0)\big)\sin(p|\underline{x}-\underline{y}|) = 0\ . \tag{B.15}$$

Note that both $I_{\delta 1} = I_{\delta 2} = 0$ for any $m \geq 0$, since for the massive case the delta function condition is never satisfied, whilst for the $m = 0$ case at $p = 0$ the integrand is vanishing. Therefore, in the $\epsilon \to 0$ limit, the infinite-time component of the covariance is given by:

$$\mathcal{C}_\infty = \frac{D_2}{8\pi^2}\frac{1}{|\underline{x}-\underline{y}|}\left[\left(\frac{1}{\epsilon}-(x^0-y^0)\right)I_1 + I_2\right]\ . \tag{B.16}$$

We were not able to find a closed analytical solution for both I_1 and I_2 for arbitrary mass.

Finite-time contribution

Let's now compute the finite-time contributions to the two-point function. This corresponds to evaluating the following integral:

$$\tilde{\mathcal{C}} = iD_2\int d^3z \int\frac{d^4p}{(2\pi)^4}\int\frac{d^4k}{(2\pi)^4}\frac{e^{-ipx}e^{-iky}e^{i(p_0+k_0)t_0}e^{-i(\underline{p}+\underline{k}).\underline{z}}}{\left[(p_0+i\epsilon)^2-E(\underline{p})^2\right]\left[(k_0+i\epsilon)^2-E(\underline{k})^2\right]}\frac{\mathbf{P}}{k_0+p_0}\ . \tag{B.17}$$

Performing the integral and extracting the principal value one gets:

$$\tilde{\mathcal{C}} = \frac{1}{2}\mathcal{C}_\infty + \Delta\mathcal{C}\ , \tag{B.18}$$

where

$$\Delta\mathcal{C} = \frac{D_2}{2} e^{-\epsilon(y_0-t_0)} \int \frac{d^4p}{(2\pi)^4} \frac{1}{E(p)} \frac{e^{-i\underline{p}.\underline{y}} e^{-ipx} e^{ip_0 t_0}}{(p_0+i\epsilon)^2 - E(p)^2} \left[\frac{e^{-iE(p)(y_0-t_0)}}{p_0 - i\epsilon + E(p)} - \frac{e^{iE(p)(y_0-t_0)}}{p_0 - i\epsilon - E(p)} \right] . \tag{B.19}$$

Performing again the p_0 integral in the complex plane (close below, since $x_0 \geq t_0$ by construction):

$$\int \frac{dp_0}{2\pi} \frac{e^{-ip_0(x^0-t_0)}}{[(p_0+i\epsilon)^2 - E(p)^2][p_0 - i\epsilon + E(p)]} = \frac{-e^{-\epsilon(x^0-t_0)}}{4E(\underline{p})^2} \left[\frac{e^{iE(\underline{p})(x^0-t_0)}}{\epsilon} + i \frac{e^{-iE(\underline{p})(x^0-t_0)}}{E(\underline{p}) - i\epsilon} \right] \tag{B.20}$$

and

$$\int \frac{dp_0}{2\pi} \frac{e^{-ip_0(x^0-t_0)}}{[(p_0+i\epsilon)^2 - E(p)^2][p_0 - i\epsilon - E(p)]} = \frac{e^{-\epsilon(x^0-t_0)}}{4E(\underline{p})^2} \left[\frac{e^{-iE(\underline{p})(x^0-t_0)}}{\epsilon} - i \frac{e^{iE(\underline{p})(x^0-t_0)}}{E(\underline{p}) + i\epsilon} . \right] \tag{B.21}$$

We can then perform the angular integral and combine the results to obtain:

$$\Delta\mathcal{C} = -\frac{D_2}{8\pi^2} \frac{e^{-\epsilon(x_0+y_0-2t_0)}}{|\underline{x}-\underline{y}|} \int dp \frac{p}{E(p)^2} \left[\frac{1}{\epsilon} \cos\left(E(p)(x_0-y_0)\right) + \frac{E(p)}{(E(p)^2+\epsilon^2)} \sin\left(E(p)(x_0+y_0-2t_0)\right) \right.$$
$$\left. - \frac{\epsilon}{(E(p)^2+\epsilon^2)} \cos\left(E(p)(x_0+y_0-2t_0)\right) \right] \sin\left(p|\underline{x}-\underline{y}|\right) . \tag{B.22}$$

We can now expand in ϵ and take the limit $\epsilon \to 0$ to obtain:

$$\Delta\mathcal{C} = -\frac{D_2}{8\pi^2} \frac{1}{|\underline{x}-\underline{y}|} \left[\left(\frac{1}{\epsilon} - (x^0+y^0-2t_0) \right) I_1 + I_3 - \pi I_{\delta 3} - \pi(x^0+y^0-2t_0) I_{\delta 4} \right] , \tag{B.23}$$

where

$$I_3 = \int_0^\infty dp \frac{p}{E(p)^3} \sin\left(E(p)(x^0+y^0-2t_0)\right) \sin(p|\underline{x}-\underline{y}|) \tag{B.24}$$

$$I_{\delta 3} = \int_0^\infty dp\ \delta(E(p))\ \frac{p}{E(p)^2} \cos\left(E(p)(x^0+y^0-2t_0)\right) \sin(p|\underline{x}-\underline{y}|) = 0, \tag{B.25}$$

$$I_{\delta 4} = \int_0^\infty dp\ \delta(E(p)) \frac{p}{E(p)} \sin\left(E(p)(x^0+y^0-2t_0)\right) \sin(p|\underline{x}-\underline{y}|) = 0 . \tag{B.26}$$

This time around, one of the two integrals involving delta functions doesn't vanish form $m = 0$, hence the Kronecker delta $\delta_{m,0}$. Note, the I_3 integral is essentially I_2 with different time components. Therefore:

$$\Delta\mathcal{C} = -\frac{D_2}{8\pi^2} \frac{1}{|\underline{x}-\underline{y}|} \left[\left(\frac{1}{\epsilon} - (x^0+y^0-2t_0) \right) I_1 + I_3 \right] . \tag{B.27}$$

Final result

It is now time to add up the two contributions. As expected, the two $1/\epsilon$ divergent terms cancel, leaving a finite well-behaved 2-point function:

$$\begin{aligned}\mathcal{C}(x,t;t_0) &= \frac{1}{2}\mathcal{C}_\infty + \bar{\mathcal{C}} = \mathcal{C}_\infty + \Delta C \\ &= \frac{D_2}{8\pi^2}\frac{1}{|\underline{x}-\underline{y}|}\left[2(y^0-t_0)I_1 + I_2 - I_3\right] \ .\end{aligned} \tag{B.28}$$

Massless case

In the massless limit, the relevant integrals simplify greatly. First, consider:

$$\begin{aligned}\lim_{m\to 0} I_1 &= |\underline{x}-\underline{y}|\int_0^\infty dp\ \cos(p(x^0-y^0))\mathrm{sinc}(p|\underline{x}-\underline{y}|) \\ &= \frac{\pi}{4}\left[\mathrm{sign}(x^0-y^0+|\underline{x}-\underline{y}|) - \mathrm{sign}(x^0-y^0-|\underline{x}-\underline{y}|)\right] \\ &= \frac{\pi}{2}\Theta(-s^2)\end{aligned} \tag{B.29}$$

where $\Theta(x)$ is the Heaviside step function and $s^2 = \Delta t^2 - \Delta x^2$ is the spacetime interval.

On the other hand:

$$\begin{aligned}\lim_{m\to 0} I_2 &= (x^0-y^0)|\underline{x}-\underline{y}|\int_0^\infty dp\ \mathrm{sinc}(p(x^0-y^0))\mathrm{sinc}(p|\underline{x}-\underline{y}|) \\ &= \frac{\pi(x^0-y^0)|\underline{x}-\underline{y}|}{|x^0-y^0+|\underline{x}-\underline{y}|| + |x^0-y^0-|\underline{x}-\underline{y}||} \\ &= \frac{\pi}{2}|\underline{x}-\underline{y}|\Theta(s^2) + \frac{\pi}{2}(x^0-y^0)\Theta(-s^2)\end{aligned} \tag{B.30}$$

and, similarly

$$\begin{aligned}\lim_{m\to 0} I_3 &= (x^0+y^0-2t_0)|\underline{x}-\underline{y}|\int_0^\infty dp\ \mathrm{sinc}(p(x^0+y^0-2t_0))\mathrm{sinc}(p|\underline{x}-\underline{y}|) \\ &= \frac{\pi(x^0+y^0-2t_0)|\underline{x}-\underline{y}|}{|x^0+y^0-2t_0+|\underline{x}-\underline{y}|| + |x^0+y^0-2t_0-|\underline{x}-\underline{y}||} \\ &= \frac{\pi}{2}|\underline{x}-\underline{y}|\Theta(x^0+y^0-2t_0-|\underline{x}-\underline{y}|) + \frac{\pi}{2}(x^0+y^0-2t_0)\Theta(-(x^0+y^0-2t_0)+|\underline{x}-\underline{y}|) \ .\end{aligned} \tag{B.31}$$

Finally, for most applications, we will be interested in the large y^0-t_0 limit, we can effectively replace the latter integral by:

$$\lim_{m\to 0} I_3 = \frac{\pi}{2}|\underline{x}-\underline{y}| \ . \tag{B.32}$$

By noting that for time-like separated events $x^0 + y^0 - 2t_0 > |\underline{x} - \underline{y}|$, we can combine all the theta-functions conditions into the following simpler result:

$$\begin{aligned}\mathcal{C}_0(x, y; t_0) &= \frac{1}{2}\mathcal{C}_\infty + \bar{\mathcal{C}} = \mathcal{C}_\infty + \Delta C \\ &= \frac{D_2}{16\pi}\left(\frac{(x^0 + y^0 - 2t_0)}{|\underline{x} - \underline{y}|} - 1\right)\Theta(-s^2)\Theta(x^0 + y^0 - 2t_0 - |\underline{x} - \underline{y}|) \ .\end{aligned} \tag{B.33}$$

Spatial gradient

The two-point function of the spatial gradient of the field is easily computed by differentiating $\mathcal{C}$ directly, thanks to the linearity of the expectation value. By carefully handling the derivatives of the distributions, we get three terms, two of which concentrated on the lightcone (due to the derivatives of the theta function). In particular:

$$\begin{aligned}\mathbb{E}[\partial_i\phi(x)\partial_j\phi(y)] =& \frac{D_2}{16\pi}\frac{(x^0 + y^0 - 2t_0)}{|\underline{x} - \underline{y}|}\left(\frac{\delta^i_j}{|\underline{x} - \underline{y}|^2} - \frac{3(x_i - y_i)(x_j - y_j)}{|\underline{x} - \underline{y}|^4}\right)\Theta(-s^2_{xy}) \\ &+ \frac{D_2}{4\pi}\frac{(x^0 + y^0 - 2t_0)}{|\underline{x} - \underline{y}|}(x_i - y_i)(x_j - y_j)\delta(-s^2_{xy}) \\ &- \left(\frac{D_2}{16\pi}\frac{(x^0 + y^0 - 2t_0)}{|\underline{x} - \underline{y}|} - 1\right)\left(2\delta(-s^2_{xy})\delta_{ij} + 4\delta'(-s^2_{xy})(x_i - y_i)(x_j - y_j)\right) \ ,\end{aligned} \tag{B.34}$$

where we have purposedly ignored the Θ-function related to the initial conditions for simplicity, as it is irrelevant in most situations of interest – t_0 is much larger than the typical scale of any Earth-based experiment. However, if we are only interested in the coincident limit (and in the sum over all directions), the solution greatly simplifies. In particular, by using the standard relation:

$$\nabla^2_x\frac{1}{|\underline{x} - \underline{y}|} = -4\pi\delta^{(3)}(\underline{x} - \underline{y}) \ , \tag{B.35}$$

we obtain (recalling the minus sign for the spatial contractions in this signature):

$$\begin{aligned}\mathbb{E}[\partial_i\phi(x)\partial^i\phi(y)] =& \frac{D_2}{16\pi}(x^0 + y^0 - 2t_0)\left(2\frac{\delta(-s^2_{xy})}{|\underline{x} - \underline{y}|} - 4\pi\delta^{(3)}(|\underline{x} - \underline{y}|)\Theta(-s^2_{xy})\right) \\ &+ \frac{D_2}{16\pi}\left(6\delta(-s^2_{xy}) + 4|\underline{x} - \underline{y}|^2\delta'(-s^2_{xy})\right) \ .\end{aligned} \tag{B.36}$$

In the non-relativistic limit:

$$\delta(-s^2_{xy}) \to \frac{\delta(|\underline{x} - \underline{y}|)}{|\underline{x} - \underline{y}|} \ , \tag{B.37}$$

and $r^2\delta'(r^2) = 0$ when integrated against any smooth test-function, whilst we always have:

$$\delta^{(3)}(\underline{x} - \underline{y}) = \frac{\delta(|\underline{x} - \underline{y}|)}{4\pi|\underline{x} - \underline{y}|^2} \ . \tag{B.38}$$

Therefore, in the non-relativistic limit we get the following covariance for the gradient of the field:

$$\mathbb{E}[\partial_i\phi(x)\partial^i\phi(y)] = \frac{D_2 T}{8\pi}\frac{\delta(|\underline{x} - \underline{y}|)}{|\underline{x} - \underline{y}|^2} = \frac{D_2 T}{2}\delta^{(3)}(\underline{x} - \underline{y}) \ , \tag{B.39}$$

where we have kept only the leading term in $T \equiv -t_0$, i.e. we assume the diffusive evolution has been going on for much larger timescales than those related to any local observation.

Appendix C

Limits of qKdS

Here we provide details leading to the various limiting geometries of the qKdS black hole described in the main text. Our analysis primarily follows [269]. First let us explore the horizon structure of the naive metric (7.23), corresponding to the roots of the blackening factor $H(r)$. Introduce a function $Q(r) \equiv r^2 H(r)$ such that the roots of Q coincide with the roots of H. Since Q is a quartic, it will have either four, two, or zero real roots. Requiring Q to have four real roots, three of which are positive and correspond to the horizons $r_c \geq r_+ \geq r_-$, imposes restrictions on the physical parameters of the black hole solution, namely, a and μ. As described in the main text, we can express the parameters a^2, R_3^2 and $\mu\ell$ in terms of the three horizons $r_\pm$ and r_c.[1] The negative root of Q, denoted r_n and sometimes called the 'negative horizon', lies behind the singularity at $r = 0$.

With these roots, we factorize Q as

$$Q(r) = -\frac{1}{R_3^2}(r - r_c)(r - r_+)(r - r_-)(r - r_n) \, . \tag{C.1}$$

It proves convenient to introduce parameters d, δ, e and ϵ to parameterize the roots of Q,

$$\begin{aligned} r_c &= e + \epsilon \, , \quad r_+ = e - \epsilon \, , \\ r_- &= d + \delta \, , \quad r_n = d - \delta \, . \end{aligned} \tag{C.2}$$

[1] For example, to reexpress R_3^2, first subtract $r_+ H(r_+) = 0$ from $r_c H(r_c) = 0$, and similarly subtract $r_- H(r_-) = 0$ from $r_+ H(r_+) = 0$. Subtracting the first of the resultant expressions from the other and rearranging one recovers (7.39).

Since r_c and $r_\pm$ are all non-negative, we immediately learn e and d are real while δ and ϵ must be non-negative real numbers. Expressing $Q(r)$ in terms of these parameters, one fixes $d = -e$ to eliminate the r^3 contribution. Additionally, the root ordering condition, $r_c \geq r_+ \geq r_-$ and $r_n = -(r_+ + r_- + r_c) < 0$ further imposes

$$0 \leq \epsilon < e \,, \quad e \leq \delta < 2e - \epsilon \,, \tag{C.3}$$

allowing us to write

$$Q = -\frac{1}{R_3^2}((r-e)^2 - \epsilon^2)((r+e)^2 - \delta^2) \,. \tag{C.4}$$

Moreover, the parameters R_3^2, a^2 and $\mu\ell$ (7.39) become

$$\begin{aligned} R_3^2 &= 2e^2 + \epsilon^2 + \delta^2 \,, \\ a^2 &= -\frac{(e-\delta)(e+\delta)(e-\epsilon)(e+\epsilon)}{2e^2+\epsilon^2+\delta^2} \,, \\ \mu\ell &= \frac{2e(\delta-e)(\delta+e)}{2e^2+\epsilon^2+\delta^2} \,. \end{aligned} \tag{C.5}$$

Notice from the root ordering (C.3) that $a^2 \geq 0$ and $\mu \geq 0$.

There are multiple cases when Q has degenerate roots, or degenerate horizons. These include: (i) the extremal or 'cold' limit, where $r_+ = r_-$; (ii) the (rotating) Nariai limit, where $r_c = r_+$, and (iii) the 'ultracold' limit, when $r_c = r_+ = r_-$ coincide. Each are explored below.

Extremal limit

The extremal limit corresponds to when the inner and outer black hole horizons coincide, $r_+ = r_-$. In this limit, the temperature of the outer black hole horizon vanishes, $T_+ = 0$, and is thus sometimes called the 'cold' black hole. Given the parameterization (C.2), $r_+ = r_-$ imposes $\delta = 2e - \epsilon$. Consequently, the parameters (C.5) become

$$a^2 = \frac{1}{R_3^2}(e-\epsilon)^2(3e-\epsilon)(e+\epsilon) \,, \quad \mu\ell = \frac{8e^2(e-\epsilon)}{R_3^2} \,, \tag{C.6}$$

with $R_3^2 = 2(3e^2 - 2e\epsilon + \epsilon^2)$, and

$$Q(r) = -\frac{1}{R_3^2}(r - (e+\epsilon))(r - e + \epsilon)^2(r + 3e - \epsilon) \,. \tag{C.7}$$

It is interesting to consider the near horizon limit of the extremal black hole, where $r \approx r_+ = e - \epsilon$. The coordinates (t, r, ϕ) become singular in this limit and we therefore perform the

coordinate transformation

$$r = e - \epsilon + \lambda\rho \ , \quad t = \frac{\tau}{\lambda} \ , \quad \phi = \varphi - \frac{a\tau}{(e-\epsilon)^2\lambda} \ , \tag{C.8}$$

where λ is a dimensionless parameter which for the time being is non-zero. Then,

$$Q(\rho) = -\frac{\lambda^2\rho^2}{R_3^2}(\lambda\rho - 2\epsilon)(\lambda\rho + 4e - 2\epsilon) \ . \tag{C.9}$$

Substituting this, performing the coordinate transformation and then taking the limit $\lambda \to 0$, the naive brane geometry (7.23) becomes

$$ds^2_{\rm ex} = -\frac{\rho^2}{\Gamma}d\tau^2 + \Gamma\frac{d\rho^2}{\rho^2} + (e-\epsilon)^2\left(d\varphi - \frac{2\rho a}{(e-\epsilon)^3}d\tau\right)^2 \ , \tag{C.10}$$

with[2]

$$\Gamma \equiv \frac{R_3^2(e-\epsilon)^2}{4\epsilon(2e-\epsilon)} = \frac{R_3^2 r_+^2}{(r_c - r_+)(r_c + 3r_+)} = \frac{r_+^2}{1 - 6r_+^2/R_3^2} \ . \tag{C.11}$$

Introducing dimensionless coordinates $(\hat\tau, \hat\rho)$ such that $\tau = \sqrt{\Gamma}\hat\tau$ and $\rho = \sqrt{\Gamma}\hat\rho$, we find

$$ds^2_{\rm ex} = \Gamma\left(-\hat\rho^2 d\hat\tau^2 + \frac{d\hat\rho^2}{\hat\rho^2}\right) + r_+^2\left(d\varphi + k\hat\rho d\hat\tau\right)^2 \ , \tag{C.12}$$

where $k \equiv -2a\Gamma/r_+^3 = -2aR_3^2/r_+(R_3^2 - 6r_+^2)$.

For completeness, the leading order contribution to the holographic CFT stress-energy tensor in the extremal background is

$$\begin{aligned} \langle T^{\hat\tau}_{\hat\tau}\rangle_0 &= \langle T^{\hat\rho}_{\hat\rho}\rangle_0 = -\frac{1}{2}\langle T^{\varphi}_{\hat\tau}\rangle_0 = \frac{1}{16\pi G_3}\frac{\mu\ell}{r_+^3} \ , \\ \langle T^{\varphi}_{\varphi}\rangle_0 &= \frac{3\mu\ell a R_3^2}{8\pi G_3(R_3^2 - 6r_+^2)}\frac{\hat\rho}{r_+^4} \ , \end{aligned} \tag{C.13}$$

which has vanishing trace to this order.

Nariai limit

The Nariai black hole is when the outer black hole horizon and cosmological horizon coincide, $r_c = r_+ = r_{\rm N}$. In this limit, naively, the temperature of the cosmological and black hole horizons vanish, however, we will see the Nariai black hole has a non-zero temperature. From the parameterization (C.2), $r_c = r_+$ is equivalent to $\epsilon = 0$, such that

$$a^2 = \frac{e^2(\delta^2 - e^2)}{R_3^2} \ , \quad \mu\ell = \frac{2e\delta^2}{R_3^2} \ , \tag{C.14}$$

[2]Here we use that in the extremal limit $R_3^2 = r_c^2 + 3r_+^2 + 2r_+r_c$, such that $r_c = \sqrt{R_3^2 - 2r_+^2} - r_+$.

with $R_3^2 = 2e^2 + \delta^2$, and

$$Q = -\frac{1}{R_3^2}(r - r_{\rm N})^2((r + r_{\rm N})^2 - \delta^2) \ , \tag{C.15}$$

which vanishes in the limit $r = r_{\rm N}$. Therefore, the (t, r, ϕ) coordinate system is insufficient to describe the Nariai geometry.

To this end, consider the following coordinate transformation

$$r = e + \epsilon\rho \ , \quad t = \frac{\tau}{\epsilon} \ , \quad \phi = \varphi - \frac{a}{e^2\epsilon}\tau \ . \tag{C.16}$$

The function Q becomes

$$Q(\rho) = \frac{\epsilon^2}{R_3^2}(1 - \rho^2)((\epsilon\rho + 2e)^2 - \delta^2) \ . \tag{C.17}$$

Taking the $\epsilon \to 0$ limit, the brane metric (7.23) takes the form

$$ds_{\rm N}^2 = \Gamma\left(-(1 - \rho^2)d\hat{\tau}^2 + \frac{d\rho^2}{(1 - \rho^2)}\right) + e^2\left(d\varphi + k\rho d\hat{\tau}\right)^2 \ , \tag{C.18}$$

where $\tau = \Gamma\hat{\tau}$ and

$$\Gamma \equiv \frac{R_3^2 e^2}{4e^2 - \delta^2} = \frac{R_3^2 r_{\rm N}^2}{6r_{\rm N}^2 - R_3^2} \ , \quad k \equiv -\frac{2a\Gamma}{r_{\rm N}^3} \ , \tag{C.19}$$

where we used $\delta = \sqrt{R_3^2 - 2r_{\rm N}^2}$.

The temperature $T_{\rm N}$ of the Nariai black hole can be found by Wick rotating the near horizon metric into an appropriate Euclidean section. To see this, rescale coordinates $\hat{\rho} = \rho\sqrt{\Gamma}$ and $\tau = \hat{\tau}\sqrt{\Gamma}$, such that the Nariai metric (C.18) becomes

$$ds_{\rm N}^2 = -f(\hat{\rho})d\tau^2 + f^{-1}(\hat{\rho})d\hat{\rho}^2 + r_{\rm N}^2(d\phi + (k/\Gamma)\hat{\rho}d\tau)^2 \ , \tag{C.20}$$

with $k/\Gamma = -2a/r_{\rm N}^2$ and $f(\hat{\rho}) = 1 - \hat{\rho}^2/\Gamma$. Next, Wick rotate $\tau \to i\tau_E$ and $a \to ia_E$, such that the Euclideanized geometry is

$$ds_{\rm N}^2 = f(\hat{\rho})d\tau_E^2 + f^{-1}(\hat{\rho})d\hat{\rho}^2 + r_{\rm N}^2\left(d\phi + \frac{2a_E\hat{\rho}}{r_{\rm N}^2}d\tau_E\right) \ . \tag{C.21}$$

We now zoom in to the near horizon region where $\hat{\rho}_i = \sqrt{\Gamma}$ and express the metric in flat polar coordinates and impose regularity to remove the conical singularity. Thus, introduce the radial coordinate

$$\rho'^2 = \frac{4(\hat{\rho} - \hat{\rho}_i)}{f'(\hat{\rho}_i)} \quad \Rightarrow \quad d\hat{\rho}^2 = (f'(\hat{\rho}_i)\rho'/2)^2 d\rho'^2 \ . \tag{C.22}$$

Moreover, to eliminate the $d\tau_E d\phi$ cross term in the line element, introduce coordinates

$$\tau_E = \frac{1}{(\gamma^2+\alpha^2)}(\gamma\tau'_E - r_{\rm N}\alpha\phi') \ , \quad \phi = \frac{1}{(\gamma^2+\alpha^2)}\left(\frac{\alpha}{r_{\rm N}}\tau'_E + \gamma\phi'\right) \ , \tag{C.23}$$

with $\gamma = \sqrt{\Gamma}/r_{\rm N}$ and $\alpha = -2a_E\Gamma/r_{\rm N}^2$. Then, expand the metric (C.21) about $\hat{\rho} = \sqrt{\Gamma}$,

$$ds_{\rm N}^2 \approx \rho'^2 d(\beta^{-1}\tau'_E)^2 + d\rho'^2 + \frac{r_{\rm N}^2}{\Gamma}d\phi'^2 \ , \tag{C.24}$$

where we used $f(\hat{\rho}) \approx f'(\hat{\rho}_i)(\hat{\rho}-\hat{\rho}_i)$ and

$$\beta = \frac{\Gamma^2}{r_{\rm N}^3 R_3^2}(6r_{\rm N}^2 - R_3^2 + 4a_E^2 R_3^2) \ . \tag{C.25}$$

The (τ'_E, ρ')-sector is that of a cone where we remove the singularity at $\rho' = 0$ by demanding τ'_E have period $\Delta\tau'_E = 2\pi\beta$. Additionally, we impose ϕ' to have period $\Delta\phi' = 0$, such that the geometry (C.24) represents flat polar coordinates. We now solve for the periodicity of $\Delta\tau_E$ in the Euclidean geometry (C.21) via[3]

$$\Delta\tau'_E = 2\pi\beta = \gamma\Delta\tau_E + r_{\rm N}\alpha\Delta\phi \ , \quad \Delta\phi' = 0 = \gamma\Delta\phi - \frac{\alpha}{r_{\rm N}}\Delta\tau_E \ , \tag{C.26}$$

leading to

$$\Delta\tau_E = \frac{2\pi\beta\gamma}{(\gamma^2+\alpha^2)} = 2\pi\sqrt{\Gamma} \ . \tag{C.27}$$

Hence, the temperature of the Nariai black hole is $T_{\rm N} = (2\pi\sqrt{\Gamma})^{-1}$.

Lastly, the holographic CFT stress-energy tensor in the rotating Nariai geometry is

$$\begin{aligned} \langle T^{\hat{\tau}}_{\hat{\tau}}\rangle_0 &= \langle T^{\rho}_{\rho}\rangle_0 = -\frac{1}{2}\langle T^{\varphi}_{\hat{\tau}}\rangle_0 = \frac{1}{16\pi G_3}\frac{\mu\ell}{r_{\rm N}^3} \ , \\ \langle T^{\varphi}_{\varphi}\rangle_0 &= \frac{3\mu\ell a R_3^2}{8\pi G_3(6r_{\rm N}^2 - R_3^2)}\frac{\rho}{r_{\rm N}^4} \ . \end{aligned} \tag{C.28}$$

When $a = 0$, we recover the stress-tensor for the static quantum Nariai black hole [264].

Ultracold limit

The ultracold limit occurs when all three horizons coincide, $r_c = r_+ = r_- \equiv r_{\rm uc}$. Thus, this is a combination of the Nariai and extremal limits, i.e., simultaneously sending $\delta \to 2e - \epsilon$ and

[3]Where it is useful to know the inverse coordinate transformation $\tau'_E = \gamma\tau_E + r_{\rm N}\alpha\phi$ and $\phi' = \gamma\phi - \frac{\beta}{r_{\rm N}}\tau_E$.

$\epsilon \to 0$. Here we will arrive at the ultracold limit directly from the Nariai limit, where we make the following change of variables:

$$\rho = \sqrt{\frac{2e-\delta}{R_3}} X \ , \quad \tau = \sqrt{\frac{R_3}{2e-\delta}} \frac{R_3 e}{4} T \ , \tag{C.29}$$

and subsequently take the limit $\delta \to 2e$ such that the Nariai geometry (C.18) becomes that of the ultracold black hole,

$$ds^2_{\rm uc} = \frac{R_3 r_{\rm uc}}{4}(-dT^2 + dX^2) + r^2_{\rm uc}\left(d\varphi - \frac{2aX}{r^3_{\rm uc}} dT\right)^2 \ . \tag{C.30}$$

The physical parameters meanwhile are $a^2 = 3e^4/R_3^2$ and $\mu\ell = 8e^3/R_3^2$.

Lukewarm black hole

Lastly, as with all Kerr-de Sitter black holes, the qKdS has a lukewarm limit, where the surface gravities of the cosmological and outer black hole horizons coincide $\kappa_c = \kappa_+$, apart from the surface gravity of the Nariai black hole. For completeness we carry out the analysis of this limiting geometry with respect to the surface gravities of the naive black hole spacetime, leaving the analysis of the lukewarm limit of the regular black hole for the main text.

To this end, the surface gravities with respect to the naive metric (7.23) are simply $\kappa_i = \frac{1}{2}|H'(r_i)|$, following the definition $\zeta^b \nabla_b \zeta^c = \kappa \zeta^c$, where there is a surface gravity associated with each root of the blackening factor $H(r)$. The temperature of each horizon is then[4]

$$T_i = \frac{\kappa_i}{2\pi} = \frac{|H'(r_i)|}{4\pi} \ . \tag{C.31}$$

Then, using $H'(r_i) = r_i^{-2} Q'(r_i)$, since $H(r_i) = 0$, we have

$$T_i = \frac{|Q'(r_i)|}{4\pi r_i^2} = \frac{1}{2\pi r_i^2 R_3^2} |[(r_i - e)((r_i + e)^2 - \delta^2) + (r_i + e)((r_i - e)^2 - \epsilon^2)]| \ . \tag{C.32}$$

Then, the temperature of the outer horizon $r_+ = e - \epsilon$ is

$$T_+ = \frac{1}{4\pi R_3^2} \frac{2\epsilon((2e-\epsilon)^2 - \delta^2)}{(e-\epsilon)^2} \ . \tag{C.33}$$

[4]One way to derive this expression of the temperature is to move to the Euclidean section of the rotating geometry (7.23), via the double Wick rotation $t \to i\tau_E$ and $a \to i a_E$ and then impose regularity to remove the conical singularity along the Euclidean time direction.

Via root ordering, this temperature is positive, and vanishes in the extremal limit. Meanwhile, the temperature of the cosmological horizon $r_c = e + \epsilon$ is

$$T_c = \frac{1}{4\pi R_3^2} \frac{2\epsilon((2e+\epsilon)^2 - \delta^2)}{(e+\epsilon)^2} \, . \tag{C.34}$$

Taking their difference,

$$T_c - T_+ = 0 \quad \Longleftrightarrow \quad e\epsilon^2(\epsilon^2 - 2e^2 + \delta^2) = 0 \, . \tag{C.35}$$

Here $e = 0$ is forbidden via the root ordering while $\epsilon = 0$ corresponds to the Nariai limit. Hence, the lukewarm limit corresponds to when $\delta^2 = 2e^2 - \epsilon^2$, with temperature $T_{\text{luke}} = \frac{\epsilon}{2\pi R_3^2}$. Moreover, since $H(r)$ is non-zero in this limit, the lukewarm geometry is safely covered by the coordinates (t, r, ϕ) with blackening factor

$$H(r) = -\frac{1}{R_3^2 r^2}((r-e)^2 - \epsilon^2)((r+e)^2 - 2e^2 + \epsilon^2) \, , \tag{C.36}$$

and where (C.5) become $R_3^2 a^2 = (e^2 - \epsilon^2)^2$ and $R_3^2 \mu\ell = 4e(e^2 - \epsilon^2)$, with $R_3^2 = 4e^2$.